

**Bangor University**

## **DOCTOR OF PHILOSOPHY**

### **The development of an electrode for the detection of potassium phosphate**

Al-Yahyawi., Zeina Mohammed Kadam

*Award date:*  
2014

*Awarding institution:*  
Bangor University

[Link to publication](#)

#### **General rights**

Copyright and moral rights for the publications made accessible in the public portal are retained by the authors and/or other copyright owners and it is a condition of accessing publications that users recognise and abide by the legal requirements associated with these rights.

- Users may download and print one copy of any publication from the public portal for the purpose of private study or research.
- You may not further distribute the material or use it for any profit-making activity or commercial gain
- You may freely distribute the URL identifying the publication in the public portal ?

#### **Take down policy**

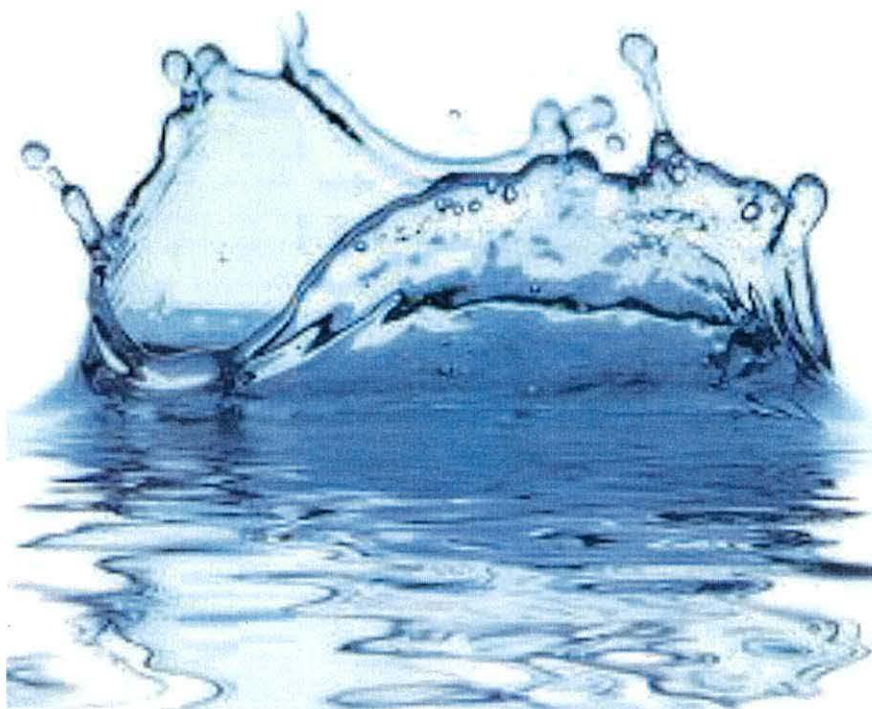
If you believe that this document breaches copyright please contact us providing details, and we will remove access to the work immediately and investigate your claim.

Download date: 09. Apr. 2024

# The development of an electrode for the detection of potassium phosphate

A thesis submitted for the degree of  
Doctor of Philosophy

---



Prifysgol Cymru • University of Wales Bangor

© January 2014

---

by

Zeina Mohammed Kadam Al-Yahyaw





# Contents

|  |               |
|--|---------------|
| Declaration and Consent .....  | II            |
| Contents .....   | ii            |
| Abstract .....   | v             |
| Acknowledgments .....  | 7             |
| <br><b>CHAPTER 1 - INTRODUCTION .....</b>  | <br><b>8</b>  |
| 1.1 Introduction .....   | 9             |
| 1.2 Electrochemical sensors .....  | 10            |
| 1.3 Potentiometric selectivity coefficients .....  | 15            |
| 1.4 Macrocyclic compounds .....  | 16            |
| 1.5 ISEs for potassium .....   | 19            |
| 1.6 Ion selective potentiometric host .....  | 23            |
| 1.7 Plasticisers .....   | 25            |
| 1.8 Ion fluxes in potentiometry .....  | 34            |
| 1.9 The electrical double layer .....  | 35            |
| 1.10 The aim of the project .....  | 36            |
| 1.11 Summary .....   | 37            |
| 1.12 References .....  | 40            |
| <br><b>CHAPTER 2 – MATERIALS AND METHODS .....</b>   | <br><b>50</b> |
| 2.1 General reagents and materials .....   | 51            |
| 2.2 General instruments and methods .....  | 52            |
| Synthesis of (((3,4,5-trinitro-1,2-phenylene)bis(oxy))bis(ethane-2,1-diyl))bis(oxy))bis(ethane-2,1-diyl) dinitrate ..... | 53            |
| Synthesis of 4-nitro benzo-15-crown-5 (1) .....  | 54            |
| Synthesis of dinitro benzo-15-crown-5 (2) .....  | 55            |
| Synthesis of 4- amino benzo-15-crown-5 (3) .....   | 56            |
| Synthesis of diamino benzo-15-crown-5 (4) .....  | 57            |
| Synthesis of 4-nitro benzo-18-crown-6 (5) .....  | 58            |
| Synthesis of dinitro benzo-18-crown-6 (6) .....  | 59            |
| Synthesis of dinitro dibenzo-18-crown-6 (7) .....  | 60            |
| Synthesis of 4- amino benzo-18-crown-6 (8) .....   | 61            |
| Synthesis of diamino benzo-18-crown-6 (9) .....  | 62            |
| Synthesis of di (amino benzo)-18-crown-6 (10) .....  | 63            |
| 2.3 Preparation methods .....  | 64            |
| 2.4 Electrode arrangement .....  | 65            |
| 2.5 Potentiometric titration .....   | 67            |
| Separate solutions method .....  | 68            |
| Mixed solutions method .....   | 68            |
| Fixed interference method .....  | 69            |
| Limit of detection .....   | 69            |
| Calibration of the electrode .....   | 69            |
| 2.6 Qualitative analysis of water samples .....  | 70            |
| 2.7 Quantitative analysis of water samples .....   | 72            |

|      |  |    |
|------|--|----|
| 2.8  | Scanning electron microscopy(SEM).....       | 73 |
| 2.9  | Energy dispersive analyser X-ray(EDAX) ..... | 74 |
| 2.10 | References.....                              | 75 |

## CHAPTER 3 – SYNTHESIS AND POTENTIOMETRIC CHARACTERISATION ..... 78

|     |  |     |
|-----|--|-----|
| 3.1 | Introduction .....   | 79  |
| 3.1 | (((3,4,5-trinitro-1,2-phenylene)bis(oxy))bis(ethane-2,1-diyl))bis(oxy))bis(ethane-2,1-diyl) dinitrate..... | 80  |
|     | Synthesis.....   | 80  |
|     | Performance .....  | 84  |
| 3.2 | 4-Nitro benzo-15-crown-5 (1) and 4-amino benzo-15-crown-5 (3).....   | 85  |
|     | Synthesis .....  | 85  |
|     | Performance .....  | 92  |
| 3.3 | Dinitro benzo-15-crown-5 (2) and diamino benzo-15-crown-5 (4).....   | 93  |
|     | Synthesis .....  | 93  |
|     | Performance .....  | 102 |
| 3.4 | 4-nitro (5) and 4-amino (8) benzo-18-crown-6 .....   | 105 |
|     | Synthesis .....  | 105 |
|     | Performance .....  | 110 |
| 3.5 | Dinitro benzo-18-crown-6 (6) and diamino benzo-18-crown-6 (9).....   | 112 |
|     | Synthesis .....  | 112 |
|     | Performance .....  | 118 |
| 3.6 | Di(nitrobenzo)-18-crown-6 (7) and di(aminobenzo)-18-crown-6 (10) .....                                     | 122 |
|     | Synthesis .....  | 122 |
|     | Performance .....  | 131 |
| 3.7 | Conclusions.....   | 133 |
| 3.8 | References.....  | 136 |

## CHAPTER 4 – PLASTICISERS ..... 139

|     |  |     |
|-----|--|-----|
| 4.1 | The selection of the solvent mediator..... | 140 |
|     | Di butyl phthalate (DBP) .....             | 141 |
|     | Nitrophenyl phenyl ether (NPPE) .....      | 144 |
|     | Diocetyl phenyl phosphonate (DOPP).....    | 146 |
|     | Di octyl phthalate (DOP) .....             | 148 |
|     | Bis (2-ethylhexyl) adipate (BEHA) .....    | 150 |
| 4.2 | Influence of membrane composition .....    | 154 |
| 4.3 | Conclusions.....                           | 156 |
| 4.4 | References.....                            | 157 |

## CHAPTER 5 - APPLICATION AND ASSESSMENT OF THE DESIGNED ELECTRODE ..... 159

|     |  |     |
|-----|--|-----|
| 5.1 | Introduction .....   | 160 |
|     | Qualitative analyses of water samples .....                | 162 |
|     | Elemental analyses.....                                    | 164 |
|     | Scanning electrochemical microscopy and EDX analyses ..... | 167 |
| 5.2 | Lifetime of the electrode.....                             | 172 |
| 5.3 | The effect of pH.....                                      | 173 |
| 5.4 | Effects of the counter ion .....                           | 174 |

|   |                          |     |
|---|--------------------------|-----|
| 5.5   | Conclusions.....         | 176 |
| 5.6   | References.....          | 177 |
| CHAPTER 6 – CONCLUSIONS AND FUTURE WORK ..... |                          | 181 |
| 6.1   | Concluding remarks ..... | 182 |
| 6.2   | Future work.....         | 185 |
| 6.3   | References .....         | 187 |



## Abstract

### **The development of an electrode for the detection of potassium phosphate**

by  
*Zeina Mohammed Kadam Al-Yahyawi*

The research associated with this work centres on the development and synthesis of selective ionophores that are capable of detecting potassium phosphate ions in aqueous solutions. This specific detection of  $K^+$  ions that are bound to a phosphate ion is crucial because both ions play a leading role in water pollution. This work describes a  $K^+$  ion-sensing system using a potentiometric method based on macrocyclic compounds.

This thesis consists of six chapters. Chapter one includes a short history and introduction of the electrochemical sensors with a description of macrocyclic compounds as ionophores which are related to this thesis work.

The second chapter describes the experimental techniques which have been used to synthesize the target compounds including single-crystal X-ray structural analysis.

Synthesis a novel ionophore (((3,4,5-trinitro-1,2-phenylene)bis(oxy))bis(ethane-2,1-diyl))bis(oxy))bis(ethane-2,1-diyl) dinitrate based on open ring macrocyclic compound structure and the synthesis and performance of ten ionophores for the electrode potentiometric applications within a PVC membrane is conveyed in chapter three. The characterisations of the those ionophores are reported including FT-IR data,  $^1H$  NMR,  $^{13}C$  NMR, HSQC NMR, 2D NMR including COSY NMR, Mass spectrometry, and single-crystal X-ray structural analysis for confirming the closing ring structures. Those ionophores are 4-nitro benzo-15-crown-5 (**1**), 4-amino benzo-15-crown-5 (**3**), dinitro benzo-15-crown-5 (**2**), diamino benzo-15-crown-5 (**4**), 4-nitro benzo-18-crown-6 (**5**), 4-amino benzo-18-crown-6 (**8**), dinitro benzo-18-crown-6 (**6**), diamino benzo-18-crown-6 (**9**), dinitro dibenzo-18-crown-6 (**7**), diamino dibenzo-18-crown-6 (**10**). In addition to that another five ionophores have been applied within a PVC membrane which there were 1-aza-18-crown-6, benzo-15-crown-5, benzo-18-crown-6, dibenzo-18-crown-6, and dicyclohexyl-18-crown-6 is reported in this chapter. The ability to synthesis these ionophores are important to

enable a review of the effects of both the ring size and the associated functional groups.

Chapter four describes the data of the effect of a range of plasticisers for incorporating the ionophores into the membrane for optimum sensor design. Those plasticisers are dibutyl phthalate, 2- nitrophenyl phenyl ether, dioctyl phenyl phosphonate, dioctyl phthalate, and bis (2-ethylhexyl) adipate. The thermal properties of all blends are studied by TG/DSC.

The assessment of the designed electrode is applied in chapter five which includes the modified electrodes with the ionophores dibenzo-18-crown-6 proving to be the most effective with a shelf life of 40 days; this ensemble also showed negligible drift. It responded in a near Nernstian fashion, and showed a low detection limit of  $3.2 \times 10^{-6} \text{ mol L}^{-1}$ , and a fast response time of 30 seconds over a concentration range of  $5 \times 10^{-5} \text{ mol L}^{-1}$  to  $1 \times 10^{-1} \text{ mol L}^{-1}$ . The morphologies of the sensor after using it is studied by imaging of the sensor in scanning electron. While the energy-dispersive X-ray spectroscopy is used to gather data about the elemental composition of the samples' surface. X-rays, which are characteristic for different elements and a composition spectrum is produced.

Finally, chapter six includes conclusions of the thesis work which involves that the resulting electrode signifies a significant advancement in the construction of a potentiometric device for the determination of potassium phosphate concentrations in solution and suggestions for future work.



## Acknowledgments

---

I feel very privileged to have had the opportunity to establish my scientific roots and I would like to deeply thank my supervisor Dr. C. Gwenin for all his guidance, patience and help through these years.

I would also like sincerely to thank Dr Holliman for his advice and help in crystallographic work. I would like to thank all the members of Dr. Gwenin research group, past and present for their friendship. In addition, I would like to thank all the secretarial, technical and the entire staff at the School of Chemistry. I would like to gratefully thank Dr Mateusz B. Pitak for his support throughout carrying out the crystallographic work at the UK National Crystallography Service (NCS), Southampton University.

I would also like to thank the government of Iraq, particularly the Ministry of Higher Education and Cultural Attaché for sponsoring me and allowing me this unique opportunity.

Finally and deeply, I would also like to thank and dedicate the work to my family and friends in Iraq and Bangor, including my parents, my brothers and sisters for their constant faith in my abilities and for my husband Mohanend and my two children, Mohammed and Noor for all of their support and understanding over these long years. This thesis is as much of them as it is me.

# **Chapter 1 - Introduction**

## 1.1 Introduction

Potassium and phosphorus are among the nutrients plants and other organisms need to flourish, as potassium phosphate delivers both it is a common substituent of fertilisers. The over use of such fertilisers result in the contamination of rivers and water supplies, thus issues of water quality still continue to attract the attention of researchers.<sup>1,2</sup> This has led to an increased level of interest in potentiometric based sensors because of their selectivity, ease of use in the field and long shelf life.<sup>3,4</sup>

Ion-selective electrodes (ISEs) are widely applied in analytical chemistry and have a steeped history of use to determine the activity of specific ions.<sup>5, 6</sup> Currently over a billion ISE measurements are performed world-wide in a large variety of fields; including physiology,<sup>7</sup> process control,<sup>8</sup> environmental analysis,<sup>9</sup> pollution monitoring,<sup>10</sup> food processing,<sup>11</sup> and water quality.<sup>12</sup> Despite this there is still an increasing interest in the development of ion-selective sensors for detecting electrolytes such as  $K^+$ .<sup>13</sup> To date, several potassium sensors based on plasticized membranes, containing different ionophores have been developed.<sup>14,15</sup> Most of them however are based on valinomycin,<sup>16,17</sup> or crown ethers<sup>18,19</sup> and report the results of a single crown ether rather than a direct comparison between the substituent and plasticiser effects.

Macrocyclic compounds, because of their selective receptor properties and their ease of structural modification, have also been engaged as ionophores in the assembly of ISEs for the determination of alkali, alkaline and many transition metal ions.<sup>20</sup> Crown ether macrocycles provide a simple receptor model and are well matched as hosts due to their conformational flexibility and the presence of multiple binding sites in their structures.<sup>21,22</sup> The complexing properties of crown ether derivatives depend on the comparative size of the ions being detected to the size of the crown ether ring as well as the number and variety of heteroatom's and functional groups.<sup>23,24</sup> Within this work a range of ionophores and plasticisers are compared for their selectivity towards potassium phosphate.



## 1.2 Electrochemical sensors

Electrochemical sensors provide an analytical instrument of great interest for both research and practical routine analysis because of their ability to be hand held and their extremely low sensitivities.<sup>25</sup> The introduction of new and reliable ISEs for various cations, anions, neutral species, gases and enzymes has been a subject of attention for many scientists in across a wide range of fields.<sup>26,27,28,29,30</sup> These electrochemical devices, whose potential directly corresponds to the concentration or activity of specific species in solution, are rapidly replacing complicated, time consuming and expensive instruments, both in scientific research and in industry.<sup>31</sup>

The history of ISEs dates back to 1906, when Max Cremer revealed pH-sensitive glasses, a discovery which was to lead to the first commercial pH glass electrodes in the 1930s.<sup>32</sup> The introduction of crystalline compounds, such as  $\text{LaF}_3$ ,  $\text{AgCl}$ , or  $\text{Ag}_2\text{S}$ , as sensing materials was discovered in the early 1960s, leading to, for example, fluoride- and halide-selective electrodes.<sup>33</sup> However, the improvement of ISEs based on these materials was delayed by the difficulty of applying crystalline materials with selectivity's for specific ions. In the 1970s, ISEs started to be widely used and applied in analytical chemistry, and have since had a long history of use to determine the activity of specific ions.<sup>5,6</sup> Currently, over a billion ISE measurements are performed world-wide and in a large variety of fields, including physiology,<sup>7</sup> process control,<sup>34</sup> environmental analysis,<sup>9</sup> food processing,<sup>35</sup> and water quality<sup>12</sup> etc.

Potentiometric ion sensors or ISEs are an important subgroup of electrochemical sensors.<sup>36,37</sup> These membrane electrodes are comprised of an internal reference system interfaced with a thin layer, which may be either solid or liquid and either conducting or non-conducting towards the ions of interest. This layer is called a membrane and forms a fundamental part of the electrode. The function and mechanism of the electrical conduction of ISEs is mainly related to the active material and the nature of the compounds used in the preparation of the membrane.

The advantages of ISEs, are their well-known principle of operation, their low cost, easy fabrication, and simple set-up. In addition the ability for electrochemical polymeric membranes to containing neutral or charged carriers (ionophores) that are

available for the determination of a large number of inorganic and organic ions is a major advantage, and as such has been the subject of extensive reviews.<sup>38,39</sup>

The chemical sensing abilities of ISEs have been further improved in the last ten years, to result in ISEs.<sup>40,41,42</sup> This has resulted from several important factors such as the lower detection limit of ISEs, new membrane ionophores, new sensing concepts, and the theoretical understanding and modelling of the potentiometric response of ISEs. The main disadvantages of potentiometric measurements are their temperature dependence, the influence of solution changes, and adsorption of solution components on membrane surfaces that can affect the nature of the charge transfer. The effect of those factors can be reduced, however, by such measures as controlling the temperature, washing the electrodes with solvents to limit the adsorption, and application of anti-fouling layers.<sup>43</sup>

### **Classification of electrochemical electrodes**

The generally accepted classification of membrane electrodes is according to the physical state of the membranes used. The electrodes are thus classified into four main types as follows:

1. Glass electrodes
2. Solid-state electrodes
  - i. Homogenous solid-state (or crystal) membrane electrodes
  - ii. Heterogeneous solid-state membrane electrodes
3. Liquid ion exchange membrane electrodes
4. Gaseous membrane electrodes
5. Biosensors

Generally, electrochemical methods are based on the transformation of chemical information into an analytically useful signal. Any sensor used in electro-analytical determination contains two basic functional units; one receptor part, which transforms the chemical information into a form of energy, and one transducer part, which transforms the energy, bearing chemical information, into a useful signal. The theory of potentiometric response includes classical equilibrium models<sup>44</sup> as well as advanced non-equilibrium models,<sup>45</sup> together with recent advances in the field of solid contact ISEs, which emphasise the application of conducting polymers as ion-to-electron transducers.<sup>46</sup>



A carrier-based ISE consists of the solvent polymeric membrane (plasticized-PVC membrane), which is a high viscosity liquid that is commonly placed between two aqueous phases, such as the sample solution and the internal electrolyte solution, has been illustrated in (Figure 1.1).

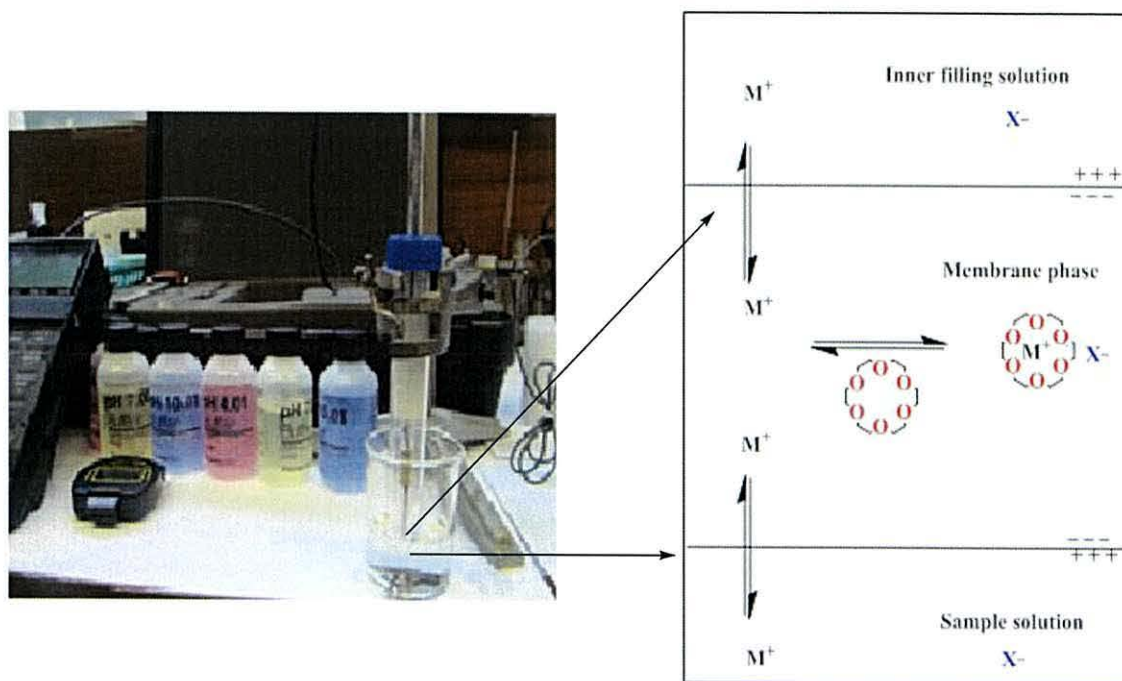


**Figure 1.1:** (Left) Photograph of in house manufactured electrode and (right) close-up of key sensor phases and equilibria

Potentiometric measurements are based on monitoring potential values under a zero current flow regime, in order to determine the analytical concentration of the desired components in an analyte. In these methods, the potential difference between an indicator electrode and the reference electrode is measured as the analytical potential. The potential of an electrochemical cell results from the changes in the free energy that occurs if the chemical phenomena reach equilibrium. This is a concept that is typically applied in quantitative analysis in relation to electrochemical cells, in which case the difference between the cathodic and the anodic potentials is the potential of the electrochemical cell and is calculated using the so-called Nernst equation. Another source of potential may be physical phenomena not involving explicit redox reactions but having non-zero free energy initial conditions.<sup>47</sup> This can also be a

potentiometric phenomenon, and is the basis of measurements that use ISEs. The Nernst equation is used to determine the concentration of the analyte, and the operation of an ISE is dependent upon the establishment of a potential difference between the solution side and the internal electrolyte side of the electrode. This potential difference occurs at the solution-membrane interface see (Figure 1.1). When the membrane is doped with an ionophore that is primarily selective for one ion this potential difference then becomes dependent upon the activity of this ion.

The function of the potential difference and the activity follow the well-known Nernst equation,<sup>48</sup> as shown;

$$E_{mem} = E^{\circ} - \frac{RT}{z_i F} \ln a_i \dots \dots \dots \text{Equation 1.1}$$

Where E is the electromotive force (emf) of the cell in volts,  $E^{\circ}$  is the emf cell constant, F is the Faraday constant,  $z_i$  and  $a_i$  represent the charges and the activity of the ion of interest respectively, and R and T are the usual thermodynamic quantities. This equation is in the form of  $y = mx + b$  and thus a plot of E verse  $\log [a]$  will give a straight line with a slope of  $2.303RT/nF$ . For the measurement of monovalent cations at 25°C,  $n = 1$  and the slope becomes 59.16 mV/dec. Thus for any ISE that measures monovalent cations and is operating according to the Nernst equation a slope of 59.16 mV/dec would be expected.

A two-electrode setup is used with the ISE as the working electrode (the membrane exposed to electrolyte solution) and a reference electrode, such as standard calomel electrode (SCE) or saturated silver/silver chloride electrode (Ag/AgCl). As shown in Figure 1.2, the electrodes are connected to a pH /mV meter and the two-half cells are placed into solution where the potential difference is measured as a function of ion concentrations. Electrochemical sensors are used to determine the concentration of specific ion species in water and air. One of the most successful types of chemical sensors is ISEs, which can be used to determine the concentration of selected ions by measurements of electrical potentials with a voltmeter as in (Figure 1.2).

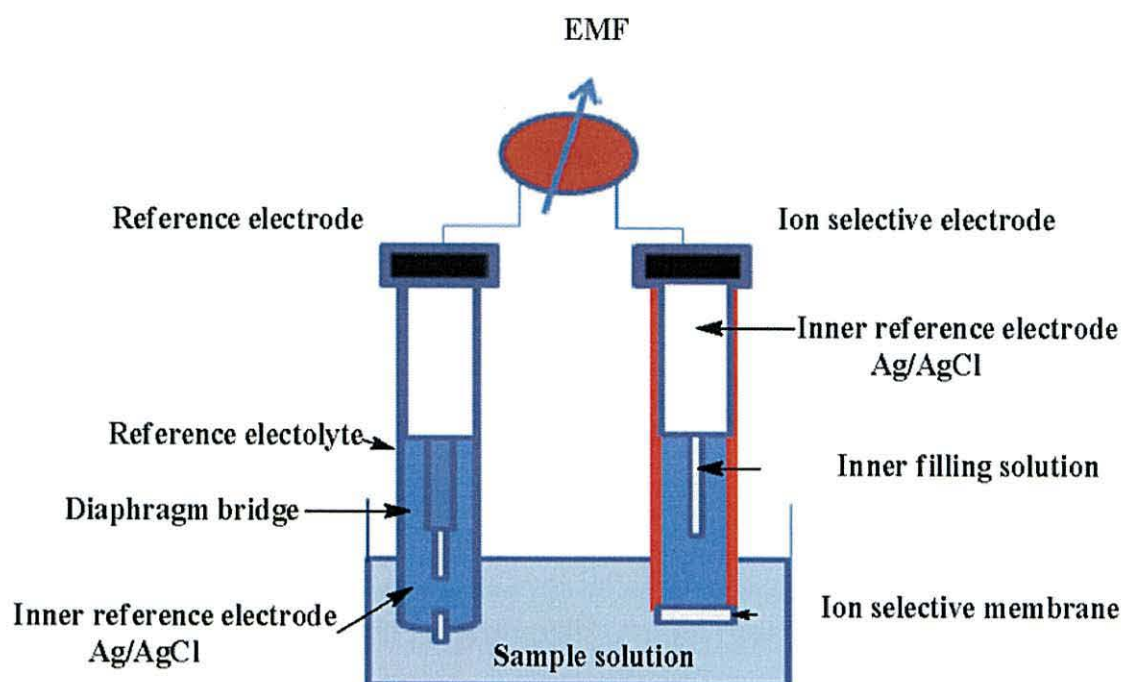


Figure 1.2: Schematic diagram of a measuring cell for traditional measurements of EMF. Redrawn from <sup>47</sup>

The operation of an ISE is dependent on the establishment of a potential difference between the solution and the internal electrolyte with the potential difference occurring at the solution-membrane interface. When the membrane is doped with an ionophore that is primarily selective for a specific ion, this potential difference becomes dependent upon the activity of the specific ion and is measured against an external reference electrode.<sup>48</sup>



### 1.3 Potentiometric selectivity coefficients

The selectivity of a sensor is determined by its ability to record concentrations of specific ions in the presence of other ions in the solution. Quantitatively, this property is described by the value of the coefficient of selectivity which is defined as the ability of an ion-selective electrode to distinguish a particular ion from others. The selectivity coefficient is  $\text{Log } K_{i,j}^{\text{Pot}}$ , but the terms ‘selectivity constant’ and ‘selectivity factor’ are frequently used instead of selectivity coefficient. However, in order to standardise the terminology associated with ISEs, use of the term ‘selectivity coefficient’ is recommended, as is the fixed interference method (FIM) for its evaluation.<sup>49</sup> For such systems, the selectivity of the ISE over other cations is one of the key parameters, primarily driven by the selectivity of the ionophore, and may be measured in one of several ways. A number of ions are taking part in any given reaction, and in the ISE case, those ions are interacting with the membrane in the presence of other ions. However, it should be noted that this difference is small in activity and concentration in dilute solutions and can be ignored in many practical applications. The selectivity of ISEs is related to the equilibrium constant of the exchange reaction of the primary ion (target ion) and interfering ions between the membrane and aqueous phase. Therefore, the selectivity is strongly dependent on the ratio of the binding constants of these ions to the ionophore in the membrane.

The goal in this work is to develop ionophores that are capable of detecting potassium phosphate ions in aqueous solution. For any ISE sensors, sensitivity to a specific ion in the required concentration range and selectivity for one specific ion over all other interfering ions are two important considerations. The two typical methods of measurement are called the FIM, which involves the measurement of two solutions where each solution contains a salt of the determined ion and the interfering ion together, and the Separate Solution Method (SSM), which involves the measurement of two separate solutions where each solution contains a salt of the determined ion only and the other solution has the interfering ion. When these methods are used, a selectivity coefficient for the sensor is determined and given as  $\text{Log } K_{i,j}^{\text{Pot}}$ . The “Pot” refers to the fact that the selectivity value was determined potentiometrically whilst  $i$  signifies the primary ion of interest, and  $j$  signifies the interfering ion. For example, typical potassium ISE’s possess selectivity values for

potassium over sodium in the order of  $\text{Log } K_{i,j}^{\text{Pot}} = -3.3$ . This is interpreted as the sensor being greater than three orders of magnitude more selective for potassium than for sodium. The activities of the primary ion,  $i$ , and the interfering ion,  $j$ , at which  $\text{Log } K_{i,j}^{\text{Pot}}$  is determined should always be specified, as the value of  $\text{Log } K_{i,j}^{\text{Pot}}$  is defined by the modified Nikolsky- Eisenman equation (Equation 1.2). The smaller the value of  $\text{Log } K_{i,j}^{\text{Pot}}$  is the greater the electrode's preference for the principal ion.<sup>49</sup>

$$\text{Log } K_{i,j}^{\text{Pot}} = \frac{(E_j - E_i)}{s} + \log c_i - \log c_j^{1/z_j} \dots \dots \dots \text{Equation 1.2}$$

#### 1.4 Macrocyclic compounds

The crowns were discovered by Charles Pedersen in 1967 by accidental isolation of a small amount from an organic reaction. The high degree of crystallinity and the solubility behaviour had motivated Pederson's attention.<sup>51</sup> It was observed that the solubility of the crown ether compounds in methanol was significantly improved when alkali metal salts were added. He finally concluded that the alkali metal ion had become incorporated in a cavity of the molecule. This initial hypothesis was soon verified to be correct and gained Pederson a share of the 1987 Nobel Prize for Chemistry.<sup>51</sup>

Crown ethers, as named by Pederson, quickly became a popular research subject in cation complexation chemistry. The development of crown ethers in the field of host-guest chemistry made remarkable advances in this field and led both analytical and organic chemists to quickly set out to develop synthetic ionophores for use in ISEs. The result of this development was that ion-selective potentiometry replaced flame atomic emission spectroscopy in the 1980s as the standard technique for the measurement of electrolyte ions in blood and urine.<sup>52</sup> As a result, this type of sensor is now one of the biggest successes of host-guest chemistry.

The essential repeating unit of any simple crown ether is the ethyleneoxy group  $-\text{CH}_2\text{CH}_2\text{O}-$ .<sup>53</sup> Their tendency to selectively form complexes with various cations has been attributed to the structural similarity with the natural ionophores; thus, the use of these compounds instead of expensive and unstable ionophores has been



encouraged.<sup>54</sup> The first compounds were dicyclo-hexyl-18-crown-6; they all contain polar as well as non-polar groups arranged in a cyclic structure. The complexation of these compounds is such that the oxygen atoms point towards the centre of the molecule to provide a polar cavity for the cation (Figure 1. 3).<sup>54</sup>

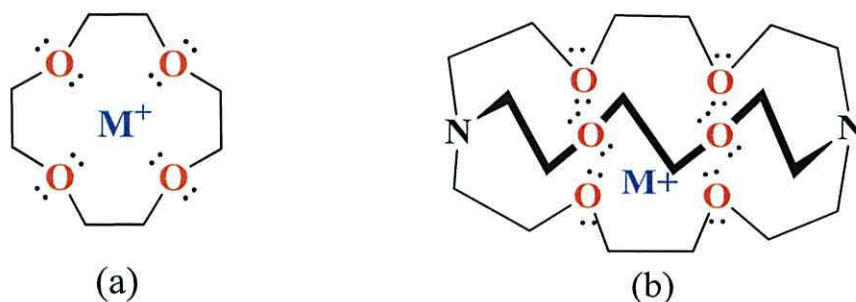


Figure 1. 3: (a) 12-crown-4, (b) [2, 2, 2] cryptand as examples of polar crown cavities

Macrocyclic compounds which then known to form intramolecular charge-transfer complexes with neutral molecules, because of their selective receptor properties and their ease of structural modification, have also been exploited as ionophores in the assembly of ISEs for the determination of alkali, alkaline and many transition metal ions.<sup>20</sup> Crown ether macrocycles provide a simple receptor model and are well matched as hosts due to their conformational flexibility and the presence of multiple binding sites in their structures.<sup>21,22</sup> The comparative size of the ions is being detected related to the size of the crown ether ring, as well as the number and variety of heteroatoms and functional groups.<sup>23,24</sup> The electronegative oxygen atoms are ideal for binding with a cation, which can be included within the cyclic host. In addition, the exterior of the host is hydrophobic.

The main step in the process of developing selective and sensitive ionophores is to study the thermodynamics of complexation. Ionophore selectivity can be discussed in terms of the thermodynamic stability of the metal ion–ionophore complex, where more stable complexes have more selective interactions.<sup>55</sup> Thermodynamic stability in these systems is a complex combination of enthalpic and entropic parameters that can be assumed for the consideration of steric size-fit parameters with pre-organisation of the ionophore. It is clear that the role of the crown ether unit

receptors is capable of lowering the kinetic barrier related with the interface transport of the carrier-guest complex. This is due to the ability of the relatively hydrophilic crown ether to “invade” the water solution across the interface.

Table 1. 1 on the following page gives a selection of thermodynamic values for alkali metal ion binding to a series of crown ethers as reported by Bradshaw and coworkers.<sup>56</sup>

*Table 1. 1: Thermodynamic values for alkali metal ion binding to a series of crown ethers as reported by Bradshaw and co-workers<sup>56</sup>*

| Crown ether type | Cavity Metal (Å) | Metal ion | Cation radius (Å) | -ΔG ((kJ/mol) | ΔH (kJ/mol) | TΔS (kJ/mol) |
|------------------|------------------|-----------|-------------------|---------------|-------------|--------------|
| 15-crown-5       | 0.86-0.92        | Na        | 0.95              | 19.7          | 20.9        | -1.30        |
|                  |                  | K         | 1.33              | 21.3          | 32.2        | -10.9        |
|                  |                  | Cs        | 1.69              | 12.6          | 49.0        | -36.4        |
| 18-crown-6       | 1.34-1.43        | Na        | 0.95              | 25.1          | 31.4        | -6.30        |
|                  |                  | K         | 1.33              | 34.7          | 56.1        | -21.3        |
|                  |                  | Rb        | 1.48              | 30.6          | 50.7        | -20.1        |
|                  |                  | Cs        | 1.69              | 27.2          | 47.3        | -20.1        |
| 21-crown-7       | ~1.70            | Na        | 0.95              | 10.0          | 43.5        | -33.5        |
|                  |                  | K         | 1.33              | 24.3          | 36.0        | -11.7        |
|                  |                  | Rb        | 1.48              | 27.6          | 40.2        | -12.6        |
|                  |                  | Cs        | 1.69              | 28.5          | 46.9        | -18.4        |

Examination of the table reveals that complexation is an enthalpically favourable process and an entropically unfavourable process, and that there may be a modest correlation between the free energy of complexation and the size-fit between the ion and ionophore. Thus, when the size matches closely, the metal ion is arranged within the cavity or pocket and gives the most symmetrical electrostatic interactions. A smaller ion will involve a proportionally smaller electrostatic interaction and thus will not be as tightly bound. However, an ion that is larger cannot fit within the pocket symmetrically and as a consequence will not benefit from all of the electrostatic stabilizing interactions provided by the ionophore. This relationship is particularly clear in the case of the 18-crown-6 and the 21-crown-7 where the average pocket sizes are in the order of 1.39 and 1.70 Å respectively. These values nicely match the ionic radius of potassium (1.33 Å) and that of caesium (1.69 Å) and as a result, the free energy of complexation for these two cations is the most



favourable ( $\Delta G = -34.7$  and  $-28.5$  kJ/mol respectively) in comparison to the other cations.

In general, two design features must be incorporated into the ionophore to achieve high selectivity for a particular guest; the pocket of the ionophore must be an appropriate size to bind the guest, and a pre-organized structure is needed to reduce the entropic and enthalpic costs of complexation. These factors are primary drivers in the complexation of alkali metal ions.<sup>55</sup>

### 1.5 ISEs for potassium

The potassium ion ( $K^+$ ) is an important cation in the human body. It is vital for preventing muscle contraction and sending all nerve impulses in animals through action potentials. Normal serum  $K^+$  levels are between 3.8 and 5.4 mmol/L.<sup>57</sup> Abnormal physiological  $K^+$  concentrations may cause several diseases. A severe shortage of potassium in body fluids, for example, may cause a potentially fatal condition known as hypokalaemia.<sup>58</sup>

Excess of  $K^+$  may increase the risk of high blood pressure and stroke.<sup>59</sup> Therefore, the determination of  $K^+$  is crucial in both clinical diagnosis and basic research. To date, various techniques have been employed to detect  $K^+$  concentration, such as ion chromatography (IC),<sup>57</sup> electrochemistry,<sup>60</sup> surface plasmon resonance (SPR),<sup>61</sup> and flame atomic absorption spectrometry (AAS).<sup>62</sup> However, these conventional methods are complex and time-consuming, and so the development of new strategies for  $K^+$  determination is needed.

Another salient area for potassium detection relates to environmental pollution caused by raw sewage released from small municipalities, remote communities, small housing complexes, tourist facilities, camps, factories, harbours and other similar sources. Until now, it has been difficult to conceive suitable treatment facilities as the problem is quite extensive in many areas.<sup>1</sup> However, with pressure on resources, the necessity to control this pollution is now stronger than ever and these small communities and facilities need an effective and easy to implement solution.

Furthermore, the ever-increasing demand for clean water supply has adversely affected water resources on a global level. As a consequence, the need to effectively protect and conserve our water necessitates either municipal or industrial scale action, with a view to encouraging reuse. Some of the most common applications of treated wastewater reuse include irrigation of agricultural land, industrial process water, recharge of aquifers, and river flow replenishment.<sup>63</sup>

Potassium and phosphorus are among the nutrients that plants and other organisms need in order to flourish. Since potassium phosphate delivers both, as such it is a common constituent of fertilizer. The overuse of such fertilizers, however, can result in the contamination of rivers and water supplies, thus issues of water quality still continue to attract the attention of researchers. This has also led to an increased level of interest in potentiometric based sensors because of their selectivity, ease of use in the field and long shelf life.<sup>2</sup>

There is increasing interest in the development sensors for detecting electrolytes such as  $K^+$ .<sup>26</sup> To date, several potassium sensors based on plasticized membranes containing different ionophores have been developed.<sup>15</sup> Most of them, however, are based on valinomycin<sup>17</sup> or crown ethers,<sup>16,18,64</sup> and report the results of a single crown ether rather than a direct comparison. When the size of the host cavity matches the diameter of a guest metal cation, high binding strength and selectivity are observed. For example, when a cavity size of 2.60-3.20 Å in a host molecule of 18-crown-6 matches the diameter of  $K^+$  (2.66 Å), the host binds with a metal cation and the oxygen donor atoms tend to interact strongly with the positively charged cation by dipole-charge interaction. The hydrocarbon skeleton of the crown ether acts as a hydrophobic outer shell to facilitate transport of the complexed metal ion across the phase boundary.

Nonactin is able to discriminate potassium ions over ammonium ions, which both have almost similar ionic radii ( $K^+ = 1.33$  Å and  $NH_4^+ = 1.43$  Å). In designing potassium ionophores for incorporation into ISEs, there are several factors to consider. The first is the size-fit requirement, as there should be a rigid framework, with a cavity appropriately sized 1.33 Å. A second consideration is the complexation geometry. Complexation is thermodynamically more favourable when the ionophore is conformationally preorganised into the correct binding geometry in order to



minimize the enthalpic cost of cation binding, so potassium ionophores should provide an octahedral binding site.<sup>65</sup>

Since it is important to be able to monitor potassium ion concentrations in human fluids, a novel concept has been described for a potassium ion biosensor that accurately, rapidly and efficiently monitors and records the presence and concentration of potassium ions with high specificity, not only in serum and urine, but also in sweat or even eye fluid. This specific biosensor design utilises a Nano manufacturing technique, i.e. Electrospinning, to produce advanced nano-bio-composites that specifically trace even minute quantities of potassium ions through the use of selective bio-receptors (ionophores) attached to high surface area nanofibers.<sup>66</sup> The ionophores for ISEs applications should be highly lipophilic to be compatible with the nonpolar membrane environment of ISEs, in addition to avoid the leaching of the ionophore from the membrane during testing. This is usually attained by attaching lipophilic groups, such as alkyl groups to the ionophore's structure. The application of the nonconducting polymers for alkali cations are illustrated in Table 1. 2.

**Table 1. 2: Characterisation of a number of reported ion selective sensors based on nonconducting polymers for alkali cations<sup>47</sup>**

| Cation          | Ionophore   | Slope (mV/decade) | Linear Range (M)                            | Most important interfering ions (log K> -2)  | Reference |
|-----------------|---|-------------------|---|--|-----------|
| Li <sup>+</sup> | Lipophilic crown-4 derivatives  | 58                | 10 <sup>-4</sup> -10 <sup>-1</sup>          | Na <sup>+</sup> , K <sup>+</sup> , NH <sub>4</sub> <sup>+</sup>                                      | 67        |
| Na <sup>+</sup> | 1-methy-1-vinyl-14-crown-5  | 55.0              | 3.16×10 <sup>-6</sup> -1.0×10 <sup>-1</sup> | K <sup>+</sup>   | 68        |
| K <sup>+</sup>  | Styrene/4(-vinyl-benzo-24-crown-8)copolymer   | 58                | 1.0×10 <sup>-6</sup> -1.0×10 <sup>-1</sup>  | -  | 69        |
| Rb <sup>+</sup> | Crown ethers incorporating anthraquinone, benzoquinone, and 1,4-dimethoxybenzene  | 54.7              | 1.0×10 <sup>-5</sup> -1.0×10 <sup>-1</sup>  | Na <sup>+</sup> , K <sup>+</sup> , Mg <sup>2+</sup> , NH <sub>4</sub> <sup>+</sup> , Li <sup>+</sup> | 70        |
| Cs <sup>+</sup> | Calix[4]arene derivative[25-(3-bromopropoxy)- 5,11, -17, 23-tetrakis(tert- butyl)-26, 27, 28- tris(1-propyloxy) calix[4] arene] | 58                | 1.0×10 <sup>-6</sup> -1.0×10 <sup>-1</sup>  | -  | 71        |

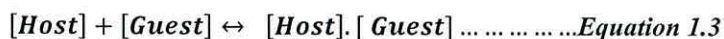


ISEs are also applied to ionic surfactants in solution, due to the change in dilute solution in activity or concentration of both the counter ions and ionic surfactants at the point of aggregation. The monomeric surfactant concentration can be determined by surfactant –ion selective electrodes (SISEs ) with practically no pre-treatment, even if the sample solutions were coloured or viscous. Ion-sensitive electrodes are usually used to consider the dimerisation, aggregation and micelle formation of ionic surfactants in aqueous solution. SISEs can provide information on the binding isotherms of the surfactant/surfactant, surfactant/polymer, and surfactant/ lipid vesicles systems, giving a performance advantage in monitoring the monomer concentration compared to other techniques.<sup>38</sup>

## 1.6 The ionophore

Supramolecular chemistry has been defined as the chemistry of molecular assemblies and of the intermolecular bond. The aim of supramolecular host design is the achievement of selectivity; in other words discrimination between one guest and others. In this research, potassium dihydrogen phosphate concentrations are the main focus due to their importance in various fields.

The main aim of this work is to design, characterise and synthesise ionophores for the complexation of potassium ions, based on the requirement for selective host-guest interactions. In order to develop the selectivity of ionophores, it is important to consider the thermodynamics of complexation. An ionophore is an ion carrier that can reversibly bind ions. Ionophore selectivity can be discussed in terms of the thermodynamic stability of the ion-ionophore complex, in which more stable complexes indicate more selectivity. The thermodynamic selectivity of a particular host for a specific cation characterizes the ratio between the host's affinities for a given cation over other guest cations. In this way, a successful selective host exhibits a strong affinity for one particular cation and a much lower affinity for others.



Therefore;

$$K = \frac{[Host].[Guest]}{[Host]+[Guest]} \dots \dots \dots \text{Equation 1.4}$$

The binding constants are thermodynamic parameters; therefore, they are related to the free energy of the association process according to the Gibbs equation:

$$\Delta G^\circ = -RT \ln K \dots \dots \dots \text{Equation 1.5}$$

The affinity of a host can be assessed by its binding constant (K), which represents the thermodynamic equilibrium constant for the binding process. Therefore, a large binding constant corresponds to a high equilibrium concentration of bound ion, hence a more stable ion-ligand complex. In energy terms, complexation of alkali cations with ionophores range from  $-20$  to  $-100 \text{ kJ mol}^{-1}$ . The difference in the free energy of each pair in the cation-ionophore complex referred to the ability of an ionophore to discriminate between different cations.

## 1.6 Ion selective potentiometric host

The concept of pre organisation is as the assembly of a host that matches both sterically and electronically the requirements of the guest before the guest is bound. Sterically, the host molecule must be able to fit physically around the guest molecule, without being too large or too small, while electronically, the host must present binding sites of opposite electrostatic charge or dipole moment to those of the guest, such as hydrogen bonding donors for hydrogen bonding acceptors.<sup>72</sup> Matching hosts and guests are described as complementary. A host must also have binding sites that have the electronic character to complement the guest, and those binding sites must be spread out on the host in such a way as to make enable them to interact with the guest in the binding conformation of the host molecule (lock and key concept). Host preorganisation is a key concept since it characterises a major difference in energy to the overall host-guest complexation energy.<sup>72</sup>

The complexation is energetically unfavourable without the solvation effect and the host must stay in this binding conformation throughout the lifetime of the host-guest complex. In the next stage, following the rearrangement, binding occurs that is energetically favourable due to the enthalpically stabilising attraction between



mutual complementary binding sites of the host and guest. The total free energy ( $\Delta G$ ) of complexation is the difference between the unfavourable reorganisation energy and favourable binding energy. The overall free energy of host-guest complexation will be condensed if the unfavourable reorganisation energy is large. On the other hand, if the host molecule is preorganised, the unfavourable reorganisation energy will be small, and the overall free energy of host-guest complexation maximised by the stability of the interaction.<sup>73</sup> In addition to the effects of solvation, the host or the ionophore must shed both its solvation shell and that of the guest in order to bind. In general, this process is favourable because the host-guest complexation is highly enthalpically suitable,<sup>74</sup> as seen in (Figure 1.4).

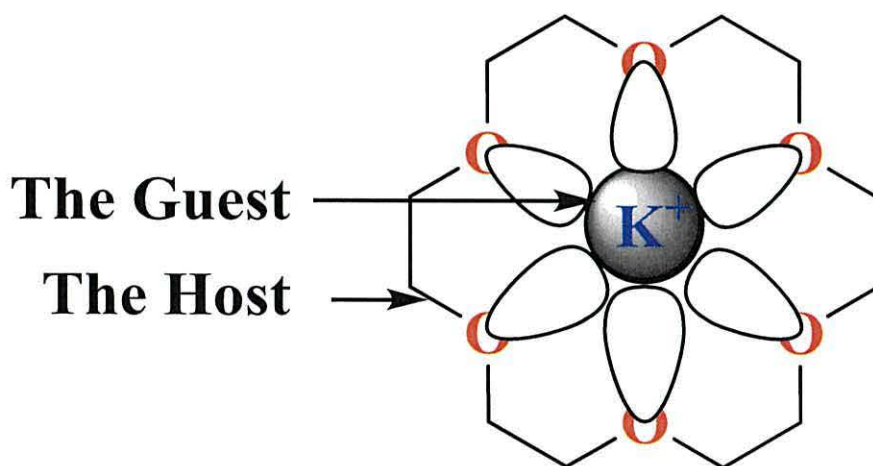


*Figure 1.4: The host–guest complexation for potassium ion in the crown cavity*

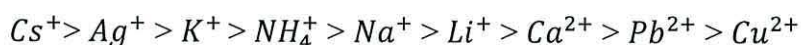
The ISE function involves the phase transfer of the aqueous ions into an organic medium of the ISE, which is typically the plasticized PVC, as will be discussed later. In fact, the transferred ions interact with the membrane components.<sup>75</sup> In the case of the ion transfer process from the aqueous phase into the polymeric membrane of the sensor, this will be controlled by the lipophilicity of the exchanged ions, such as a phase transfer equilibrium when the incorporated ionophore is a simple ion-exchanging species. The ion-exchanger should be highly soluble in the organic phase and insoluble in the solution under test. This state can be achieved by using substances with long hydrocarbon chains in their structure. These organic ion-exchangers bind small ions selectively either at charged sites of opposite sign or in



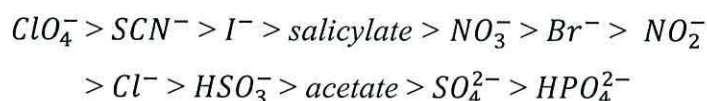
some cases at co-ordination sites. The sites must be capable of entering into a rapid mobile ion exchange equilibrium with the ions of interest.<sup>76</sup>

The selectivity performance of an ion-exchanger based ISE, where the ionophore does not have any chemical recognition abilities, certainly reflects the relative lipophilicities of the studied ions, which mean the higher ion lipophilicity results in a greater sensor response to the ion.<sup>77</sup> After a number of studies showed this with ion-exchanging ISEs and liquid-liquid extraction assays, a lipophilicity-dependent selectivity pattern was concluded. This pattern, however, is valid only when the response is a function of the ion lipophilicity.

For the cations, the corresponding pattern is:



In parallel, the respective pattern for the anions is as follows:



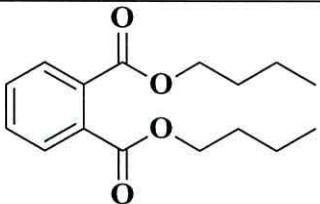
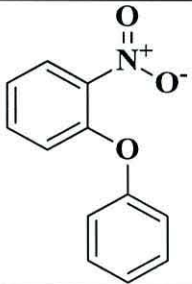
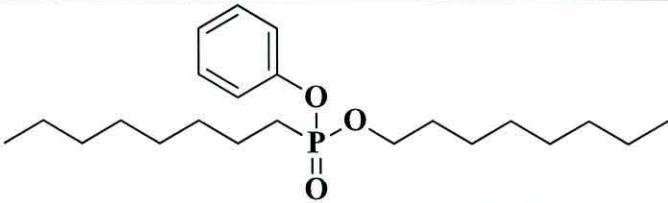
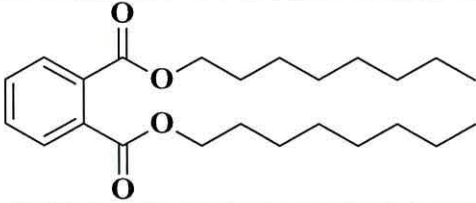
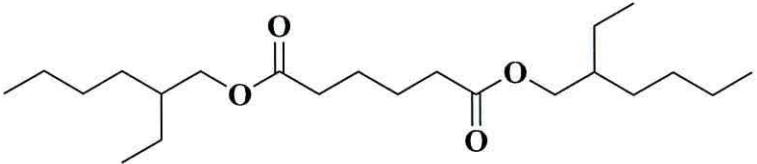
These patterns are known as the Hofmeister series.<sup>78</sup> On the other hand, the incorporation of a selectively binding ionophore into the ion-sensing membrane decreases the overall free energy for the transfer of the ionophore-bound ions to the organic phase, in contrast with that of the simply aqueous ions. When the ionophore binds to an ion strongly, its influence on the ion phase transfer equilibrium is higher.<sup>79</sup>

## 1.7 Plasticisers

Plasticisers increase the plasticity or fluidity of the material to which they are added. The membrane solvent has to be physically compatible with the polymer so as to give an organic phase.<sup>41</sup> Furthermore; it may affect the selectivity performance, since the selectivity's of the carrier-based ISEs are significantly influenced by the membrane solvent. The solvent used must be highly hydrophobic and in general have a low dielectric constant and a high molecular weight. It should have a low vapour pressure to avoid major evaporation and a sufficiently high viscosity that it does not

pass through the membrane pores quickly. Also, it must be completely inert to reaction with the electrode body. In addition, other considerations to be taken in to account include availability of the solvent in pure form, degree of dissolution of the particular active component used, and hydrophobizing properties. Several different plasticizers have been used in this study, as detailed in Table 1. 3.

*Table 1. 3: The plasticisers' structures used in this study*

| Plasticisers                | The structures   |
|-----------------------------|--|
| dibutyl phthalate ester     |    |
| 2- nitrophenyl phenyl ether |   |
| dioctyl phenyl phosphonate  |  |
| dioctyl phthalate           |  |
| bis(2-ethylhexyl) adipate   |  |

For the plasticizers used in the preparation of the polymeric membrane must be compatible with the polymer and electrode component, and furthermore need to be

disolved in tetrahydrofuran or cyclohexanone, the solvent used in the membrane preparation. Those plasticizers with high lipophilicity are preferred to incorporate the the ionophore in the membrane.<sup>80</sup>

The solvent polymeric membrane contains several constituents; a selective ionophore, a membrane solvent, an organic polymer (the most common is polyvinylchloride, PVC), and in some circumstances an ionic additive (lipophilic salt such as potassium tetrakis(4-chlorophenyl) borate or KTpCIPB). The ionophore is the selective ion carrier that reversibly binds ions and transports them across the hydrophobic membrane. Some of the common membrane solvents are dioctyl phthalate (DOP), dioctyl sebacate (DOS), or nitrophenyl octyl ether (NPOE), as shown in (Figure 1.5) which it have a high dielectric constant. In order to give a homogenous organic phase, the membrane solvent must be physically compatible with the polymer; otherwise it will be extracted, yielding an unstable membrane composition. The selectivity of the carrier-based ISEs is highly influenced by the membrane solvent, and is predictable due to the polarity of the plasticizer. For example, NPOE is a polar membrane solvent compared to DOS, and changes the plasticizer polarity from polar plasticizer NPOE to unpolar DOS or nitrophenyl octyl ether (NPOE).

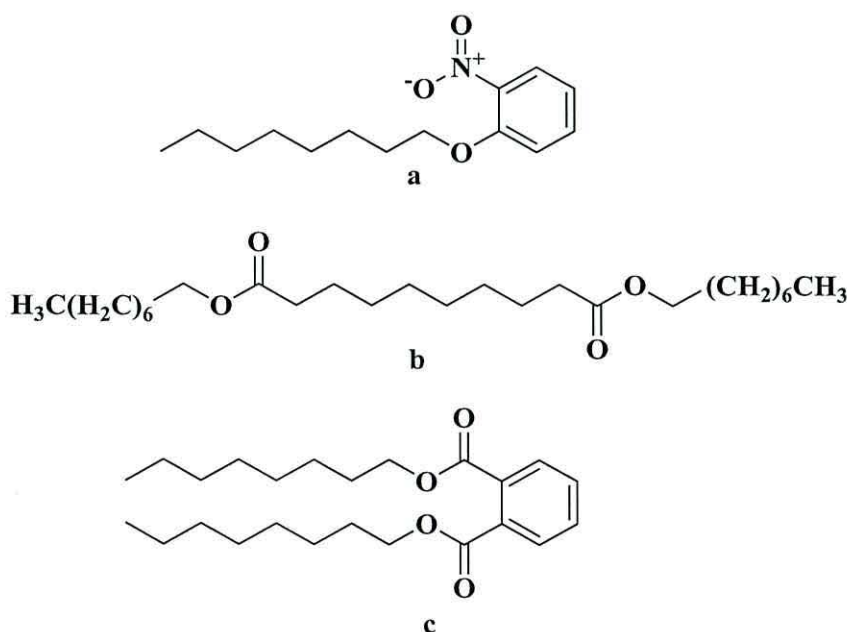


*Figure 1.5: Different structures of plasticisers a: nitrophenyl octyl ether, b: dioctyl sebacate, c: dioctyl phthalate ester*



NPOE and DOP are often used as plasticizers of potassium selective electrodes, since they have been described to yield good results. Measurements with ISEs are a form of potentiometry, where the ISE produces a potential that is proportional to the analyte concentration (an ion).<sup>81</sup> Nonetheless, the plasticizer selection is performed in line with its compatibility with the ionophore (solubility reasons), in addition to the final ISE application. The most common plasticizers employed in ISE fabrication and their names/abbreviations are given in Table 1. 4.

**Table 1. 4: The most used common plasticizers and their names/abbreviations are employed in the ISE fabrication**

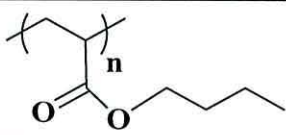
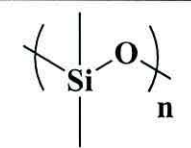
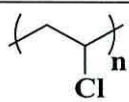
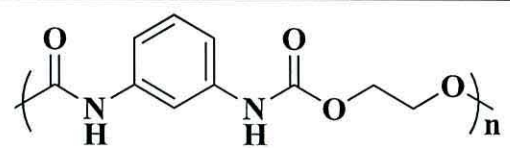
| Plasticizer's name                              | Plasticizer's abbreviations | References |
|---|-----------------------------|------------|
| bis(2-ethylhexyl) adipate                       | DOA                         | 82         |
| bis(2-ethylhexyl) sebacate                      | BEHS                        | 83         |
| dodecyl phthalate                               | DDP                         | 84         |
| 2-nitrophenyl phenyl ether                      | <i>o</i> -NPPE              | 85         |
| <i>o</i> -nitrophenyl octyl ether               | <i>o</i> -NPOE              | 86,41      |
| dibutyl sebacate                                | DBS                         | 87         |
| tri- <i>n</i> -butyl phosphate                  | TBP                         | 40         |
| bibenzyl ether                                  | DBE                         | 68         |
| bis(2-ethylhexyl) sebacate                      | DOS                         | 88,89      |
| bis-(1-butylpentyl) adipate                     | BBPA                        | 46,90      |
| bis(2-ethylhexyl) phthalate (dioctyl phthalate) | DOP                         | 83         |
| dibutyl phthalates                              | DBP                         | 91         |
| benzyl acetate                                  | BA                          | 92         |

The earliest examples of such polymeric membranes were prepared as ionophore solutions in an organic water immiscible solvent infused into some type of porous support, such as a porous glass filter. In 1970, polymeric membrane matrices were presented to improve the mechanical stability, and in particular, resistance to external pressure of such devices.<sup>93</sup> It is important that, in all these cases, the polymers do not form any type of channel or have any other three-dimensional architecture. Instead, the ideal polymer provides a rubberlike homogenous hydrophobic medium, ionophore complexes and ionic sites can move easily, as they can in a water-immiscible organic solvent. The sample-dependent phase boundary potential can only be found if the ions of interest can move easily back and forth between the aqueous sample and the membrane phase, so crystalline polymers and amorphous

polymers that form hard glasses at room temperature are not suitable as ISE membrane matrices.<sup>93</sup>

Different matrices, such as polyvinyl chloride (PVC) polyurethanes, acrylates, silicone rubbers, and perfluoropolymers are represented in Table 1. 5 have been used in electrochemical sensors, while (PVC) continues to be the most common matrix polymer for ISE membranes.<sup>94</sup>

*Table 1. 5: Different polymer matrixes used for assembling ISE*

| Polymer matrixes | The structures   |
|------------------|--|
| Polyacrylate     |    |
| Silicone rubber  |    |
| PVC              |   |
| Polyurethane     |  |

While PVC continues to be the most common matrix polymer for ISE membranes for providing the required physical properties,<sup>94</sup> in recent times, polymers have started to be used as homogeneous membrane matrices. For the preparation of a sensing membrane, a usual composition is as follows: 33% (w/w) PVC as the polymeric matrix, 66% plasticizer for the matrix homogenization, and 1% ionophore. In polymeric membranes using valinomycin as the neutral ion carrier in silicone rubber or PVC without the addition of lipophilic ionic sites, the polymer can provide the required physical properties (e.g. resistance and mechanical stability).



Many successful polymers are soft and rubberlike amorphous materials that only transform into a glassy state at below room temperature.<sup>90</sup> Others, such as polyvinyl chloride or Teflon AF, have a glass transition temperature that is high, but can be lowered to below room temperature by blending with plasticizers. It should be stressed that these ISEs exhibit a Nernstian response, due to the possible ionic impurity presence in the PVC used, as well as in the presence of the other membrane components. Moreover, membranes with no ionic sites have not been found to respond to the target ion concentration, as they combine almost totally pure membrane ingredients.<sup>90</sup>

The glass transition temperature ( $T_g$ ) of the polymer is the temperature required for an amorphous solid to become brittle on cooling, or soft on heating which is a sign of the suitability of the polymer to be involved in a sensing membrane. The ( $T_g$ ) value should therefore be below room temperature. Suitable polymers are liquids and fully miscible with the polymer, have much lower molecular weights than the polymer itself but have sufficiently low vapour pressures so that evaporation during the use of the ISE is not a concern. Plasticizers are not only components of many ISE membranes, but are also used in many polymeric consumer products.

The matrix formed by the polymer or the blend of polymer and plasticizer must dissolve all the components that provide the ISE membrane with selectivity, namely the free ionophore, the ionophore complex, and the ionic sites. In the case of an electrically neutral ionophore, this means that precipitation of not only the ionophore itself but also salts formed by the ionic sites and the ionophore complex must be avoided. In the laboratory, the formation of crystalline precipitates is often readily recognized with the naked eye. However, the result of the aggregation of membrane components can also result in small crystals or noncrystalline aggregates that may be easily overlooked, so the routine observation of ISE membranes containing new ionophores or ionic sites using optical microscopy is recommended.<sup>95</sup> If the designed membranes are fluid enough under the ambient conditions, they allow the diffusion of the membrane components, present reasonable ionic conductivities, and illustrate the proper mechanical properties to be utilised for routine processes. If the polymers are characterized by high  $T_g$  values (e.g. the  $T_g$  value of high molecular weight PVC is 80 °C), the use of plasticizers will be necessary. Conversely, if the polymers are



characterized by low  $T_g$  values, such as soft polyurethanes with a low content of crystalline units, silicone rubber, poly (vinylidene chloride) or poly siloxanes, the use of plasticizers is not needed.<sup>47</sup> Different polymer types have been examined for their application to membrane preparation. The popular one is PVC derivatives with 1.8% carboxylate groups. The respective sensing devices, based on several neutral carriers, have been seen to present similar characteristics to those of the PVC matrices. It is recommended to covalently attach all the membrane components, including the ionophore, to the polymer matrix. Both charged and also uncharged ionophores have been covalently bonded, seemingly with no essential loss in the electrode performance.<sup>90</sup>

### Total-equilibrium models

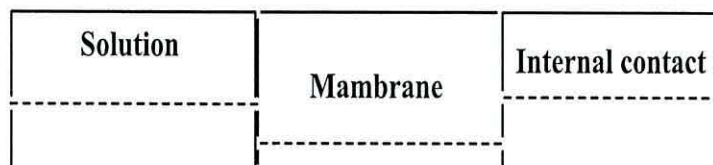
In all the classical models, the electric membrane potential ( $E_M$ ) of an ion sensor is represented by the sum of a boundary potential ( $E_{PB}$ ) at the sample/ion-sensitive membrane (film) boundary (PB) and by the diffusion potential inside the membrane or film ( $E_D$ ). The constant added includes the potential at the internal interfaces (internal contact).

$$E_M = E_{PB} + E_D + \text{constant} \dots \dots \dots \text{Equation 1.6}$$

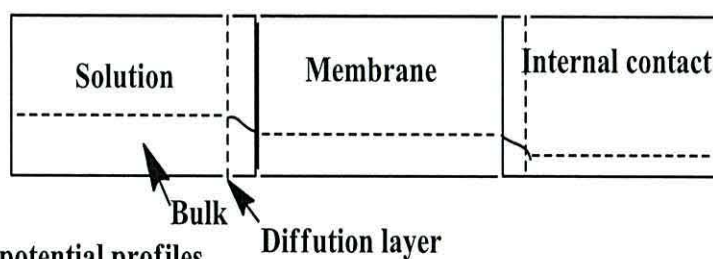
In the classical modelling of the response of ion sensors, two possibilities are considered-one recognizes diffusion potential, while the other disregards it.<sup>48</sup> These two approaches are presented in (Figure 1.6).

## A. Concentration profiles

Total equilibrium

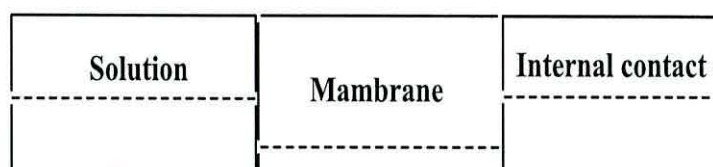


Advanced models



## B. Electrical potential profiles

Total equilibrium models



Advanced models

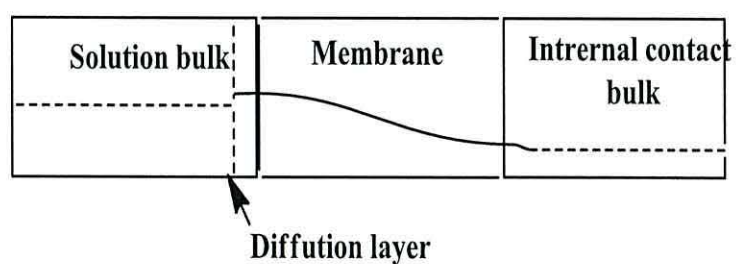


Figure 1.6: The diffusion potential inside the PVC membrane.<sup>48</sup>

### Phase-boundary-potential approach

The measured potential is typically referred to as electromotive force, EMF. At room temperature, a 10-fold increase in the activity of the ion  $i$  with the charge  $z_i$  results in an increase in the EMF of  $59.2 \text{ mV}/z_i$ , as predicted for  $25^\circ\text{C}$  by the Nernst detail below. The origin of this EMF response is directly related to the sample dependence of the electrical potential difference across the phase boundary between the sample phase and the hydrophobic ion-selective phase.

Phase boundary potentials are much more common than the non-electrochemist may suspect, and are quite easy to understand. The phase boundary potential at the interface between two phases that contain only one salt (the so-called distribution potential) does not depend on concentration of this salt, unless its concentration is so high that activity coefficients differ substantially from unity. On a qualitative level, from the view of thermodynamics, the concentration independence of the phase boundary potential in this particular case can be described quantitatively with a very general equation that describes the phase boundary potential, EPB, at equilibrium, i.e. energies of the ion  $i$  in the two phases. The derivation of this equation from electrochemical potentials is direct.<sup>96</sup>

Clearly, as long as the addition of more salt into the two-phase system raises the activities of the ion  $i$  in both phases by the same factor, the phase boundary potential, EPB, do not depend on the salt concentration.<sup>97</sup>

The phase-boundary potential model is based on two idealizing assumptions, as follows:

- (1) The phase-boundary potential at the sample/membrane interface (phase boundary)

$E_M = E_{PB}$ . Migration effects in the membrane are ignored, which means that the kinetic parameters of all the charged species involved (i.e. all ionic mobilities) are equal. Consequently, the diffusion potential is ignored, which formally means that  $E_D = 0$ . In other words, the electroneutrality in the membrane, except of the boundary, is assumed (*the electroneutrality assumption*). Otherwise, the diffusion potential is



assumed to be  $E_D \neq 0 = \text{const}$  (*the pseudo-electroneutrality assumption*) and, in this way, is ignored.

(2) Electrochemical equilibrium is assumed at the sample/membrane interface; therefore the difference in chemical potential for any ion able to cross the interface is balanced by a difference of the inner electrical potentials  $E_M$  ( $E_M$  is called the equilibrium potential). In the case of one or multiple salts distributing between two immiscible liquids,  $E^\circ_{PB, i}$  is different for every ion involved since this value depends on ionic solvation.

However, since there is only one physical phase boundary, there is also only one value for the phase boundary potential, EPB, between the two phases. In the example of the single salt distributing between the two phases, the same value of EPB is obtained to the cation as when it is applied to the anion, which can be understood upon realizing that the charges  $z_i$  of the two ions differ.

Furthermore, it is assumed that the electric potentials and the concentrations of ions in the phases in contact are independent of distance and time, which is known as the *total-equilibrium assumption*.<sup>98</sup>

## 1.8 Ion fluxes in potentiometry

Commonly, the sample and the inner solution do not have identical compositions. Because ions can diffuse across the organic membrane phase according to several mechanisms, this concentration asymmetry tempts a process toward a true equilibrium. This process is so slow that it can be ignored if the solution concentrations of the relevant species are higher than  $\sim 1 \mu\text{M}$ . However, if lower concentrations are involved, transmembrane ion fluxes may have a decisive influence on the response of ISEs. This model is very close to reality, even if the composition of the inner solution is different from that of the sample. The ion-exchange property of the hydrophobic membrane largely blocks the incorporation of the aqueous cation and its counter ion into the organic phase. Additionally, the high selectivity will hinder the exchange of the analyte ion with an interfering ion.<sup>99</sup>

## 1.9 The electrical double layer

The electrode/solution interface has critical importance when considering electron transfer reactions, and the processes which occur at the interface need to be understood. The electrode/solution behaves like a capacitor (Figure 1. 7), a component of an electrical circuit made from two metal sheets separated by a dielectric material, and which stores energy. Helmholtz developed a simple model which describes the electrode/solution interface as an electrical double layer. When a potential is applied to the electrode with respect to a reference electrode, a charge exists on the electrode,  $qm$ , For the interface as a whole to remain neutral, the solution must also have an equal but opposite charge,  $qs$ , at all times.<sup>99,100</sup>

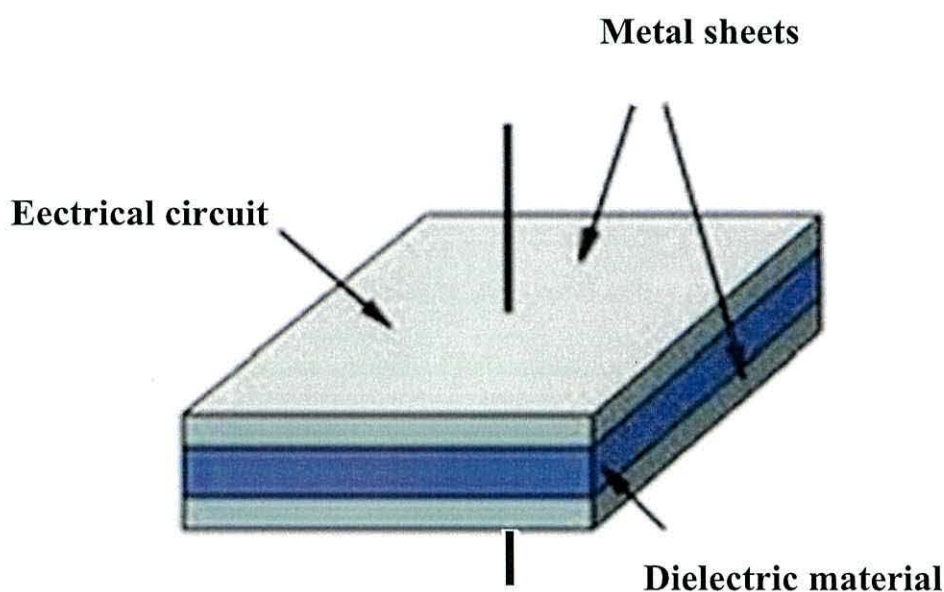


*Figure 1. 7: Metal sheets separated by a dielectric material for presenting a capacitor*

The charge in solution arises from the electrostatic rearrangement of electrolyte ions near to the surface of the electrode. It can also be caused by the reorientation of the dipole of solvent molecules. An excess of anions or cations is built up at the electrode surface, forming the electrical double layer. At the centre of these adsorbed species is the inner Helmholtz plane (IHP). While the line drawn through the centre of these solvated ions defines the outer Helmholtz plane (OHP), but these ions are non-specifically adsorbed to the electrode surface, as only long distance electrostatic

forces are involved and so the interaction is independent of the chemical properties of the ion.<sup>99,101</sup> (Figure 1.8) contains solvated ions which approach the electrode, but to a distance which is limited by the solvation shell of the ion.

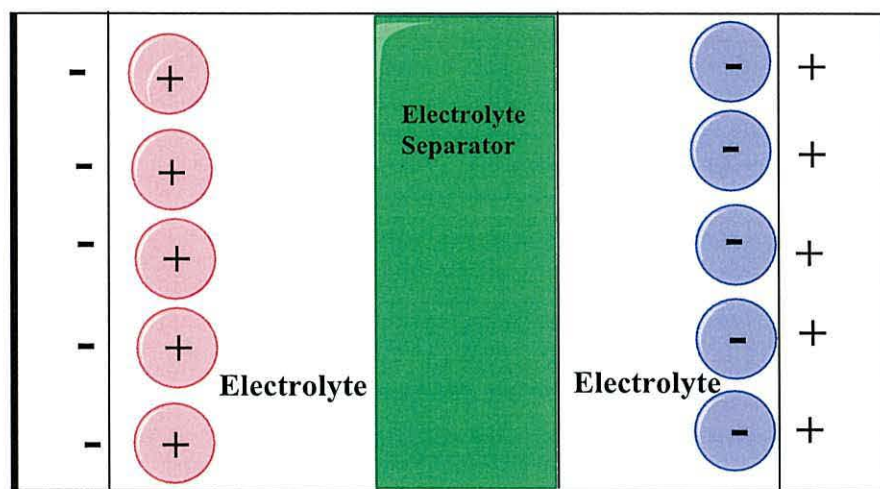


Figure 1.8: The electrical double layer of the Helmholtz plane. Redrawn from <sup>99</sup>

The area including the OHP and extending into the bulk solution is known as the diffuse layer, the thickness of which is dependent upon the concentration of ions in the solution, for example, the thickness is less than  $\sim 100 \text{ \AA}$  for concentrations greater than  $0.1 \text{ M}$ .<sup>99</sup>

### 1.10 The aim of the project

The need for fast, on-site monitoring methods allowing the analysis of a large number of samples has led to the investigation of ion-selective electrode (ISE) technology for potassium phosphate measurement.

This project consists of four parts. The aim of first part was to synthesise of a new opened cavity crown ether structure and the ten closed cavity ionophores and performance them as potentiometric sensors within a PVC membrane to refer to the role of the cavity in binding process with cation and the performance effect for them.



Those ionophores were 4-nitro benzo-15-crown-5 (1), 4-amino benzo-15-crown-5 (3), dinitro benzo-15-crown-5 (2), diamino benzo-15-crown-5 (4), 4-nitro benzo-18-crown-6 (5), 4-amino benzo-18-crown-6 (8), dinitro benzo-18-crown-6 (6), diamino benzo-18-crown-6 (9), dinitro dibenzo-18-crown-6 (7), diamino dibenzo-18-crown-6 (10). In addition to that another five ionophore have been applied within a PVC membrane which there were 1-aza-18-crown-6, benzo-15-crown-5, benzo-18-crown-6, dibenzo-18-crown-6, and dicyclohexyl-18-crown-6. The second part was the experimental data of the effect of a range of plasticisers for incorporating the ionophores into the membrane for optimum sensor design. Those plasticisers were dibutyl phthalate, 2- nitrophenyl phenyl ether, dioctyl phenyl phosphonate, dioctyl phthalate, and bis (2-ethylhexyl) adipate. The third part was to assess the practical applicability of the sensor in real samples. The target for this part was to determine of potassium ions in samples ranged from rivers running through farmland, to wells, tap water and potable water, finally waste water. The analysis was comparable with those obtained by the AAS analysis. The designed electrode will be important for the construction of a potentiometric device for the determination of potassium phosphate concentrations in solution.as well as in studying the PVC plasticised membrane properties for this kind of sensors.

### 1.11 Summary

Potassium is widely distributed in the earth's surface, seawater as a mono-valent cation. It occurs naturally in the form of several mineral salts not as metallic potassium which refers to ionic potassium. Potassium occurs in foods mainly associated with weak organic acids. Potassium is also found in mineral, spring, and potable waters. Another important nutrient is phosphorus which plays a main role in vital processes that are essential to the life of animals and plants. The main source of phosphorus in nature is the slow weathering of rocks and soils. Plants take-up phosphates through their roots and incorporate them into their cells and tissues. When plants are eaten, the phosphorus they contain passes to animals and returns phosphorus to the soil through microbial decomposition. In stable environments, the total quantity of phosphorus consequently stays rather constant as it cycles round the ecosystem.

In recent time high percentage of the artificial phosphates produced are applied to agricultural land as fertiliser to promote high yields of crops. The other part of phosphate chemicals is come from many sources, including detergent manufacture; Sewage is one important route by which phosphates may enter rivers, animal feeds and industrial processes. The comparatively low and stable levels of phosphorus cycling through river ecosystems have increased as a result of human activities.

Higher inputs of potassium together with other nutrients such as phosphate from human sources may stimulate plant growth in rivers and causes 'blooms' of algae or known as 'eutrophication' This process is the process of decomposition strips oxygen from the river water. There are encouraging signs that policies to reduce the problem of eutrophication are starting to have an effect. This strategy is required to bring about long-term improvements in the nutrient status of rivers. In addition to the removal of nutrients at sewage treatment works, this will focus on reducing inputs at source and better agricultural waste management.

The rising potassium and phosphate content of the reservoir water led the drinking-water collection company to request the monitoring system to conduct an extensive inquiry into the causes of this pollution which regulated by the EU through the Urban Waste Water Treatment Directive, (annual mean total phosphorus concentrations of 1–2 mg/l) and the Water Framework Directive that will enforce "good ecological and chemical status" by 2015. Conventional measuring methods are costly and time consuming, because they require complex processes for pre-treatment and expensive instruments for samples to be quantitatively analyzed. The high cost and long delays of such methods have limited. There is thus a clear need for a fast, portable and cost effective sensor for such detection, especially for use *in situ*.<sup>111</sup>

ISEs based on ionophore-impregnated polymer membranes are becoming ever more attractive for trace analysis; offering a wide variety of potential for an even wider variety of applications. Here we report a series of macrocyclic compounds with different substituents; which have been examined for their potential to detect potassium phosphate in the presence of other potassium counter ions.

Furthermore, the goal in this work is to develop new and selective ionophores that are capable of detecting ions in aqueous solution. Since ISEs offer one way to achieve this goal, new potassium ionophores were designed to be incorporated into these electrodes. For any ISE sensors, sensitivity to a specific ion in the required concentration range and selectivity for one specific ion are important considerations.

The ionophores for ISEs applications should be highly lipophilic, in order to be compatible with the nonpolar membrane environment of ISEs and to prevent the leaching of the ionophore from the membrane during testing. This is usually achieved by attaching groups, such as nitro or amino groups to the ionophore's structure.



### 1.12 References

- [1] J. P. Panizzon, V. R. M. Macedo, V. Machado, and L. M. Fiuza, **Microbiological and physical–chemical water quality of the rice fields in Sinos River’s basin, Southern Brazil**, *Environ. Monit. Assess.*, 2013, **185**, 2767-2775.
- [2] D. Kemp, C. J. Bond, D. M. Franks and C. Cote, **Mining, water and human rights: making the connection**, *J. Clean. Prod.*, 2010, **18**, 1553-1562.
- [3] A. Khudhair Hassan, B. Saad, S. Ab Ghani, R. Adnan, A. Abdul Rahim, N. Ahmad, M. Mokhtar, S. T. Ameen, and S. Mustafa Al-Araji, **Ionophore-based potentiometric sensors for the flow-Injection determination of promethazine hydrochloride in pharmaceutical formulations and human urine**, *Sensors*, 2011, **11**, 1028-1042.
- [4] S. Peper and C. Gonczy, **Potentiometric response characteristics of membrane-based  $\text{Cs}^+$ -selective electrodes containing ionophore-functionalized polymeric microspheres**, *Int. J. Chem.*, 2011, **2011**, 1-8.
- [5] A. Craggs, B. Doyle, S. Hassan, G.J. Moody, and J.D.R. Thomas, **PVC ion-selective electrodes based on calcium bis-[dialkyl- and di-(4-alkylphenyl) phosphates] and mixed solvent mediators**, *Talanta*, 1980, **27**, 277-280.
- [6] R. De Marco and C. Phan, **Determination of phosphate in hydroponic nutrient solutions using flow injection potentiometry and a cobalt-wire phosphate ion-selective electrode**, *Talanta*, 2003, **60**, 1215-1221.
- [7] I.A. Newman, **Ion transport in roots: measurment of fluxes using ion-selective microelectrodes to characterize transporter function**, *Plant. Cell. Environ.*, 2001, **24**, 1-14.
- [8] J. Izquierdo, L. Nagy, Á. Varga, I. Bitter, G. Nagy, and R. M. Souto, **Scanning electrochemical microscopy for the investigation of corrosion processes: Measurement of  $\text{Zn}^{2+}$  spatial distribution with ion selective microelectrodes**, *Electrochim. Acta*, 2012, **59**, 398-403.
- [9] A. Abbaspour, E. Mirahmadi, A. Khalafi and S. Babamohammadi, **A highly selective and sensitive disposable carbon composite PVC-based membrane for determination of lead ion in environmental samples**, *J. Hazard. Mater.*, 2010, **174**, 656-661.

- [10] A. Jang, Z. Zou, K. K. Lee, C. H Ahn, and P. L Bishop, **State-of-the-art lab chip sensors for environmental water monitoring**, *Meas. Sci. Technol.*, 2011, **22**, 1-18.
- [11] L. D. Mello and L. T. Kubota, **Review of the use of biosensors as analytical tools in the food and drink industries**, *Food Chem.*, 2002, **77**, 237-256.
- [12] A. Ceresa, E. Bakker, B. Hattendorf, D. Gunther, and E. Pretsch, **Potentiometric polymeric membrane electrodes for measurement of environmental samples at trace levels: New requirements for selectivities and measuring protocols, and comparison with ICPMS**, *Anal. Chem.*, 2001, **73(2)**, 343-351.
- [13] J. Ping, Y. Wang, Y. Ying, and J. Wu, **Application of electrochemically reduced graphene oxide on screen-printed ion-selective electrode**, *Anal. Chem.*, 2012, **84**, 3473-3479.
- [14] J. Steinlechner, S. Ast, C. Krüger, A. P. Singh, T. Eberle, V. Handchen, and R. Schnabel, **Absorption measurements of periodically poled potassium titanyl phosphate (PPKTP) at 775 nm and 1550 nm**, *Sensors*, 2013, **13**, 565-573.
- [15] J. Q. Ang, B. T. Nguyen, C. S. Toh, **A dual  $K^+$ - $Na^+$  selective Prussian blue nanotubes sensor**, *Sens. Actuators B*, 2011, **157**, 417-423.
- [16] N. Zine, J. Bausells, F. Vocanson, R. Lamartine, Z. Asfari, F. Teixidor, E. Crespo, I. A. M. de Oliveira, J. Samitier and A. Errachid, **Potassium-ion selective solid contact microelectrode based on a novel 1,3-(di-4-oxabutanol)-calix[4]arene-crown-5 neutral carrier**, *Electrochim. Acta*, 2006, **51**, 5075-5079.
- [17] P. C. Hauser, D. W. L. Chiang and G. A. Wright, **A potassium-ion selective electrode with valinomycin based poly(vinyl chloride) membrane and a poly(vinyl ferrocene) solid contact**, *Anal. Chim. Acta*, 1995, **302**, 241-248.
- [18] S. Kim, H. Kim, K. H. Noh, S. H. Lee, S. K. Kim and J. S. Kim, **Potassium ion-selective membrane electrodes based on 1,3-alternate calix[4]crown-5-azacrown-5**, *Talanta*, 2003, **61**, 709-716.
- [19] P. Thuérya, B. Mascib, M. Takimoto, and T. Yamato, **Supramolecular assemblages from uranyl complexes of calixarenes and potassium complexes of 18-crown-6 or dibenzo-18-crown-6**, *Inorg. Chem. Comm.*, 2007, **10 (7)**, 795-799.



- [20] Y. Kudo, J. Usami, S. Katsuta, and Y. Takeda, **On the difference between ion-pair formation constants of crown ether-complex ions with picrate ion in water determined by solvent extraction and by potentiometry**, *J. Mol. Liq.*, 2006, **123**, 29-37.
- [21] M. Ouchi and T. Hakushi, **Cation binding by thallium(I) selective crown ethers**, *Coord. Chem. Rev.*, 1996, **148**, 171-181.
- [22] C. Barral, I. Rodríguez, A. Regueiro, M. Esteban, D. Platas, C. Blas, and A. Rodríguez, **A merged experimental and theoretical conformational study on alkaline-earth complexes with lariat ethers derived from 4,13-diaza-18-crown-6**, *Inorg. Chim. Acta*, 2011, **370**, 270-278.
- [23] R. K. Mahajan, M. Kumar, V. Sharma, and I. Kaur, **Silver(I) ion-selective membrane based on Schiff base--butylcalix[4]arene**, *Analyst*, 2001, **126** (4), 505-507.
- [24] R. M. Z. Kakhki and G. Rounaghi, **Selective uranyl cation detection by polymeric ion selective electrode based on benzo-15-crown-5**, *Mater. Sci. Eng., C*, 2011, **31** (8), 1637-1642.
- [25] Y. Vlasov, Y. Ermolenko, and A. Legin, **Chemical sensors and their systems**, *J. Anal. Chem.*, 2010, **65**(9), 880-898.
- [26] F. Xiaoyu, L. Haitao, Z. Jie, L. Fanbo, Z. Lingli, Z. Youyu, and Y. Shouzhuo, **A novel label-free fluorescent sensor for the detection of potassium ion based on DNAzyme**, *Talanta*, 2012, **89**, 57-62.
- [27] S. Zhang, J. Xia and X. Li, **Electrochemical biosensor for detection of Adenosine based on structure-switching aptamer and amplification with reporter probe DNA modified Au nanoparticles**, *Anal. Chem.*, 2008, **80**, 8382-8388.
- [28] T. Hianik and J. Wang, **Electrochemical aptasensors ? Recent achievements and perspectives**, *Electroanalysis*, 2009, **21**, 1223-1235.
- [29] J. M. Pingarrón, P. Y. Sedefio, and A. G. Cortés, **Gold nanoparticle-based electrochemical biosensors**, *Electrochim. Acta*, 2008, **53** (19), 5848-5866.
- [30] Y. Liu, B. Li, D. Cheng, and X. Duan, **Simple and sensitive fluorescence sensor for detection of potassium ion in the presence of high concentration of sodium ion using berberine–G-quadruplex complex as sensing element**, *Microchem. J.*, 2011, **99** (2), 503-507.



- [31] B. M.A., **New trends in removing heavy metals from industrial wastewater**, *Arab.J. .Chem.*, 2011, **4**, 361-377.
- [32] T. Matsuo and M. Esashi, **Methods of ISFET fabrication**, *Sens. and Actuators*, 1981, **1**, 77-96.
- [33] D. Ammann, E. Pretsch, W. Simon, E. Lindner, A. Bezegh, E. Pungor, **Lipophilic salts as membrane additives and their influence on the properties of macro- and micro-electrodes based on neutral carriers**, *Anal. Chim. Acta*, 1985, **171**, 119-129.
- [34] J. Izquierdo, L. Nagy, Á. Varga, I. Bitter, G. Nagy, and R. M. Souto, **Scanning electrochemical microscopy for the investigation of corrosion processes: Measurement of  $Zn^{2+}$  spatial distribution with ion selective microelectrodes**, *Electrochim. Acta*, 2012, **59**, 398-403.
- [35] L. D. Mello and L. T. Kubota, **Review of the use of biosensors as analytical tools in the food and drink industries**, *Food Chem.*, 2002, **77**, 237-256.
- [36] E. Bakker and E. Pretsch, **Potentiometric sensors for trace-level analysis**, *Trends Anal. Chem.*, 2005, **24 (3)**, 199-207.
- [37] M. Ulrika, R. Sylwia, L. Andrzej, and B. Johan, **Impedance study of the ion-to-electron transduction process for carbon cloth as solid-contact material in potentiometric ion sensors**, *Electrochim. Acta*, 2011, **56 (28)**, 10683-10687.
- [38] L. Guobao, M. Hongmin, and H. Jingcheng, **Surfactant ion-selective electrodes: A promising approach to the study of the aggregation of ionic surfactants in solution**, *Soft Matter*, 2012, **8 (4)**, 896-909.
- [39] P. Ciosek and W. Wróblewski, **Potentiometric electronic tongues for foodstuff and biosample. Recognition—An Overview**, *Sensors*, 2011, **11**, 4688-4701.
- [40] A. Ramanavičiūsa, A. Ramanavičienė, A. Malinauskas, **Electrochemical sensors based on conducting polymer—polypyrrole**, *Electrochim. Acta*, 2006, **51 (27)**, 6025-6037.
- [41] J. A. Ortuño, C. Serna, A. Molina, E. Torralba, **Ion transfer square wave voltammetry of ionic liquid cations with a solvent polymeric membrane ion sensor**, *Electroanalysis*, 2009, **21 (21)**, 2297-2302.
- [42] E. Pretsch, **The new wave of ion-selective electrodes**, *Anal. Chem.*, 2002, **74 (15)**, 420-426.

- [43] A. L. Gui, E. Luais, J. R. Peterson, and J. J. Gooding, **Zwitterionic phenyl layers: Finally, stable, anti-biofouling coatings that do not passivate electrodes**, *Appl. Mater. Interfaces*, 2013, **5**, 4827-4835.
- [44] B. Juan, **Physical electrochemistry of nanostructured devices**, *Phys. Chem. Chem. Phys.*, 2008, **10** (1), 49-72.
- [45] J. Šimůnek, N. J. Jarvis, M.T. Genuchten, A. Gärdenäs, **Review and comparison of models for describing non-equilibrium and preferential flow and transport in the vadose zone**, *J. Hydrology.*, 2003, **272**, 14-35.
- [46] B. Johan, I. Ari, and L. Andrzej, **Potentiometric ion sensors based on conducting polymers**, *Electroanalysis*, 2003, **15** (5-6), 366-374.
- [47] F. Faridbod, M. R. Ganjali, R. Dinarvand and P. Norouzi, **Developments in the field of conducting and non-conducting polymer based potentiometric membrane sensors for ions over the past decade**, *Sensors*, 2008, **8**, 2331-2412.
- [48] J. Bobacka, A. Ivaska, and A. Lewenstam, **Potentiometric ion sensors**, *Chem. Rev.*, 2008, **108**, 329-351.
- [49] R. P. Buck and E. Linder, **Recommendations for nomenclature of ion-selective electrodes (IUPAC Recommendations 1994)**, *Pure. Appl. Chem.*, 1994, **66** (12), 2527-2536.
- [50] H. Cabezas, J. P. O'Connell, **Some uses and misuses of thermodynamic models for dilute liquid solutions**, *Ind. Eng. Chem. Res.*, 1993, **32**, 2892-2904.
- [51] C. J. Pedersen, **The discovery of crown ethers (Noble lecture)**, *Angew. Chem. Int. Ed. Engl.*, 1988, **27**, 1021-1027.
- [52] P. Buhlmann, E. Pretsch, and E. Bakker, **Carrier-based ion-selective electrodes and bulk optodes. 2. ionophores for potentiometric and optical sensors**, *Chem. Rev.*, 1998, **98**, 1593-1687.
- [53] C. J. Pedersen, **Cyclic polyethers and their complexes with metal salts**, *J. Am. Chem. Soc.*, 1967, **20** (26), 7017-7036.
- [54] A. Elbasyouny, H. J. Briigge, K. von Deuten, M. Dickel, A. Knochel, K. U. Koch, J. Kopf, D. Melzer, and G. Rudolph, **Host-guest complexes of 18-crown-6 with neutral molecules possessing the structure element XH<sub>2</sub> (X = oxygen, nitrogen, or carbon)**, *J. Am. Chem. Soc.*, 1983, **105**, 6568-6577.



- [55] J. M. Lehn, **Supramolecular chemistry: Concepts and perspectives**, *Cambridge; Willy*, 1995.
- [56] J. S. Bradshaw, R. M. Izatt, A. V. Bordunov, C. Y. Zhu, and J. K. Hathaway, **Comprehensive Supramolecular Chemistry**, *Elsevier*, 1996, **1**, 35-95.
- [57] B. S. Yu, L.H. Nie, and S. Z. Yao, **Ion chromatographic study of sodium, potassium and ammonium in human body fluids with bulk acoustic wave detection**, *J. Chromatogr., B*, 1997, **693** (1), 43-49.
- [58] T. J. Schaefer, R. W. Wolford, **Disorders of potassium**, *Emerg. Med. Clin. N. Am.*, 2005, **23**, 723-747.
- [59] M. F.S. Teixeiraa, B. H. Freitas, P. M. Seraphimb, L. O. Salmazoa, M. A. Nobrea, and S. Lanfredi, **Development of an electrochemical sensor for potassium ions based on  $\text{KSr}_2\text{Nb}_5\text{O}_{15}$  modified electrode**, *Proced. Chem.*, 2009, **1** (1), 293-296.
- [60] A. J. Michalska, C. Appaih, L. Yook Heng, S. Walkiewicz, and E. A. H. Hall, **An experimental study of membrane materials and inner contacting layers for ion-selective  $\text{K}^+$  electrodes with a stable response and good dynamic range**, *Anal. Chem.*, 2004, **76**, 2031-2039.
- [61] C. Hongxia, G. Yeong, K. Sung, C. Heung, O. Cheol, L. Jaebeom, K. Kwangnak, **Potassium ion sensing using a self-assembled calix[4]crown monolayer by surface plasmon resonance**, *Sens. Actuators B: Chem.*, 2008, **133**, 577-581.
- [62] A. Jesus, M. M. Silva, and M. G. R. Vale, **The use of microemulsion for determination of sodium and potassium in biodiesel by flame atomic absorption spectrometry**, *Talanta*, 2008, **74**, 1378-1384.
- [63] M. S. Islam and M. Tanaka, **Impacts of pollution on coastal and marine ecosystems including coastal and marine fisheries and approach for management: a review and synthesis**, *Mar. Pollut. Bull.*, 2004, **48** (7-8), 624-649.
- [64] P. Thuéry, B. Masci, M. Takimoto and T. Yamato, **Supramolecular assemblages from uranyl complexes of calixarenes and potassium complexes of 18-crown-6 or dibenzo-18-crown-6**, *Inorg. Chem. Comm.*, 2007, **10**, 795-799.



- [65] D. M. Pranitis and M. E. Meyerhoff, **Continuous monitoring of ambient ammonia with a membrane-electrode-based detector**, *Anal. Chem.*, 1987, **59** (19), 2345-2350.
- [66] R. Xue and P.I. Gouma, **Novel nanocomposite-based potassium ion biosensor**, *AIP Conf. Proc.*, 2009, **1137**, 279-280.
- [67] W. S. Han, M. Y. Park, K. C. Chung, D. H. Cho, and Tae. K. Hong, **All solid state hydrogen ion selective electrode based on a tribenzylamine neutral carrier in a poly(vinyl chloride) membrane with a poly(aniline) solid contact**, *Electroanalysis*, 2001, **13** (11), 955-959.
- [68] L. H. C. Sudeshna, **A new sodium ion selective electrode based on a novel silacrown ether**, *Sens. Actuators B: Chem.*, 2006, **114**, 849-854.
- [69] M. R. Ganjali, A. Moghimi, and G. W. Buchanan, **The synthesis of styrene/4'-vinylbenzo-24-crown-8 copolymer and its use in potassium-ion selective electrodes**, *J. Includ. Phenom. Mol. Rec. Chem.*, 1998, **30**, 29-43.
- [70] Z. Xia, I. H. A. Badr, S. L. Plummer, L. Cullen, and L.G. Bachas, **Synthesis and evaluation of a bis(crown ether) ionophore with a conformationally constrained bridge in ion-selective electrodes**, *Anal. Sci.*, 1998, **14**, 169-173.
- [71] M. A. Barmchia, M. F. Mousavib, M. A. Zanjanchic, M. Shamsipurd, and S. Taghvaeie, **Cesium- selective poly (vinyl chloride) membrane electrode based on a new calix [4] arene derivative in the 1,3- alternate conformation**, *Anal. Lett.*, 2002, **35** (5), 767-783.
- [72] M. H. Filby, J. W. Steed, **A modular approach to organic, coordination complex and polymer based podand hosts for anions**, *Coord. Chem. Rev.*, 2006, **250** (23-24), 3200-3218.
- [73] S. L. Tobey and E. V. Anslyn, **Studies into the thermodynamic origin of negative cooperativity in ion-pairing molecular recognition**, *J. Am. Chem. Soc.*, 2003, **125** (36), 10963-10970.
- [74] D. B. Smithrud and F. Diederich, **Strength of molecular complexation of apolar solutes in water and in organic solvents is predictable by linear free energy relationships: a general model for solvation effects on apolar binding**, *J. Am. Chem. Soc.*, 1990, **112** (10), 339-343.

- [75] J. R. L. Guerreiro, V. Freitas, and M. G. F. Sales, **New sensing materials of molecularly-imprinted polymers for the selective recognition of Chlortetracycline**, *Microchem. J.*, 2011, **97 (2)**, 173-181.
- [76] T. Jaskari, M. Vuorio, K. Kontturi, J. A. Manzanares, and J. Hirvonen, **Ion-exchange fibers and drugs: An equilibrium study**, *J. Controlled Release*, 2001, 219-229.
- [77] M. Telting-Diaz and E. Bakker, **Effect of lipophilic ion-exchanger leaching on the detection limit of carrier-based ion-selective electrodes**, *Anal. Chem.*, 2001, **73**, 5582-5589.
- [78] K. Wojciechowska, M. Kuchareka, W. Wróblewska, and P. Warszyński, **On the origin of the Hofmeister effect in anion-selective potentiometric electrodes with tetraalkylammonium salts**, *J. Electroanal. Chem.*, 2010, **638 (2)**, 204-211.
- [79] F. Faridbod, M. R. Ganjali, R. Dinarvand, P. Norouzi, and S. Riahi, **Review, schiff's bases and crown ethers as supramolecular sensing materials in the construction of potentiometric membrane sensors**, *Sensors*, 2008, **8**, 1645-1703.
- [80] L. D. Nghiema, P. Mornanea, I. D. Potter, J. M. Perera, R. W. Cattrall, and S. D. Kolev, **Extraction and transport of metal ions and small organic compounds using polymer inclusion membranes (PIMs)**, *J. Membr. Sci.*, 2006, **281 (1-2)**, 7-41.
- [81] C. Mihali and N. Vaum, **Use of plasticizers for electrochemical sensors**, *InTech.*, 2012, 125-140.
- [82] A. Rzewuska, M. Wojciechowski, E. Bulska, E. Hall, K. Maksymiuk, and A. Michalska, **Composite polyacrylate–poly(3,4- ethylenedioxythiophene) membranes for improved all-solid-state ion-selective sensors**, *Anal. Chem.*, 2008, **80**, 321-327.
- [83] J. Bobacka, **Conducting polymer-based solid-state ion-selective electrodes**, *Trends Anal. Chem.*, 2006, **18 (1)**, 7-18.
- [84] J. Bobacka, **Potential stability of all-solid-state ion-selective electrodes using conducting polymers as ion-to-electron transducers**, *Anal. Chem.*, 1999, **71 (21)**, 4932-4937.



- [85] M. Rahman, P. Kumar, D. Park and Y. Shim, **Review, Electrochemical sensors based on organic conjugated polymers**, *Sensors*, 2008, **8**, 118-141.
- [86] M. R. Ganjali, M. Emami, M. S. Niasari, and M. Yousefi, **Determination of trace amounts of Cr(III) in presence of Cr(VI) by a novel potentiometric membrane sensor based on a new tridentate S,N,O schiff's base**, *Anal. Lett.*, 2003, **36 (13)**, 2735-2747.
- [87] M. Fibbioli, K. Bandyopadhyay, S. G. Liu, L. Echegoyen, O. Enger, F. Diederich, D. Gingery, P. Bühlmann, H. Persson, U. W. Suter, and E. Pretsch, **Redox-active self-assembled monolayers for solid-contact polymeric membrane ion-selective electrodes**, *Chem. Mater.*, 2002, **14 (4)**, 1721-1729.
- [88] T. Lindfors, and A. Ivaska, **Stability of the inner polyaniline solid contact layer in all-solid-state K<sup>+</sup>-selective electrodes based on plasticized poly(vinyl chloride)**, *Anal. Chem.*, 2004, **76 (15)**, 4387-4394.
- [89] L. Tom, S. Fredrik, H. Lajos, G. Róbert, **FTIR-ATR study of water uptake and diffusion through ion-selective membranes based on plasticized poly(vinyl chloride)**, *Electroanalysis*, 2009, **21 (17-18)**, 1914-1922.
- [90] F. Faridbod, M. R. Ganjali, R. Dinarvand, and P. Norouzi, **The fabrication of potentiometric membrane sensors and their applications**, *African. J. Biotech.*, 2007, **6 (25)**, 2960-2987.
- [91] H. Z. Langroodi, and S. Meghdadi, **Application of N-quinoline-2-carboxamido-8-aminoquinoline in fabrication of a Ho(III)-PVC membrane sensor**, *J. Chem.*, 2011, **8(S1)**, 237-244.
- [92] A. K. Singh, S. Mehtab, and A. K. Jain, **Selective electrochemical sensor for copper (II) ion based on chelating ionophores**, *Anal. Chim. Acta*, 2006, **575 (1)**, 25-31.
- [93] G. J. Moody, R. B. Oke and J. D. R. Thomas, **A calcium-sensitive electrode based on a liquid ion exchanger in a poly(vinyl chloride) matrix**, *Analyst*, 1970, **95 (1136)**, 910-918.
- [94] A. Rouhollahia, M. R. Ganjaliala, M. Shamsipur, **Lead ion selective PVC membrane electrode based on 5,5'-dithiobis-(2-nitrobenzoic acid)**, *Talanta*, 1998, **46 (6)**, 1341-1346.



- [95] K. N. Phillips, C. Lantz, P. Bühlmann, **Visible and FTIR microscopic observation of bithiourea ionophore aggregates in ion-selective electrode membranes**, *Electroanalysis*, 2005, **17 (22)**, 2019-2025.
- [96] E. Bakker, P. Bühlmann, E. Pretsch, **The phase-boundary potential model**, *Talanta*, 2004, **63(1)**, 3-20.
- [97] M. G. Afshar, G. A. Crespo, and E. Bakker, **Direct ion speciation analysis with ion-selective membranes operated in a sequential potentiometric/time resolved chronopotentiometric sensing mode**, *Anal. Chem.*, 2012, **84**, 8813-8821.
- [98] B. Juan, **Physical electrochemistry of nanostructured devices**, *Phys. Chem. Chem. Phys.*, 2008, **10 (1)**, 49-72.
- [99] E. Bakker and E. Pretsch, **The new wave of ion-selective electrodes**, *Anal. Chem.*, 2002, **1 (15)**, 420-426.
- [100] E. Lust, R. Truu, and K. Lust, **Electroreduction of peroxodisulfate anion at Bi(III) single-crystal plane electrode**, *Russ. J. Electrochem.*, 2000, **36 (11)**, 1195-1202.
- [101] Stephen W. Feldberg, **Implications of extended heterogeneous electron transfer. Part 1. Coupling of semi-infinite linear diffusion and heterogeneous electron transfer with a decaying exponential dependence upon distance from the outer Helmholtz plane**, *J. Electroanal. Chem.*, 1986, **198**, 1-18.
- [111] C. Warwick, A. Guerreiro, and A. Soares, **Sensing and analysis of soluble phosphates in environmental samples: A review**, *Biosens. Bioelectron.*, 2013, **41**, 1-11.

## **Chapter 2 – Materials and methods**

## 2.1 General reagents and materials

Chemicals used were obtained from commercial suppliers or prepared from them by the methods described. Solvents which were required to be dry, e.g. ether, tetrahydrofuran, and toluene were dried over sodium wire and benzophenone under nitrogen, while dichloromethane was dried over calcium hydride. Petroleum ether used was of boiling point 40-60 °C. Reactions carried out under inert conditions were under a slow stream of nitrogen. Those carried out at low temperatures were cooled using a bath of methylated spirits and liquid nitrogen.

All reagents and solvents used were of reagent grade unless otherwise stated. Silica gel (Merck 7736) and silica gel plates used for column chromatography and thin layer chromatography were obtained from Aldrich; separated components were detected using variously UV light, I<sub>2</sub> and phosphomolybdic acid solution in IMS followed by charring. Anhydrous magnesium sulphate was used to dry organic solutions.

For electrochemical applications, all reagents and solvents for synthesis were purchased from Aldrich, and were of analytical grade unless otherwise noted. Low molecular weight poly vinyl chloride (PVC), dibutyl phthalate (DBP), dioctyl phthalate (DOP), and Bis(2-ethyl hexyl) adipate from Aldrich, 2-Nitro phenyl phenyl ether (NPPE) from Fluka. All the interfering ions were purchased from Alfa Aesar and all the ionophores structures are benzo-18-crown-6, 1- Aza-18-crown 6, benzo-15-crown-5, di benzo-18-crown-6, dicyclo hexyl-18-crown-6 and potassium salts of all anions and dioctyl phenyl phosphonate (DOPP) were purchased from Sigma-Aldrich. Electrolyte solutions were freshly prepared using high-purity Millipore deionized water (18 M $\Omega$ .cm).



## 2.2 General instruments and methods

All potentiometric measurements were made at room temperature using a portable pH and pH / ISE Meter model 290 A plus A Metrohm double junction Ag/AgCl reference electrode model 80 × 8 mm/ 4 mm containing saturated potassium chloride in the outer compartment was used in conjunction with the proposed electrode. A combined pH electrode model Thermo Orion, Low Maintenance pH Triode, 9107BN was used for all pH measurements.

NMR spectra were carried out on an Advance Bruker 400 spectrometer; for both  $^1\text{H}$  spectra the machine and  $^{13}\text{C}$  spectra was ran at 500 MHz in  $\text{CDCl}_3$  or DMSO solutions. Chemical shifts for  $^1\text{H}$  /  $^{13}\text{C}$  are quoted in  $\delta$  relative to chloroform ( $\delta$  7.27 ppm), and  $\text{CDCl}_3$  ( $\delta$  77.16 ppm). Mass spectra were recorded on a Bruker Microtof. MALDI mass spectrometry values are given plus sodium, potassium or hydrogen to an accuracy of 2 d.p., Melting point data was obtained using a Mel-Temp capillary melting point apparatus.

In this study, infrared (IR) spectra were obtained carried out on Bruker FT-IR spectrometer at  $4\text{ cm}^{-1}$  resolution, from  $(4000\text{ to }500)\text{ cm}^{-1}$ . A neat KBr disc was used as a blank sample before the data acquisition of each spectrum.

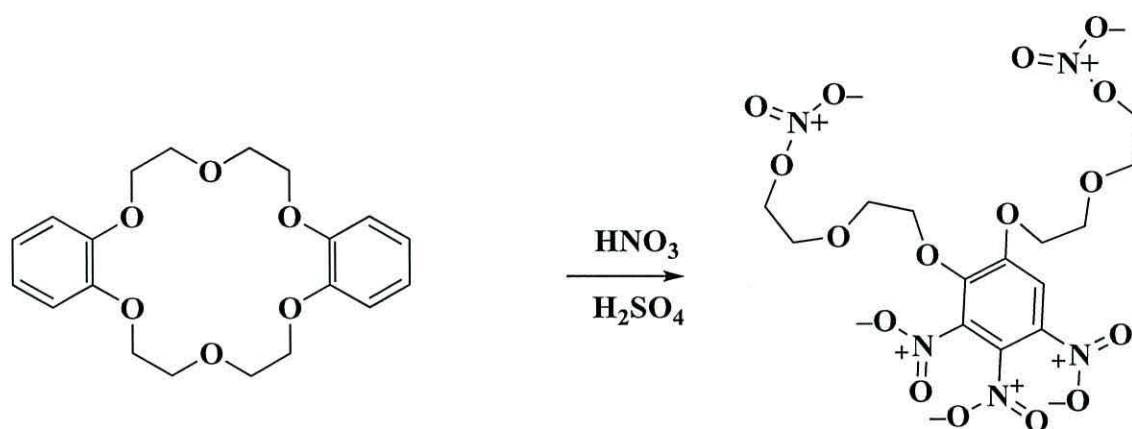
Analyses of the collected water samples were conducted *via* atomic absorption spectrometry (Varian 220F3). The membranes morphologies were characterised by using a scanning electron microscope (SEM) (Hitachi S-520) and energy dispersive analyser X ray (EDAX) (Oxford Instruments 7497 EDX with Link ISIS computer software).

X-ray crystallography was performed with the use of synchrotron X-rays at Diamond Light Source UK, beamline I19 ( $\lambda = 0.6889\text{ \AA}$ ) on a Crystal Logic diffractometer and Rigaku Saturn 724 detector equipped with an Oxford Cryosystems Cryostream device. Data were processed using the Rigaku CrystalClear package and Bruker APEX2 software.<sup>1</sup>

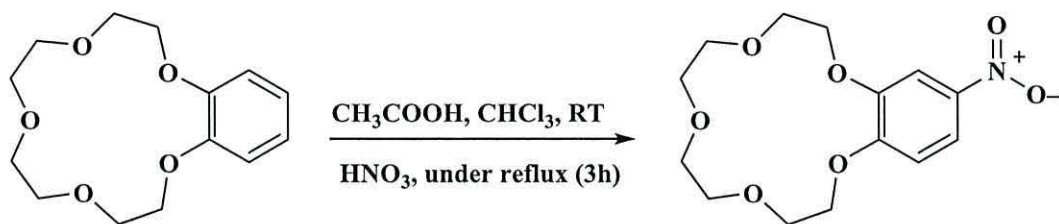
For conventional service crystallography the beam line operates at a typical energy of 18 keV (Zr K absorption edge) and a Rigaku ACTOR robotic sample changing

system is available. Single-crystal X-ray diffraction data were collected and solved at the National Crystallography Service at Southampton University at 100 K on Rigaku AFC12 goniometer equipped with an enhanced sensitivity (HG) Saturn 724+ detector mounted at the window of an FR-E+ Superbright MoK $\alpha$  rotating anode generator with HF Varimax optics,<sup>2</sup> and unit cell parameters were refined against all data. An empirical absorption correction was carried out using SADABS.<sup>3</sup>

**Synthesis of (((3,4,5-trinitro-1,2-phenylene)bis(oxy))bis(ethane-2,1-diyl))bis(oxy))bis(ethane-2,1-diyl) dinitrate**

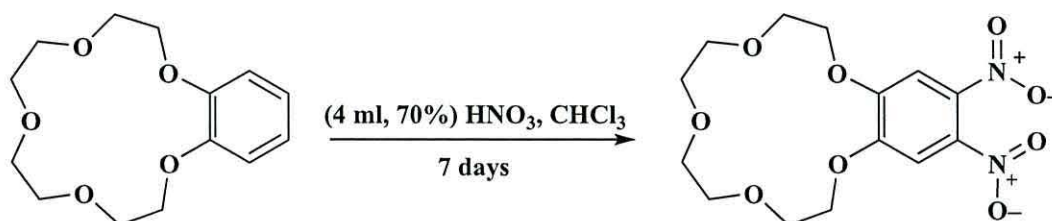


Nitric acid (1 ml) was added via syringe over 10-15 min to a stirred solution of dibenzo-18-crown-6 (100 mg, 0.27 mmol) and sulphuric acid (1 ml) at room temperature. The mixture was stirred overnight. TLC showed no starting material was left. The mixture was poured on ice water (50 ml) and then extracted with ethyl acetate ( $2 \times 30$  ml) and dried over magnesium sulphate and solvent was removed under reduced pressure. The precipitated product was washed with water ( $3 \times 50$  ml) and purified by column chromatography eluting with petrol / ethyl acetate (1:1) to give a pale yellow solid (0.112 mg, 80%).  $^1\text{H}$  NMR (400 MHz,  $\text{CDCl}_3$ ):  $\delta$  7.73 (s, 1H), 4.65 – 4.60 (m, 2H), 4.59 – 4.51 (m, 4H), 4.42 – 4.35 (m, 2H), 3.97 – 3.91 (m, 2H), 3.85 – 3.81 (m, 2H), 3.79 – 3.75 (m, 2H), 3.74 – 3.69 (m, 2H);  $^{13}\text{C}$  NMR (101 MHz,  $\text{CDCl}_3$ ):  $\delta$  154.06, 145.24, 138.84, 136.63, 110.60, 74.41, 71.91, 71.77, 70.27, 69.97, 69.01, 67.40, 67.24. MALDI-TOF mass found,  $m/z$  534.06.

**Synthesis of 4-nitro benzo-15-crown-5 (1)**

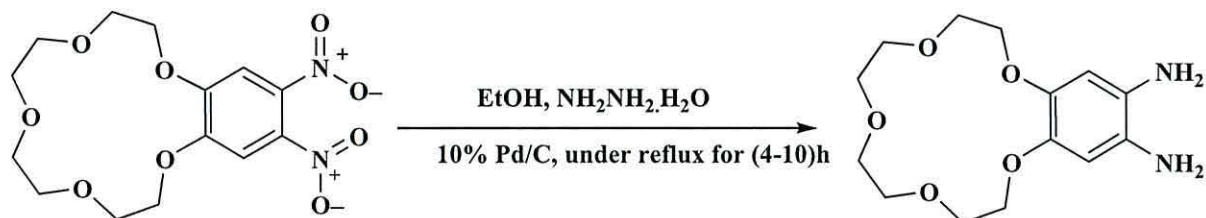
The synthesis for 4-nitro benzo-15-crown-5 was carried out as previous published by the following alterations.<sup>4, 5</sup> Benzo-15-crown-5 (100 mg, 0.37 mmol) was dissolved in acetic acid (1 ml) at room temperature then cooled down with ice for -5 °C. At that temperature HNO<sub>3</sub> (1 ml) was added to the solution over 30 min; the solution was stirred at -5 °C for an hour and at room temperature for 48 hrs. TLC showed no starting material was left. The mixture was poured on ice water then extracted with ethyl acetate (2 × 30 ml). The organic layer was washed with water (3 × 30 ml), and finally dried over anhydrous MgSO<sub>4</sub>. The solvent was removed under reduced pressure. The crude product was purified by column chromatography eluting with petrol /ethyl acetate (1:1). The compound 4-nitro benzo-15-crown-5 was isolated as a pale yellow solid. Recrystallization from methanol gave pale yellow needle crystals (100 mg, 85%, mp 90-92 °C, lit.<sup>6,7</sup> mp 91-94 °C) which showed FTIR (neat) ; 1588 (NO<sub>2</sub>); 1137 (C-O)  $\nu_{\text{max}}/\text{cm}^{-1}$ ; <sup>1</sup>H NMR (400 MHz, CDCl<sub>3</sub>):  $\delta$  7.92 (dd, *J* = 8.9, 2.6 Hz, 1H), 7.74 (d, *J* = 2.6 Hz, 1H), 6.89 (d, *J* = 8.9 Hz, 1H), 4.27 – 4.21 (m, 4H), 4.00 – 3.95 (m, 4H), 3.82 – 3.74 (m, 8H). (s, 4H); <sup>13</sup>C NMR (101 MHz, CDCl<sub>3</sub>):  $\delta$  154.09, 148.24, 141.59, 118.24, 111.27, 108.12, 77.16, 70.55, 70.54, 69.85, 69.79, 68.83, 68.76, 68.57, 68.42. MALDI-TOF mass found, *m/z* 336.117.



**Synthesis of dinitro benzo-15-crown-5 (2)**

Solid benzo-15-crown-5 (200 mg, 0.47 mmol) was added slowly over thirty minutes to concentrated nitric acid (4 mL, 70%) with stirring.<sup>8</sup> After finishing the addition of the acid,  $\text{CHCl}_3$  (3 mL) was added to the yellow solution and the two layers were stirred for seven days. After this time the acid was diluted with an equal volume of distilled water. The product was extracted with chloroform ( $3 \times 15$  mL). The organic layer was evaporated to dryness leaving a yellow waxy residue. The crude product was purified by column chromatography eluting with petrol /ethyl acetate (2:1). The compound dinitro benzo-15-crown-5 was isolated as a pale yellow semi solid. Recrystallization from methanol gave a yellow needle crystal (220 mg 82% mp 158-161 °C, lit.<sup>6</sup> mp 168 °C),<sup>6</sup> FTIR (neat); 1586 ( $\text{NO}_2$ ); 1136 (C-O)  $\nu_{\text{max}}/\text{cm}^{-1}$ ;  $^1\text{H}$  NMR (400 MHz,  $\text{CDCl}_3$ ):  $\delta$  7.31 (s, 2H), 4.28 – 4.22 (m, 4H), 3.97 – 3.91 (m, 4H), 3.79 – 3.69 (m, 8H);  $^{13}\text{C}$  NMR (101 MHz,  $\text{CDCl}_3$ ):  $\delta$  151.98, 136.84, 108.55, 71.23, 70.23, 69.74, 68.76. MALDI-TOF mass found,  $m/z$  381.097.

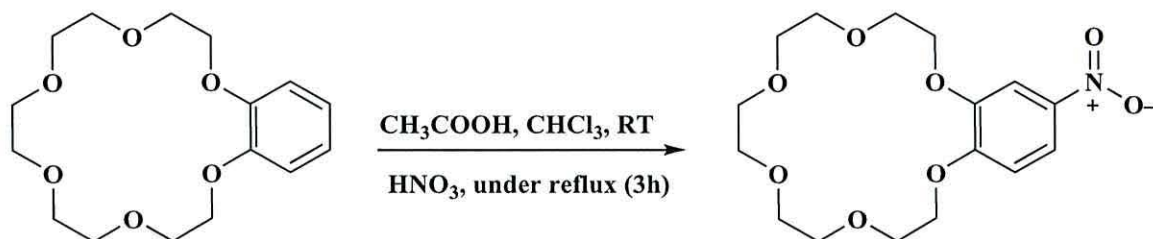


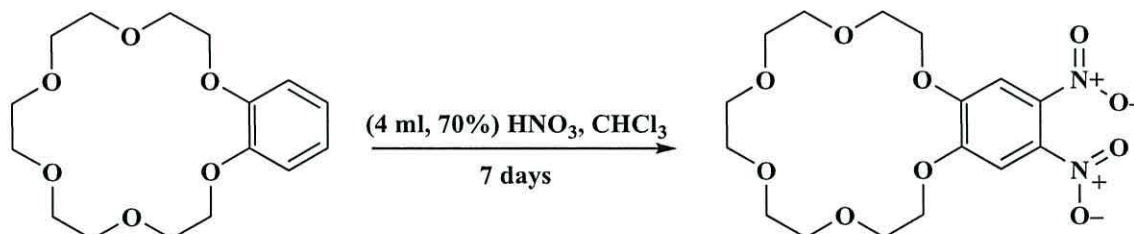
**Synthesis of diamino benzo-15-crown-5 (4)**

Dinitro benzo-15-crown-5 (50 mg, 0.13 mmol) was dissolved in ethanol (40 ml) under nitrogen atmosphere. The mixture was heated to reach 40 °C. At that temperature the Pd/C (10%) catalyst (13 mg) was added. The mixture then refluxed at 105 °C.<sup>5</sup> To that mixture a solution of ethanol (20 ml) and hydrazine hydrate (0.44 ml, 8.9 mmol) was added over thirty minutes. The reaction mixture was refluxed for 3-8 hrs. until the starting nitro compound was completely consumed (TLC monitoring), and the catalyst was filtered off from celite plug bed. The filtrate was concentrated in vacuum, water was added to the residue, and the mixture was extracted with chloroform. The extracts were concentrated under vacuum. The pure product was collected from dichloromethane as a solid compound from that solvent. The compound diamino benzo-15-crown-5 was isolated as a tan solid. (40 mg, 96%, mp 79-81 °C, lit.<sup>9</sup> 82-86 °C). FTIR (neat) data at: 3354, 3213 (NH<sub>2</sub>); 1125 (C-O)  $\nu_{\text{max}}/\text{cm}^{-1}$ . Which showed <sup>1</sup>H NMR (400 MHz, MeOD):  $\delta$  6.49 (s, 2H), 4.87 (s, 4H), 4.07 – 4.01 (m, 4H), 3.86 – 3.81 (m, 4H), 3.72 (s, 8H); <sup>13</sup>C NMR (101 MHz, MeOD):  $\delta$  143.52, 130.33, 107.12, 71.04, 70.92, 70.56. MALDI-TOF mass found,  $m/z$  321.106.



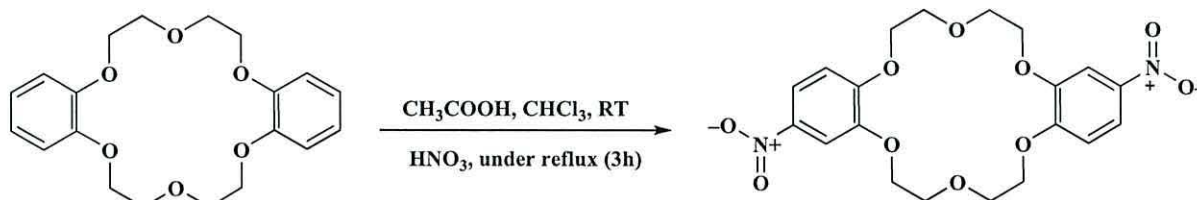
### Synthesis of 4-nitro benzo-18-crown-6 (5)



**Synthesis of dinitro benzo-18-crown-6 (6)**

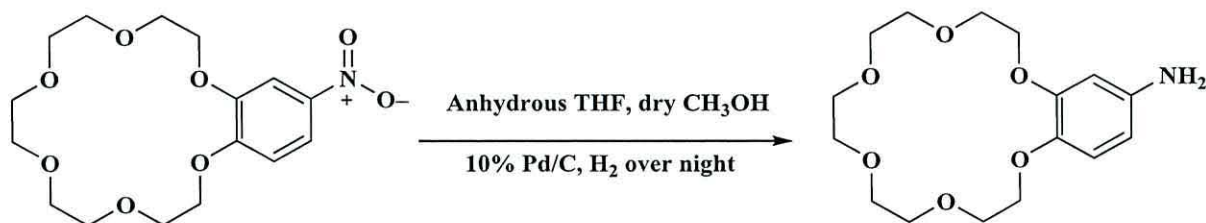
In a Quick fit round bottom flask (25 ml) concentrated nitric acid (7 mL, 70%) was stirred. To that flask, benzo-18-crown-6 (200 mg, 0.64 mmol) was added slowly for half an hour. After finishing the addition to the acid,  $\text{CHCl}_3$  (5 mL) was added to the yellow solution and the two layers were stirred for seven days.<sup>8</sup> After this time the acid was diluted with (7 ml) of distilled water. The product was extracted with chloroform ( $4 \times 20$  mL). The organic layer was evaporated to dryness leaving a yellow waxy residue. The crude product was purified by column chromatography eluting with petrol /ethyl acetate (5:2). The compound dinitro benzo-18-crown-6 was isolated as a pale yellow solid (220 mg, 88%, mp 191-193 °C, lit.<sup>7</sup> mp 198-201 °C). FTIR: 1581 ( $\text{NO}_2$ ); 1135 (C-O)  $\nu_{\text{max}}/\text{cm}^{-1}$ ;  $^1\text{H}$  NMR (400 MHz,  $\text{CDCl}_3$ ):  $\delta$  7.31 (s, 2H), 4.32 – 4.25 (m, 4H), 3.94 – 3.90 (m, 4H), 3.74 – 3.71 (m, 4H), 3.70 – 3.67 (m, 4H), 3.66 (s, 4H);  $^{13}\text{C}$  NMR (101 MHz,  $\text{CDCl}_3$ ):  $\delta$  151.38, 136.59, 107.98, 70.61, 70.40, 70.22, 69.35, 68.65. MALDI-TOF mass found,  $m/z$  425.119.

### Synthesis of dinitro dibenzo-18-crown-6 (7)



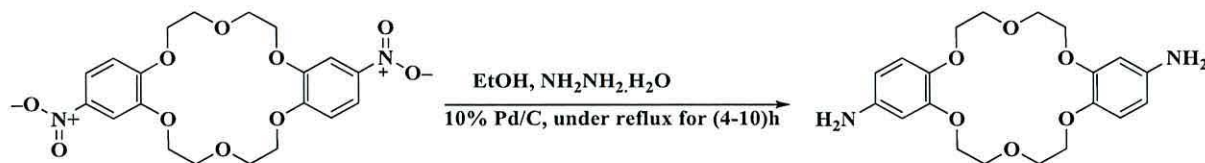
Dibenzo-18-crown-6 (100 mg, 0.27 mmol) was dissolved in  $\text{CHCl}_3$  (2 ml) in a round bottom flask. Acetic acid (1ml) was added to the solution over 10 min (the addition of the acid was one drop every five seconds), then the solution was stirred at room temperature for an additional 5 min. A solution of  $\text{HNO}_3$  (2 mml) and acetic acid (4 mml) was added over 15-20 min *via* syringe.<sup>11,12</sup> The solution was stirred at room temperature for 1 h and then heated to reflux for 3 h whereupon a precipitate formed. The solution was left to reach room temperature, and the precipitate of was filtered and washed three times with water to get rid of the residue acid and finally dried over anhydrous  $\text{MgSO}_4$  and the solvent was removed under reduced pressure. The crude product was purified by column chromatography eluting with petrol /ethyl acetate (40 %). The compound dinitro dibenzo-18-crown-6 was collected as a pale yellow solid (63 mg, 51%, mp 227-232 °C, lit. <sup>9</sup> 247-252 °C). Which showed FTIR ; 1580 ( $\text{NO}_2$ ); 1130 (C-O)  $\nu_{\text{max}}/\text{cm}^{-1}$ ;  $^1\text{H}$  NMR (400 MHz,  $\text{CDCl}_3$ ):  $\delta$  7.89 (dd,  $J = 8.9, 2.5$  Hz, 2H), 7.71 (d,  $J = 2.6$  Hz, 2H), 6.87 (d,  $J = 8.9$  Hz, 2H), 4.29 – 4.20 (m, 8H), 4.08 – 3.99 (m, 8H);  $^{13}\text{C}$  NMR (101 MHz, DMSO):  $\delta$  154.21, 148.11, 141.02, 118.09, 111.72, 107.01, 68.93, 68.88, 68.83, 68.48, 68.44. MALDI-TOF mass found,  $m/z$  473.124.



**Synthesis of 4- amino benzo-18-crown-6 (8)**

4-nitro benzo-18-crown-6 (100 mg, 0.30 mmol) was dissolved in anhydrous THF and dry CH<sub>3</sub>OH (2ml 1:1). The solution was degassed using nitrogen, then 10 % Pd/C (15 mg) was added and the mixture was stirred under hydrogen atmosphere overnight to complete hydrogenation.<sup>5</sup> The mixture diluted with methanol (10 ml) then filtered through a silica gel/Celite plug. The solvent was removed under reduced pressure. The compound 4- amino benzo-18-crown-6 was isolated as a tan solid. (80 mg, 87%, mp 79-81 °C, lit.<sup>9</sup> 82-86 °C). FTIR (neat); 3351, 3211 (NH<sub>2</sub>); 1121 (C-O)  $\nu_{\text{max}}/\text{cm}^{-1}$ ; <sup>1</sup>H NMR (400 MHz, CDCl<sub>3</sub>)  $\delta$  6.73 (d,  $J$  = 8.4 Hz, 1H), 6.30 (d,  $J$  = 2.6 Hz, 1H), 6.23 (dd,  $J$  = 8.4, 2.5 Hz, 1H), 4.14 – 4.05 (m, 4H), 3.94 – 3.90 (m, 2H), 3.89 – 3.85 (m, 2H), 3.79 – 3.69 (m, 8H), 3.68 (s, 4H); <sup>13</sup>C NMR (101 MHz, CDCl<sub>3</sub>):  $\delta$  150.45, 141.96, 141.60, 117.50, 107.44, 102.96, 71.02, 70.97, 70.95, 70.93, 70.88, 70.80, 70.64, 70.13, 69.85, 68.95. MALDI-TOF mass found,  $m/z$  350.140.



**Synthesis of di (amino benzo)-18-crown-6 (10)**

In a two necked round bottom flask (100ml), di (nitro benzo)-18-crown-6 (70 mg, 0.15 mmol) was dissolved in ethanol (40 ml) under nitrogen atmosphere. At 40 °C, the of Pd/C catalyst (10%) (13 mg) was added. The mixture then refluxed at 105 °C. Then a solution of ethanol (20 ml) and hydrazine hydrate (0.49 ml, 9.9 mmol) was added over (45 minutes). The reaction mixture was refluxed for 4—10 hrs. until the starting nitro compound was completely consumed by (TLC monitoring), and the catalyst was filtered off. The filtrate was concentrated under vacuum, water was added to the residue, and the mixture was extracted with chloroform. The extracts were concentrated in vacuum. The purification of the organic layer was recrystallized from methanol. The compound diamino benzo-18-crown-6 was isolated as a tan solid. (50 mg, 90%, mp 199-203 °C, lit.<sup>13</sup> 220-240 °C). FTIR; 3394, 3213 (NH<sub>2</sub>); 1120 (C-O)  $\nu_{\text{max}}/\text{cm}^{-1}$ ; <sup>1</sup>H NMR (400 MHz, CDCl<sub>3</sub>):  $\delta$  6.73 (d,  $J$  = 1.6 Hz, 1H), 6.71 (d,  $J$  = 1.6 Hz, 1H), 6.28 (t,  $J$  = 2.5 Hz, 2H), 6.22 (t,  $J$  = 2.8 Hz, 1H), 6.20 (t,  $J$  = 2.8 Hz, 1H), 4.14 – 4.07 (m, 8H), 4.02 – 3.97 (m, 4H), 3.97 – 3.93 (m, 4H); <sup>13</sup>C NMR (101 MHz, CDCl<sub>3</sub>):  $\delta$  150.32, 150.17, 141.92, 141.79, 141.59, 141.46, 117.10, 116.81, 107.41, 107.28, 102.83, 102.61, 70.52, 70.46, 70.44, 70.31, 70.18, 70.01, 68.92, 68.85. MALDI-TOF mass found,  $m/z$  413.129.



### 2.3 Preparation methods

#### Preparation of the sensor

The membranes were prepared as described in literature<sup>14, 15</sup> using 812 mg polyvinyl chloride (PVC), 185 mg dibutyl phthalate (DBP) and 3 mg of ionophore, dissolved in *ca.* 10 ml of anhydrous tetrahydrofuran (THF). Once completely dissolved, the solution was poured into a glass template as in (Figure 2.1) (Top). To obtain membranes with reproducible characteristics, the solvent evaporation was carefully controlled otherwise the morphology and thickness of the membranes shows significant variation which ultimately affected the sensor response. The transparent membranes of 500  $\mu$ m thickness were removed carefully from the glass plate as (Figure 2.1) (bottom).

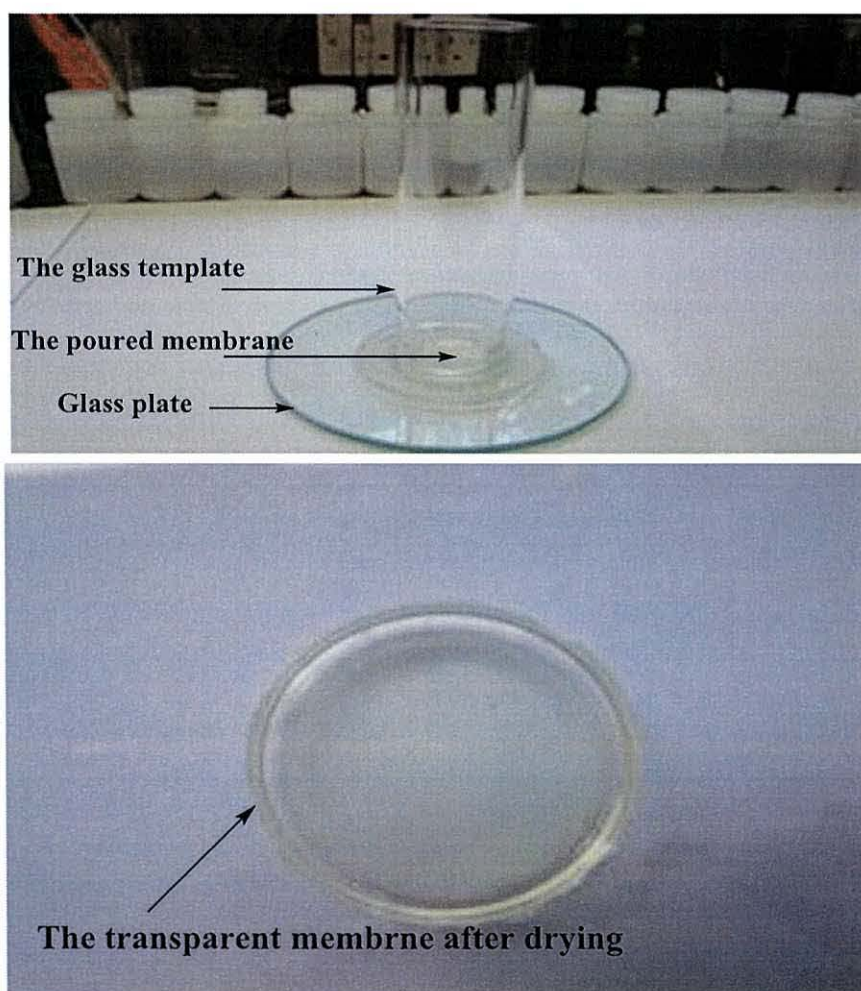
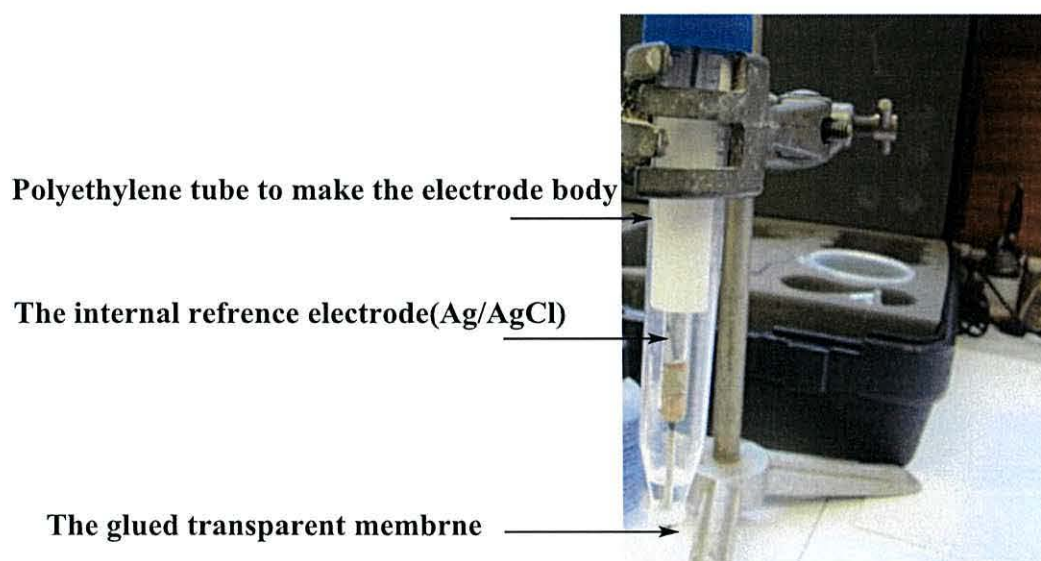


Figure 2.1: (Top) Preparation the sensor (bottom) the dry sensor template

## 2.4 Electrode arrangement

Discs (9.0 mm diameter) were obtained from the template membrane and glued to polyethylene tubes (12 cm length, 5.0 mm I.D.) using THF. For checking the proper sealing of the membrane to the end of the PVC tube (Figure 2. 2), the electrode was immersed in distilled water and air was blown through the electrode body. The appearance of any air bubble was the sign of improper sealing, which can be cured by changing the membrane, and repeating the gluing process. The electrode usually is completed by filling the internal reference solution ( $10^{-2}$  mol/dm<sup>3</sup> K<sub>2</sub>HPO<sub>4</sub> solution) and placing the internal reference electrode (Ag/AgCl) in the inner solution.

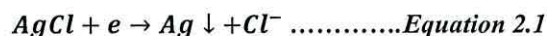


*Figure 2. 2: The electrode arrangement*

The finished electrode needed treatment in  $10^{-2}$  mol/dm<sup>3</sup> K<sub>2</sub>HPO<sub>4</sub> solution for at least 3 hour before any measurement in order to get better and stable response. The sensor electrode was immersed in a solution (10 mM, pH 9) until use. Construction the electrochemical cell

For these selective electrodes it is recommended that a glass Ag/AgCl (1.0 mm diameters) as an internal reference electrode reference electrode to avoid introducing

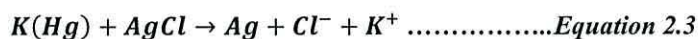
interferes into the test solution. According to the IUPAC convention, the Ag/AgCl electrode can be written:



and for the potassium



Addition of reaction gives the cell reaction



The Nernst slope for this cell is 59.16 mV at 25°C

The inner filling solution was freshly made of each set of experiments and an electrical contact was made *via* a porous plug. The ground sleeve junction provided the electrical contact between the outer filling solution and test solution. The indicator electrodes were conditioned by soaking in a 10 mM alkaline phosphate solutions for 24 h and stored in the same solution when not in use,<sup>16</sup> as in (Figure 2.3).

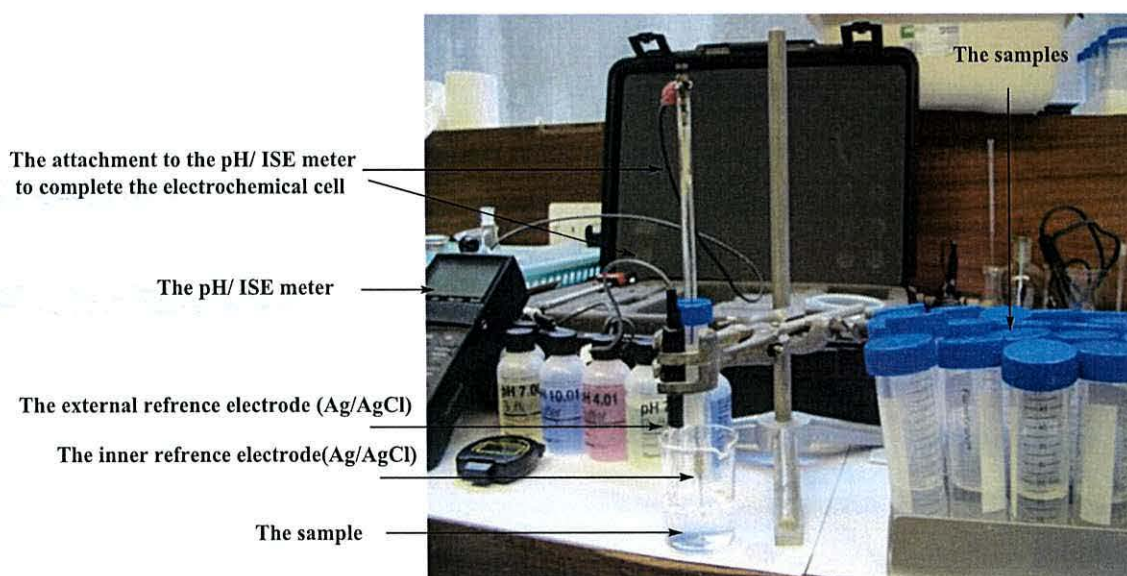


*Figure 2.3: The electrochemical cell in operation for measurements the samples*



## 2.5 Potentiometric titration

A calibration plot for an ISE is a plot of the potential difference of the cell against the logarithm of the activity or concentration of the primary ion in the experimental cell. In this work, the calibration curves were produced on concentration basis. The linearity of the slope and the response range are taken as criteria for functional electrodes.

Measurements of electromotive force (EMF) of the complete cell comprising the sensing electrode and reference electrode were made. The solutions were held at  $25 \pm 0.5^\circ\text{C}$  and stirred magnetically. Standard solutions were prepared daily using distilled water. Measurements were made by recording the potential for the most dilute standard first and wiping the electrode with tissue before progressing to the next standard. For dilute standards, the response was allowed to stabilise for 1-3 minutes whilst for all other standards a steady potential was reached within 30 seconds.

### Selectivity Coefficients

One of the important parameters for an ISE is the selectivity coefficient. This is a measure of the response to the primary or analyte ion in the presence of an interfering ion. Unfortunately, the term selectivity coefficient is misleading. The values are not constants and vary depending upon activity and the method of determination. The selectivity coefficient is defined by the potentiometric selectivity coefficient. Two classic methods, i.e., SSM and FIM, can be used to obtain selectivity coefficients  $K_{I,J}^{Pot}$  that are unbiased, i.e., equal to the thermodynamically defined ones. The prerequisite is that the selectivity coefficients are determined under conditions where the response to each of the ions in the investigated activity range is Nernstian; i.e., the respective ion is potential determining.

### Separate solutions method

The calibration curve for the primary ion is measured. If its slope is close to Nernstian,  $E_i^\circ$  is calculated by extrapolating the response to  $a_i = 1\text{M}$ . This is done by using the theoretical slope from measured values at different activities, to obtain the mean and standard deviation. A significantly smaller slope than theoretical or a slope of the opposite sign than expected may occur at high activities as a consequence of counter ion interference. In such a case, the portion of the calibration curve at lower activities may be used if it is close to Nernstian.

The selectivity coefficients<sup>17, 18</sup> of the electrode ( $k_{i,j}$ ) were determined by a SSM using the respective potassium salts. The concentrations were adjusted to 10 mM. The values were calculated using

$$\text{Log } K_{i,j}^{\text{Pot}} = (E_j - E_i)/S + \log c_i - \log c_j^{1/z_j} \dots\dots\dots \text{Equation 2.4}$$

where  $E_i$  and  $E_j$  represent the potential readings measured for  $\text{K}^+$  and the interfering ion, respectively,  $S$  is the theoretical slope of the electrode for  $\text{K}^+$  (59.2 mV at 25°C),  $c_i$  and  $c_j$  are the concentrations of  $\text{K}^+$  and the interfering ion, respectively, and  $z_j$  is the charge of the interfering ion.

The bias caused by ions leaching from the membrane can be eliminated (a) by using appropriate inner reference electrolyte solutions that prevent leaching,<sup>19</sup> (b) by measuring calibration curves with membranes that had not been in contact with the primary ions, starting with the most discriminated ions in sequence of decreasing discrimination,<sup>20</sup> or (c) by using complexing agents for the primary ions in the sample.<sup>21</sup>

### Mixed solutions method

The mixed solutions method overcomes the disadvantage with the separate solutions method and was utilised for all selectivity coefficient determinations. Solutions were prepared with a fixed level of interfering and varying levels of the analyte. A calibration curve was prepared and the so called  $18/z_i$  mV method was used.

**Fixed interference method**

The calibration curve for the primary ion is measured without additional background electrolyte and the lower detection limit is determined from its two linear portions and the calibration curve for the primary ion is measured in the presence of an interfering ion.

**Limit of detection**

We have used the IUPAC recommended definition of limit of detection which is calculated from the calibration curve. Extrapolation of two straight lines for the calibration curve gives rise to a point to yield an activity for the primary ion. It is interesting to note that this is also used in the intersection method for the determination of limits of detection are influenced in many cases by interferes which cannot be removed from the sample. The slight solubility of the electro active, material will also restrict the detection limit and it is for this reason that covalent attachment was expected to yield improved values. The purity of the water and reagents used to prepare standards and samples will also affect detection limits.

**Calibration of the electrode**

The ion selective PVC membrane electrode was calibrated by immersion along with the reference electrode, in appropriate aliquots of a stock solution which introduced to the cell, and the corresponding potentials were determined. The potential readings were plotted against logarithmic values of the concentration at pH 9.0. Then the potential was recorded after stabilisation to  $\pm 0.2$  mV. A calibration graph was then constructed by plotting the recorded potentials as a function of logarithmic concentrations solutions. The resulting graph was used for subsequent determination of unknown concentration.



## 2.6 Qualitative analysis of water samples

The collected water samples were tested for common anions as described.<sup>22,23,8</sup> Anatyte (1.0 ml) was added to a dry, clean test tube. There were common different tests per water sample location. These tests outlined below were done in order to note any interference ions that may be present in the water samples.

### Test for halides

The silver nitrate test was performed to test for any halides present in the water samples. This was achieved by adding a drop of nitric acid for acidifying the water sample, then adding a drop of silver nitrate ( $\text{AgNO}_3$ ). The reaction, if any, was noted and then excess dilute  $\text{NH}_3$  solution was added.

A positive result for chloride would show formation of a white precipitate upon addition of silver nitrate to the acidified water sample, which was then completely soluble when excess dilute  $\text{NH}_3$  solution was added. The formation of a cream precipitate, which was partially soluble in excess dilute  $\text{NH}_3$  indicated the presence of bromides; and the formation of a yellow precipitate, which was insoluble in excess dilute  $\text{NH}_3$  solution, showed that iodides were present.

### Test for carbonates and bicarbonates

The test for the presence of carbonates was done by the idea of production of  $\text{CO}_2$  gas which indicates a positive result. While for bicarbonates was done by addition of magnesium sulphate, a white precipitate of magnesium carbonate is formed, which is soluble in dilute ammonia solution. The bicarbonates do not react with magnesium sulphate.

A few drops of dilute hydrochloric acid ( $\text{HCl}$ ) were added to the water sample and evolved gas tested with limewater. This was done by keeping the mouth of the test tube covered for a while, then releasing any pressure will build-up occasionally.

Once the reaction was complete, the test tube should have contained  $\text{CO}_2$ . The gas was then poured into the test tube containing limewater, then given a gentle shake to mix the gas properly into it, and the comments recorded.

When testing for the presents of bicarbonates, a few drops of magnesium sulphate ( $\text{MgSO}_4$ ) solution was added and followed by the addition of a few drops of dilute ammonia ( $\text{NH}_3$ ) solution. Positive results in the first test would have shown fizzing due to the release of  $\text{CO}_2$  gas, which upon addition to limewater would have turned milky; this could have been from either carbonates or bicarbonates. The test carbonates would have distinguished as a white precipitate, which is soluble in  $\text{NH}_3$  solution due to the formation of magnesium carbonate; whereas bicarbonates do not react with magnesium sulphate.

### **Test for nitrates**

The presence of nitrates in the water samples was also established. A positive result showed the formation of a brown ring at the junction of the two liquid layers. This was due to the formation of  $[\text{Fe}(\text{NO})]\text{SO}_4$ .

Each test tube contained 2.0 ml of water sample. 4.0 ml of concentrated sulphuric acid ( $\text{H}_2\text{SO}_4$ ) was added slowly to the water sample and cooled on ice. A saturated solution of iron (II) sulphate was prepared and using a Pasteur pipette, a little was run down the side of the test tube, resulting in the formation of two layers. The junction of these two layers was simply observed and any colour change noted.

### **Test for sulphates and sulphites**

The first test in this sub-section is that for sulphates. By addition of barium chloride, a white precipitate of barium sulphate is formed which is insoluble in hydrochloric acid.

The second of these tests is for the sulphite was done by addition of dilute hydrochloric acid, redox the sulphite to sulphur dioxide. This strong emitted gas turns moist litmus paper red, and moist potassium dichromate paper changes from brown to green. The final test in this sub-section is another for sulphites, and, if positive, results in the reduction of  $\text{Mn}^{7+}$  to  $\text{Mn}^{2+}$  which causes decolourisation of the purple acidified potassium permanganate.

## 2.7 Quantitative analysis of water samples

The collected water samples were tested for their hardness, *i.e.* the presence of  $\text{Ca}^{2+}$  ions, the data was not showing.<sup>23</sup>

### Preparation of the calcium standard solution

0.25 g of calcium carbonate ( $\text{CaCO}_3$ ) was added to a 100 ml beaker and dissolved with 10.0 ml of de-ionised (Milli-Q system) water. Concentrated hydrochloric acid was added drop-wise until the entire solid had dissolved and no further gas was evolved. The solution was then transferred to a 250 ml volumetric flask and made up to the mark with de-ionised (Milli-Q system) water.

### Standardisation of ethylenediamine tetra-acetic acid

A clean, dry 50 ml burette was filled with approximately 0.01 M EDTA. 25.0 ml of the  $\text{CaCO}_3$  standard solution was pipetted into a 250 ml conical flask, and 25.0 ml of pH 10 ammonia/ammonium chloride buffer solution was added to it. A few drops of Eriochrome Black T solution were also added, and then the mixture was titrated with EDTA. This procedure was done in triplicate and the data used to determine the exact molarity of the EDTA.



### **Titration of calcium in water samples**

5.0 ml of the water sample was pipetted into a clean, dry 250 ml conical flask. A drop of 1:1 triethanolamine was added to mask any traces of iron, and a drop of 2.0 M sodium hydroxide (NaOH) was added to precipitate out any  $\text{Mg}^{2+}$  present as magnesium hydroxide, as well as to obtain the desired pH for the indicator. A few crystals of Patton-Reeder indicator were added before titrating with EDTA.<sup>24</sup>

### **Elemental analyses of water samples**

Analyses of the collected water samples were conducted *via* atomic absorbance spectroscopy method.

### **Atomic absorbance spectroscopy**

The presence and concentration of trace metals was determined using AAS which works by introducing the sample into a flame. Here, the metals are atomized, and light at a specific wavelength corresponding to the atom's valence level transition is applied to the sample. The absorbance of the light is recorded and the concentration of the metal is calculated from a standard calibration curve prepared prior to analysis.<sup>25</sup>

The concentrations of Ag, Cd, Co, Cu, Fe, Pb and Zn were determined by AAS, using a Varian Spectra AA 220FS/220Z instrument, in an air-acetylene flame. The concentrations of As and Ca were determined by AAS using the same instrument, but using a nitrous oxide-acetylene flame.

## **2.8 Scanning electron microscopy(SEM)**

Prior to SEM analysis, non-conducting samples were affixed with carbon tape to an aluminium stub and then the samples were coated in gold for 5 minutes at 10 mA and 1.2 kV using a Polaron Equipment Ltd. SEM coating unit E5000. The samples were gold-coated (Figure 2. 4) in order to make the surface conductive. This helps to

prevent charge build-up on the surface during SEM analysis and reduces noise in the image.



*Figure 2. 4: The membranes after coating them with gold*

To characterise further the membranes morphologies, examination was continued with the use of a SEM (Hitachi S-520) A beam of finely focussed electrons scans over the sample; this releases secondary electrons (to show topography) and backscattered electrons (to show contrast). An electron beam current of 10 kV was found to give the best results; these are detected and amplified to give an image of the surface of the sample.

## **2.9 Energy dispersive analyser X-ray(EDAX)**

The individual membranes were coated with a thin layer of gold (1 to 5 nm). Electron probe microanalysis was completed using the energy dispersive X ray analyser (EDXA) (Oxford Instruments 7497 EDX with Link ISIS computer software.) using an electron beam current of 14kV. A light element window was fitted and was capable of detecting X-ray emissions from elements with an atomic number of 5 (boron) and greater

## 2.10 References

- [1] R. Rigaku, **Cell determination and data collection**, *Crystal Clear-SM Expert*, 2010, **2.0 r5**.
- [2] S. J. Coles and P. A. Gale, **Changing and challenging times for service crystallography**. *Chem. Sci.*, 2012, **3**, 683-689.
- [3] G. M. Sheldrick, **Structure refinement: SHELXL97**, *Acta Cryst.*, 2008, **A64**, 112-122.
- [4] M. Y. Keating and G. A. Rechnitz, **Potentiometric digoxin antibody easurements with antigen-ionophore based membrane electrodes**, *Anal. Chem.*, 1984, **56**, 801-806.
- [5] J. Yang, C. Hwang, and M. Chen, **Bimodal fluorescence signaling based on control of the excited-state conformational twisting and the ground-state protonation processes**, *Tetrahedron Lett.*, 2007, **48**, 3097-3102.
- [6] E. Vasile, F. Dumitru, A. Razvan, O. Oprea, and C. Andronescu, **Novel ureido-4'-aminobenzo-15-crown-5-ether periodic mesoporous silicas**, *D. J. Nano. Biostr.*, 2013, **8 (1)**, 433-444.
- [7] A. D. Grebenyuk, S. A. Andreev, I. A. Stempnevskaya, M. G. Levkovich, and A. K. Tashmukhamedove, **Nitration of benzo crown ethers with potassium nitrate in polyphosphoric acid**, *Chem. Heterocycl. Compd.*, 2000, **36 (12)**, 1449-1456.
- [8] M. B. Deshmukh, K. N. Alasundkar, S. M. Salunkhe, D. K. Salunkhe, S. A. Sankpal, D. R. Patil, and P. V. Anbhule., **Synthesis, X-ray diffraction and optical spectral study of benzo-18-crown-6 containing monoazo dyes**, *Indian J. Chem.*, 2009, **48 B**, 737-740.
- [9] W. M. Feigenbaum, R. H. Michel, **Novel polyamides from macrocyclic ethers**, *J. Polym. Sci., Part A: Polym. Chem.*, 1971, **9 (3)**, 817-820.
- [10] R. Ungaro, B. El Haj, and J. Smid, **Substituent effects on the stability of cation complexes of 4'-substituted monobenzo crown ethers**, *J. Am. Chem. Soc.*, 1976, , 5198-5202.
- [11] M. J. Deetz, M. Shang, and B. D. Smith, **A macrobicyclic receptor with versatile recognition properties: simultaneous binding of an ion pair and**



- selective complexation of dimethylsulfoxide**, *J. Am. Chem. Soc.*, 2000, **122**, 6201-6207.
- [12] S. A. Duggan, G. Fallon, S. J. Langford, V. Lau, J. F. Satchell, and M. N. Paddon-Row, **Crown-linked porphyrin systems**, *J. Org. Chem.*, 2001, **66**, 4419-4426.
- [13] C. J. Pedersen, **Cyclic polyethers and their complexes with metal salts**, *J. Am. Chem. Soc.*, 1967, **89**, 7017-7021.
- [14] F. Faridbod, M. R. Ganjali, R. Dinarvand, and P. Norouzi, **The fabrication of potentiometric membrane sensors and their applications**, *Afri. J. Biotech.*, 2007, **6 (25)**, 2960-2987.
- [15] A. Babakhanian, M. B. Gholivand, M. Mohammadi, M. Khodadadian, A. Shockravi, M. Abbaszadeh, and A. Ghanbary, **Fabrication of a novel iron(III)-PVC membrane sensor based on a new 1,1[1]-(iminobis(methan-1-yl-1-ylidene))dinaphthalen-2-ol synthetic ionophore for direct and indirect determination of free iron species in some biological and non-biological samples**, *J. Hazard. Mater.*, 2010, **177**, 159-166.
- [16] A. Babakhaniana, M. B. Gholivanda, M. Mohammadib, M. Khodadadianc, A. Shockravib, M. Abbaszadehb, and A. Ghanbary, **Fabrication of a novel iron(III)-PVC membrane sensor based on a new 1,1[1]-(iminobis(methan-1-yl-1-ylidene))dinaphthalen-2-ol synthetic ionophore for direct and indirect determination of free iron species in some biological and non-biological samples**, *J. Hazard. Mater.*, 2010, **177**, 159-166.
- [17] T. Katsua, K. Ido, K. Takaishib, and H. Yokosu, **Thallium(I)-selective membrane electrodes based on calix[6]arene or calix[5]arene derivatives**, *Sens. Actuators, B, Chem.*, 2002, **87**, 331-335.
- [18] E. P. E. Bakker, **Potentiometric sensors for trace-level analysis**, *Trends Anal. Chem.*, 2005, **24 (3)**, 199-207.
- [19] T. Sokalski, A. Ceresa, M. Fibbioli, T. Zwickl, E. Bakker, and E. Pretsch, **Lowering the detection limit of solvent polymeric ion-selective membrane electrodes. 2. Influence of composition of sample and internal electrolyte solution**, *Anal. Chem.*, 1999, **71**, 1210-1214.
- [20] E. Bakker, **Determination of unbiased selectivity coefficients of neutral carrier-based cation-selective electrodes**, *Anal. Chem.*, 1997, **69**, 1061-1069.

- [21] R. Bereczki, B. Takacs, J. Langmaier, M. Neely, R. E. Gyurcsanyi, K. Toth, G. Nagy, and E. Lindner, **How to assess the limits of ion-selective electrodes: Method for the determination of the ultimate span, response range, and selectivity coefficients of neutral carrier-based cation selective electrodes**, *Anal. Chem.*, 2006, **78**, 942-950.
- [22] A. I. Vogel and G. Svehla, **In Vogel's qualitative inorganic analysis**, Longman, Harlow, 1996.
- [23] A. I. Vogel, **Vogel's textbook of quantitative chemical analysis**, Pearson Education Ltd, Essex, 2000.
- [24] K. H. Gelberg, L. Church, G. Casey, M. London, D. S. Roerig, J. Boyd, and M. Hill, **Nitrate levels in drinking water in rural New York state**, *Environ. Res. A*, 1999, **80**, 34-40.
- [25] K. C. Thompson and R. J. Reynolds, **In atomic absorption, fluorescence and flame emission spectroscopy: a practical approach**, Griffin, London, 1978.

## **Chapter 3 – Synthesis and potentiometric characterisation**



### 3.1 Introduction

The chapter concerns the production of a range of dipotassium hydrogen phosphate sensors based on crown ethers. The resulting sensors have been evaluated for their effectiveness in the determination of potassium phosphate ions in solutions. The ionophores structures reported here have been illustrated in (Figure 3. 1) below.

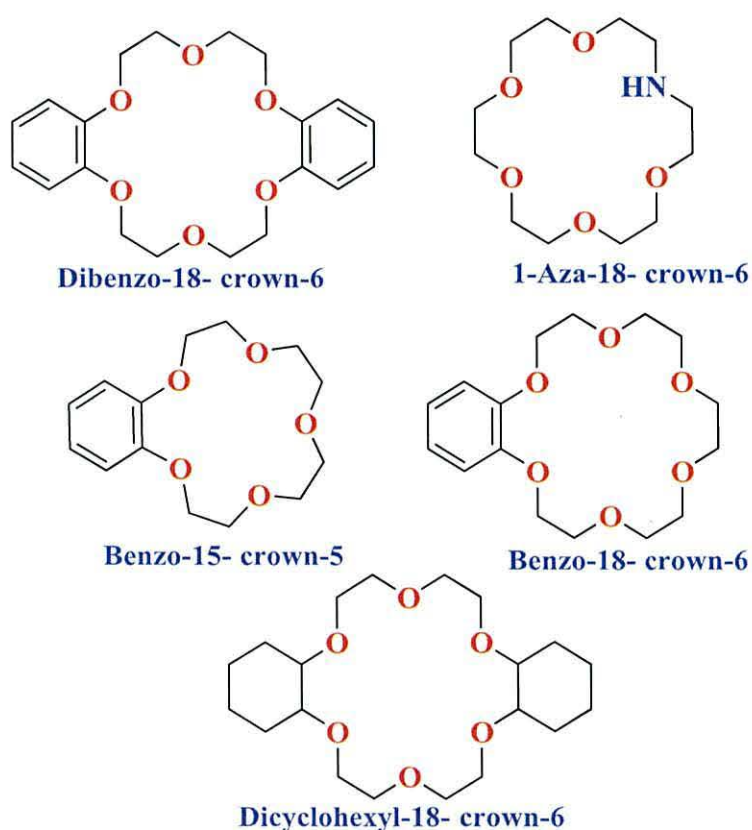


*Figure 3. 1: The structures of the ionophores*

In the present study, the synthesis and complexation of macromolecules based on crown ether compounds that are bound to potassium are described. The rings are then functionalised with either withdrawing or donating groups to enhance the binding process.

The development of plasticised polymeric membrane sensors has been a thesis target for the liquid membrane phases. This has led to an increased level of interest in

potentiometric based sensors because of their selectivity, ease of use in the field and long shelf life.<sup>1,2</sup> Crown ether macrocycles provide a simple receptor model and are well matched as hosts due to their conformational flexibility and the presence of multiple binding sites in their structures.<sup>3,4,5</sup> The complexation properties of crown ether derivatives depend on the comparative size of the ions being detected to the size of the crown ether ring as well as the number and variety of heteroatom's and functional groups.<sup>6,7,8</sup> In order to select the best solvent mediator, tests are usually required.<sup>9</sup> The properties of the ISEs are tested with different membrane compositions, and the electrode with the necessary characteristics is selected. The most important characteristics include linear response range, slope (sensitivity), and also selectivity towards the ions present in the analysed solution.<sup>10</sup>

### **3.1 (((3,4,5-trinitro-1,2-phenylene)bis(oxy))bis(ethane-2,1-diyl))bis(oxy))bis(ethane-2,1-diyl) dinitrate**

#### **Synthesis**

All NMR spectra and Mass Spectrometry data are given in Appendix in attached CD. The <sup>1</sup>H NMR spectrum shows a singlet at δ 7.73 ppm (1H) due to the aromatic proton which represent in Ha from (Figure 3. 2). The asymmetric structure of the compound exhibited a multiplet at δ 4.65 – 4.60 ppm belongs to two protons to the far end in the opened crown cavity represent in He, a multiplet at δ 4.59 – 4.51 ppm belongs to the four protons of the opened crown cavity represent in Hb, j, the multiplet at δ 4.42 – 4.35 ppm belongs to the two protons in the opened crown cavity next to the benzene ring from side represents in Hf, and the multiplet at δ 3.97 – 3.91 ppm belongs to the two protons represents in Hg. The rest signals represented by the multiplets at δ 3.85 – 3.81 ppm represents in Hd, δ 3.79 – 3.75 ppm represents in Hc, δ 3.74 – 3.69 ppm represents in Hh belong to the other left protons in the opened crown cavity because of the asymmetric structure of this compound which confirmed by COSY spectrum (Figure 3. 3) and also COSY spectrum confirms the coupling between Hb with Hc from side and the coupling between Hj with Hh from the other side. On the other hand this spectrum shows another coupling between He with Hd from side and Hf with Hg from the other side.

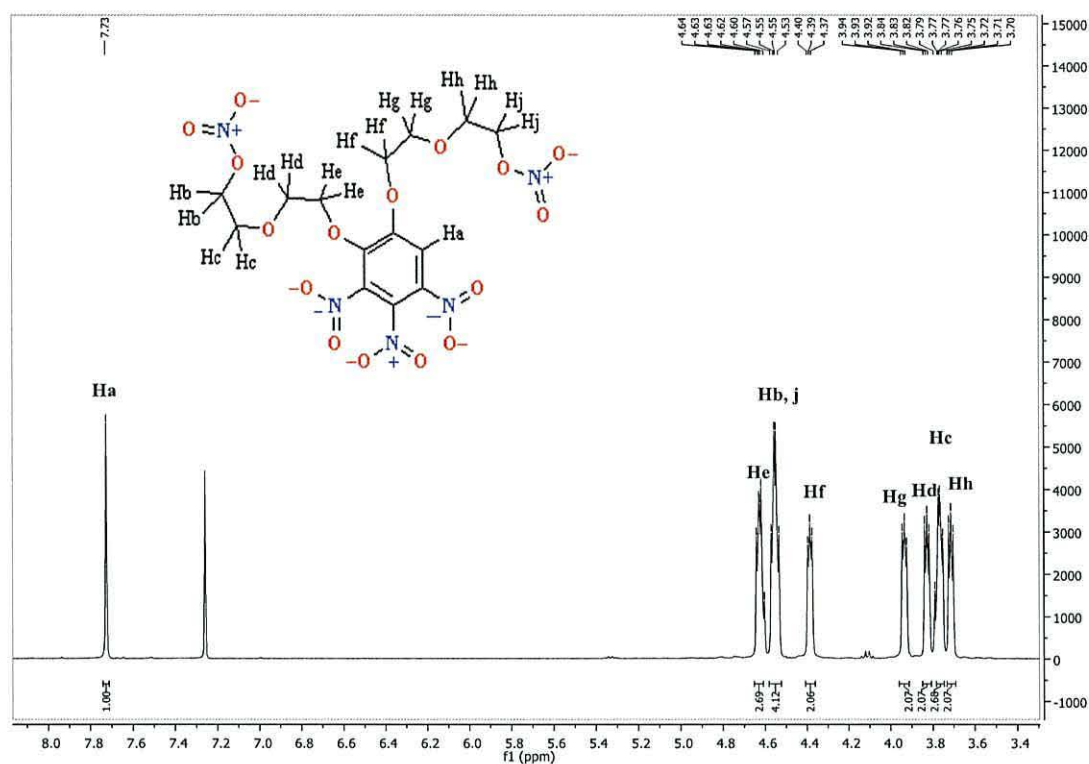


Figure 3. 2:  $^1\text{H}$  NMR spectrum of (((3,4,5-trinitro-1,2-phenylene)bis(oxy))bis(ethane-2,1-diyl))bis(oxy))bis(ethane-2,1-diyl) dinitrate

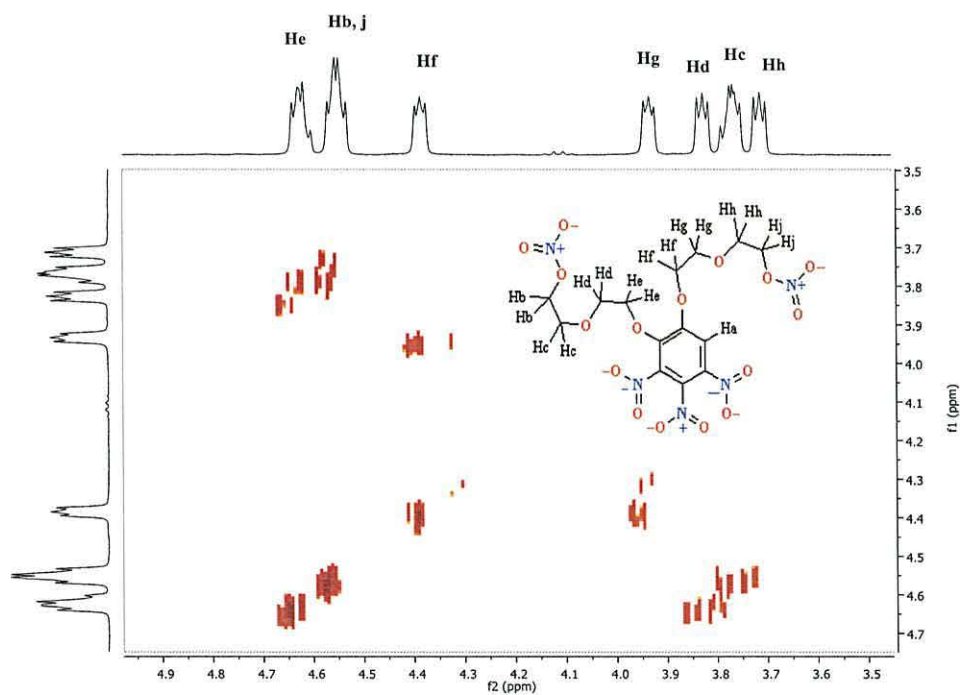


Figure 3. 3: The COSY spectrum of (((3,4,5-trinitro-1,2-phenylene)bis(oxy))bis(ethane-2,1-diyl))bis(oxy))bis(ethane-2,1-diyl) dinitrate



The  $^{13}\text{C}$  NMR spectrum (Figure 3. 4) exhibits signals at  $\delta$  154.06, 145.24, 138.84, 136.63, 110.60 ppm due to aromatic carbon atoms attached to the opened cavity ring, while the series of the signals at  $\delta$  74.41, 71.91, 71.77, 70.27, 69.97, 69.01, 67.40, 67.24 ppm belong to the carbon atoms of the ether groups which represent the opened cavity ring.

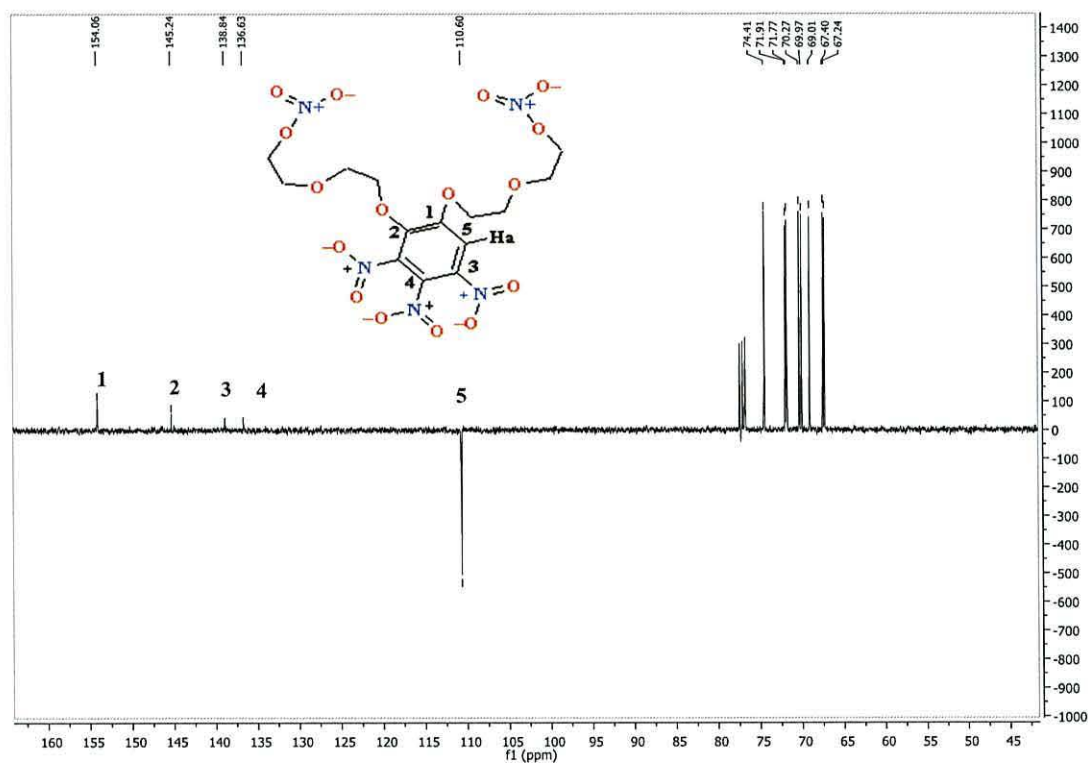
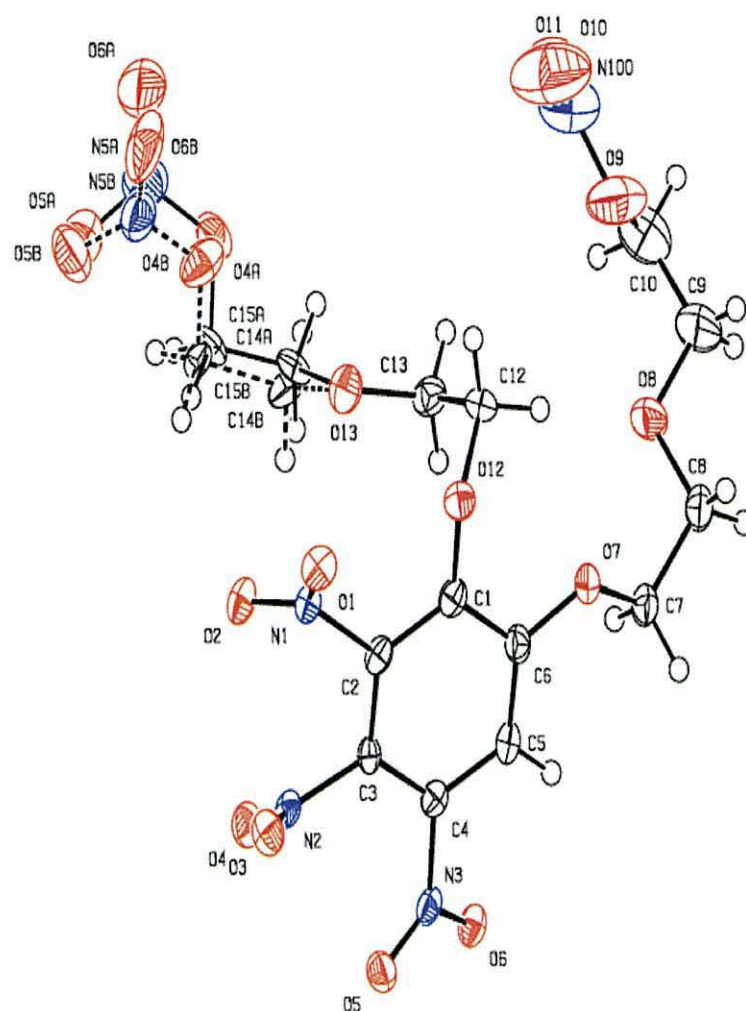


Figure 3. 4:  $^{13}\text{C}$  NMR spectrum of (((3,4,5-trinitro-1,2-phenylene)bis(oxy))bis(ethane-2,1-diyl))bis(oxy))bis(ethane-2,1-diyl) dinitrate

Single-crystal X-ray structural analyses (Figure 3. 5, Table 3. 1) verifies the expected structural arrangements of the ionophore (((3,4,5-trinitro-1,2-phenylene)bis(oxy))bis(ethane-2,1-diyl))bis(oxy))bis(ethane-2,1-diyl) dinitrate.

The important target for the X-ray structure is to confirm the desired the opened ring for those macrocyclic compounds with the strongly withdrawing nitro group separated from the crown cavity by the phenyl group by this kind of the synthesis procedure.



**Figure 3. 5:** molecular structure of (((3,4,5-trinitro-1,2-phenylene)bis(oxy))bis(ethane-2,1-diyl))bis(oxy))bis(ethane-2,1-diyl) dinitrate. Two components of positional disorder are shown. Displacement ellipsoids – 50% probability.

Table 3. 1: Crystal data and structure refinement details.

|  |   |
|--|---|
| Empirical formula  | C <sub>14</sub> H <sub>17</sub> N <sub>5</sub> O <sub>16</sub>            |
| Formula weight   | 511.33  |
| Temperature  | 100(2) K  |
| The wave length  | 0.71075 Å   |
| Crystal system   | Monoclinic  |
| Space group  | <i>P</i> 2 <sub>1</sub> / <i>c</i>  |
| Unit cell dimensions<br><i>a</i> = 5.021(4) Å<br><i>b</i> = 12.6385(10) Å<br><i>c</i> = 33.71(3) Å | $\alpha = 90^\circ$<br>$\beta = 90.9440(10)^\circ$<br>$\gamma = 90^\circ$ |
| Volume   | 2139(3) Å <sup>3</sup>  |
| <i>Z</i>   | 4   |
| Density (calculated)   | 1.588 Mg / m <sup>3</sup>   |
| Absorption coefficient   | 0.148 mm <sup>-1</sup>  |
| <i>F</i> (000)   | 1056  |
| Crystal  | Plate; pale yellow  |
| Crystal size   | 0.13 × 0.07 × 0.01 mm <sup>3</sup>  |
| $\theta$ range for data collection   | 3.22 – 25.02°   |
| Index ranges   | –5 ≤ <i>h</i> ≤ 5, –13 ≤ <i>k</i> ≤ 15, –34 ≤ <i>l</i> ≤ 40               |
| Reflections collected  | 10680   |
| Independent reflections  | 3710 [ <i>R</i> <sub>int</sub> = 0.0496]                                  |
| Completeness to $\theta = 24.21^\circ$   | 98.8 %  |
| Absorption correction  | Semi-empirical from equivalents   |
| Max. and min. transmission   | 0.9985 and 0.9811   |
| Refinement method  | Full-matrix least-squares on <i>F</i> <sup>2</sup>                        |
| Data / restraints / parameters   | 3710 / 144 / 371  |
| Goodness-of-fit on <i>F</i> <sup>2</sup>   | 1.132   |
| Final <i>R</i> indices [ <i>F</i> <sup>2</sup> > 2σ( <i>F</i> <sup>2</sup> )]                      | <i>R</i> 1 = 0.1045, <i>wR</i> 2 = 0.2691                                 |
| <i>R</i> indices (all data)  | <i>R</i> 1 = 0.1280, <i>wR</i> 2 = 0.2914                                 |
| Largest diff. peak and hole  | 1.495 and –0.626 e Å <sup>-3</sup>  |

## Performance

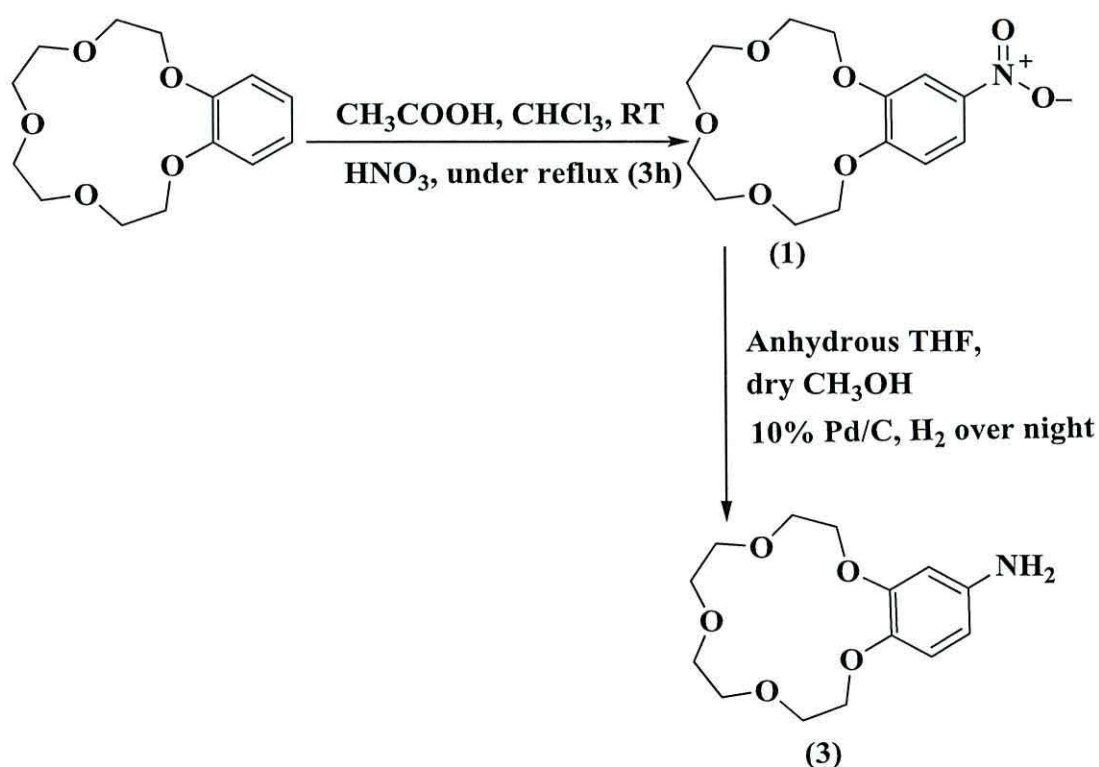
The potentiometric response of the ISE modified with ionophore (((3,4,5-trinitro-1,2-phenylene)bis(oxy))bis(ethane-2,1-diyl))bis(oxy))bis(ethane-2,1-diyl) dinitrate was investigated for the potassium phosphate. Appropriate aliquots of the stock solution were introduced to the cell and the corresponding potentials determined. The unstable potential readings were showed which prevented to be recorded with a very long time. This first attempt to get this opened ring structure to be comparable with closed ones was studied to show the effect of the interactions between the cavity ring of the ionophore and the cation itself.



### 3.2 4-Nitro benzo-15-crown-5 (1) and 4-amino benzo-15-crown-5 (3)

#### Synthesis

All NMR spectra and Mass Spectrometry data are given in Appendix in attached CD. Firstly, the compounds 4-nitro benzo-15-crown-5 (1) and 4-amino benzo-15-crown-5 (3) were synthesized according to<sup>11, 12</sup> described below. Benzo-15-crown-5 was used as a starting material for the preparing 4- Nitro benzo-15-crown-5 by dissolving it in acetic acid at room temperature then cooling down with ice because it is an exothermic reaction. Then HNO<sub>3</sub> (70%) was added. The solution was stirred at room temperature for 48 h and extracted with ethyl. The crude product was purified by flash chromatography (petrol /ethyl acetate 1:1) to give a pale yellow solid; as pictured in Scheme 3.1.



*Scheme 3.1: Synthesis of 4-nitro benzo-15-crown-5(1) and 4-aminobenzo-15-crown-5(3)*

The  $^1\text{H}$  NMR and  $^{13}\text{C}$  NMR spectra are shown below and in Appendix. The data confirm that the product (1) was formed. The  $^1\text{H}$  NMR exhibits double of doublet at

$\delta$  7.92 ppm ( $J = 8.9, 2.6$  Hz, 1H) due to the aromatic protons next to the carbon atom which is connected to the nitro group Hb in (Figure 3.6). While the aromatic protons appear as doublets at  $\delta$  7.74 ppm ( $J = 2.6$  Hz) and  $\delta$  6.89 ppm ( $J = 8.9$  Hz), presented by Ha, and Hc respectively. The series of multiplets at  $\delta$  4.27 – 4.21 ppm belongs to the four protons and  $\delta$  4.00 – 3.95 ppm belongs to the other four protons, while the singlet at  $\delta$  3.80, 3.78 ppm for the last eight protons are due to the ether bridges of the crown cavity compound.

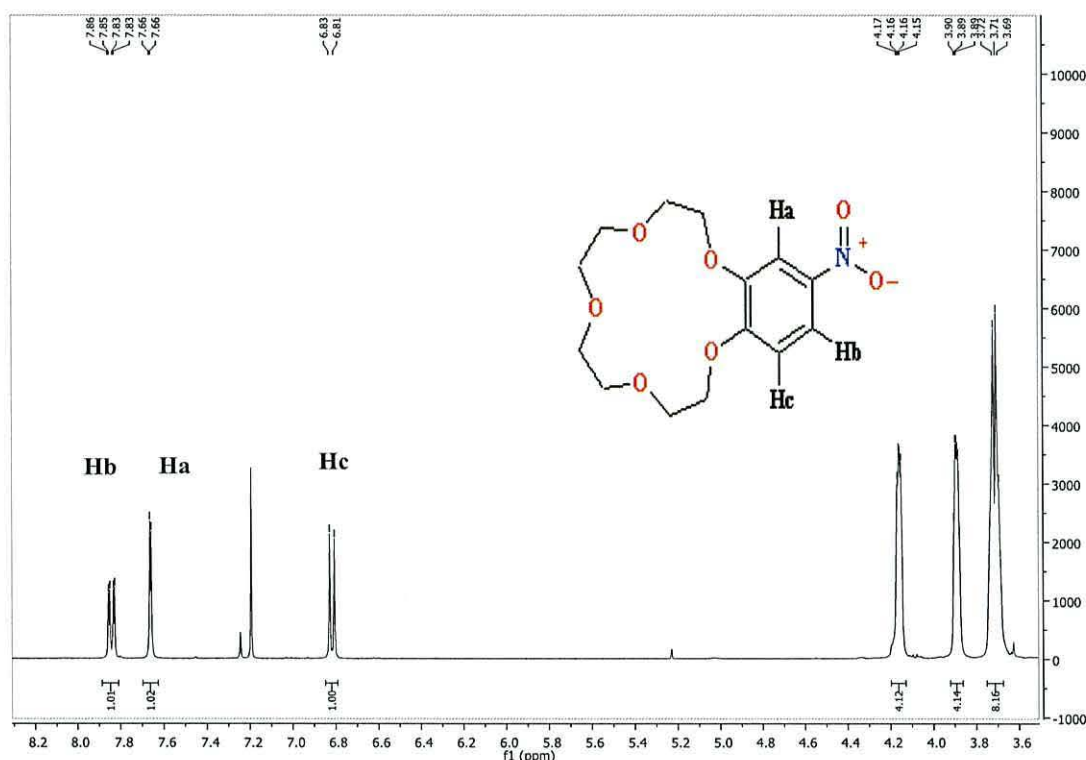


**Figure 3.6:** The characteristic signal of the protons (Ha, Hb, and Hc) adjacent to a nitro group of 4-nitro benzo-15-crown-5(1) compound

The  $^{13}\text{C}$  NMR spectrum is less ambiguous than the  $^1\text{H}$  NMR spectrum. The  $^{13}\text{C}$  NMR spectrum exhibits signals at  $\delta$  154.09, 148.24 ppm due to the aromatic carbon atoms which attached to the crown cavity. The signals in downfield at  $\delta$  141.59 ppm belongs to the carbon connected to the nitrogen atom of the nitro group. While the signals at  $\delta$  118.24, 111.27 ppm belong to non-equivalent  $\text{sp}^2$ -carbons connected to the nitro group in aromatic structure of the crown compound. While the signal at  $\delta$  108.12, belongs to the other carbon atom in benzo group. The series of the signals are at  $\delta$  77.16, 70.55, 70.54, 69.85, 69.79, 68.83, 68.76, 68.57, 68.42 ppm belong to

the carbon atoms of the ether bridges of the crown compound. Single-crystal X-ray structural analyses (Figure 3.7, Table 3. 2) verifies the expected structural arrangements of (1).

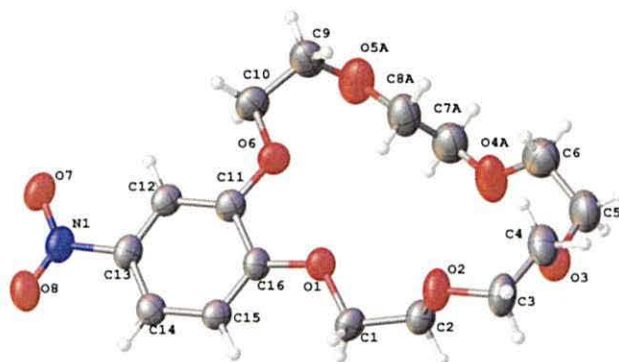


**Figure 3.7:** Molecular structure of 4-nitro benzo-15-crown-5(1) compound. Only one component is shown. Displacement ellipsoids- 50% probability.

**Table 3. 2:** Crystal data and structure refinement details of 4-nitro benzo-15-crown-5(1).

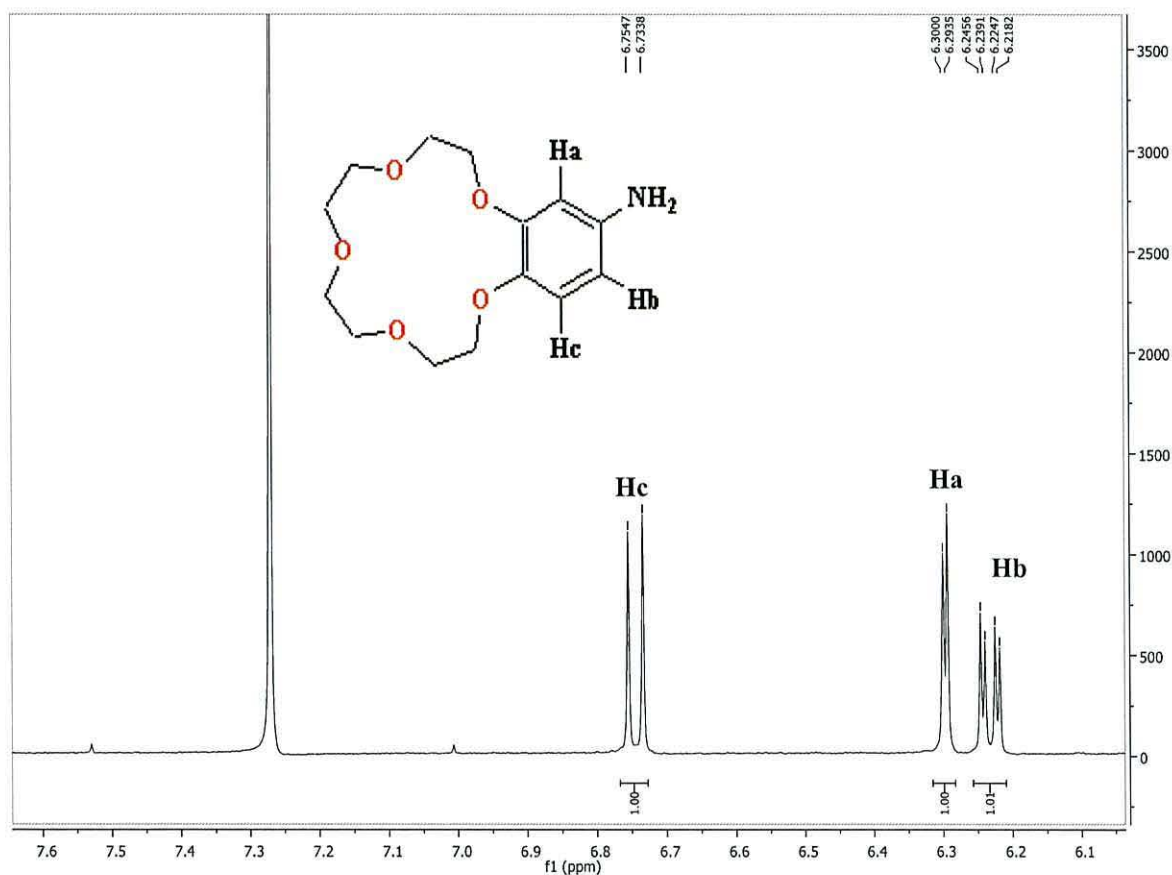
|  |  |
|--|--|
| Empirical formula                          | C <sub>16</sub> H <sub>23</sub> NO <sub>8</sub>            |
| Formula weight                             | 357.35   |
| Temperature                                | 100(2) K   |
| The wave length                            | 0.68890 Å  |
| Crystal system                             | Monoclinic   |
| Space group                                | <i>P</i> 2 <sub>1</sub> / <i>n</i>                         |
| Unit cell dimensions                       | $\alpha = 90^\circ$  |
| $a = 17.594(13)$ Å                         | $\beta = 112.95(2)^\circ$                                  |
| $b = 4.912(5)$ Å                           | $\gamma = 90^\circ$  |
| $c = 21.955(17)$ Å                         |  |
| Volume                                     | 1747(3) Å <sup>3</sup>                                     |
| Z  | 4  |
| Density (calculated)                       | 1.359 Mg / m <sup>3</sup>                                  |
| Absorption coefficient                     | 0.109 mm <sup>-1</sup>                                     |
| $F(000)$                                   | 760  |
| Crystal                                    | Lath; colourless   |
| Crystal size                               | 0.07 × 0.02 × 0.01 mm <sup>3</sup>                         |
| $\theta$ range for data collection         | 3.40 – 24.21°  |
| Index ranges                               | $-20 \leq h \leq 20, -4 \leq k \leq 5, -26 \leq l \leq 26$ |
| Reflections collected                      | 9330   |
| Independent reflections                    | 3033 [ $R_{int} = 0.0852$ ]                                |
| Completeness to $\theta = 24.21^\circ$     | 98.5 %   |
| Absorption correction                      | Semi-empirical from equivalents                            |
| Max. and min. transmission                 | 0.9989 and 0.9924  |
| Refinement method                          | Full-matrix least-squares on $F^2$                         |
| Data / restraints / parameters             | 3033 / 132 / 263   |
| Goodness-of-fit on $F^2$                   | 0.959  |
| Final $R$ indices [ $F^2 > 2\sigma(F^2)$ ] | $R1 = 0.0737, wR2 = 0.1870$                                |
| $R$ indices (all data)                     | $R1 = 0.1242, wR2 = 0.2270$                                |
| Largest diff. peak and hole                | 0.311 and -0.244 e Å <sup>-3</sup>                         |



Importantly this confirms the desired the closed ring for these macrocyclic compounds with the strongly withdrawing nitro group separated from the crown cavity by the phenyl group. In addition, these data also show the nature of the bonding suggests that the structure should be relatively rigid. This type of atomic arrangement should be preferable to optimise efficient electron bonding with potassium cation in the crown cavity and the phosphate anion as a counter ion for this structure.

In structure **(1)** in crystal form an average length of all bonds is  $1.611 \pm 0.090$  Å, remarkably identical to the effective ionic radius of  $K^+$  cation (1.33 Å) and van der Waals radius of oxygen atom, 1.40–1.52 Å.<sup>13</sup> While for synthesis the compound **(3)**, the starting material was 4-nitro benzo-15-crown-5 (**1**) was dissolved in anhydrous THF and dry  $CH_3OH$ . The solution was degassed using nitrogen, and then 10% Pd/C was added under hydrogen atmosphere.<sup>12</sup> The mixture was stirred overnight to complete hydrogenation. The mixture diluted with more methanol then filtered through a silica gel/Celite plug. The solvent was removed from the solution by evaporation of the solvent mixture under reduced pressure. The purification was done by recrystallization from methane in a good yield. The compound was isolated as a tan solid.

The  $^1\text{H}$  NMR and  $^{13}\text{C}$  NMR spectra confirm that the product (**3**) was formed. The  $^1\text{H}$  NMR spectra shows a doublet signal at  $\delta$  6.73 ( $J = 8.4$  Hz) and at  $\delta$  6.29 ( $J = 2.6$  Hz) belong to the protons on carbon atom in the far end to the carbon attached to the amino group, while the other proton on carbon atoms next to the carbon attached to the amino group appear as doublet and double of doublet at signals  $\delta$  6.30 ( $J = 2.6$  Hz) and at  $\delta$  6.22 ( $J = 8.4, 2.6$  Hz) (Figure 3. 8). The signals of multiplets at  $\delta$  4.11 – 4.04,  $\delta$  3.92 – 3.85,  $\delta$  3.78-3.72 belong to the four, four, and eight protons respectively for ether bridges of the crown structure.



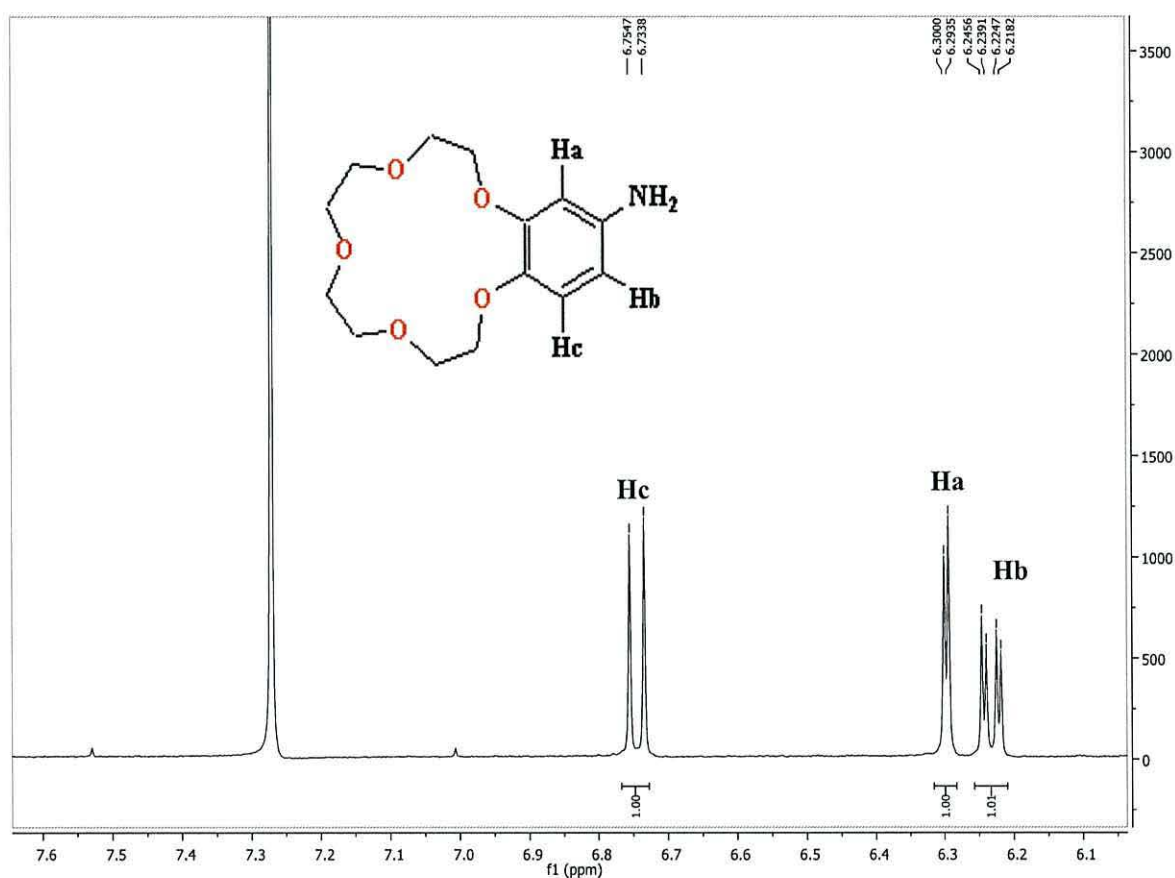


**Figure 3. 8:** The characteristic signal of the protons (Ha , Hb, and Hc) adjacent to an amino group 4-aminobenzo-15-crown-5 (3)

As a comparison between those two groups; the nitro and the amino in a benzo ring of the 4-nitro benzo-15-crown-5 (1) and 4-amino benzo-15-crown-5 (3) macrocyclic compounds. (Figure 3.9) shows the effect of the withdrawing and the donating groups for those ionophores on the chemical shift.



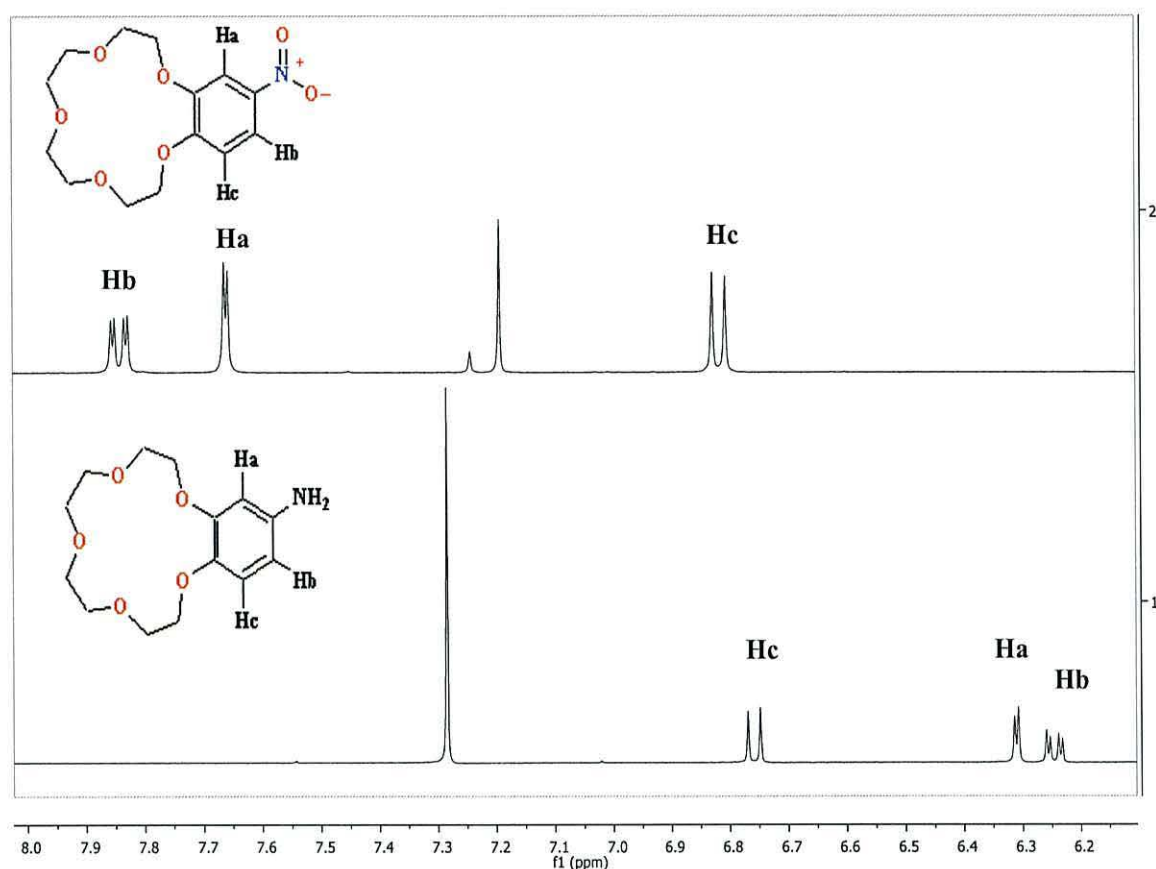


**Figure 3.9:** The characteristic signal of the protons (Ha, Hb, and Hc) as a comparison between the nitro and the amino groups in a benzo ring of the 4-nitro benzo-15-crown-5(1) and 4-amino benzo-15-crown-5(3) macrocyclic compounds

The  $^{13}\text{C}$  NMR spectrum in Appendix exhibits a signal at  $\delta$  150.67, 142.12 ppm due to the aromatic carbon atoms which attached to the crown cavity. The signal in downfield at  $\delta$  141.39 ppm belongs to the carbon connected to the amino group. While the signals at  $\delta$  117.51, 107.52 ppm belong to non-equivalent  $\text{sp}^2$ -carbons connected to the amino group in aromatic structure of the crown compound. The signal at  $\delta$  102.83 ppm belongs to the other carbon atom in benzo group. The series of the signals are at  $\delta$  71.08, 70.99, 70.90, 70.59, 70.08, 69.74, 68.80 ppm belong to the carbon atoms of the ether bridges of the crown compound.

### Performance

The potentiometric response of the ISE modified with ionophore (1) and (3) was investigated against the potassium phosphate. Series of diluted solution were introduced to the cell and the corresponding potentials determined. The potential readings were plotted against the logarithmic values of the concentration over a range of  $5 \times 10^{-5} \text{ mol L}^{-1}$  to  $1 \times 10^{-1} \text{ mol L}^{-1}$  (Figure 3.10) and (Figure 3.11). The slope of the calibration line for 4- nitro benzo-15-crown-5 ionophore was  $14.282 \pm (1.1) \text{ mV per decade}$ ; with the considered error bars for the sensor which relates to the sensor composition.<sup>14</sup>

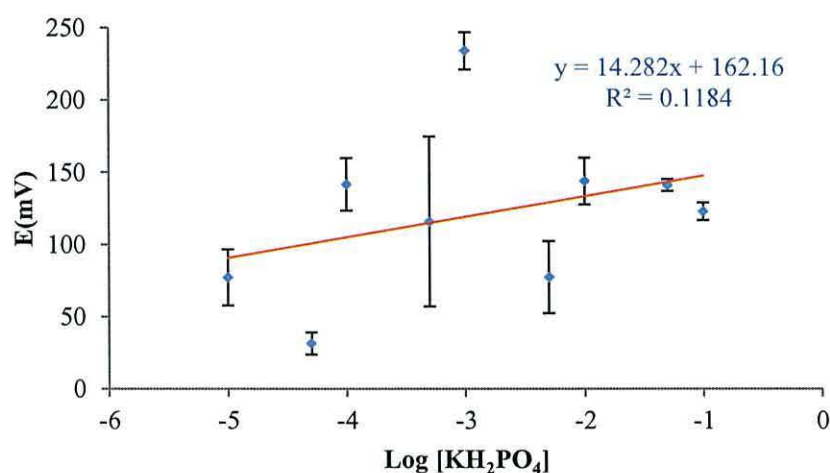


Figure 3.10: The application of ionophore 4- nitro benzo-15-crown-5 (1) for Nernstian response ( $n = 3$  and error bars (where visible) indicate the standard deviation)

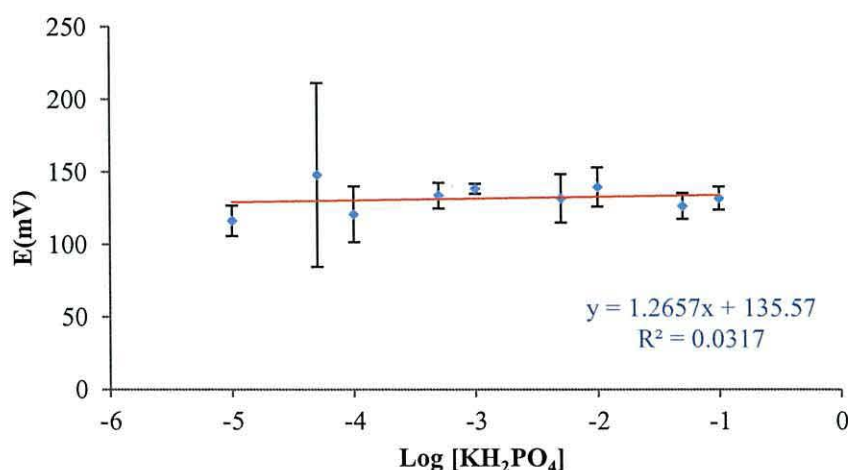


Figure 3.11: The application of ionophore 4- amino benzo-15-crown-5 (3) for Nernstian response ( $n = 3$  and error bars (where visible) indicate the standard deviation)

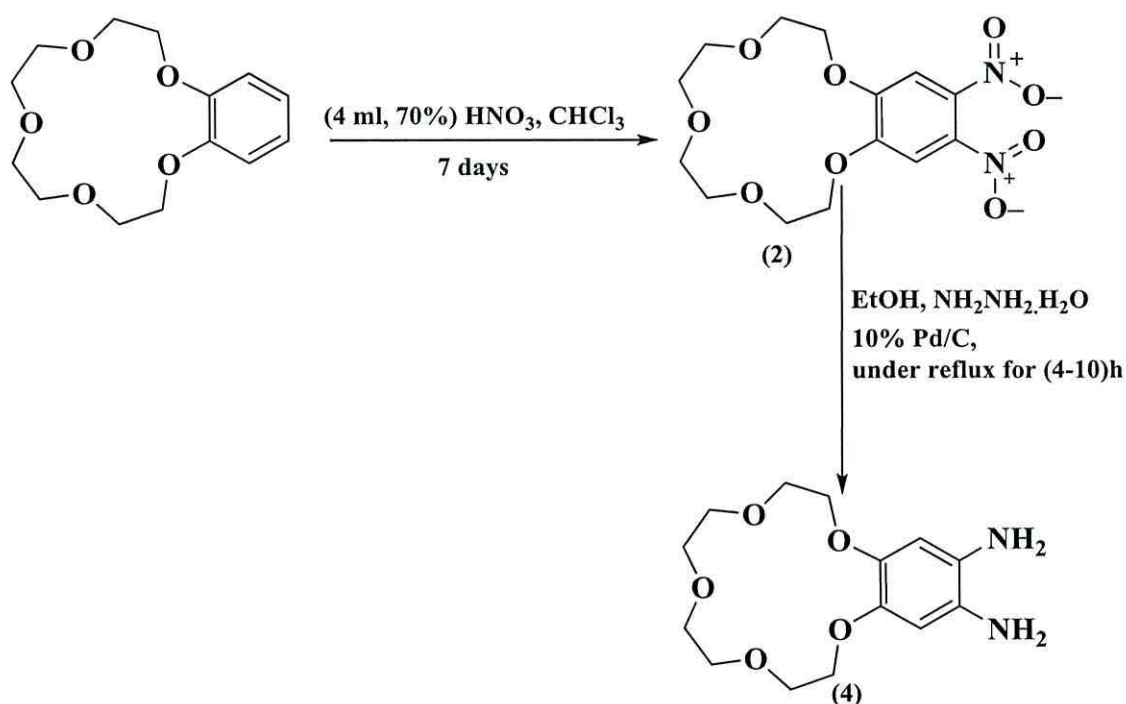
The slope of the calibration line for 4- amino benzo-15-crown-5 ionophore was  $1.2657 \pm (1.1)$  mV per decade and the  $R^2$  was 0.0317 due to there is not any correlation between those two factors with Nernstian response owed to the sensor composition from (1) or (3) as ionophors in PVC membrane.<sup>14</sup>

### 3.3 Dinitro benzo-15-crown-5 (2) and diamino benzo-15-crown-5 (4)

#### Synthesis

All NMR spectra and Mass Spectrometry data are given in Appendix in attached CD. The compounds dinitro benzo-15-crown-5 (2) and diamino benzo-15-crown-5 (4) was synthesized according to Scheme 3.2 described below. Solid benzo-15-crown-5 was added to concentrated nitric acid then  $\text{CHCl}_3$  was added to the yellow solution and the two layers were stirred for seven days. After this time the acid was diluted with an equal volume of distilled water.<sup>15</sup> The product was extracted with chloroform and evaporated to dryness leaving a yellow waxy residue. The purification of the organic layer has been done by flash chromatography (petrol /ethyl acetate 2:1). The compound was isolated as a pale yellow crystal solid. Yield (82%). The  $^1\text{H}$  NMR and  $^{13}\text{C}$  NMR spectra shown below confirm that the product (2) was formed.





*Scheme 3.2: Synthesis of dinitro benzo-15-crown-5 (2) and diamino benzo-15-crown-5 (4)*

The  $^1\text{H}$  NMR spectra exhibits a singlet at  $\delta$  7.31 ppm (2H) is due to the aromatic protons next to the carbon atom is connected to the nitro groups which represent in Ha, b from (Figure 3.12). While the multiplet at  $\delta$  4.28- 4.22 ppm which belongs to four protons in the crown cavity next to the benzene ring, and the other multiplet at  $\delta$  3.97 – 3.91 ppm belongs to the other four protons in the crown cavity next to the multiplet next to the benzene ring.

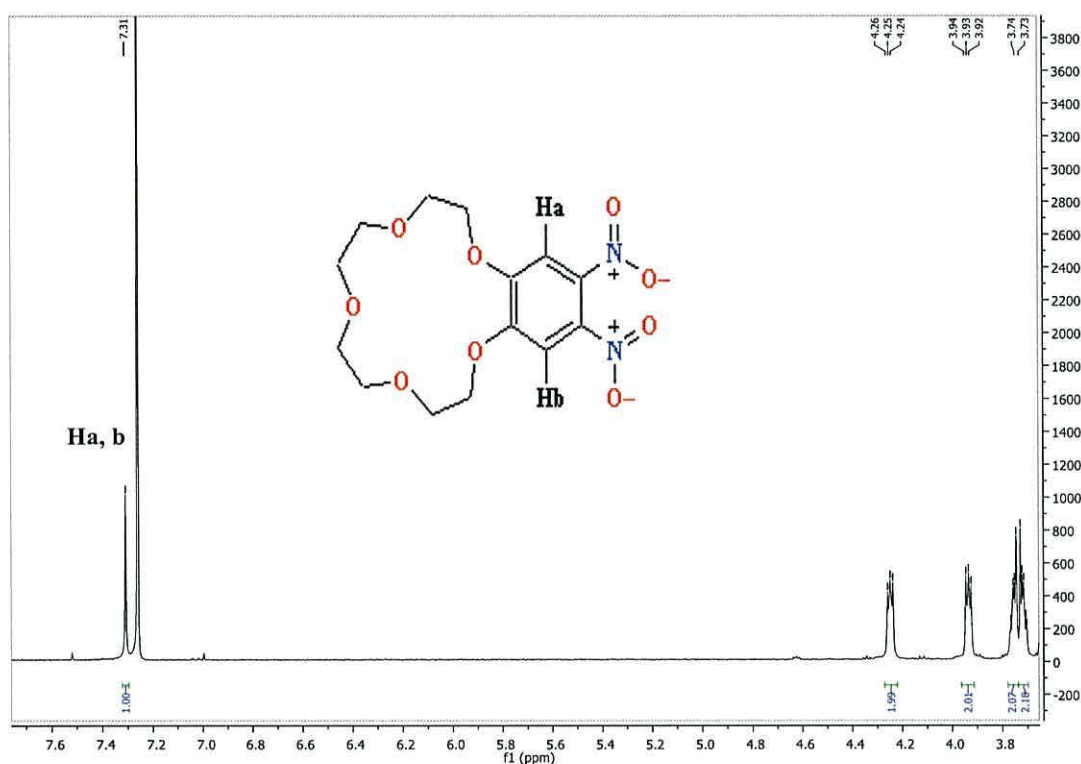


Figure 3.12:  $^1\text{H}$  NMR spectrum of dinitro benzo-15-crown-5 (2)

Finally the last multiplet at  $\delta$  3.79 – 3.69 ppm belongs to the other four protons in the crown cavity in the far end of the benzene ring and all of those multiplets are due to the ether bridges of the crown cavity compound which confirmed by COSY spectrum (Figure 3.13) and which also confirms the theoretical schemes.

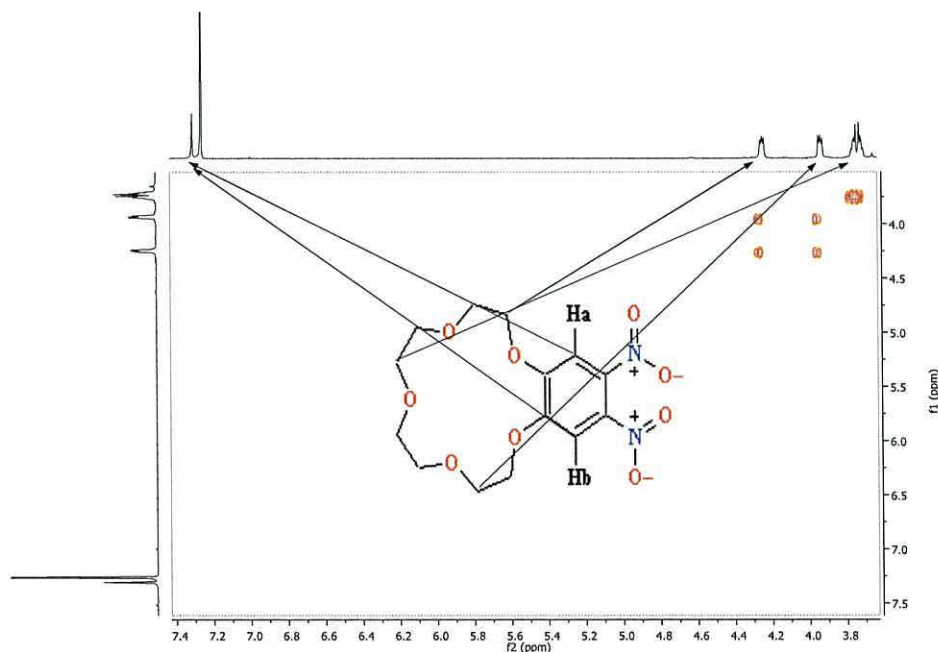


Figure 3.13: The COSY spectrum of dinitro benzo-15-crown-5 (2)

The  $^{13}\text{C}$  NMR spectrum (Figure 3.14) exhibits a signal at  $\delta$  151.98 ppm due to aromatic carbons atom attached to the cavity ring, while the signal at  $\delta$  136.84 ppm belongs to the other aromatic carbons atom linked to the nitro groups, and the other aromatic carbons represents in the signal at  $\delta$  108.55 ppm. While the series of the signals at  $\delta$  71.23, 70.23, 69.74, 68.76 ppm belong to the carbon atoms of ether groups.

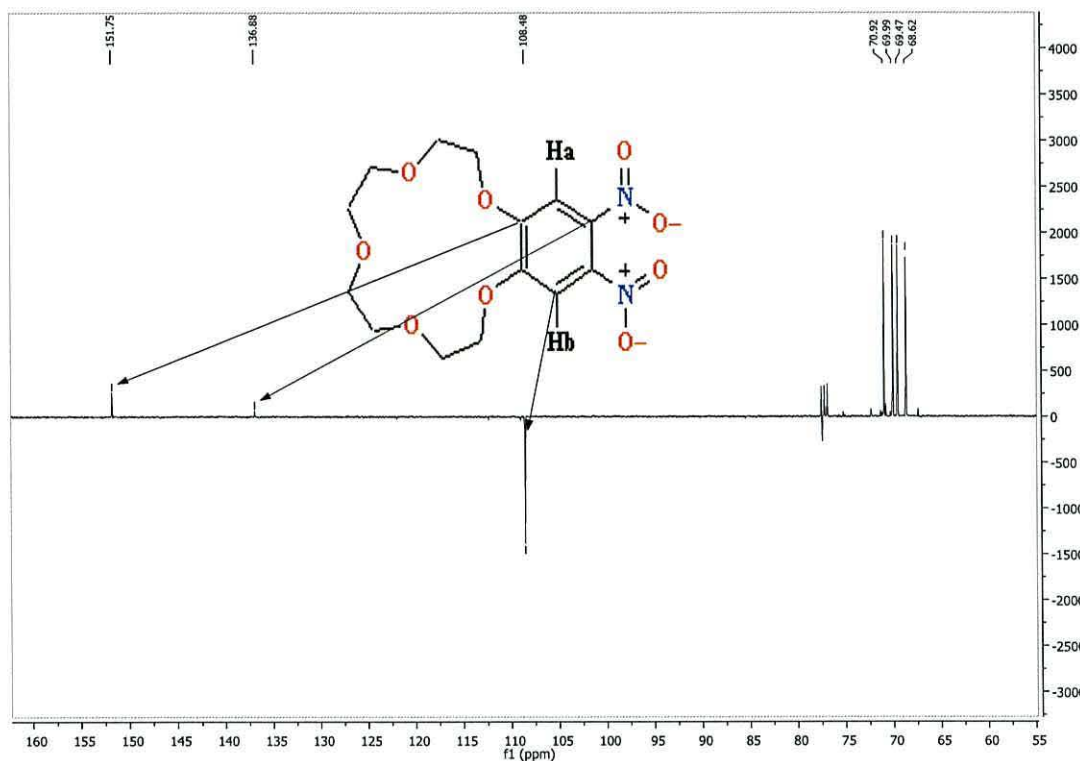


Figure 3.14: DEPT-Q NMR spectrum of dinitro benzo-15-crown-5 (2)

The  $^1\text{H}$  NMR and  $^{13}\text{C}$  NMR spectra shown below and in Appendix confirms that the product was (4) formed. The compound (4) was synthesized by dissolving di nitro benzo-15-crown-5 in ethanol. The mixture then heated to add the Pd/C (10%) catalyst and refluxed and the mixture of ethanol (20 ml) and hydrazine hydrate was added. The reaction mixture was refluxed and the catalyst was filtered off from celite plug bed. The pure tan product was collected from dichloromethane as a solid compound from that solvent.

Attempts to grow suitable crystals of this complex were successful to get the expected structured (2). Single-crystal X-ray structural analyses (Figure 3.15)



verified the expected structural arrangements of (2). Importantly this confirms the desired the closed ring cavity for these macrocyclic compounds with the strongly withdrawing nitro group separated from the crown cavity by the phenyl group. In addition, these data also show that these groups are approximately collinear and the nature of the bonding suggests that the structure should be relatively rigid. This type of atomic arrangement should be preferable to optimise efficient bonding with potassium cation in the crown cavity and the phosphate anion as a counter ion for this structure.

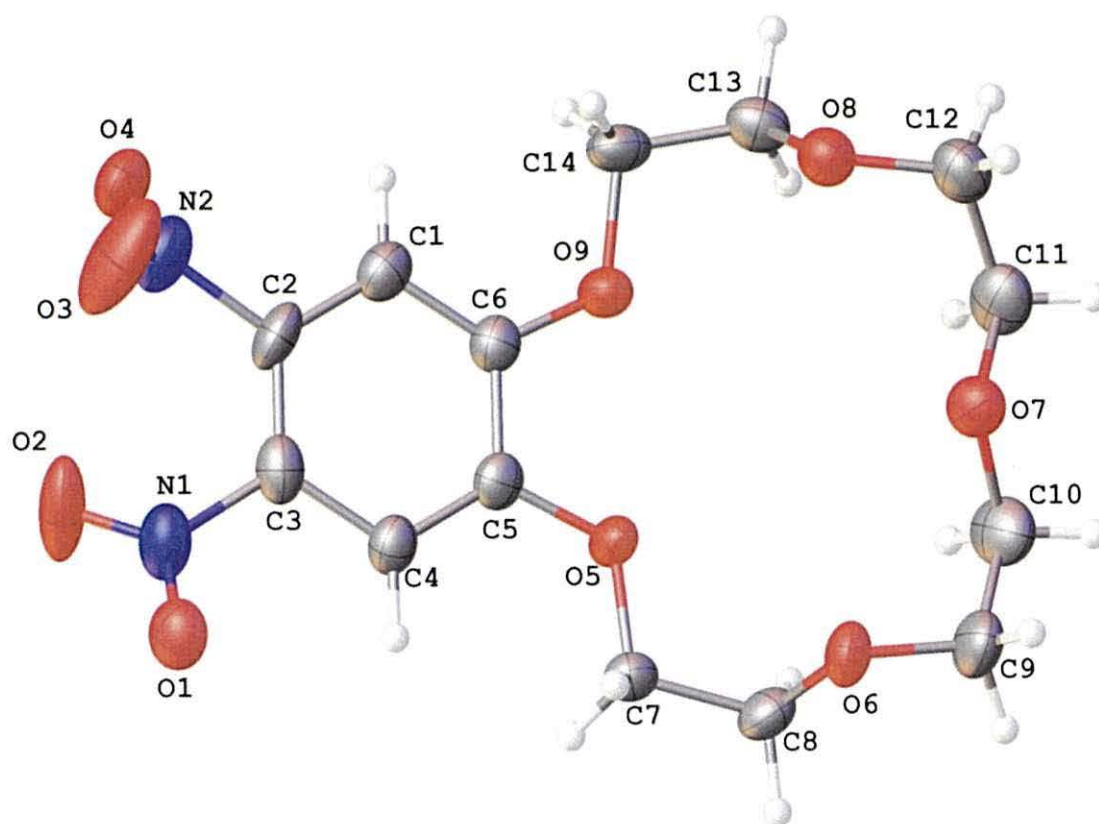


*Figure 3.15: Molecular structure of dinitro benzo-15-crown-5 (2). Displacement ellipsoids – 50% probability*

An X-ray crystal structure as well provided further clarification see Table 3. 3 and Table 3. 4.

*Table 3. 3: Crystal data and structure refinement details of dinitro benzo-15-crown-5 (2).*

|  |  |
|--|--|
| Empirical formula  | C <sub>14</sub> H <sub>18</sub> N <sub>2</sub> O <sub>9</sub>            |
| Formula weight   | 358.30   |
| Temperature  | 100(2) K   |
| The wave length  | 0.68890 Å  |
| Crystal system   | Monoclinic   |
| Space group  | <i>P</i> 21/ <i>n</i>  |
| Unit cell dimensions<br><i>a</i> = 11.613(7) Å<br><i>b</i> = 4.912(5) Å<br><i>c</i> = 21.955(17) Å | $\alpha = 90^\circ$<br>$\beta = 109.584(5)^\circ$<br>$\gamma = 90^\circ$ |
| Volume   | 1604.5(18) Å <sup>3</sup>  |
| <i>Z</i>   | 4  |
| Density (calculated)   | 1.483 Mg / m <sup>3</sup>  |
| Absorption coefficient   | 0.126 mm <sup>-1</sup>   |
| <i>F</i> (000)   | 752  |
| Crystal  | Platelet; yellow   |
| Crystal size   | 0.03 × 0.03 × 0.01 mm <sup>3</sup>                                       |
| $\theta$ range for data collection   | 2.94 – 24.21°  |
| Index ranges   | –13 ≤ <i>h</i> ≤ 13, –10 ≤ <i>k</i> ≤ 10, –20 ≤ <i>l</i> ≤ 20            |
| Reflections collected  | 13146  |
| Independent reflections  | 2903 [ <i>R</i> <sub>int</sub> = 0.1204]                                 |
| Completeness to $\theta = 24.21^\circ$   | 99.1 %   |
| Absorption correction  | Semi-empirical from equivalents  |
| Max. and min. transmission   | 0.9987 and 0.9962  |
| Refinement method  | Full-matrix least-squares on <i>F</i> <sup>2</sup>                       |
| Data / restraints / parameters   | 2903 / 0 / 227   |
| Goodness-of-fit on <i>F</i> <sup>2</sup>   | 1.059  |
| Final <i>R</i> indices [ <i>F</i> <sup>2</sup> > 2σ( <i>F</i> <sup>2</sup> )]                      | <i>R</i> 1 = 0.0695, <i>wR</i> 2 = 0.1406                                |
| <i>R</i> indices (all data)  | <i>R</i> 1 = 0.1140, <i>wR</i> 2 = 0.1657                                |
| Largest diff. peak and hole  | 0.315 and –0.317 e Å <sup>-3</sup>                                       |

**Table 3. 4:** Atomic coordinates [ $\times 10^4$ ], equivalent isotropic displacement parameters [ $\text{\AA}^2 \times 10^3$ ] and site occupancy factors.  $U_{eq}$  is defined as one third of the trace of the orthogonalized  $U^{ij}$  tensor of dinitro benzo-15-crown-5 (2).

| Atom | x               | y       | z     | $U_{eq}$ S.o.f. |
|------|-----------------|---------|-------|-----------------|
| C1   | 5083(4)2106(5)  | 2765(3) | 40(1) | 1               |
| C2   | 4283(4)1449(5)  | 3113(3) | 42(1) | 1               |
| C3   | 3742(4)19(5)    | 2857(3) | 39(1) | 1               |
| C4   | 3981(4)–816(5)  | 2228(2) | 35(1) | 1               |
| C5   | 4769(4)–163(5)  | 1877(2) | 32(1) | 1               |
| C6   | 5320(4)1316(5)  | 2137(2) | 34(1) | 1               |
| C7   | 4683(4)–2408(5) | 1021(3) | 36(1) | 1               |
| C8   | 5211(4)–2864(5) | 373(3)  | 42(1) | 1               |
| C9   | 7177(5)–3187(6) | 226(3)  | 53(1) | 1               |
| C10  | 7507(5)–1564(6) | 46(3)   | 54(1) | 1               |
| C11  | 8594(5)711(6)   | 609(3)  | 50(1) | 1               |
| C12  | 9268(4)1561(6)  | 1366(3) | 47(1) | 1               |
| C13  | 7775(4)3194(5)  | 1639(3) | 41(1) | 1               |
| C14  | 6882(4)3153(5)  | 2095(3) | 42(1) | 1               |
| N1   | 2825(4)–646(5)  | 3179(2) | 48(1) | 1               |
| N2   | 4109(4)2281(5)  | 3811(3) | 53(1) | 1               |
| O1   | 2783(3)–2083(4) | 3243(2) | 48(1) | 1               |
| O2   | 2127(4)263(4)   | 3351(3) | 74(1) | 1               |
| O3   | 4321(5)1564(5)  | 4452(2) | 95(2) | 1               |
| O4   | 3815(3)3673(4)  | 3713(2) | 51(1) | 1               |
| O5   | 5089(3)–841(3)  | 1269(2) | 36(1) | 1               |
| O6   | 6472(3)–3229(4) | 761(2)  | 44(1) | 1               |
| O7   | 8272(3)–832(3)  | 786(2)  | 42(1) | 1               |
| O8   | 8570(3)1888(4)  | 1895(2) | 41(1) | 1               |
| O9   | 6086(3)1824(3)  | 1757(2) | 39(1) | 1               |

The  $^1\text{H}$  NMR spectrum in Appendix, exhibits a singlet at  $\delta$  6.49 ppm (2H) due to the aromatic protons next to the carbon atom is connected to the amino groups which represent in Ha, b from (Figure 3.16). While the other singlet at  $\delta$  4.87 ppm which relates to protons from the amino groups. This is confirmed by the COSY spectrum (Figure 3.17). The multiplet at  $\delta$  4.07 – 4.01 ppm belongs to four protons in the crown cavity next to the benzene ring. The other multiplet at  $\delta$  3.86 – 3.81 ppm belongs to the other four protons in the crown cavity next to the multiplet next to the benzene ring. Finally the singlet at  $\delta$  3.72 ppm belongs to the other eight protons in the crown cavity furthest from the benzene ring due to the ether bridges of the crown cavity.



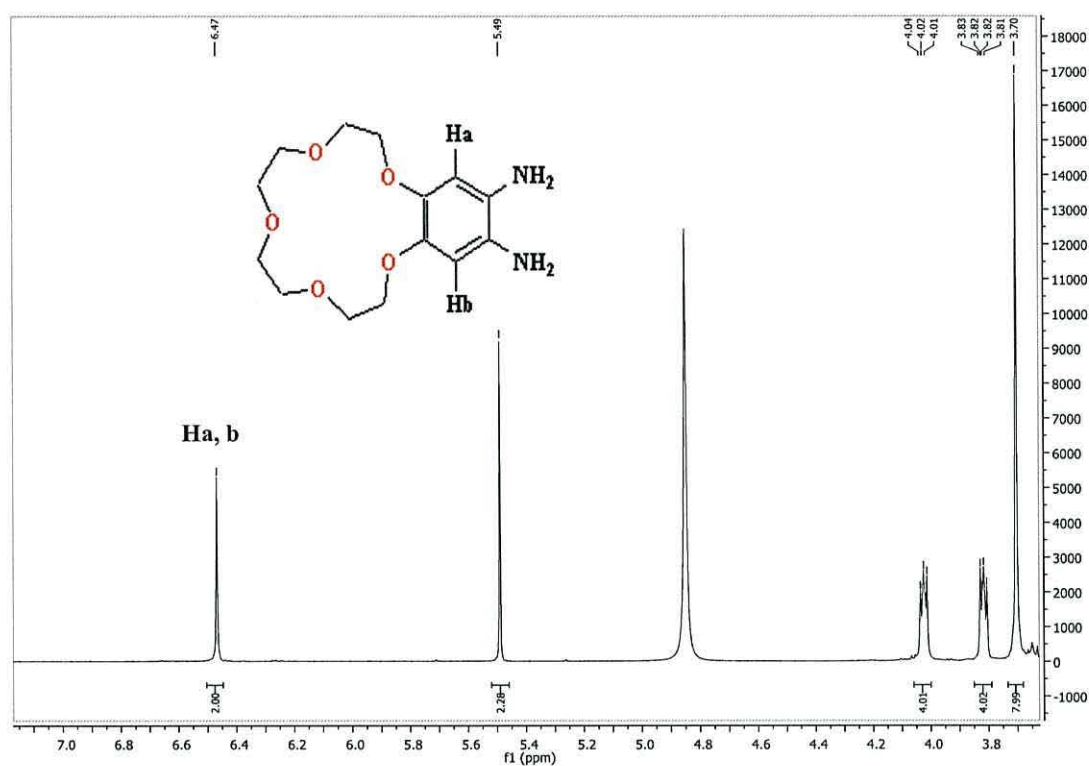


Figure 3.16: <sup>1</sup>H NMR spectrum of diamino benzo-15-crown-5 (4)

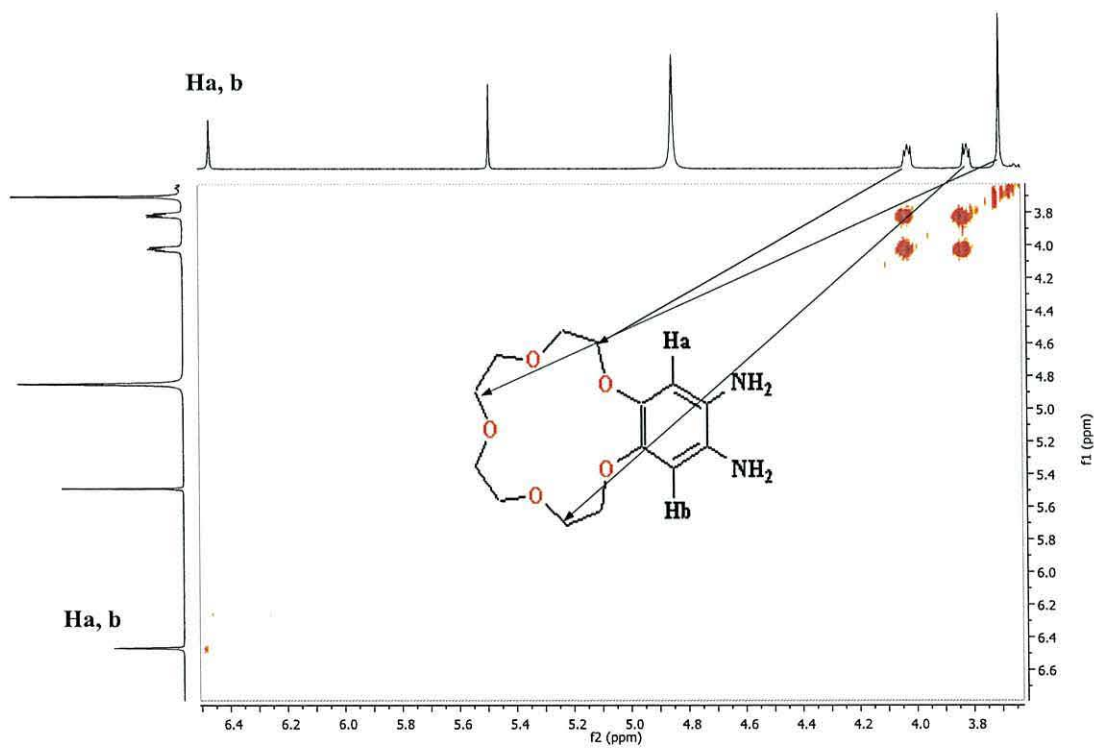
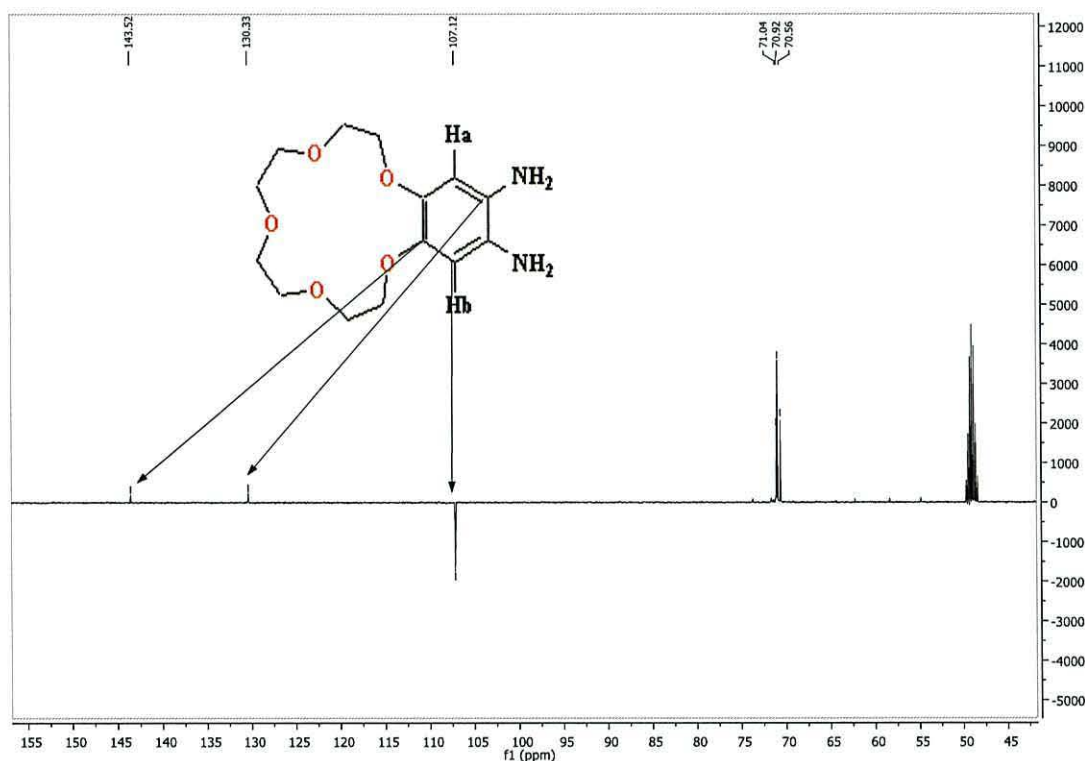


Figure 3.17: The COSY spectrum of di amino benzo-15-crown-5 (4)

The  $^{13}\text{C}$  NMR spectrum (Figure 3.18) exhibits a signal at  $\delta$  143.52 ppm belongs to aromatic carbons atom attached to the cavity ring, while the signal at  $\delta$  130.33 ppm belongs to the other aromatic carbons atom linked to the amino groups, and the other aromatic carbons represents in the signal at  $\delta$  107.12 ppm.



**Figure 3.18: DEPT-Q NMR spectrum of diamino benzo-15-crown-5 (4)**

For a comparison purposes, (Figure 3.19) shows the differences in the spectra's between those two functional groups on benzo ring attached to the crown cavity for ionophore (2) and ionophore (4) compounds respectively. The effect of the withdrawing group shifts more to the down field on the opposite of the donating group which shifts more to the high field.

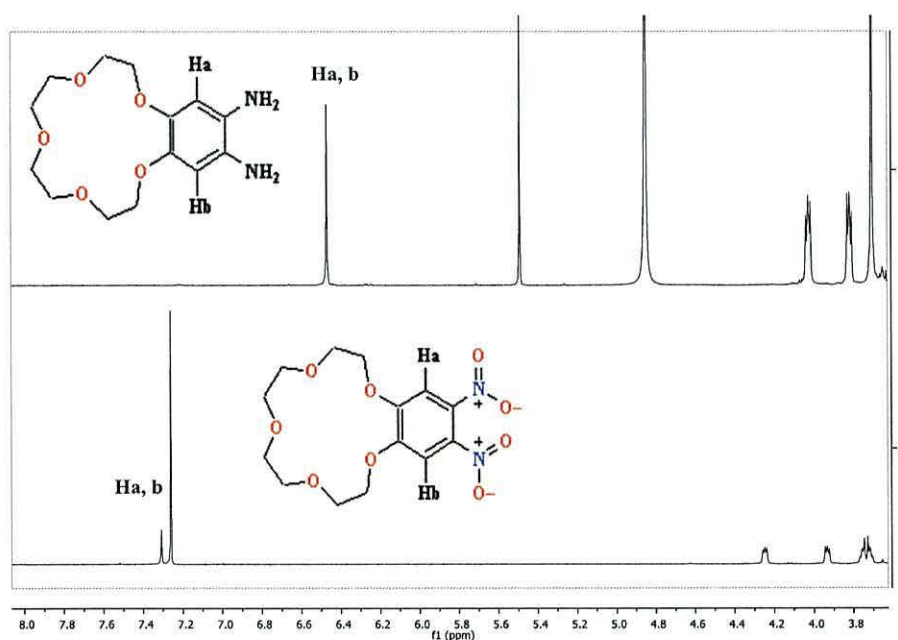


Figure 3.19: The characteristic signal of the protons (Ha, b) as a comparison between the nitro and the amino groups in a benzo ring of the dinitro benzo-15-crown-5 (2) and diamino benzo-15-crown-5 (4) macrocyclic compounds respectively.

### Performance

The potentiometric response of the ISE modified with ionophore (2) was investigated for the potassium phosphate. Appropriate aliquots of the stock solution were introduced to the cell and the corresponding potentials determined. The potential readings were plotted against the logarithmic values of the concentration over a range of  $5 \times 10^{-5} \text{ mol L}^{-1}$  to  $1 \times 10^{-1} \text{ mol L}^{-1}$  as in (Figure 3.20).

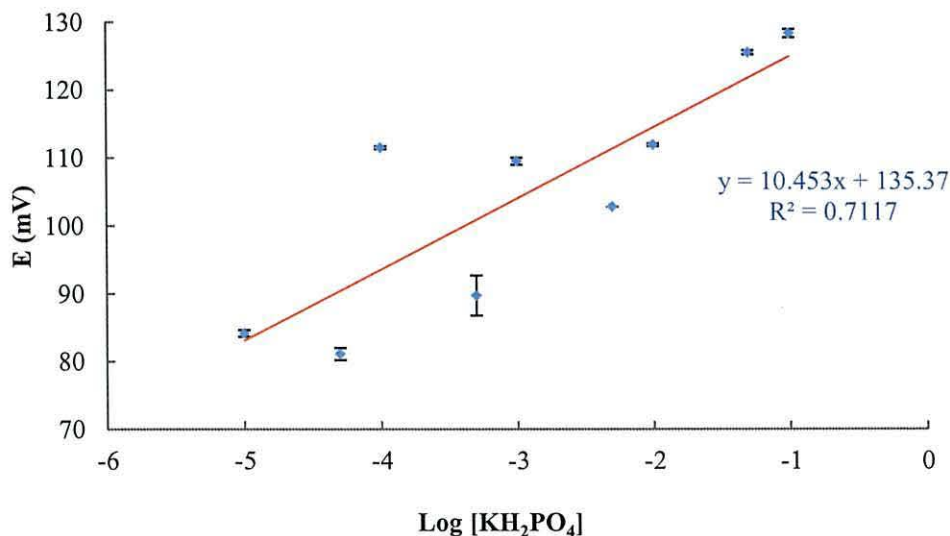
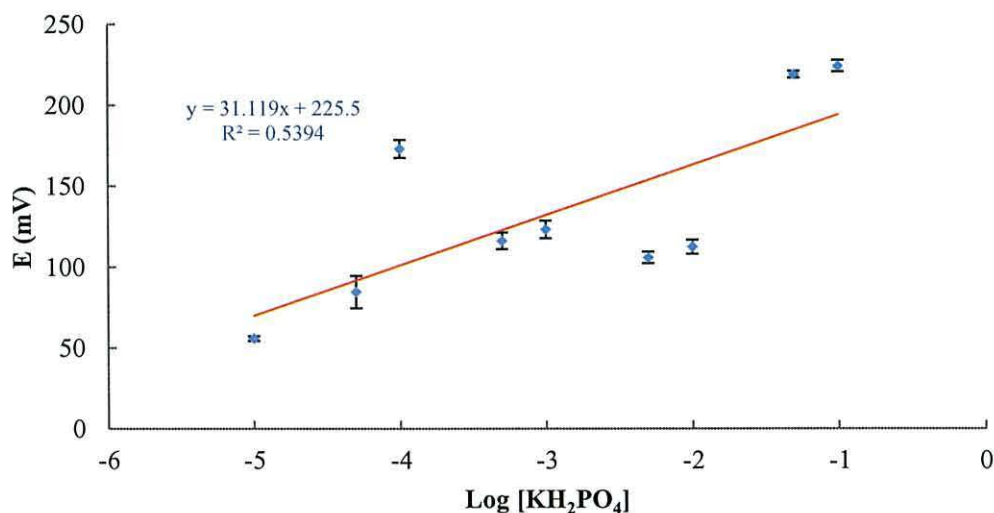


Figure 3.20: The application of dinitro benzo-15-crown-5 (2) ionophore for Nernstian response ( $n = 3$  and error bars (where visible) indicate the standard deviation)



The slope of the calibration line for ionophore (2) was  $10.45 \pm (1.1)$  mV per decade and the limit of detection was  $1.9 \times 10^{-4}$  mol L<sup>-1</sup>; when the error bars are considered it can be seen that the low concentration have increased errors this is thought to be due to the associated increase in response time for the sensor which relates with the sensor composition.<sup>14</sup>

The potentiometric response of the ISE modified with ionophore (4) was also investigated against the potassium phosphate. Appropriate aliquots of the stock solution were introduced to the cell and the corresponding potentials determined. The potential readings were plotted against the logarithmic values of the concentration over a range of  $5 \times 10^{-5}$  mol L<sup>-1</sup> to  $1 \times 10^{-1}$  mol L<sup>-1</sup> (Figure 3.21).



**Figure 3.21:** The application of the synthesised ionophore diamino benzo-15-crown-5 (4) for Nernstian response ( $n = 3$  and error bars (where visible) indicate the standard deviation)

The slope of the calibration line for ionophore (4) was  $31.11 \pm (1.1)$  mV per decade and the limit of detection was  $1.6 \times 10^{-5}$  mol L<sup>-1</sup>; with the low error bars.<sup>14</sup> In addition to that, the calibration of the potentiometric response for the ionophore 1-aza-18-crown-6 is explained as in (Figure 3.22).

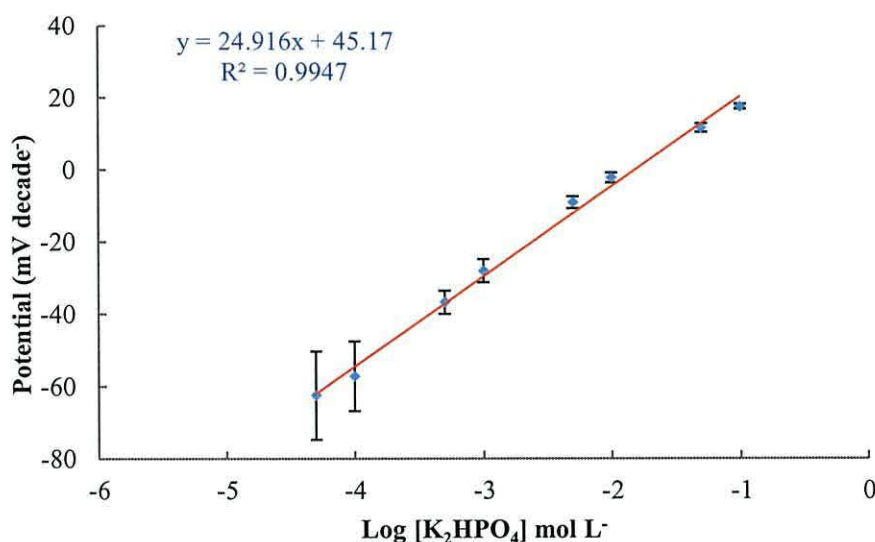


**Figure 3.22:** Potential response of the potassium ISE containing ionophore 1-aza-18-crown-6 vs. Ag/AgCl reference electrode for increasing concentrations of potassium phosphate ion at pH 9. ( $n = 3$  and error bars error bars (where visible) indicate the standard deviation)

The slope of the calibration line for 1-aza-18-crown-6 ionophore was  $24.916 \pm (1.1)$  mV per decade and the limit of detection was  $4.5 \times 10^{-4}$  mol L<sup>-1</sup>; at low concentration the error bars are considered.<sup>14</sup> While the potentiometric response of the membrane of the dicyclohexyl-18-crown-6 ionophore can be seen in (Figure 3.23).

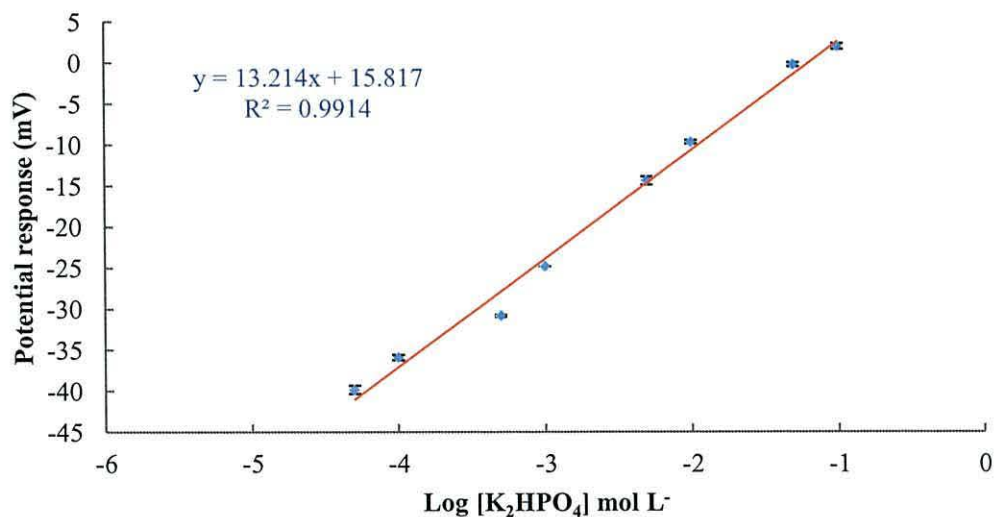


**Figure 3.23:** Potential response of the potassium ISE containing dicyclohexyl-18-crown-6 ionophore vs. Ag/AgCl reference electrode for increasing concentrations of potassium phosphate ion at pH 9. ( $n = 3$  and error bars error bars (where visible) indicate the standard deviation)

(Figure 3.23) shows the low potentiometric response by the slope of the calibration line for dicyclohexyl-18-crown-6 ionophore was  $13.21 \pm (1.1)$  mV per decade and the limit of detection was  $1.2 \times 10^{-4}$  mol L<sup>-1</sup>; the sensor composition of dicyclohexyl-18-crown-6 has high level of error bars.<sup>14</sup> The missing of the aromatic system has an effect of non-Nernstian response due to lose the delocalisation of the charges in the whole macrocyclic compound system in the PVC membrane.

On the other hand; the high potential response of the benzo-18-crown-6 ionophore in the membrane can be seen in (Figure 3.24).

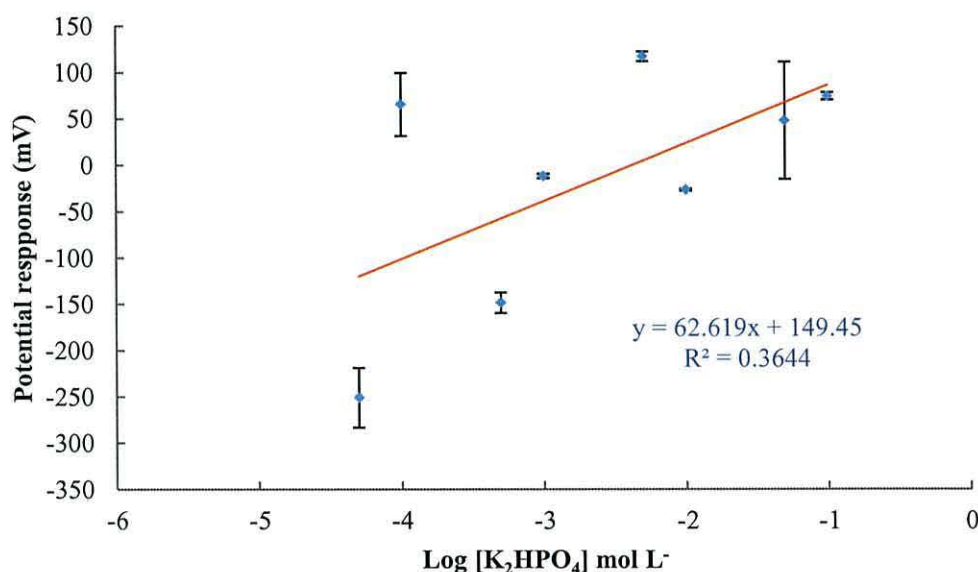


**Figure 3.24:** Potential response of the potassium ISE containing benzo-18-crown-6 ionophore vs. Ag/AgCl reference electrode for increasing concentrations of potassium phosphate ion at pH 9. ( $n = 3$  and error bars error bars (where visible) indicate the standard deviation)

The high value of the potentiometric response of the calibration line for benzo-18-crown-6 ionophore was  $62.61 \pm (1.1)$  mV per decade and the limit of detection was  $1.1 \times 10^{-4}$  mol L<sup>-1</sup>; the error bars are related to the sensor structure from this ionophore within the PVC membrane.<sup>14</sup>

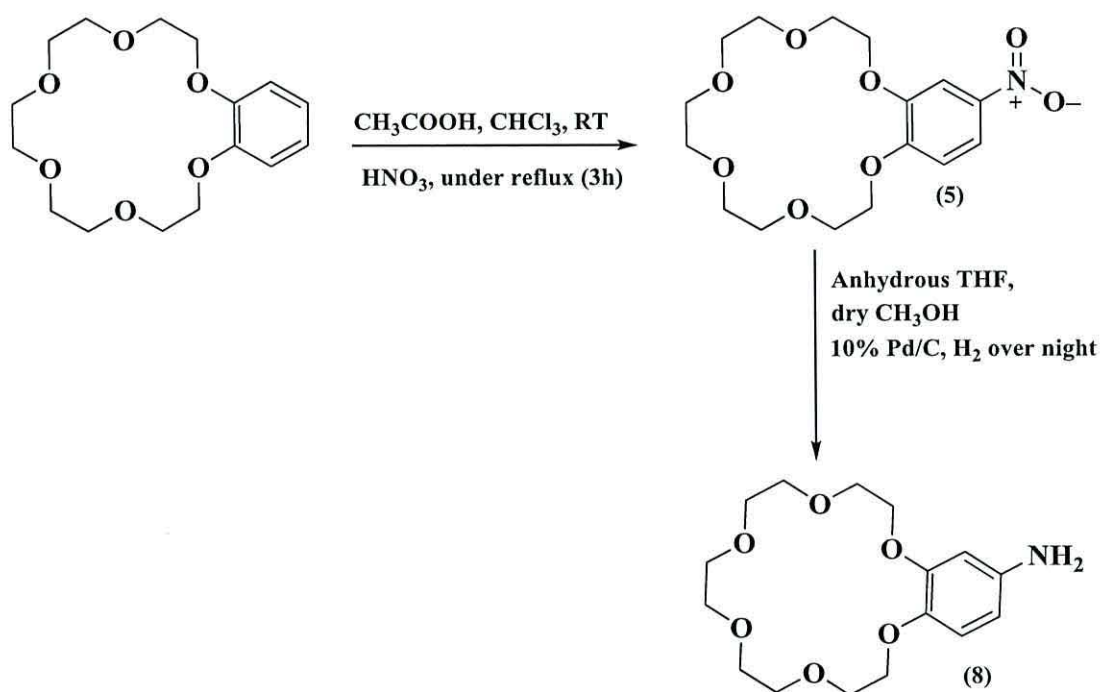
### 3.4 4-nitro (5) and 4-amino (8) benzo-18-crown-6

#### Synthesis

All NMR spectra and Mass Spectrometry data are given in Appendix in attached CD. The compounds 4-nitro benzo-18-crown-6 (5) and 4-amino benzo-18-crown-6 (8)



were synthesized according to Scheme 3.3. Benzo-18-crown-6 was dissolved in  $\text{CHCl}_3$ . Acetic acid was added to the solution then a mixture of  $\text{HNO}_3$  in acetic acid was added stirred at room temperature then heated to reflux then the reaction has been cooled down to room temperature and extracted with ethyl.<sup>12</sup> The purification of the organic layer was done by flash chromatography (petrol /ethyl acetate 1:1). The compound was isolated as a pale yellow solid in yield 80%.



*Scheme 3.3: Synthesis of 4-nitro benzo-18-crown-6(5) and 4-amino benzo-18-crown-6(8)*

The  $^1\text{H}$  NMR and  $^{13}\text{C}$  NMR spectra shown below and in Appendix confirm that the product (5) was formed. The  $^1\text{H}$  NMR spectrum exhibits a doublet of doublets at  $\delta$  7.89 (dd,  $J = 8.9, 2.6$  Hz, 1H) due to the aromatic protons next to the carbon atom which connected to the nitro group which represent in Hb (Figure 3.25). While the other aromatic protons appear as doublet at  $\delta$  7.74 ppm (d,  $J = 2.6$  Hz, 1H) which belongs to Ha and as another doublet at  $\delta$  6.88 ppm (d,  $J = 8.9$  Hz, 1H) which belongs to Hc. The series of multiplet at  $\delta$  4.27 – 4.20 ppm (m, 4H), 3.98 – 3.92 (m, 4H), 3.80 – 3.75 (m, 4H), are due to the ether bridges of the crown cavity compound. The  $^{13}\text{C}$  NMR spectrum exhibits signals at  $\delta$  154.58 and  $\delta$  146.14 ppm due to the

aromatic carbon atoms which attached to the crown cavity. The signals in downfield at  $\delta$  145.26 ppm belong to the carbon connected to the nitrogen atom of the nitro group. The signals at  $\delta$  118.09, 111.44, and 108.38 ppm belong to the other carbons of the benzene ring, while the other series of signals at  $\delta$  71.13, 70.94, 70.88, 70.76, 70.71, 69.38, 69.31, and 69.25 ppm belong to the carbon atoms of the ether bridges of the crown compound.

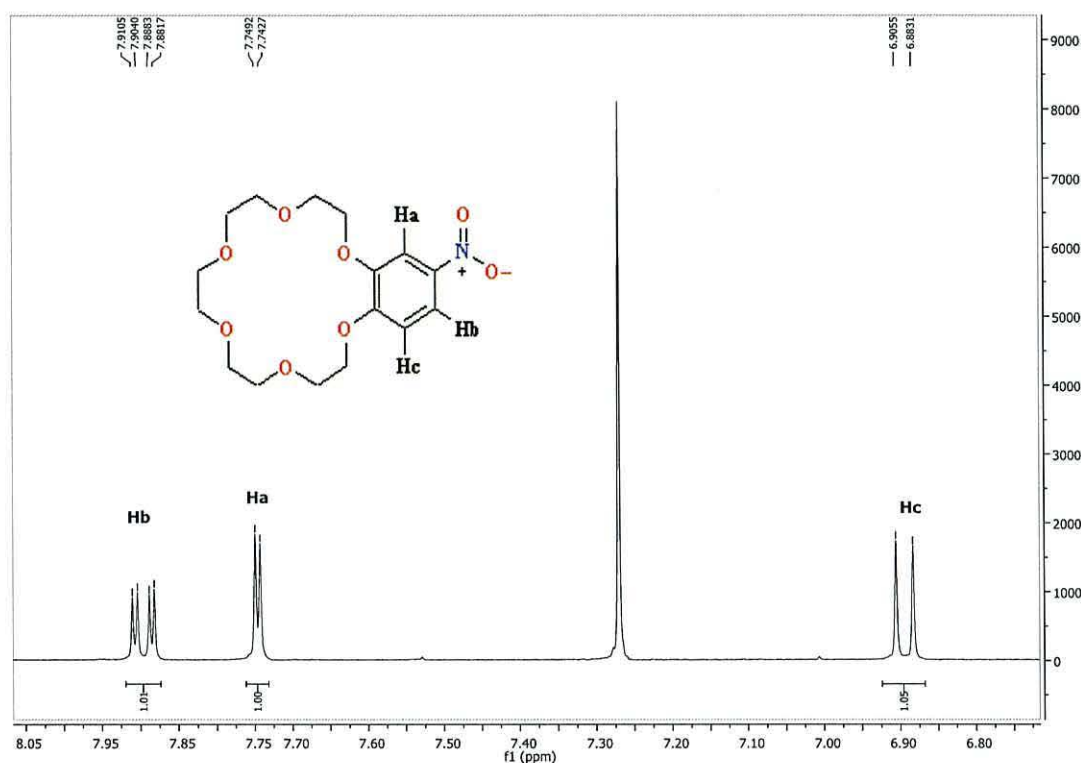


**Figure 3.25:** The characteristic signal of the protons (Ha, Hb, and Hc) adjacent to the nitro group 4-nitro benzo-18-crown-6 (5)

For the synthesis of product (8), the starting material 4-nitro benzo-18-crown-6 was dissolved in anhydrous THF and dry  $\text{CH}_3\text{OH}$ . Then the solution was degassed using nitrogen and 10% Pd/C was added as a catalyst.<sup>12</sup> The mixture was stirred overnight to complete the hydrogenation process. The compound was isolated as a tan solid. The  $^1\text{H}$  NMR and  $^{13}\text{C}$  NMR spectra shown confirm that the product (8) was formed. The  $^1\text{H}$  NMR spectrum exhibits at  $\delta$  6.73 ppm (d,  $J = 8.4$  Hz, 1H) which represents in Ha belongs to the proton on carbon atom in the far end to the carbon attached to the amino group, while the other proton on carbon atoms next to the carbon attached to the amino group appears as doublet at  $\delta$  6.30 ppm (d,  $J = 2.6$  Hz, 1H) which

represents in Hc and a doublet of doublets at  $\delta$  6.23 ppm (dd,  $J = 8.4, 2.5$  Hz, 1H) which represents in Hb. The signals of multiplets and singlet at  $\delta$  4.14 – 4.05 ppm (m, 4H),  $\delta$  3.94 – 3.90 (m, 4H) ppm,  $\delta$  3.89– 3.85 (m, 2H) ppm,  $\delta$  3.79 – 3.69 ppm (m, 8H), and the singlet at  $\delta$  3.68 ppm (s, 4H) belongs to the ether bridges of the crown structure; as seen in (Figure 3.26). As a comparison between these two groups on benzo group attached to the crown cavity for these two ionophores are as in (Figure 3.27).

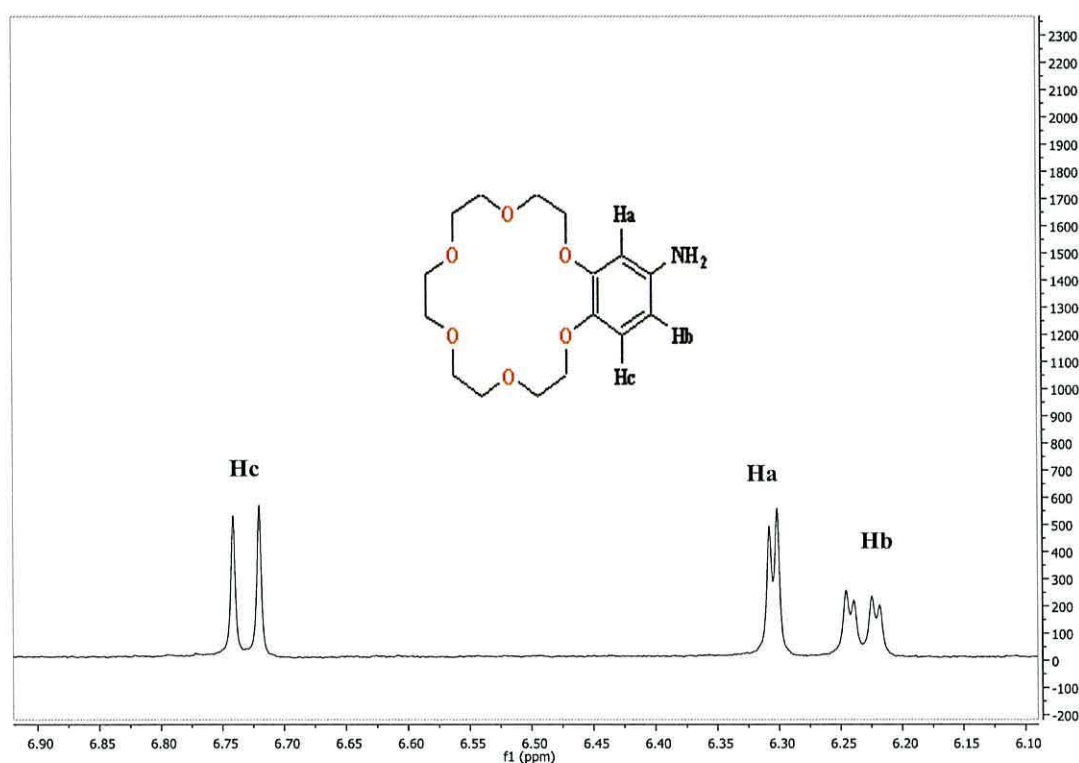


**Figure 3.26:** The characteristic signal of the protons (Ha, Hb, and Hc) adjacent to an amino group of 4-amino benzo-18-crown-6 (8)



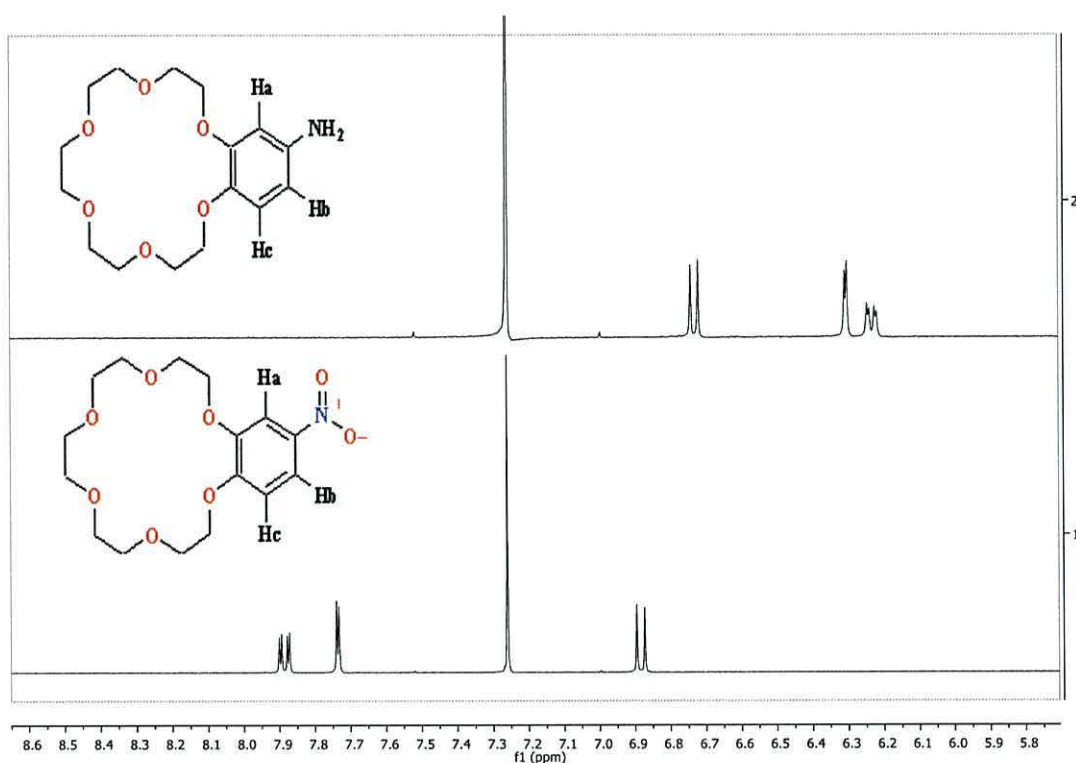


**Figure 3.27:** The characteristic signal of the protons (Ha, Hb, and Hc) as a comparison between the nitro and the amino groups in a benzo ring of the 4-nitro benzo-18-crown-6(5) and 4-amino benzo-18-crown-6 (8) macrocyclic compounds

The  $^{13}\text{C}$  NMR spectrum (Figure 3. 28) exhibits a signal at  $\delta$  150.45 ppm belongs to carbon atom attached to the amino group, while the signals at  $\delta$  141.96, 141.60 ppm belong to the two carbon atoms attached to the ether groups in the structure. The signals at  $\delta$  117.50, 107.44 ppm belong to the carbon atoms next to the carbon attached to the amino group and the signal at  $\delta$  102.96 ppm belongs to the other aromatic carbon atom in benzo group. While the series of the signals at  $\delta$  71.02, 70.97, 70.95, 70.93, 70.88, 70.80, 70.64, 70.13, 69.85, 68.95 ppm belong to the carbon atoms of ether groups in the crown structure.

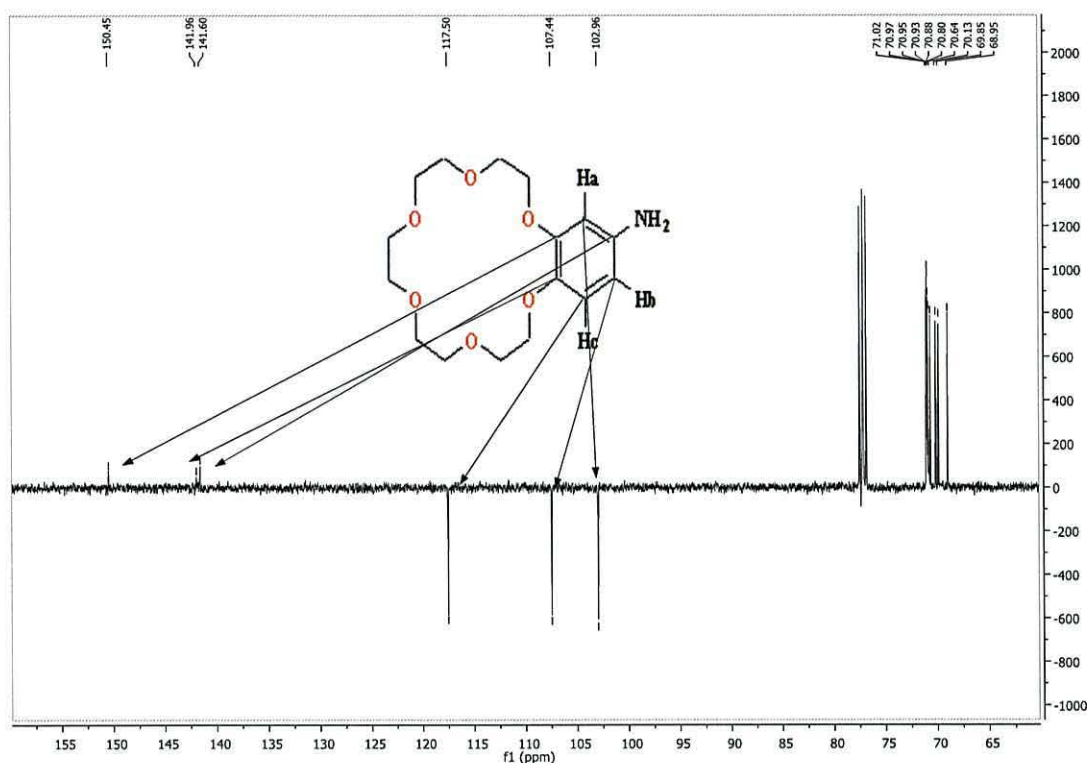
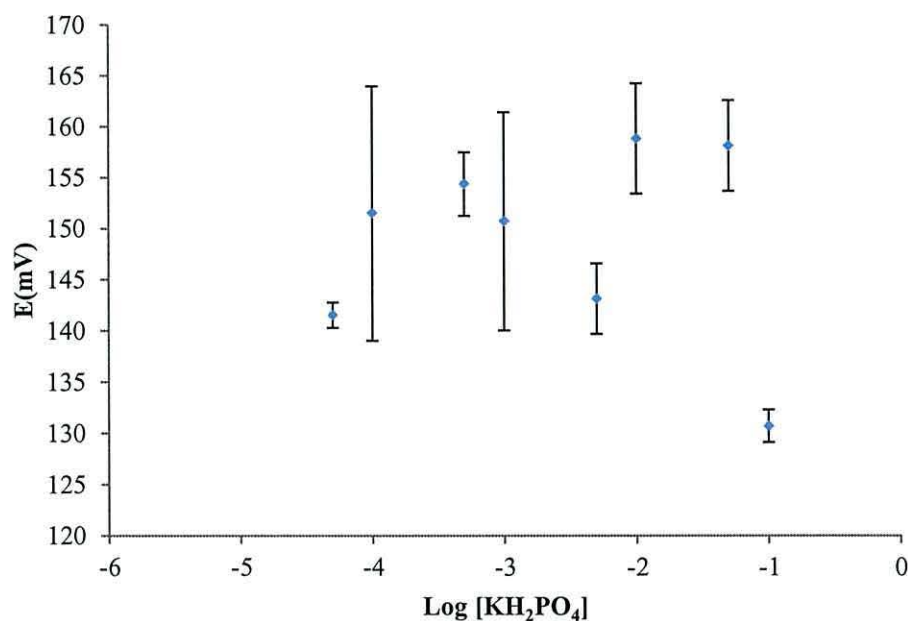


Figure 3. 28: DEPT-Q spectrum of 4-amino benzo-18-crown-6 (8)

## Performance

The potentiometric response of the ISE modified with 4-nitrobenzo-18-crown-6 ionophore (5) was investigated against the potassium phosphate. Appropriate aliquots of the stock solution were introduced to the cell and the corresponding potentials determined. The potential readings were plotted against the logarithmic values of the concentration over a range of  $5 \times 10^{-5} \text{ mol L}^{-1}$  to  $1 \times 10^{-1} \text{ mol L}^{-1}$  (Figure 3.29).



**Figure 3.29:** The application of the synthesised ionophore 4-nitro benzo-18-crown-6(5) for Nernstian response ( $n = 3$  and error bars (where visible) indicate the standard deviation)

The slope of the calibration line for (5) ionophore was  $-0.8525 \pm (1.1)$  mV per decade which refers to the non Nernstain response for this ionophore.<sup>14</sup>

For the potentiometric response of the ISE modified with ionophore (8). The potential readings were plotted against the logarithmic values of the concentration over a range of  $5 \times 10^{-5}$  mol L<sup>-1</sup> to  $1 \times 10^{-1}$  mol L<sup>-1</sup> (Figure 3.30).

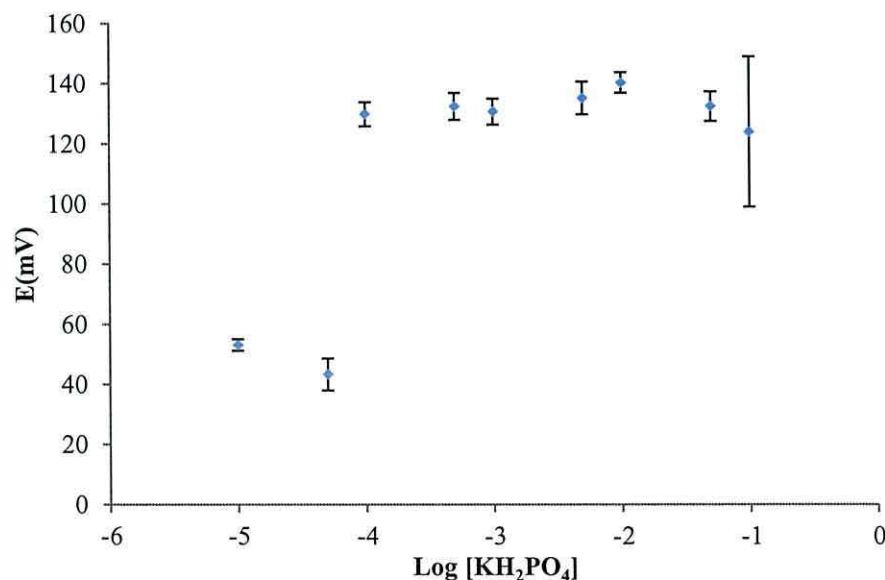


**Figure 3.30:** The application of the synthesised ionophore 4-amino benzo-18-crown-6(8) for Nernstian response ( $n = 3$  and error bars (where visible) indicate the standard deviation)

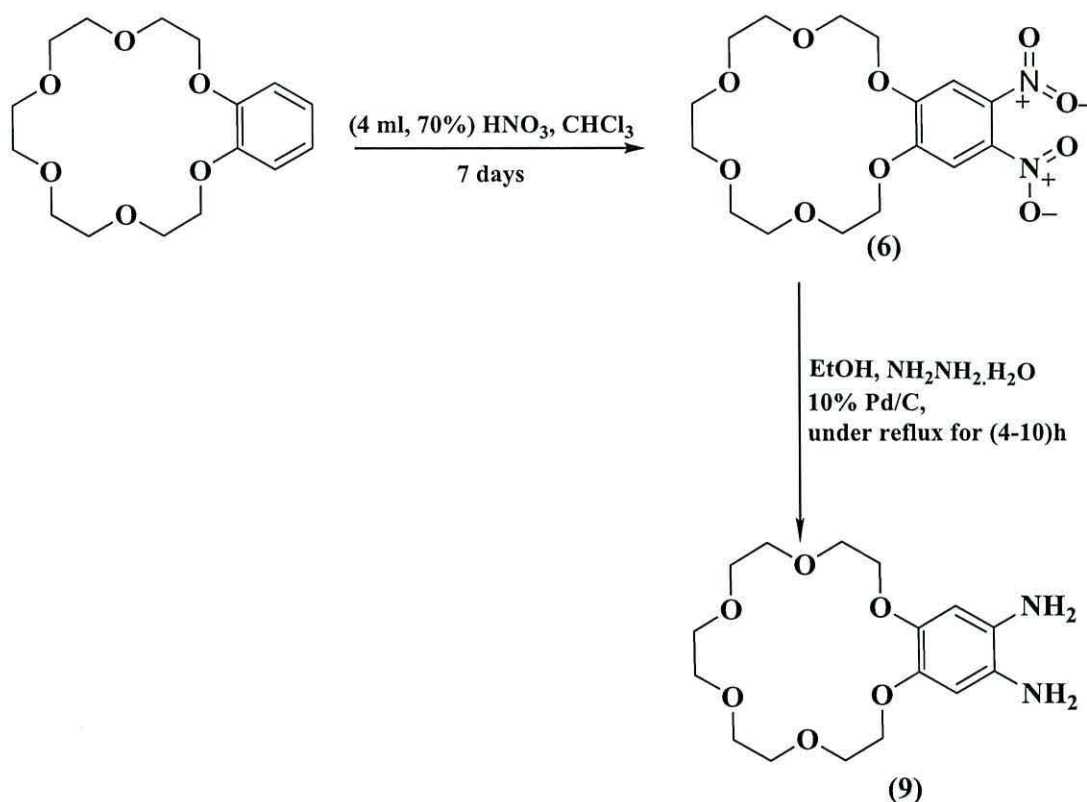


The slope of the calibration line for 4-aminobenzo-18-crown-6 ionophore (8) was  $18.90 \pm (1.1)$  mV per decade and the limit of detection was  $1.8 \times 10^{-4}$  mol L<sup>-1</sup> at high error bars for the concentrated solutions.<sup>14</sup>. The low value of the R<sup>2</sup> refers to the poor response for 4-aminobenzo-18-crown-6 as an ionophore in the PVC membrane.

### **3.5 Dinitro benzo-18-crown-6 (6) and diamino benzo-18-crown-6 (9)**

#### **Synthesis**

All NMR spectra and Mass Spectrometry data are given in Appendix in attached CD. The compounds dinitro benzo-18-crown-6 (6) and diamino benzo-18-crown-6 (9) was synthesized according to Scheme 3.4 described below. Solid benzo-18-crown-6 was added slowly to a concentrated nitric acid (70%), then CHCl<sub>3</sub> (5 mL) was added to the solution and stirred for seven days.<sup>15</sup> The product was extracted with chloroform and evaporated to dryness leaving a yellow waxy residue. The purification of the organic layer has been done by flash chromatography (petrol /ethyl acetate 5:2). The compound was isolated as a pale yellow solid in Yield (88%).



*Scheme 3.4: The scheme of synthesis dinitro benzo-18-crown-6 (6) and diamino benzo-18-crown-6 (9)*

The <sup>1</sup>H NMR spectrum exhibits a singlet at δ 7.31 ppm (2H) due to the aromatic protons next to the carbon atom which connected to the nitro groups which represent in Ha, b from (Figure 3.31). The multiplet at δ 4.32 – 4.25 ppm belongs to the four protons in the crown cavity next to the benzene ring. The other multiplet at δ 3.94 – 3.90 ppm belongs to the other four protons in the crown cavity. Finally the last multiplet at δ 3.74 – 3.71 ppm belongs to the other four protons in the crown cavity in the far end of benzene ring, while the singlet at δ 3.66 ppm belong to the last four protons due to the ether bridges of the crown cavity compound which confirmed by COSY spectrum in Appendix which also confirms the theoretical schemes.

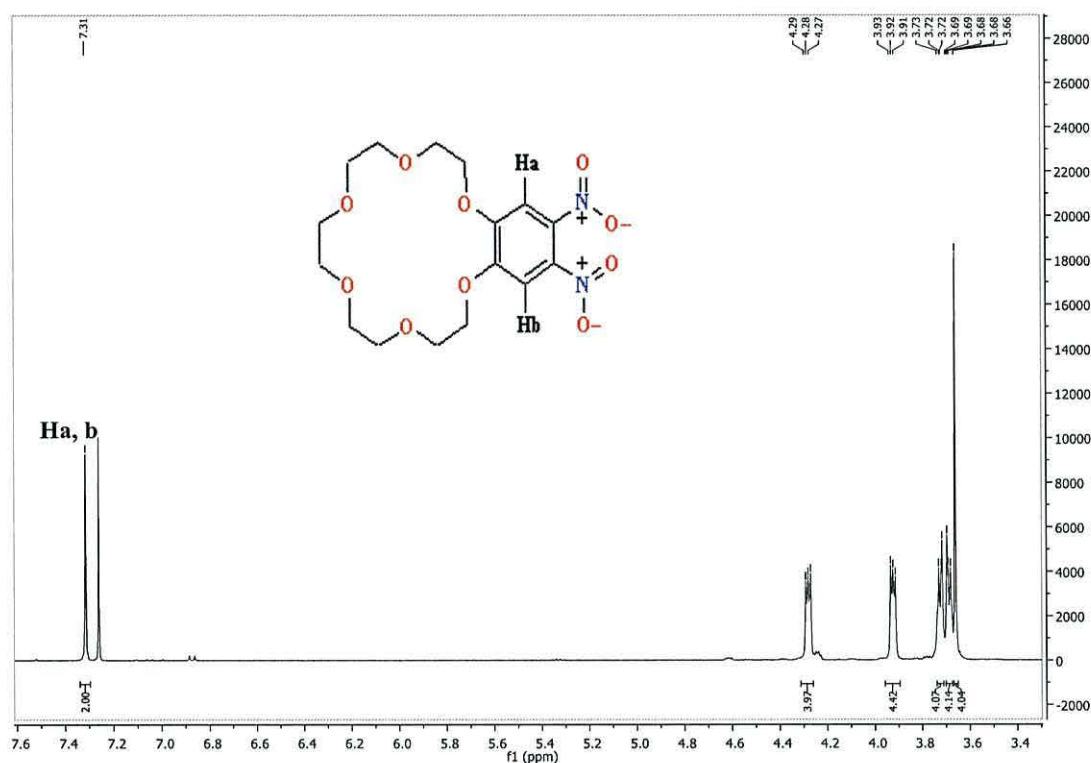


Figure 3.31: The  $^1\text{H}$  NMR spectra of ininitro benzo-18-crown-6 (6) ionophore

The  $^{13}\text{C}$  NMR spectrum exhibits a signal at  $\delta$  151.38 ppm belongs to aromatic carbons atom attached to the cavity ring, while the signal at  $\delta$  136.59 ppm belongs to the other aromatic carbons atom linked to the nitro groups, and the other aromatic carbons represents in the signal at  $\delta$  107.98 ppm. While the series of the signals at  $\delta$  70.61, 70.40, 70.22, 69.35, 68.65 ppm belong to the carbon atoms of ether groups in the crown structure.

The synthesis of (9) was done by applying a nitrogen atmosphere to the di nitro benzo-18-crown-6 compound. Then the mixture was dissolved in ethanol and Pd/C catalyst was added. The mixture then refluxed and a mixture of ethanol and hydrazine was added to it. The reaction mixture was refluxed and filtered off. The purification of the organic layer has been done by recrystallization from methanol. The compound was isolated as a tan semi solid in yield of (91%).

The  $^1\text{H}$  NMR spectrum of (9) exhibits a singlet at  $\delta$  6.32 (2H) due to the aromatic protons next to the carbon atom which connected to the amino groups which represent in Ha, b (Figure 3.32). While the multiplet at  $\delta$  4.07 – 4.00 ppm refers to



protons belong to four protons in the crown cavity next to the benzene ring and this confirmed by COSY spectrum in (Figure 3.33) and HSQC spectrum in (Figure 3.34). The multiplet at  $\delta$  3.87 – 3.80 ppm belongs to the other four protons in the crown cavity next to the benzene ring, and the other multiplet at  $\delta$  3.73 – 3.63 ppm belongs to the last twelve protons in the crown cavity in the furthest end to the benzene ring due to the ether bridges of the crown cavity.

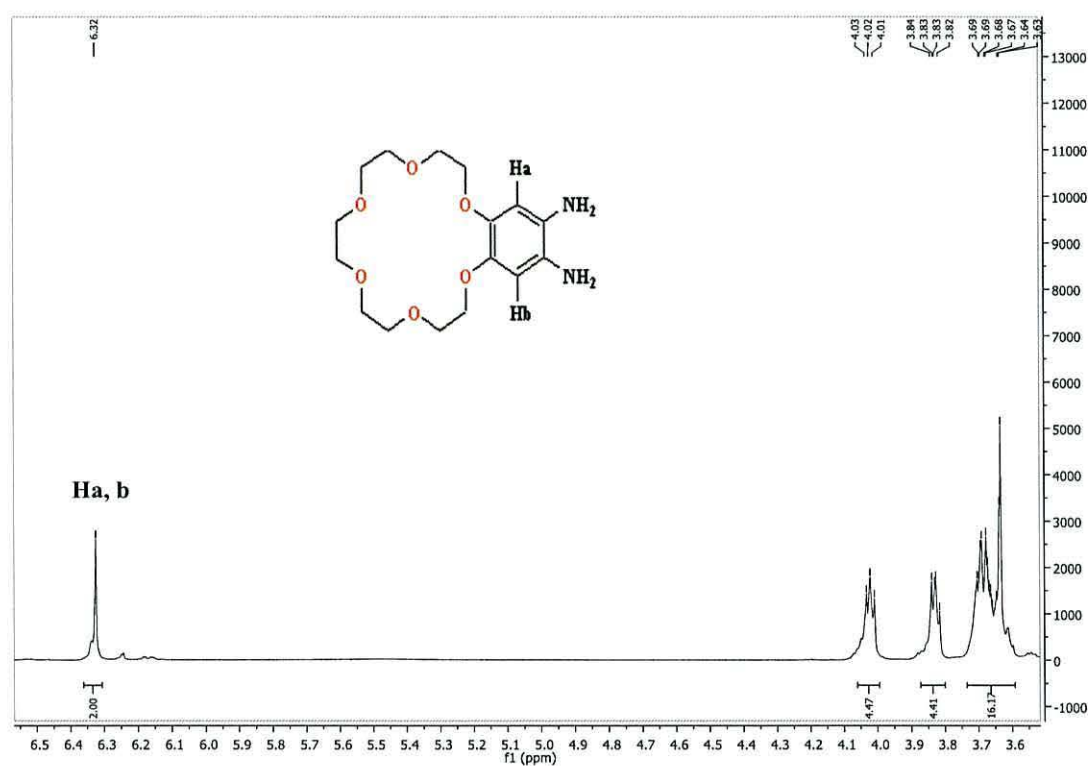


**Figure 3.32:**  $^1\text{H}$  NMR spectrum of diamino benzo-18-crown-6 (**9**)

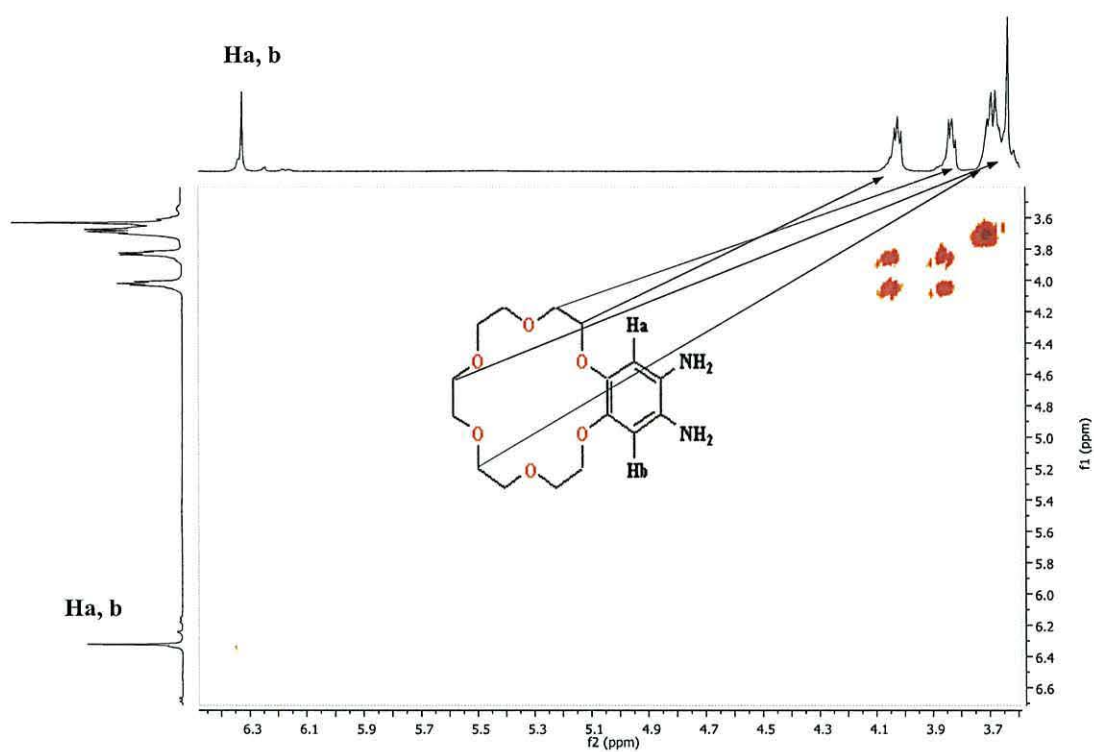


Figure 3.33: COSY spectrum of di amino benzo-18-crown-6 (9)

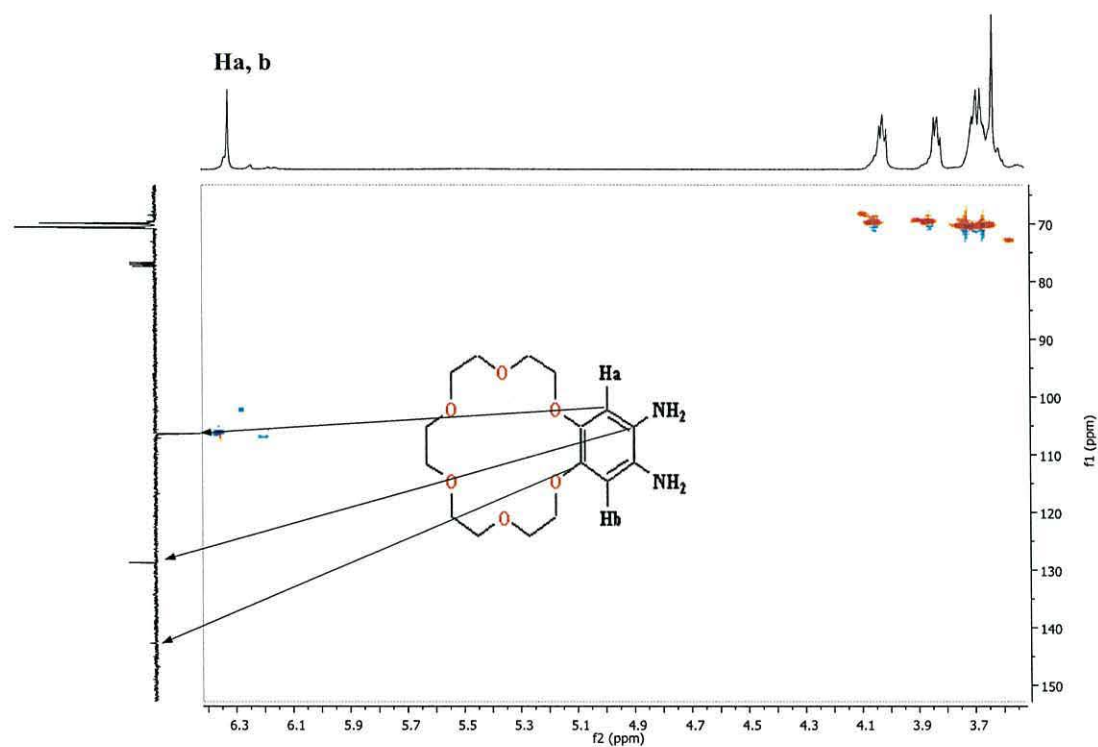


Figure 3.34: HSQC spectrum of di amino benzo-18-crown-6 (9)

The  $^{13}\text{C}$  NMR spectrum as in (Figure 3.35) exhibits a signal at  $\delta$  142.80 ppm belongs to aromatic carbons atom attached to the cavity ring, while the signal at  $\delta$  128.81 ppm belongs to the other aromatic carbons atom linked to the amino groups, and the other aromatic carbons represents in the signal at  $\delta$  106.47 ppm. The series of the signals at  $\delta$  70.83, 70.67, 70.09, 69.98 ppm belong to the carbon atoms of ether groups in the crown structure.

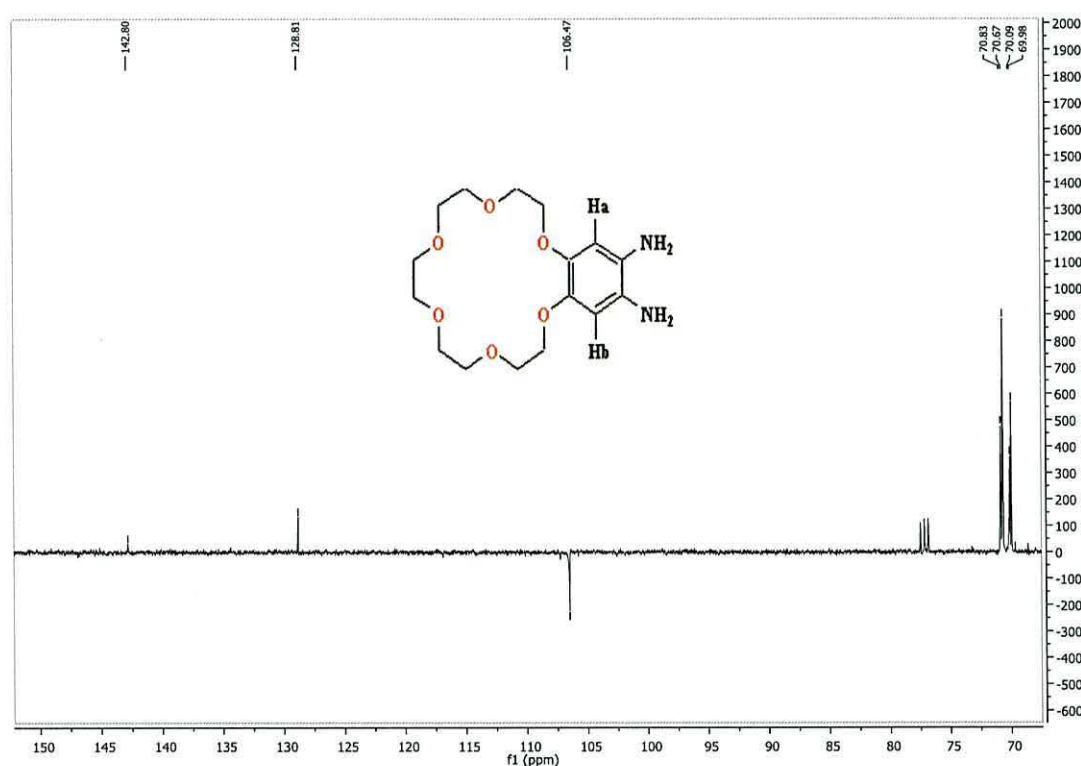
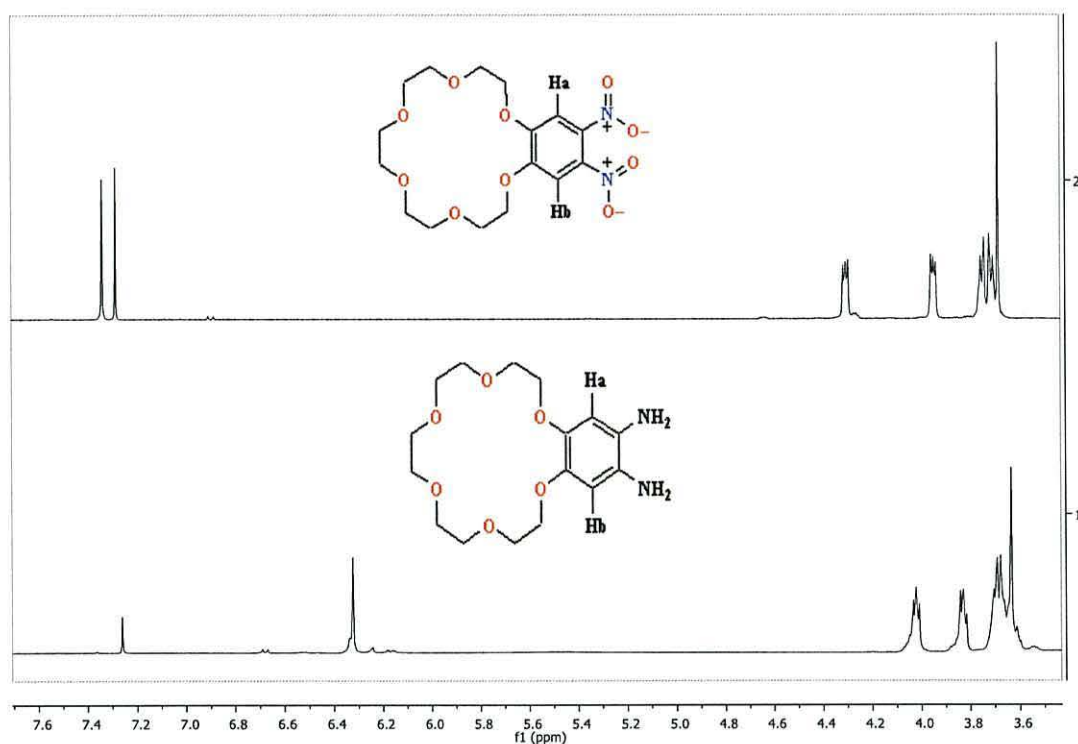


Figure 3.35: DEPT-Q NMR spectrum of Di amino benzo-18-crown-6 (9)

(Figure 3.36) shows characteristic signal of the protons (Ha, b) as a comparison between the nitro and the amino groups in a benzo ring dinitro benzo-18-crown-6 (6) and diamino benzo-18-crown-6 (9) macrocyclic compounds.





**Figure 3.36:** A comparison between the nitro and the amino groups in a benzo ring dinitro benzo-18-crown-6 (6) up and diamino benzo-18-crown-6 (9) down ionophores in <sup>1</sup>H NMR spectrum.

## Performance

The potentiometric response of the ISE modified with ionophore (6) was investigated against the potassium phosphate. The potential readings were plotted against the logarithmic values of the concentration over a range of  $5 \times 10^{-5} \text{ mol L}^{-1}$  to  $1 \times 10^{-1} \text{ mol L}^{-1}$  (Figure 3.37).

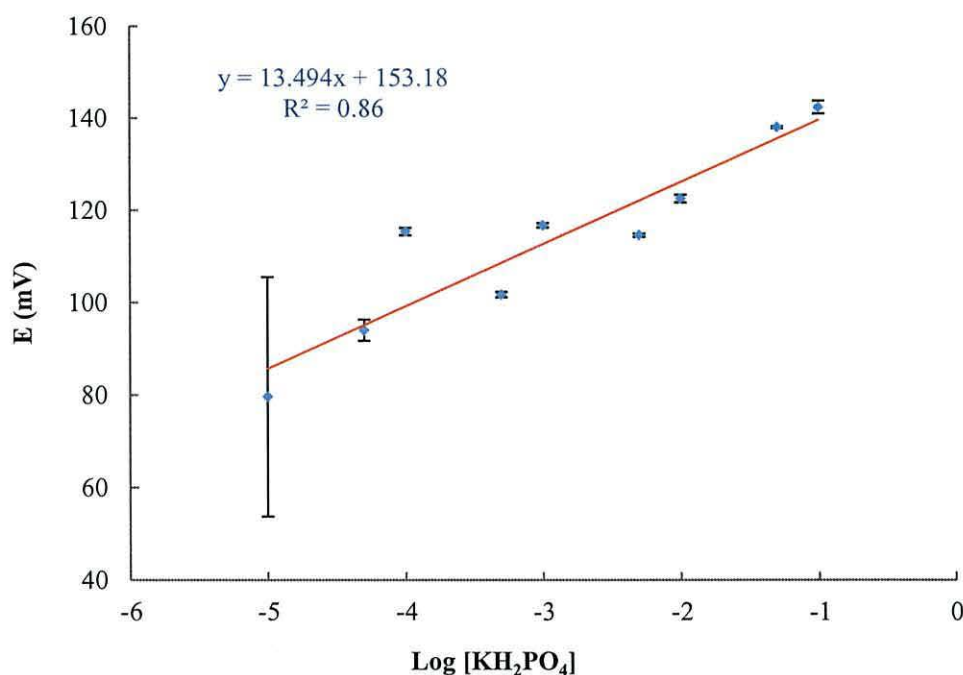


**Figure 3.37:** The application of the synthesised ionophore dinitro benzo-18-crown-6 (**6**) for Nernstian response ( $n = 3$  and error bars (where visible) indicate the standard deviation)

The slope of the calibration line for (**6**) ionophore was  $13.494 \pm (1.1)$  mV per decade; while the detection limit was  $1.5 \times 10^{-5}$  mol L<sup>-1</sup>. At the low concentration the error bars have increased which relates to the non Nernstian response for the (**6**) ionophore.<sup>14</sup> While the low potentiometric response of the ISE modified with ionophore (**9**) was investigated against the potassium phosphate (Figure 3.38).

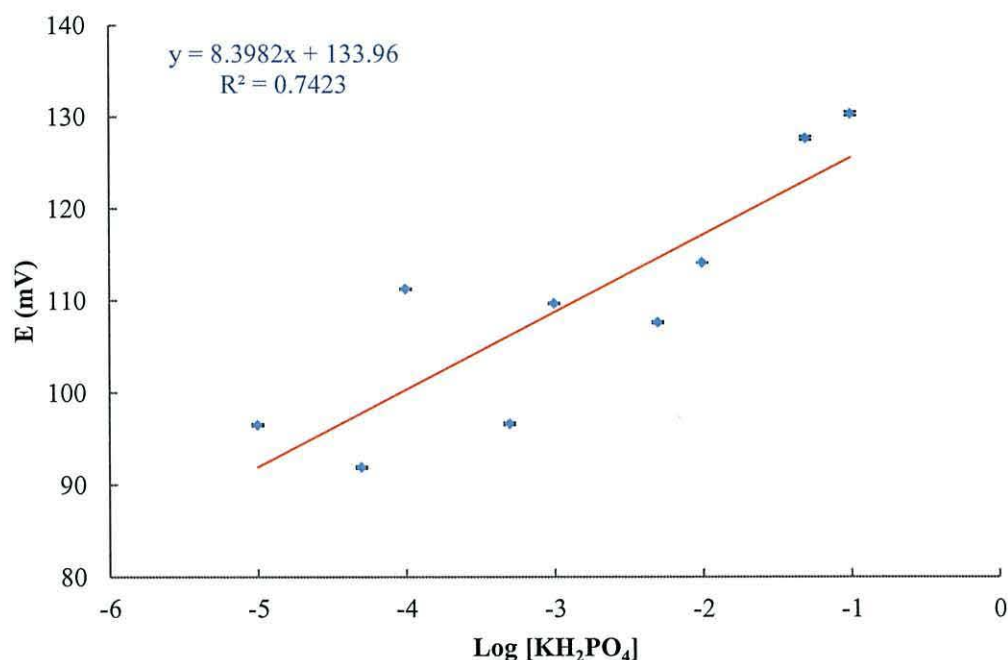


**Figure 3.38:** The application of diamino benzo-18-crown-6 (9) for Nernstian response ( $n = 3$  and error bars (where visible) indicate the standard deviation)

The low potentiometric slope of the calibration line for ionophore (9) was  $8.3982 \pm (1.1)$  mV per decade and the limit of detection was  $5.8 \times 10^{-4}$  mol L<sup>-1</sup> which relates to the sensor composition.<sup>14</sup> The low potentiometric response due to the ion pair on the nitrogen in amino groups touches the delocalised ring electrons in phenyl ring and makes delocalisation system with them. That means that the ion pairs no longer fully available to combine with potassium ions in solution. The nitrogen is still the most electronegative atom in the molecule, and so the delocalised electrons will be attracted towards it.

The potentiometric response of the ISE modified with dibenzo-18-crown-6 ionophore was investigated against the potassium phosphate and the corresponding potentials determined. The potential readings were plotted against the logarithmic values of the concentration over a range of  $5 \times 10^{-5}$  mol L<sup>-1</sup> to  $1 \times 10^{-1}$  mol L<sup>-1</sup> (Figure 3.39).



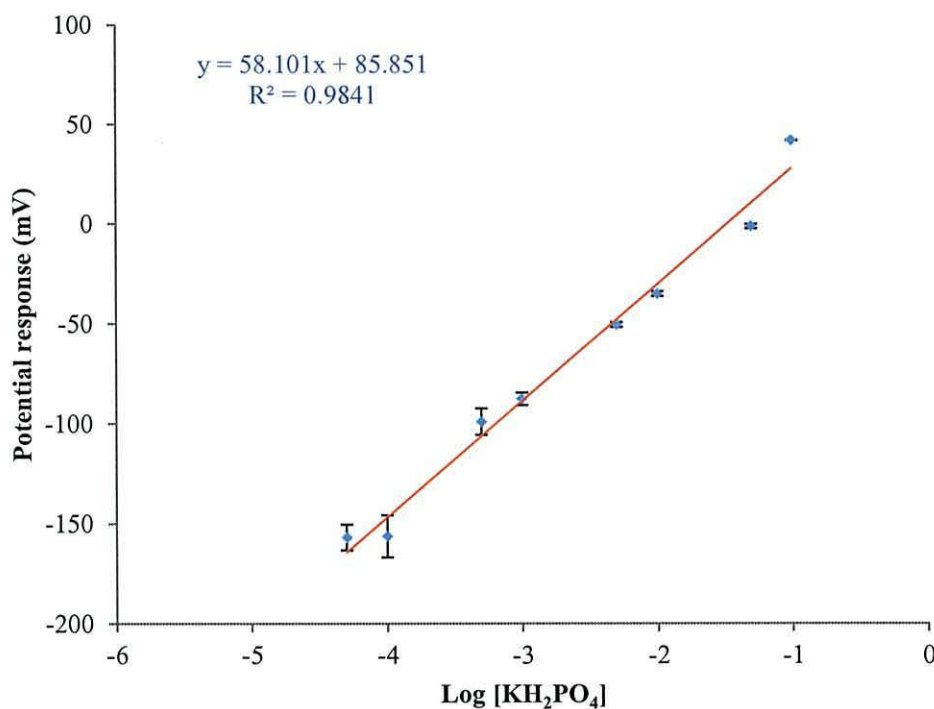


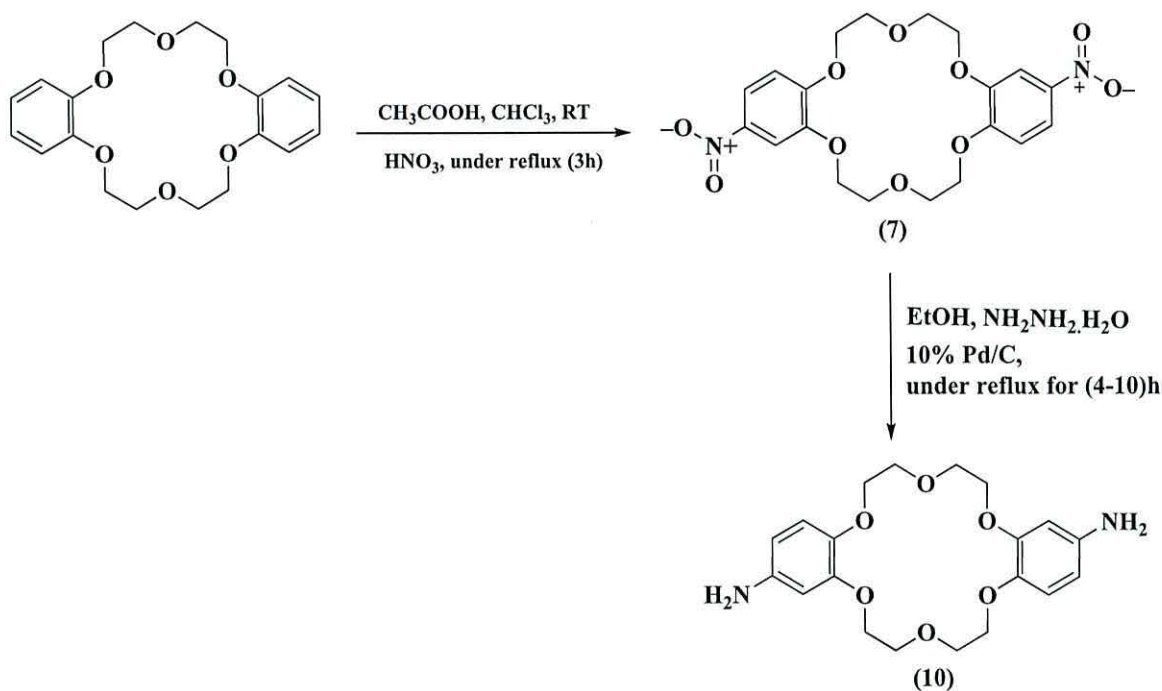
**Figure 3.39:** Potential response of the potassium ISE containing di benzo-18-crown-6 ionophore vs. Ag/AgCl reference electrode for increasing concentrations of potassium phosphate ion at pH 9. ( $n = 3$  and error bars error bars (where visible) indicate the standard deviation)

According to the IUPAC, the slope of the calibration line was  $58.1 \pm (1.1)$  mV per decade and the limit of detection was  $3.2 \times 10^{-6}$  mol L<sup>-1</sup>; This means that the response time depends on the particular working conditions. For instance, whether after increasing or decreasing the primary ion concentration in the middle of the dynamic response range or near the detection limit; Moreover, it may depend on the concentration of the solution in which the electrode is initially conditioned (and on conditioning time) or kept when not in use.<sup>14</sup>

### 3.6 Di(nitrobenzo)-18-crown-6 (7) and di(aminobenzo)-18-crown-6 (10)

#### Synthesis

All NMR spectra and Mass Spectrometry data are given in Appendix in attached CD. Di (nitrobenzo)-18-crown-6 (7) and di (aminobenzo)-18-crown-6 (10) were synthesised according to Scheme 3.5 described.



*Scheme 3.5: Synthesis of di (nitrobenzo)-18-crown-6 (7) and di (aminobenzo)-18-crown-6 (10)*

Dibenzo-18-crown-6 was dissolved in  $\text{CHCl}_3$  and acetic acid was added to the solution and stirred. Then a mixture solution of  $\text{HNO}_3$  and acetic acid was added.<sup>16,17</sup> The solution was stirred then heated to reflux whereupon a precipitate formed. The purification of the organic layer has been done by flash chromatography (40% petrol /ethyl acetate). The compound (7) was collected as a pale yellow solid in good yield.

The  $^1\text{H}$  NMR spectrum exhibits a doublet at  $\delta$  7.89 ppm (dd,  $J = 8.9, 2.5$  Hz, 2H) which belongs to the aromatic protons next to the carbon atom which connected to the nitro groups which represent in H b, b' from (Figure 3.40). The doublet signal at  $\delta$  7.71 ppm ( $J = 2.6$  Hz) refers to aromatic protons next to the one attached to the nitro

group represents in Ha, a' in the same figure, the other aromatic doublet signal at  $\delta$  6.87 ppm ( $J = 8.9$  Hz) represents in Hc, c'. The multiplet at  $\delta$  4.07 – 4.01 ppm belongs to eight protons in the crown cavity next to the benzene ring, and the other multiplet at  $\delta$  4.08 – 3.99 ppm belongs to the other eight protons in the crown cavity due to the ether bridges of the crown cavity compound. This is confirmed by the COSY spectrum (Figure 3.41) also confirms the *Trans* structure for this product due to the connecting between Hb, b' with Ha, a' from side and Hb, b' with Hc, c' from the other side.

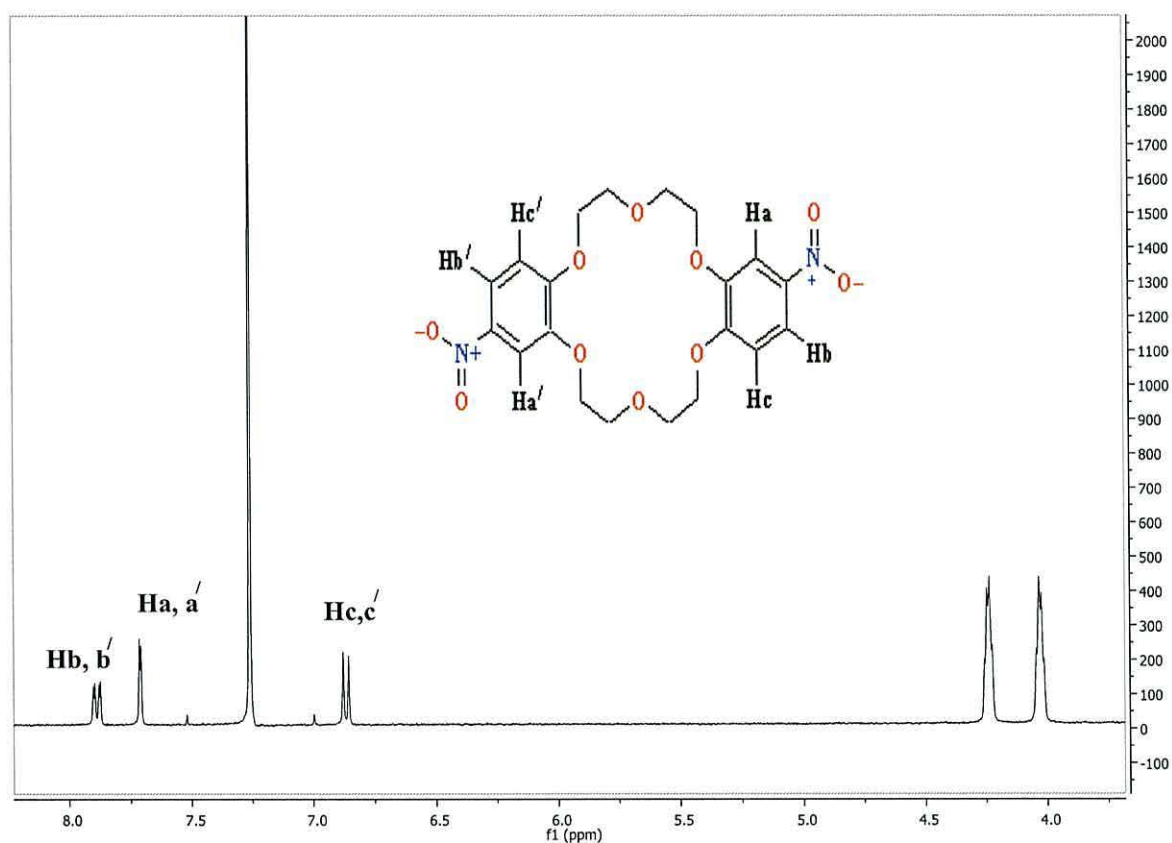


Figure 3.40:  $^1\text{H}$  NMR spectrum of di(nitrobenzo)-18-crown-6 (7)



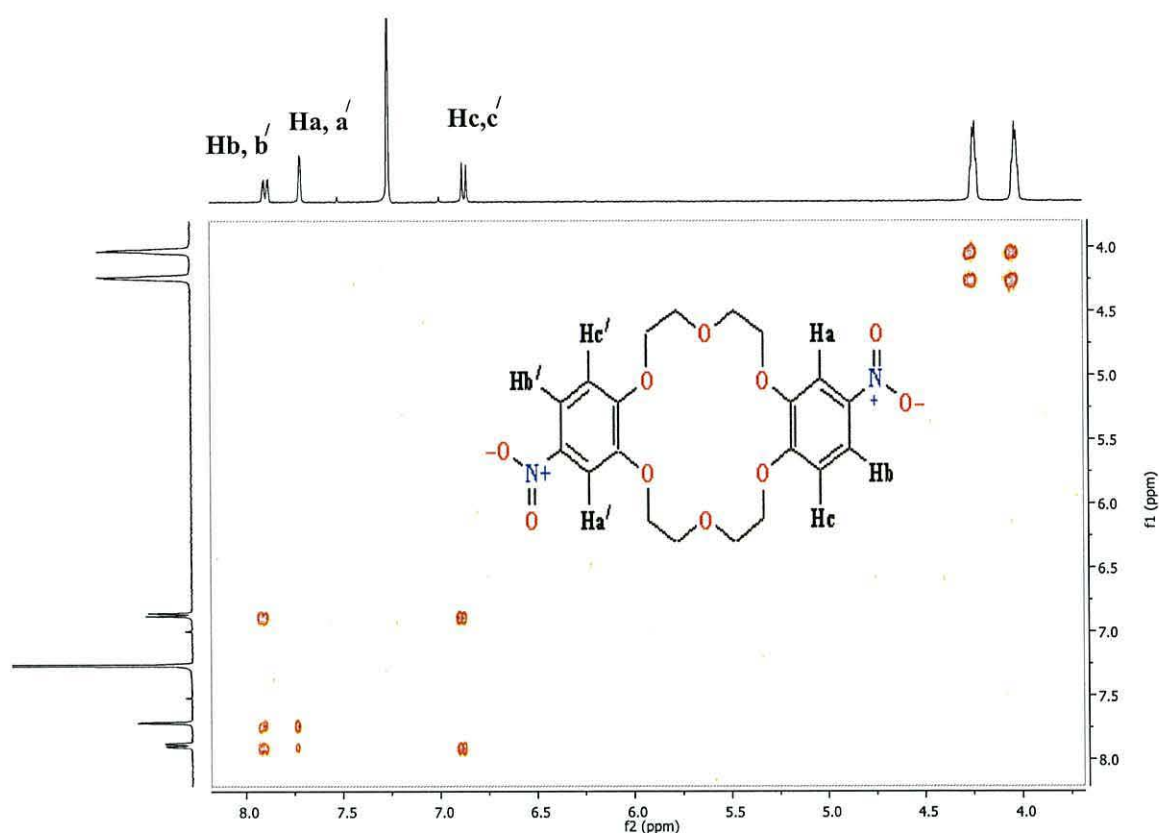


Figure 3.41: The COSY spectrum of di (nitrobenzo)-18-crown-6 (7)

The  $^{13}\text{C}$  NMR spectrum in (Figure 3.42) shows a signal at  $\delta$  154.21 ppm belongs to aromatic carbons atom attached to the cavity ring, while the signal at  $\delta$  148.11 ppm belongs to the other aromatic carbons atom linked to the cavity ring. While the signal at  $\delta$  141.02 ppm belongs to the other aromatic carbons atom linked to the carbon the nitro group. The rest aromatic carbon represent in  $\delta$  118.09, 111.72, 107.01 ppm signals. The series of the signals at  $\delta$  68.93, 68.88, 68.83, 68.48 and 68.44 ppm which belong to the carbon atoms of ether groups in the crown structure.

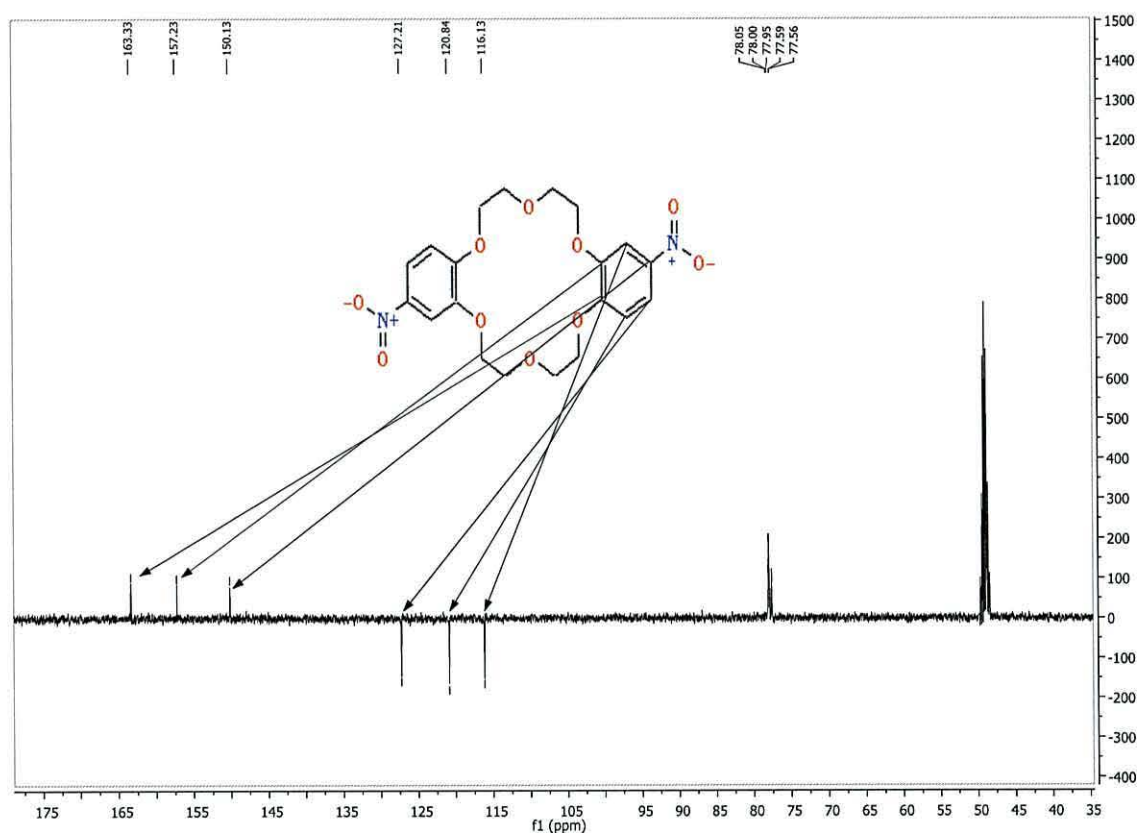


Figure 3.42: DEPT-Q NMR spectrum of di (nitrobenzo)-18-crown-6 (7)

The HSQC spectrum of compound (7) as in (Figure 3.43) represents the connecting between Hb, b' and the carbon atom of  $\delta$  118.09 ppm. While the proton of Ha, a' connect to the carbon of  $\delta$  111.72 ppm, and Hc, c' proton connect to the carbon of  $\delta$  107.01 ppm. As a result HSQC spectrum confirms the structure of *trans* (dinitrobenzo)-18-crown-6 compound.

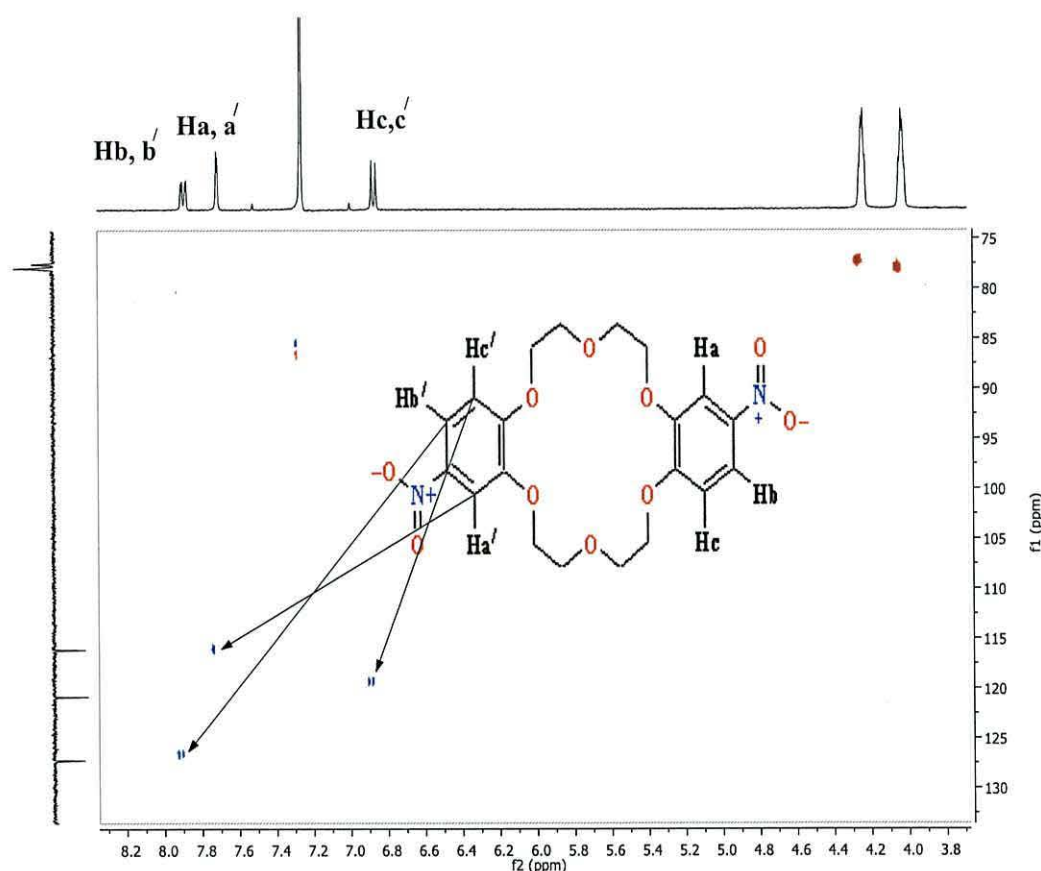


Figure 3.43: The HSQC spectrum di (nitrobenzo)-18-crown-6 (7)

While the synthesis of compound (10) from compound (7) by dissolving it in ethanol under nitrogen atmosphere. Then the catalyst of Pd/C (10%) was added. The mixture then refluxed and a solution of ethanol and hydrazine hydrate was added. The reaction mixture was refluxed and the catalyst was filtered off. The mixture was extracted with chloroform. The purification of the organic layer was done by recrystallization from methanol. The compound was isolated as a tan.

The  $^1\text{H}$  NMR exhibits a doublet at  $\delta$  6.73 ppm ( $J = 1.6$  Hz) belongs to the aromatic protons which represent in Hc, c' from (Figure 3.44). The doublet signal at  $\delta$  6.71 ppm ( $J = 1.6$  Hz) refers to other aromatic protons next to the carbon attached to the amino group represents in H a, a' in the same figure, the other aromatic triplets signal at  $\delta$  6.28 ppm ( $J = 2.5$  Hz) represents in H b, b'. While the other triplets at 6.22 ppm ( $J = 2.8$  Hz), and 6.20 ppm ( $J = 2.8$ ) belong to the protons amino groups. The cavity protons represent in the multiplet signals at  $\delta$  4.14 – 4.07 ppm for eight protons, and



at  $\delta$  4.02 – 3.97 ppm for other four protons, and finally for the last four, the signals at  $\delta$  3.97 – 3.93 ppm in the crown cavity due to the ether bridges of the crown cavity compound which confirmed by COSY spectrum (Figure 3.45) and also confirms the *Trans* structure for this product due to the connecting between Hc, c' with Hb, b' from side and Ha, a' with Hb, b' from the other side and as well COSY spectrum explained clearly the amino protons in this structure.

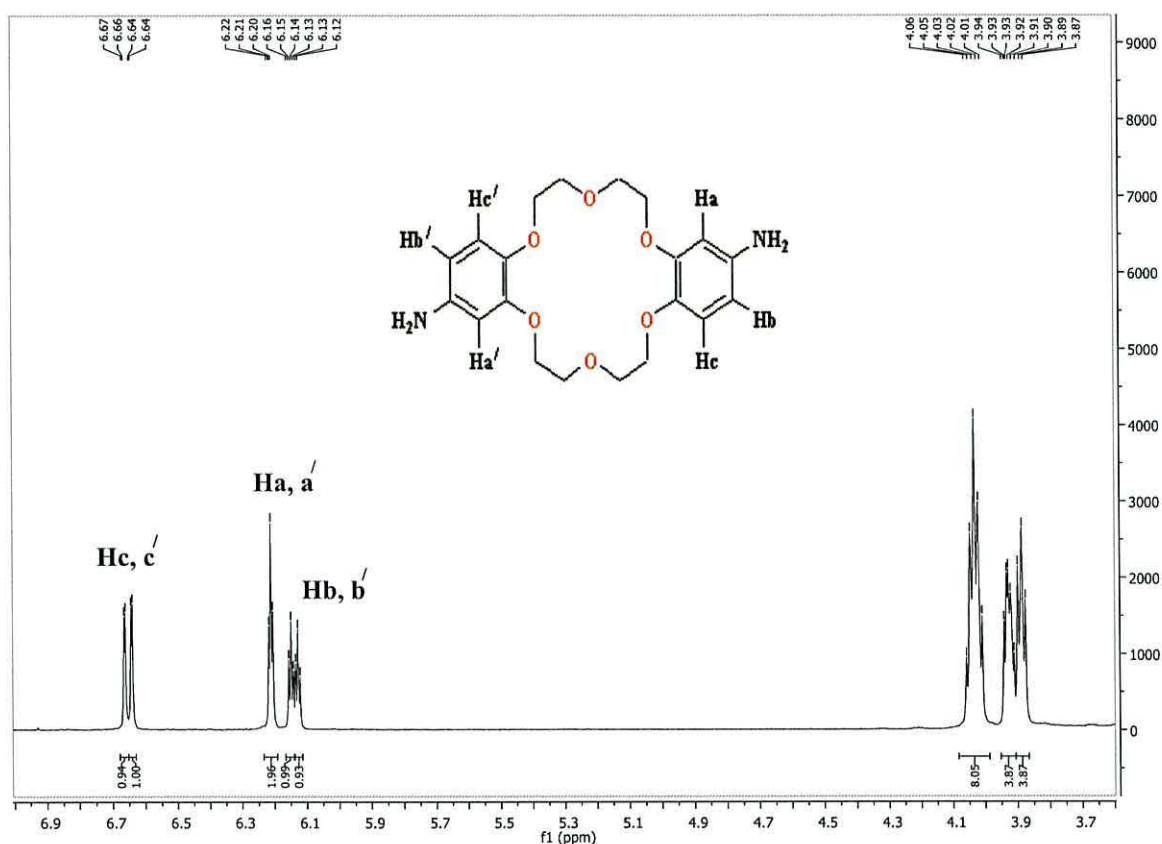


Figure 3.44:  $^1\text{H}$  NMR spectrum of synthesis of di(aminobenzo)-18-crown-6 (10)

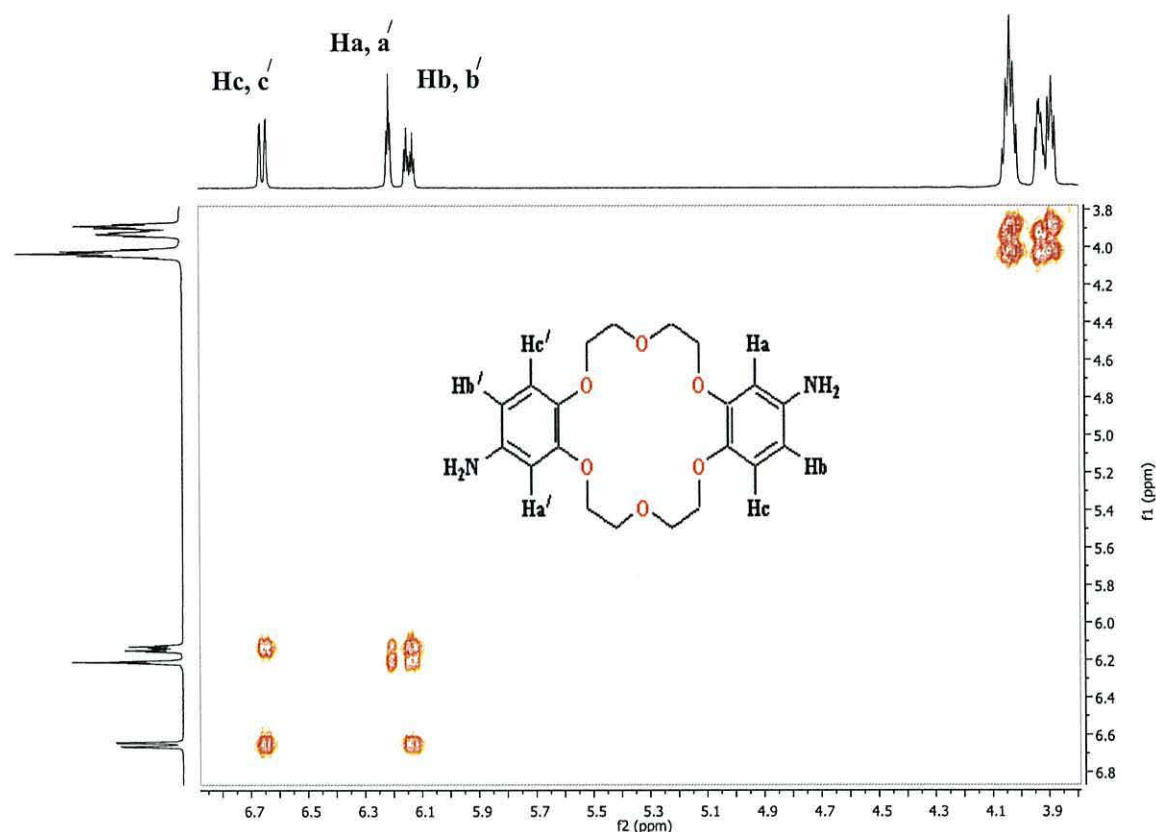


Figure 3.45: The COSY spectrum of di (aminobenzo)-18-crown-6 (10)

The <sup>13</sup>C NMR spectrum in (Figure 3.46) exhibits a signal at  $\delta$  150.32 ppm belongs to aromatic carbons atom attached to the cavity ring, while the signal at  $\delta$  150.17 ppm belongs to the aromatic carbon atom linked to the carbon the amino group. The other aromatic carbons atom linked to the cavity ring are at  $\delta$  141.92 ppm, and the other aromatic carbons represent in  $\delta$  117.10,  $\delta$  116.81,  $\delta$  107.41,  $\delta$  107.28,  $\delta$  102.83,  $\delta$  102.61 ppm. While the series of the signals at  $\delta$  70.52,  $\delta$  70.46,  $\delta$  70.44,  $\delta$  70.31,  $\delta$  70.01,  $\delta$  68.92 and  $\delta$  68.85 ppm belong to the carbon atoms of ether groups in the crown structure. In addition to the <sup>13</sup>C NMR spectrum, The HSQC spectrum explained clearly that the proton of Hc, c' on the carbon at  $\delta$  117.10 ppm, and the proton of Hb, b' on the carbon at  $\delta$  107.41 ppm, and the proton of Ha, a' on the carbon at  $\delta$  102.83 ppm.

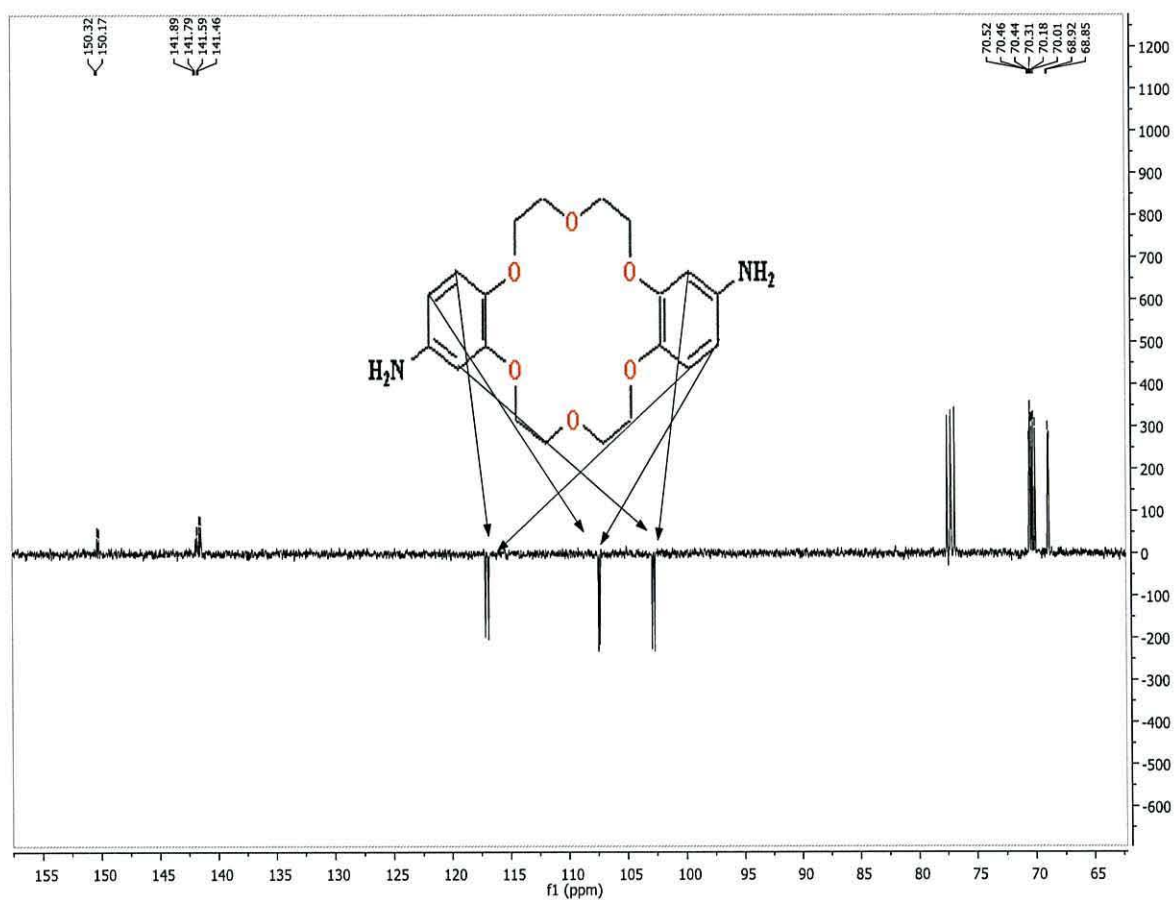


Figure 3.46: DEPT-Q NMR spectrum of di(aminobenzo)-18-crown-6 (10)

The close agreement between the  $^1\text{H}$  NMR and  $^{13}\text{C}$  NMR spectra was obtained for (10) and that confirmed by HSQC spectrum (Figure 3.47).



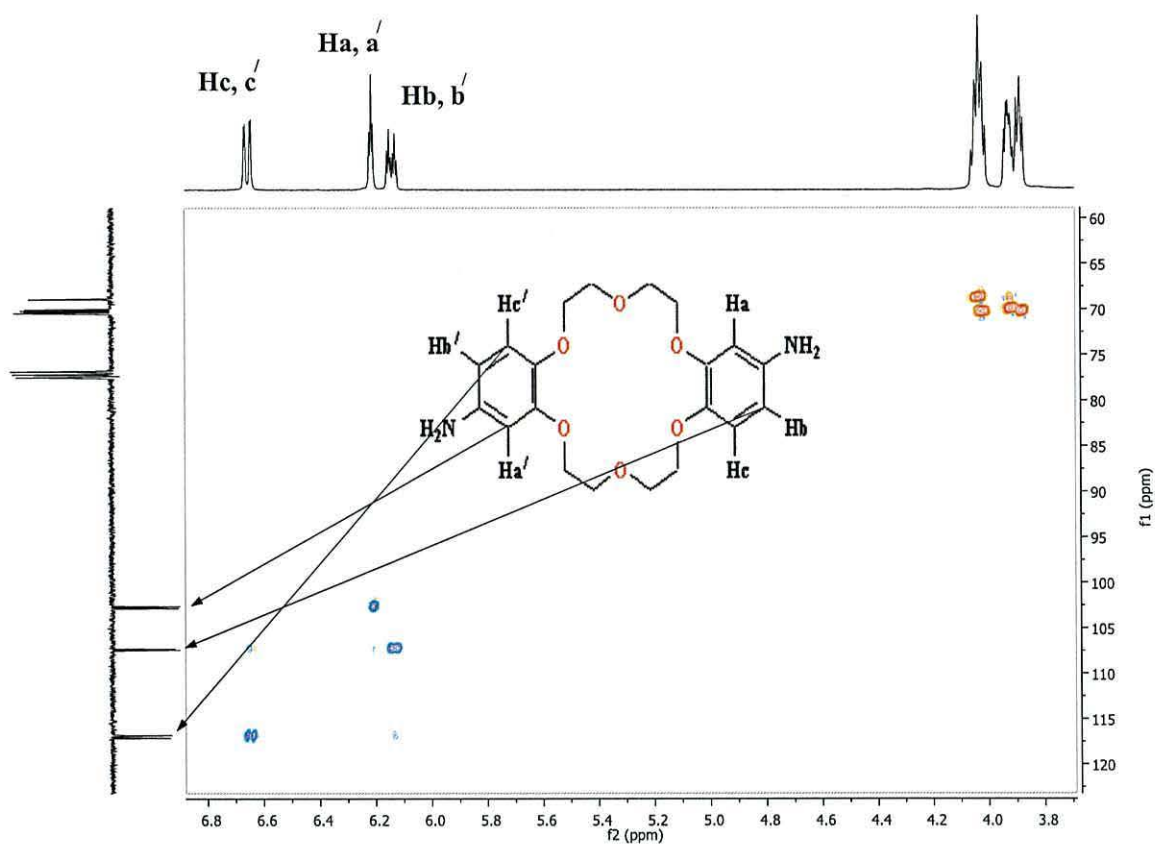
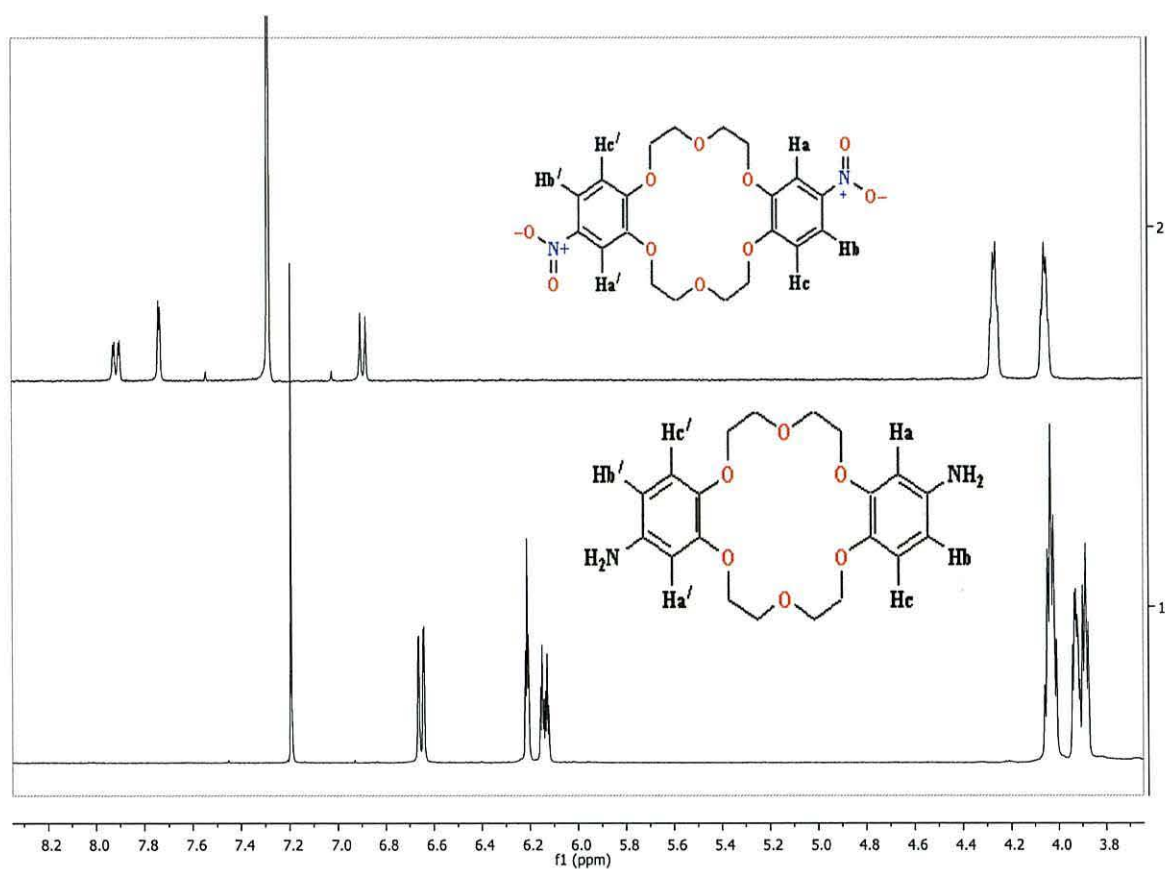


Figure 3.47: The HSQC spectrum of di(aminobenzo)-18-crown-6 (10)

As a comparison between these two groups on benzo ring attached to the crown cavity for compound (7) and compound (10) was elucidated by (Figure 3.48).



*Figure 3.48: The characteristic signal of the protons ( $H_{a,a'}$ ,  $H_{b,b'}$ , and  $H_{c,c'}$ ) as a comparison between the nitro and the amino groups in a benzo ring of the di (nitrobenzo)-18-crown-6 (7) and di(aminobenzo)-18-crown-6 (10) macrocyclic compounds.*

## Performance

The potential of potassium ion solutions were measured within a concentration range of  $5 \times 10^{-5} \text{ mol L}^{-1}$  to  $1 \times 10^{-1} \text{ mol L}^{-1}$ . Each solution was stirred and the potential reading was recorded after stabilisation to  $\pm 0.2 \text{ mV}$ . The potentiometric response of the ISE modified with ionophore (7) was investigated for the potassium phosphate solutions. The potential readings were plotted against the logarithmic values of the concentration over a range of  $5 \times 10^{-5} \text{ mol L}^{-1}$  to  $1 \times 10^{-1} \text{ mol L}^{-1}$  (Figure 3.49).

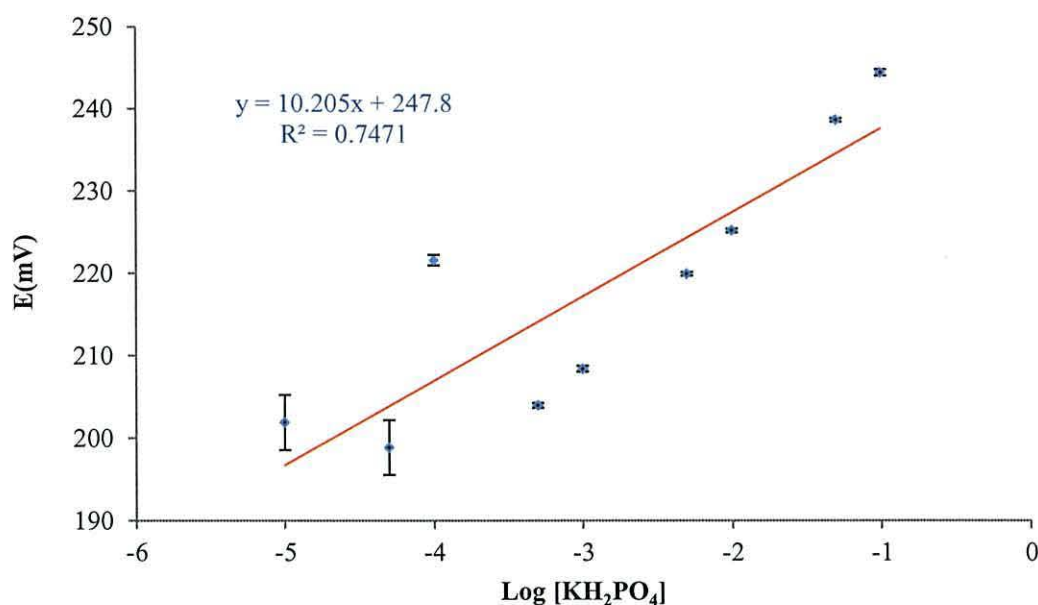


Figure 3.49: The application of (Trans) di (nitrobenzo)-18-crown-6 (7) for Nernstian response ( $n = 3$  and error bars (where visible) indicate the standard deviation) (2 STDE)

The slope of the calibration line for ionophore (7) was  $10.20 \pm (1.1)$  mV per decade and the limit of detection was  $3.9 \times 10^{-4}$  mol L<sup>-1</sup>; While, the potentiometric response of the ISE modified with ionophore (10) was determined of the concentration over a range of  $5 \times 10^{-5}$  mol L<sup>-1</sup> to  $1 \times 10^{-1}$  mol L<sup>-1</sup> (Figure 3.50).

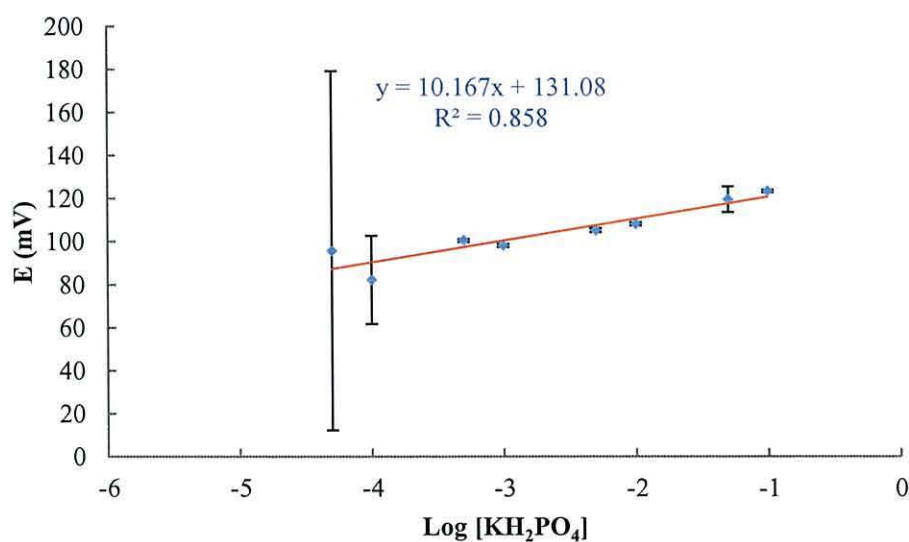


Figure 3.50: The application of di (amino benzo)-18-crown-6 (10) for Nernstian response ( $n = 3$  and error bars (where visible) indicate the standard deviation)



The slope of the calibration line for ionophore (10) was  $10.16 \pm (1.1)$  mV per decade and the limit of detection was  $1.9 \times 10^{-3}$  mol L<sup>-1</sup>; when the error bars are considered it can be seen that the low concentration have increased errors this is thought to be due to the associated increase in response time for the sensor which relates with the sensor composition.<sup>14</sup>

### 3.7 Conclusions

The potential performance for the synthesised ionophores in this work has been summarised in Table 3. 5.

*Table 3. 5: The Potential performance for the synthesised ionophores in this work*

| The sensor ionophore                          | (1)     | (2)     | (3)    | (4)     | (5)    | (6)     | (7)     | (8)     | (9)    | (10)    |
|---|---------|---------|--------|---------|--------|---------|---------|---------|--------|---------|
| The plasticiser                               | DBP     | DBP     | DBP    | DBP     | DBP    | DBP     | DBP     | DBP     | DBP    | DBP     |
| The response time(seconds)                    | 80      | 88      | 120    | 90      | 110    | 95      | 125     | 135     | 160    | 95      |
| The correlation coefficient (R <sup>2</sup> ) | 0.1184  | 0.7117  | 0.0317 | 0.5394  | 0.0115 | 0.8600  | 0.7471  | 0.4835  | 0.7423 | 0.8580  |
| The Nernstian response mV/decade              | 14.2820 | 10.4530 | 1.2657 | 31.1190 | 0.8525 | 13.4940 | 10.2050 | 18.9060 | 8.3982 | 10.1670 |

The potentiometric response for the synthesised ionophores has shown that the best performance in less than one minute belongs to the sensor ionophore (10) which gave the correlation coefficient  $R^2 = 0.858$ . The ionophores (7), (9) gave  $R^2 = 0.7471$  and  $R^2 = 0.7423$ , respectively. While the potentiometric response for the (10) ionophore is 10.167 mV/decade and the potentiometric response for the ionophores (7), (9) is 10.205 mV/decade and 8.3982 mV/decade. On the other hand the (4) ionophore has showed a response value of 31.119 mV/decade with low correlation coefficient which is 0.5394.

The synthesis of those ionophore molecules is important for the identification of their structures ability for binding with potassium phosphate in water samples studying their chemical properties for applying in other fields.<sup>18,19</sup>

The electrodes were constructed for the determination of potassium phosphate, with dibenzo-18-crown-6 (ionophore) proving to be the most effective ionophore with a shelf life of 40 days with negligible drift. It responded in a near Nernstian fashion, and showed a low detection limit of  $3.2 \times 10^{-6} \text{ mol L}^{-1}$ , and a fast response time over a concentration range of  $5 \times 10^{-5} \text{ mol L}^{-1}$  to  $1 \times 10^{-1} \text{ mol L}^{-1}$ . The resulting electrode signifies a significant advancement in the construction of a potentiometric device for the determination of di-potassium hydrogen phosphate concentrations in solution. The use of dibenzo-18-crown-6 showed the potential towards a method for the quantitative determination potassium ions in water samples. Furthermore, the goal in this work is to develop selective ionophores that are capable of detecting ions in aqueous solution. Since ISEs offer one way to achieve this goal, new potassium phosphate ionophores were designed to be incorporated into these electrodes. For any ISE sensors, sensitivity to a specific ion in the required concentration range and selectivity for one specific ion are important considerations.

The ionophores for ISEs applications should be highly lipophilic, in order to be compatible with the nonpolar membrane environment of ISEs and to prevent the leaching of the ionophore from the membrane during testing. This is usually achieved by attaching groups, such as nitro or amino groups to the ionophore's structure. Here we report a series of synthesised macrocyclic compounds with different substituents; which have been examined for their potential to detect potassium phosphate in the presence of other potassium counter ions. The ISE based on 4-amino benzo-18-crown-6 and diamino benzo-15-crown-5 exhibited a Nernstian response for potassium phosphate over a wide concentration range of  $5 \times 10^{-5} \text{ mol L}^{-1}$  to  $1 \times 10^{-1} \text{ mol L}^{-1}$  with a low limit of detection of  $1.8 \times 10^{-4} \text{ mol L}^{-1}$  and  $6 \times 10^{-5} \text{ mol L}^{-1}$  respectively. The resulting electrode exhibited a shelf life of 50- 60 days with negligible drift.

The electrodes were constructed for the determination of potassium phosphate, it responded in a near Nernstian fashion, and showed a low detection limit and a fast response time over a concentration range of  $5 \times 10^{-5} \text{ mol L}^{-1}$  to  $1 \times 10^{-1} \text{ mol L}^{-1}$ .

The best potentiometric response of the ISE modified with dibenzo-18-crown-6 ionophore was investigated against the potassium phosphate. The slope of the calibration line was  $58.1 \pm (1.1)$  mV per decade and the limit of detection was  $3.2 \times 10^{-6}$  mol L<sup>-1</sup>; On the other hand; The potentiometric response for the synthesised ionophores has cleared that the best performance in less than one minute belongs to the sensor ionophore (10) which gave the correlation coefficient  $R^2 = 0.858$ , and for the ionophores (7), (9) are  $R^2 = 0.7471$  and  $R^2 = 0.7423$  respectively. While as a Nernstian response for the (10) ionophore is 10.167 mV/decade and the potentiometric response for the ionophores (7), (9) is 10.205 mV/decade and 8.3982 mV/decade. On the other hand the (4) ionophore has showed a near Nernstian response which is 31.119 mV/decade with low correlation coefficient which is  $R^2 = 0.5394$ .



### 3.8 References

- [1] A. Khudhair Hassan, B. Saad, S. Ab Ghani, R. Adnan, A. Abdul Rahim, N. Ahmad, M. Mokhtar, S. T. Ameen, and S. Mustafa Al-Araji, **Ionophore-based potentiometric sensors for the flow-Injection determination of promethazine hydrochloride in pharmaceutical formulations and human urine**, *Sensors*, 2011, **11**, 1028-1042.
- [2] S. Peper, and C. Gonczy, **Potentiometric response characteristics of membrane-based  $\text{Cs}^+$ -selective electrodes containing ionophore-functionalized polymeric microspheres**, *Int. J. Electrochem.*, 2011, **2011**, 1-8.
- [3] M. Ouchi and T. Hakushi, **Cation binding by thallium(I) selective crown ethers**, *Coord. Chem. Rev.*, 1996, **148**, 171-181.
- [4] S. Hwang, K. H. Lee, G. H. Ryu, Y. H. Jang, S. B. Lee, W. Y. Lee, J. I. Hong, and D. S. Chung, **Relative binding affinities of alkali metal cations to [18]starand in methanol: computational and experimental studies**, *J. Org. Chem.*, 2000, **65**, 536-542.
- [5] I. Carreira-Barral, A. Rodríguez-Rodríguez, M. Regueiro-Figueroa, D. Esteban-Gómez, C. Platas-Iglesias, and A.D. Blas, **A merged experimental and theoretical conformational study on alkaline-earth complexes with lariat ethers derived from 4,13-diaza-18-crown-6**, *Inorg. Chim. Acta*, 2011, **370**, 270-278.
- [6] M. G. Babashkina, D. A. Safin, M. Bolte, and A. Klein, **Synthesis and characterization of crown ether-containing N-phosphorylated Thioureas  $\text{RC(S)NHP(O)(OiPr)}_2$  ( $\text{R} = 1\text{-aza-15-crown-5}$ ,  $1\text{-aza-12-crown-4}$ ) and their  $\text{Co(II)}$  and  $\text{Ni(II)}$  complexes**, *Heteroat. Chem.*, 2010, **21(7)**, 486-491.
- [7] M. Saaid, B. Saad, I. A. Rahman, A. S. M. Ali and M. I. Saleh, **Extraction of biogenic amines using sorbent materials containing immobilized crown ethers**, *Talanta*, 2010, **80**, 1183-1190.
- [8] R. M. Z. kakhki and G. Rounaghi, **Selective uranyl cation detection by polymeric ion selective electrode based on benzo-15-crown-5**, *Mater. Sci. Eng.: C*, 2011, **31**, 1637-1642.

- [9] J. A. Ortuño, C. Serna, A. Molina, and E. Torralba, **Ion transfer square wave voltammetry of ionic liquid cations with a solvent polymeric membrane ion sensor**, *Electroanalysis*, 2009, **21 (21)**, 2297-2302.
- [10] M. O'Rourke, N. Duffy, R. De Marco, and I. Potter, **Electrochemical impedance spectroscopy—A Simple method for the characterization of polymer inclusion membranes containing aliquat 336**, *Membranes*, 2011, **1**, 132-148.
- [11] M. Y. Keating and G. A. Rechnitz, **Potentiometric digoxin antibody measurements with antigen-ionophore based membrane electrodes**, *Anal. Chem.*, 1984, **56**, 801-806.
- [12] J. Yang, C. Hwang, and M. Chen, **Bimodal fluorescence signaling based on control of the excited-state conformational twisting and the ground-state protonation processes**, *Tetrahedron Lett.*, 2007, **48**, 3097-3102.
- [13] A. N. Chekhlov, **Preparation and crystal structure of bis[(dibenzo-18-crown-6)potassium]bis( $\mu$ 2-chloro)- tetrachlorodicuprate(II)**, *Russ. J. Gen. Chem*, 2009, **79 (9)**, 1821-1824.
- [14] M. Carlo, **Response time of ion-selective electrodes: Current usage versus IUPAC recommendations**, *Anal. Chim. Acta*, 2004, **512**, 183-190.
- [15] M. B. Deshmukh, K. N. Alasundkar, S. M. Salunkhe, D. K. Salunkhe, S. A. Sankpal, D. R. Patil, and P. V. Anbhule., **Synthesis, X-ray diffraction and optical spectral study of benzo-18-crown-6 containing monoazo dyes**, *Indian J. Chem.*, 2009, **48 B**, 737-740.
- [16] M. J. Deetz, M. Shang, and B. D. Smith, **A macrobicyclic receptor with versatile recognition properties: simultaneous binding of an ion pair and selective complexation of dimethylsulfoxide**, *J. Am. Chem. Soc.*, 2000, **122**, 6201-6207.
- [17] S. A. Duggan, G. Fallon, S. J. Langford, V. Lau, J. F. Satchell, and M. N. Paddon-Row, **Crown-linked porphyrin systems**, *J. Org. Chem.*, 2001, **66**, 4419-4426.
- [18] J. P. Panizzon, V. R. M. Macedo, V. Machado, L. M. Fiuza, **Microbiological and physical–chemical water quality of the rice fields in Sinos River's basin, Southern Brazil**, *Environ. Monit. Assess.*, 2013, **185**, 2767-2775.

- [19] D. Kemp, C. J. Bond, D. M. Franks and C. Cote, **Mining, water and human rights: making the connection**, *J. Clean. Prod.*, 2010, **18**, 1553-1562.



## **Chapter 4 – Plasticisers**

#### 4.1 The selection of the solvent mediator

Plasticisers are organic substances that can be added to polymers in order to enhance certain of their characteristics, such as their elasticity and mechanical properties. Plasticisers are very important in the design of the selective polymeric membrane for potentiometric sensors, because they fix the dielectric constant of the membrane and improve the selectivity of those devices.<sup>1</sup>

The physical properties of the polymer have been modified by blending the polymer with a plasticizer or with a second polymer, and the flexibility of the polymer can thereby be improved. Examples of polymers that have been blended with poly (lactic acid) PLA which is a biodegradable thermoplastic that can be formed from renewable resources, because of its good mechanical properties and processibility as well as biocompatibility.<sup>2</sup>

The plasticisers that have previously been used in electrochemical sensors are *ortho*-nitrophenyloctyl ether (NPOE),<sup>3</sup> dibutyl phthalate (DBP),<sup>4</sup> bis(2-ethylhexyl) adipate (BEHA),<sup>5</sup> dioctylphthalate (DOP),<sup>6</sup> and bis (2-ethylhexyl) sebacate (BEHS).<sup>7,8</sup> In this work, new ion-selective electrodes for potassium phosphate have been developed and tested, employing benzo-18-crown-6, dibenzo-18-crown-6, benzo-15-crown-5, 1-aza-18 crown-6, and dicyclohexyl-18-crown-6 ionophores and other derivatives in polyvinyl chloride (PVC) membranes. The design and synthesis of highly selective ionophores has received much attention because of the important role played by these sensors in many applications.<sup>9, 10, 11</sup> The concept of this research involves host guest supramolecular chemistry, where the ionophores serve as hosts for cation guests.<sup>12, 13, 14</sup>

Many types of sensors have been developed to measure the concentration of potassium ions in potassium phosphate solutions. Various plasticisers including dibutylphthalate (DBP), dioctylphthalate (DOP), dioctylphenylphosphonate (DOPP), 2-Nitro phenyl phenyl ether (NPPE), and bis(2- ethyl hexyl) adipate (BEHA) were tested for the best Nernstian response. It should be noted that the nature of the plasticiser influences both the dielectric constant of the membrane and the exchange smobility of the ionophore are in its complex.<sup>15, 16</sup>

The solvent mediator used must be highly hydrophobic and in general have a low dielectric constant and a high molecular weight. It should have a low vapour pressure to avoid major evaporation and a sufficiently high viscosity that it does not pass through the membrane pores quickly.<sup>15, 16</sup>

The performances of several sets of membrane-based cation-selective polymeric membrane electrodes with different plasticisers were investigated, as the selectivity of ISEs are greatly influenced by the membrane solvent and also controlled by plasticisers. For the plasticisers used in the preparation of the polymeric membrane of ISEs, these must be compatible with the polymer and electrode component, and furthermore need to be dissolved in tetrahydrofuran or cyclohexanone, the solvent used in the membrane preparation. Those plasticisers with high lipophilicity are preferred.<sup>17</sup>

The calibration parameters were obtained by continuous calibration of each prepared sensor. On the basis of those parameters, certain properties were evaluated during this study that defines the quality of the electrode in relation to its lifetime. The calibration curves were used to calculate such parameters as slope, the detection limit, and the linear response, with all of this work done through data adjustment by the linear equation method following the Nernst law for monovalent ions. The different structures and molecular weights of the plasticisers effect, as shown in Table 4. 1.

*Table 4. 1: The molecular weights and empirical formulae of the different plasticisers used in this study*

| The plasticisers      | Di butyl phthalate                             | 2- nitrophenyl phenyl ether                    | Di octyl phenyl phosphonate                      | Di octyl phthalate                             | Bis(2-ethyl hexyl dipate)                      |
|-----------------------|--|--|--|--|--|
| The formula           | 278.35   | 215.20   | 382.52   | 390.56   | 370.58   |
| The empirical formula | C <sub>16</sub> H <sub>22</sub> O <sub>4</sub> | C <sub>12</sub> H <sub>9</sub> NO <sub>3</sub> | C <sub>22</sub> H <sub>39</sub> O <sub>3</sub> P | C <sub>24</sub> H <sub>38</sub> O <sub>4</sub> | C <sub>22</sub> H <sub>42</sub> O <sub>4</sub> |

#### **Di butyl phthalate (DBP)**

This chapter investigated the effect of using different solvent mediators in the sensing membrane on the performance of an ISE based on a PVC membrane. Membranes were prepared from PVC, tetrahydrofuran (THF), and also the plasticiser



DBP. The DBP sensor for potassium ions ( $K^+$ ) in the presence of  $PO_4^{3-}$  was the first sensor to be prepared and tested. Its structure is shown in (Figure 4. 1).

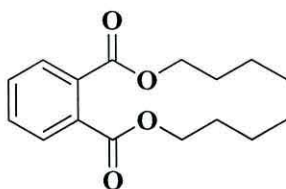


**Figure 4. 1: Di butyl phthalate plasticiser chemical structure**

DBP was used as the solvent mediator, As can be seen from its structure, the two chains of dibutyl ester linked to the phthalalic acid structure enhance the polarity and create hydrogen bonding with PVC in the sensor membrane. This enables it to remain for longer without leaching into the solution. However, it is still an inert organic material with a high boiling point around  $340^{\circ}C$  and a low vapour pressure of 1 mmHg ( $147^{\circ}C$ ). (Figure 4. 2) show the thermal properties of this plasticiser which studied by DSC- TGA thermogram of the samples and showed crystalline melting peaks at nearly  $285^{\circ}C$ .

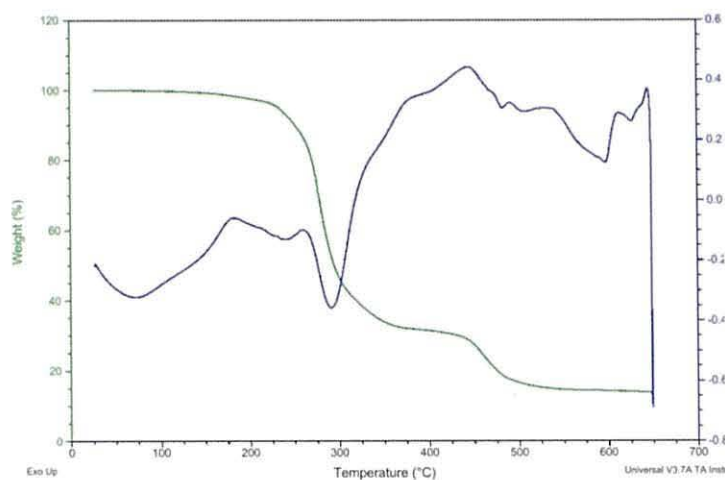


**Figure 4. 2: DSC- TGA thermogram shows the thermal properties of the DBP plasticiser**

Electrodes based on this plasticiser produced better results than other plasticised PVC membrane electrodes over a wide response concentration range of  $5 \times 10^{-5} \text{ mol L}^{-1}$  to  $1 \times 10^{-1} \text{ mol L}^{-1}$ , and a low limit of detection of  $3.2 \times 10^{-6} \text{ mol L}^{-1}$ . A calibration standard solution of potassium phosphate was freshly prepared, in a range of  $0.1 \text{ mol L}^{-1}$  to  $0.5 \times 10^{-5} \text{ mol L}^{-1}$ . The dibenzo-18-crown-6 sensor with DBP as a solvent mediator and a silver/silver chloride (Ag/AgCl) reference electrode were used to measure the potential from the solutions in triplicate. The electrodes were immersed in solutions for up to five minutes to stabilise the readings. The stability had shown of using that kind of plasticiser with an ionophore of dibenzo-18-crown-6 ionophore in a PVC matrix.

A new polymer sensor was then prepared and the measurements repeated, with the same results being obtained. Therefore, it was concluded that the DB18C6 sensor had affinity for  $\text{K}^+$  in the presence of DBP as a solvent mediator, which is the specific type of plasticiser most commonly used in PVC. The PVC polymer chains are attracted to one another, and therefore form a very rigid structure. The phthalate plasticisers are added to PVC to help the chains slide against each other, therefore softening the PVC because of the structure of a phthalate ester. The plasticiser DBP produced better results than other plasticisers in the Nernstian response slope, which was 58.1 mV per decade, with a correlation coefficient of 0.9841 for the linear part, as shown in (Figure 4. 3). The polymer's flexibility (elongation) or ease of processing (workability) increased gradually.

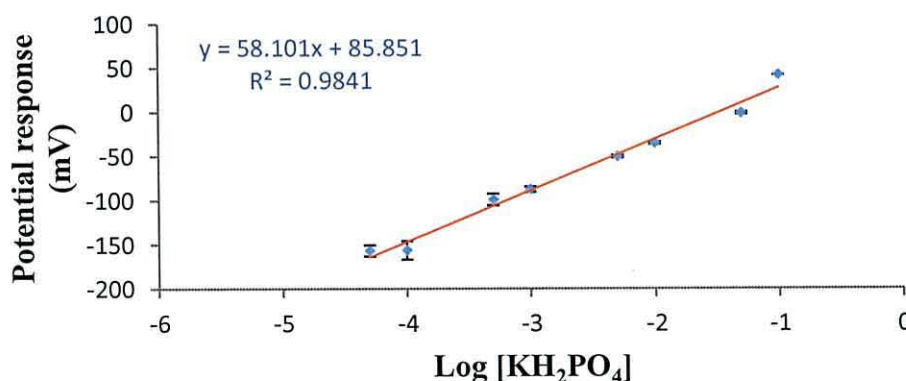


**Figure 4. 3:** Potential response of the potassium ISE containing DBP as a plasticiser and dibenzo-18-crown-6 as an ionophore vs. an Ag/AgCl reference electrode, for increasing concentrations of potassium phosphate ion at pH 9 ( $n = 3$  and error bars [where visible] indicate the standard deviation)

### Nitrophenyl phenyl ether (NPPE)

The nitrophenyl phenyl ether plasticisers (NPPE) sensors were prepared and tested with dibenzo-18-crown-6 ionophore for the potassium ion ( $K^+$ ) in the presence of  $PO_4^{3-}$ . The NPPE plasticiser is shown in (Figure 4. 4) were investigated in the sensing membrane for the performance of an ISE based on a PVC membrane.

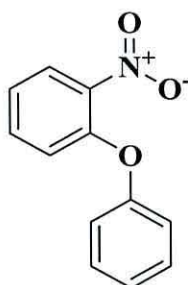


*Figure 4. 4: Nitrophenyl phenyl ether plasticiser chemical structure*

NPPE was used as a solvent mediator and it can be seen from its structure that it has a nitro group as a substituent to the benzene group with the phenyl. These plasticisers are commonly used due to their favourable physical interactions with high-molecular-weight polymer which is 215.20 g/mol for NPPE plasticiser.<sup>15</sup> These physical interactions cause the polymer and the solvent mediator to form a homogenous physical unit with a high boiling point of 106-108 °C/0.01 mmHg. (Figure 4. 5) shows the thermal properties of this plasticiser were studied by DSC-TGA thermogram of the samples and the DSC curve presents a melting process at 275 °C by the exothermic peak.

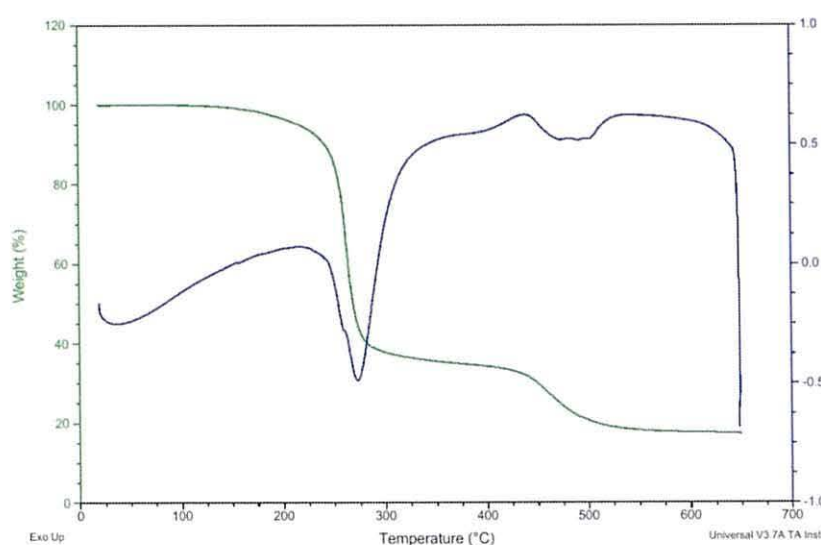


*Figure 4. 5: DSC - TGA thermogram shows the thermal properties of the nitrophenyl phenyl ether plasticiser*



Electrodes based on this solvent mediator produced non-Nernstian results in terms of the response concentration range of  $5 \times 10^{-4} \text{ mol L}^{-1}$  to  $1 \times 10^{-1} \text{ mol L}^{-1}$ , and low limit of detection of  $1.2 \times 10^{-4} \text{ mol L}^{-1}$ .

The dibenzo-18-crown-6 sensor with NPPE as a solvent mediator and a silver/silver chloride (Ag/AgCl) reference electrode were used to measure the potential from the solutions in triplicate. The non-stabilisation of the potential readings was due to use that kind of plasticiser with an ionophore of dibenzo-18-crown-6 in a PVC matrix. This can be seen in (Figure 4. 6). A new polymer sensor was prepared and the measurements repeated, and the same results were obtained. The use of NPPE derivatives, as more hydrophobic plasticisers in comparison to DBP, should enhance the performance of membrane-selective electrodes in PVC membrane electrodes with no added ion-exchanger, with respect to low detection limits. However, the use of NPPE derivatives did not enhance the performance of membrane-selective PVC electrodes with respect to slope sensitivity, response time or pH effect. Therefore, it was concluded that the dibenzo-18-crown-6 sensor does not have affinity for  $\text{K}^+$  in the presence of NPPE as a plasticiser.

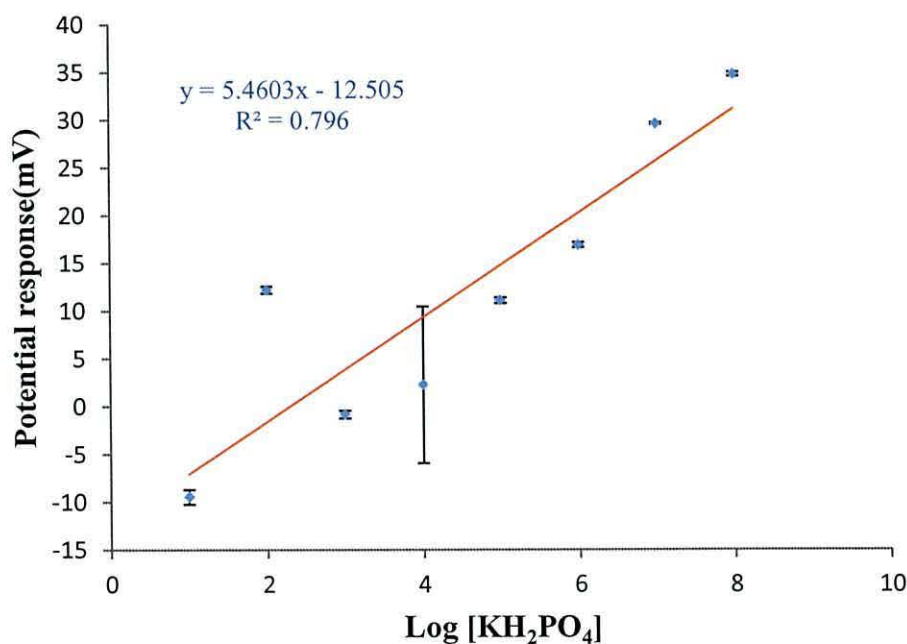


*Figure 4. 6: Potential response of the potassium ISE containing the nitrophenyl phenyl ether as a plasticiser and dibenzo-18-crown-6 as an ionophore vs. an Ag/AgCl reference electrode, for increasing concentrations of potassium phosphate ion at pH 9 ( $n = 3$  and error bars [where visible] indicate the standard deviation)*

The solvent mediator's nature can significantly affect the selectivity of an ISE reversible to the cations by the degree of substitution or by the number of non-ionic polar groups capable of specifically interacting with the plasticiser, primarily in the mechanism of the formation of hydrogen bonds. Thus, despite the presence of polar groups in its molecule which make it capable of forming hydrogen bonds with Lewis bases, change of the basicity of the solvent mediator only slightly affects selectivity to the potassium cation.

As it can be seen from the graph the linearity started deviated from the linear case by moving to the diluted solution, which explained clearly by error bars and the main reason of that was the long response time for the steady potential reading.

### Dioctyl phenyl phosphonate (DOPP)

The dioctyl phenyl phosphonate plasticiser's sensor of dibenzo-18-crown-6 ionophore for the potassium ion ( $K^+$ ) in the presence of  $PO_4^{3-}$  were prepared and tested. The dioctyl phenyl phosphonate plasticiser is shown in (Figure 4. 7) have two octyl chains attached to a phosphonate substituent to the benzene ring.

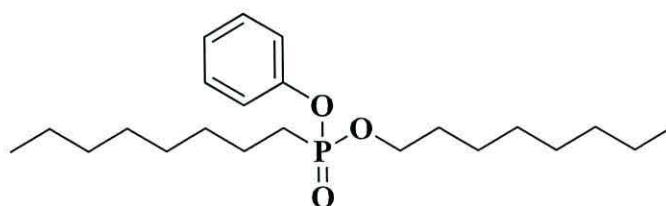
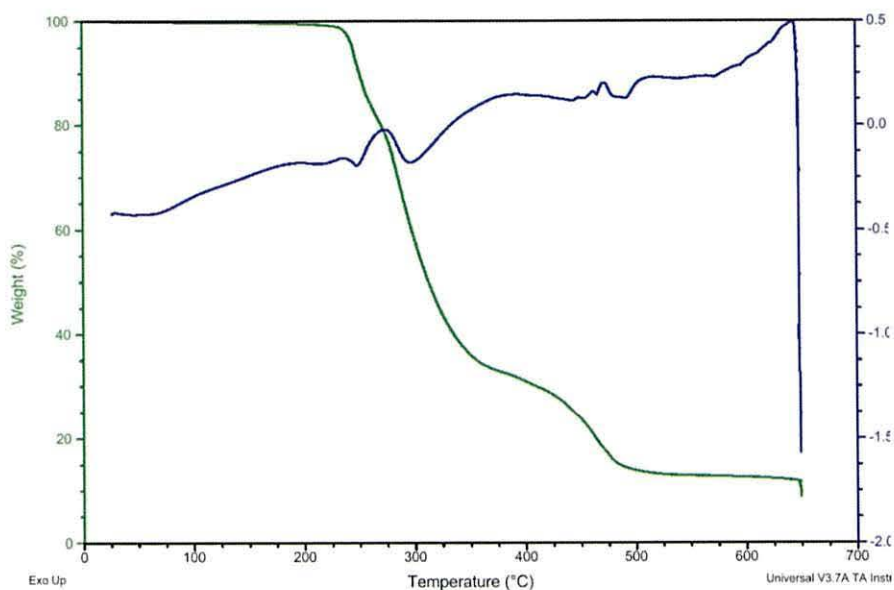


Figure 4. 7: Dioctyl phenyl phosphonate plasticiser chemical structure

The effect of this solvent mediator in the sensing membrane on the performance of an ISE based on a PVC membrane was investigated. The plasticiser DOPP was used and, as can be seen from its structure, the two long dioctyl chains linked to the phosphonoic acid with a phenyl ring structure give it polarity and create hydrogen bonding with the PVC in the sensor membrane. The solvent mediator is not covalently bound to the PVC molecule, meaning that it can diffuse out into the PVC. Nevertheless, it is still an inert organic material with a high boiling point of 207 C and high density of 0.967 g/mL at 25 C. (Figure 4. 8 ) shows the thermal properties

of this plasticiser were studied by DSC- TGA thermogram of the samples and the DSC curve presents a melting process at 280 °C by the exothermic peak.



**Figure 4. 8: DSC- TGA thermogram shows the thermal properties of the diethyl phenyl phosphonate plasticiser**

Electrodes based on this solvent mediator produced better results than other plasticised PVC membrane electrodes, with the exception of DBP, in terms of a response concentration range of  $1 \times 10^{-3} \text{ mol L}^{-1}$  to  $1 \times 10^{-1} \text{ mol L}^{-1}$ , with a low limit of detection of  $5.1 \times 10^{-4} \text{ mol L}^{-1}$ . A new polymer sensor was prepared and the measurements recorded, with the same results being found, as shown in (Figure 4. 9). Therefore, it was deduced that the dibenzo-18-crown-6 sensor had less affinity for  $\text{K}^+$  in the presence of DOPP as a plasticiser, in comparison with DBP. As it can be seen from the graph the linearity started deviated from the linear case by moving to the diluted solution or due to the chemical structure for the plasticiser which incorporates the ionophore in the PVC membrane.



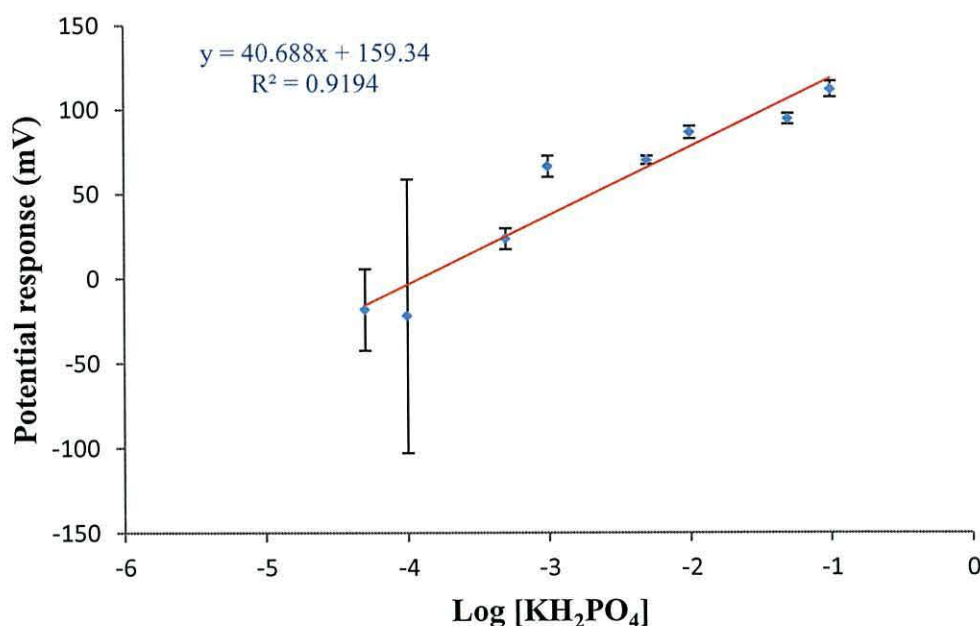


*Figure 4. 9: Potential response of the potassium ISE containing the di octyl phenyl phosphonate as a plasticisers and dibenzo-18-crown-6 as an ionophore vs. an Ag/AgCl reference electrode, for increasing concentrations of potassium phosphate ion at pH 9 ( $n = 3$  and error bars [where visible] indicate the standard deviation)*

### Di octyl phthalate (DOP)

The dioctyl phthalate sensor for the potassium ion ( $K^+$ ) in the presence of  $PO_4^{3-}$  was prepared and tested. The structure of this solvent mediator is as shown in (Figure 4. 10), with two octyl chains attached to the two phthalate groups as substituents of the benzene ring.

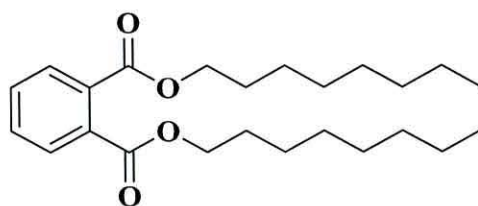


*Figure 4. 10: Di octyl phthalate plasticiser chemical structure*

The calibration standard solutions of  $K_2HPO_4$  were freshly prepared in series, in a range of  $0.1 \text{ mol L}^{-1}$  to  $0.5 \times 10^{-5} \text{ mol L}^{-1}$ . The dibenzo-18-crown-6 sensor with DOP as a solvent mediator and a silver/silver chloride (Ag/AgCl) reference electrode were used to measure the potential from the solutions in triplicate. The electrodes were immersed in solutions for up to five minutes to stabilise them. Stable readings were obtained and the potential had drifted, which showed a fair stability in using that kind

of solvent mediator with an ionophore of dibenzo-18-crown-6 in a PVC matrix, as shown in (Figure 4. 11). Because of the reduction in the cohesive intermolecular forces along the polymer chains, the chains move more freely relative to one another and the toughness of the polymer is reduced, which can be attributed to the high molecular weight for this solvent mediator.

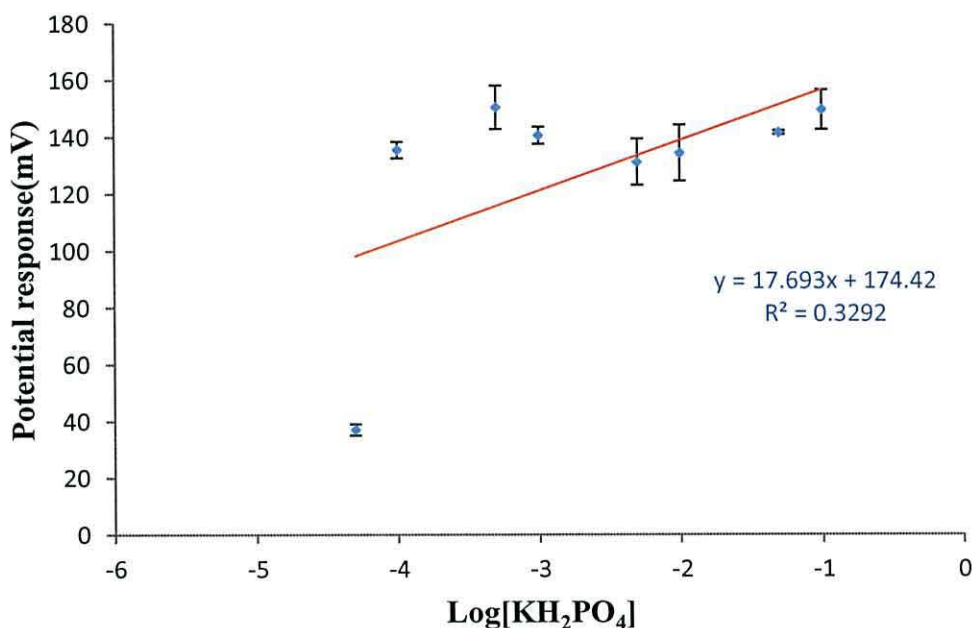


**Figure 4. 11:** Potential response of the potassium ISE containing dioctyl phthalate as a plasticiser and dibenzo-18-crown-6 as an ionophore vs. an Ag/AgCl reference electrode, for increasing concentrations of potassium phosphate ion at pH 9 ( $n = 3$  and error bars [where visible] indicate the standard deviation)

The effect of this solvent mediator in the sensing membrane on the performance of an ISE based on a PVC membrane was investigated. DOP was used as a solvent mediator and as can be seen from its structure, the two long dioctyl chains linked to the phthalic acid give it polarity and create hydrogen bonding with PVC in the sensor membrane. However, it is still an inert organic material with a high boiling point of 384 °C and high density of 0.967 g/mL at 25 °C. Together with the high vapour pressure of 1.2 mmHg (93 °C), all of these physical properties boost its ability to be incorporated in PVC membrane. (Figure 4. 12) shows the thermal properties of this plasticiser were studied by TGA / DSC thermogram of the samples and the DSC curve presents a melting process at 320 °C by the exothermic peak.

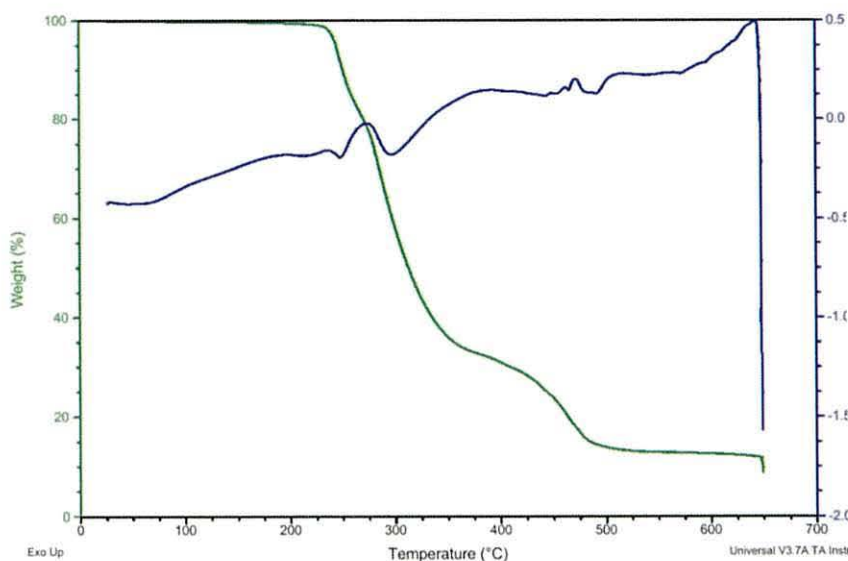


**Figure 4. 12:** DSC- TGA thermogram shows the thermal properties of the Di-octyl phthalate plasticiser

Electrodes based on this solvent mediator produced better results than other plasticised PVC membrane electrodes, with the exception of DBP, in terms of the response concentration range of  $5.5 \times 10^{-3} \text{ mol L}^{-1}$  to  $3 \times 10^{-1} \text{ mol L}^{-1}$ , and low limit of detection of  $3.1 \times 10^{-3} \text{ mol L}^{-1}$ . A new membrane sensor was prepared and the measurements repeated, with the same results obtained. Therefore, it was deduced that the dibenzo-18-crown-6 sensor had a slight affinity for  $\text{K}^+$  in the presence of DOP as a solvent mediator.

#### Bis (2-ethylhexyl) adipate (BEHA)

The Bis (2-ethylhexyl) adipate (BEHA) of dibenzo-18-crown-6 ionophore sensor for the potassium ion ( $\text{K}^+$ ) in the presence of  $\text{PO}_4^{3-}$  was prepared and tested. The Bis (2-ethylhexyl) adipate plasticiser (Figure 4. 13) is a long aliphatic chain of an ethyl hexyl group with two carboxylic groups.

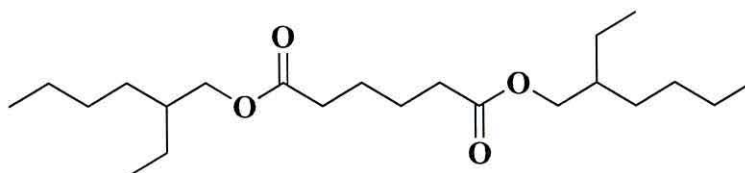


**Figure 4. 13:** Bis (2-ethylhexyl) adipate plasticiser chemical structure



The effect of this plasticiser in the sensing membrane on the performance of an ISE based on a PVC membrane was investigated. BEHA was used as a solvent mediator and it can be seen from its structure that the two long dioctyl chains linked to the phthalic acid give it polarity and create hydrogen bonding with PVC in the sensor membrane. Despite this, it is still an inert organic material with a high boiling point of 175 °C and high density of 0.925 g/mL at 25 °C. (Figure 4. 14) shows the thermal properties of this plasticiser were studied by TGA / DSC thermogram of the PVC membrane with BEHA plasticiser and the DSC curve presents a melting process at 300 °C by the exothermic peak.

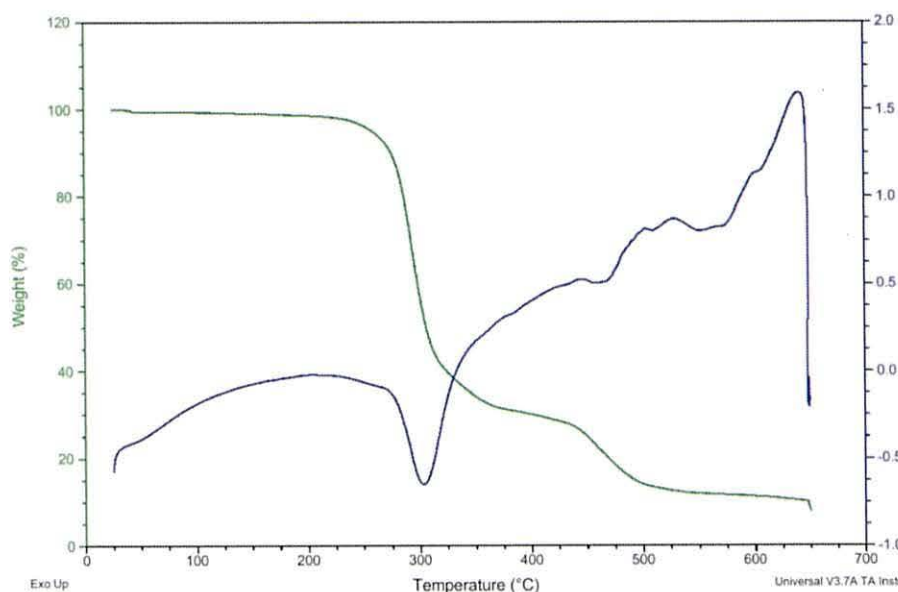


**Figure 4. 14: DSC- TGA thermogram shows the thermal properties of the Bis (2-ethylhexyl) adipate plasticiser**

In spite of the physical properties of this solvent mediator, it doesn't seem to have the ability to be incorporated into a PVC membrane, which is clear from its non-Nernstian slope for its measurements. The non-stability of using this kind of plasticiser with dibenzo-18-crown-6 ionophore in a PVC matrix has been shown in (Figure 4. 15). For confirmation of these results, a new polymer sensor was prepared and the measurements repeated, but the same results were obtained. Therefore, it was deduced that the dibenzo-18-crown-6 sensor had no affinity for  $K^+$  in the presence of BEHA as a solvent mediator.

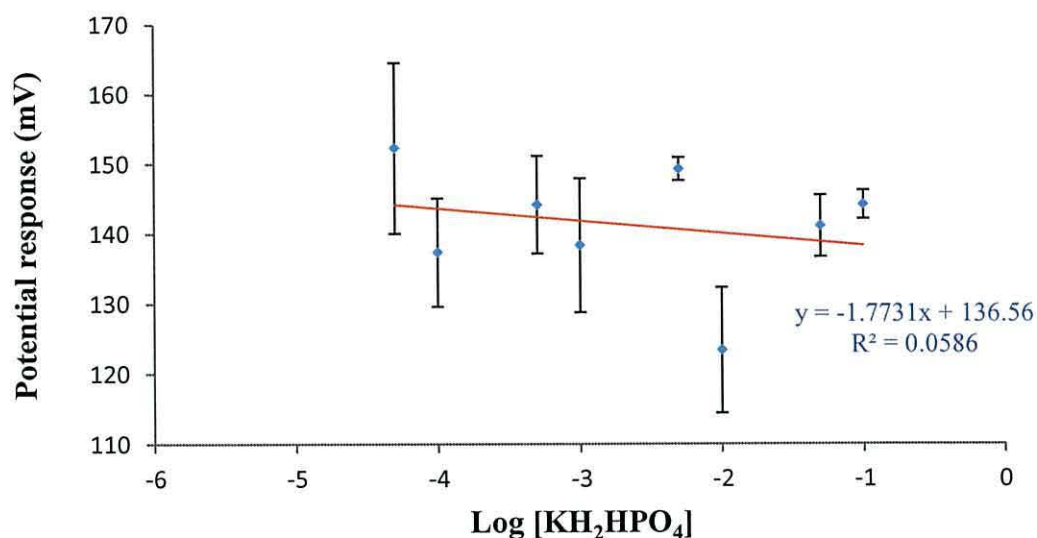


**Figure 4. 15:** Potential response of the potassium ISE containing the Bis(2-ethylhexyl) adipate as a plasticiser and dibenzo-18-crown-6 as an ionophore vs. an Ag/AgCl reference electrode, for increasing concentrations of potassium phosphate ion at pH 9 ( $n = 3$  and error bars [where visible] indicate the standard deviation)

In addition to all above thermal properties; the polarity properties for each plasticiser was done by introduce each plasticiser for two different polarity solvents (petroleum ether/ethyl acetate) 10:1 and TLC analysis was applied as in (Figure 4. 16).

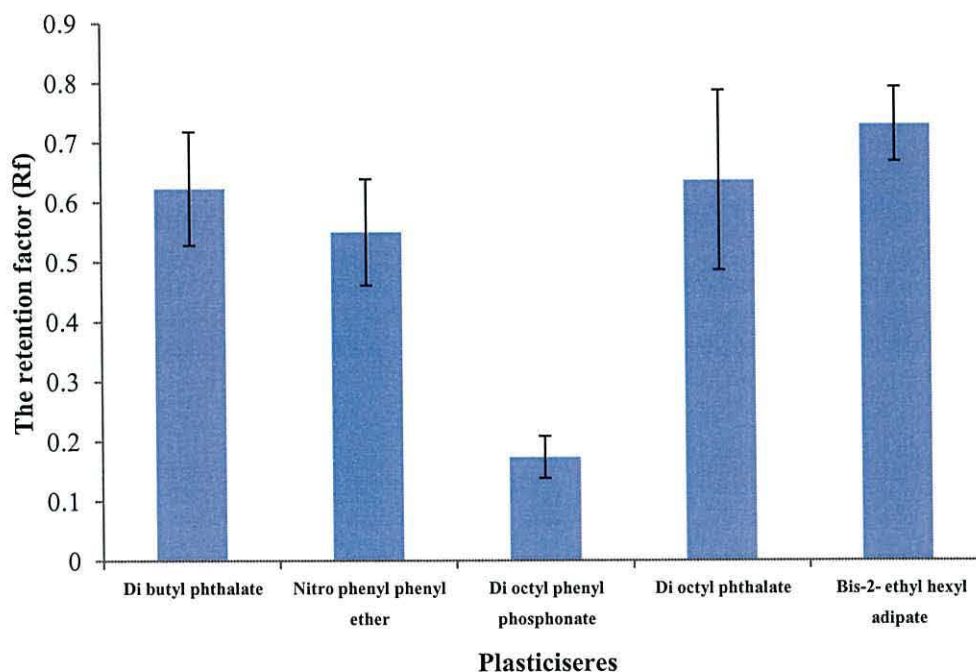


**Figure 4. 16:** The retention factors of the different plasticisers DBP, DOPP, DOP, NPPE, and BEHA, using TLC (petrol: ethyl acetate) 10:1. ( $n = 3$  and error bars [where visible] indicate the standard deviation)

It can be seen from the graph that the order of the polarity of these plasticisers in the direction from the highest polarity to the lowest one in this way DOPP > 2-NPPE > DBP > DOP > BEHA. As a result of that arrangement, the potential response of the membranes of these plasticisers is in the order as in (Figure 4. 17).

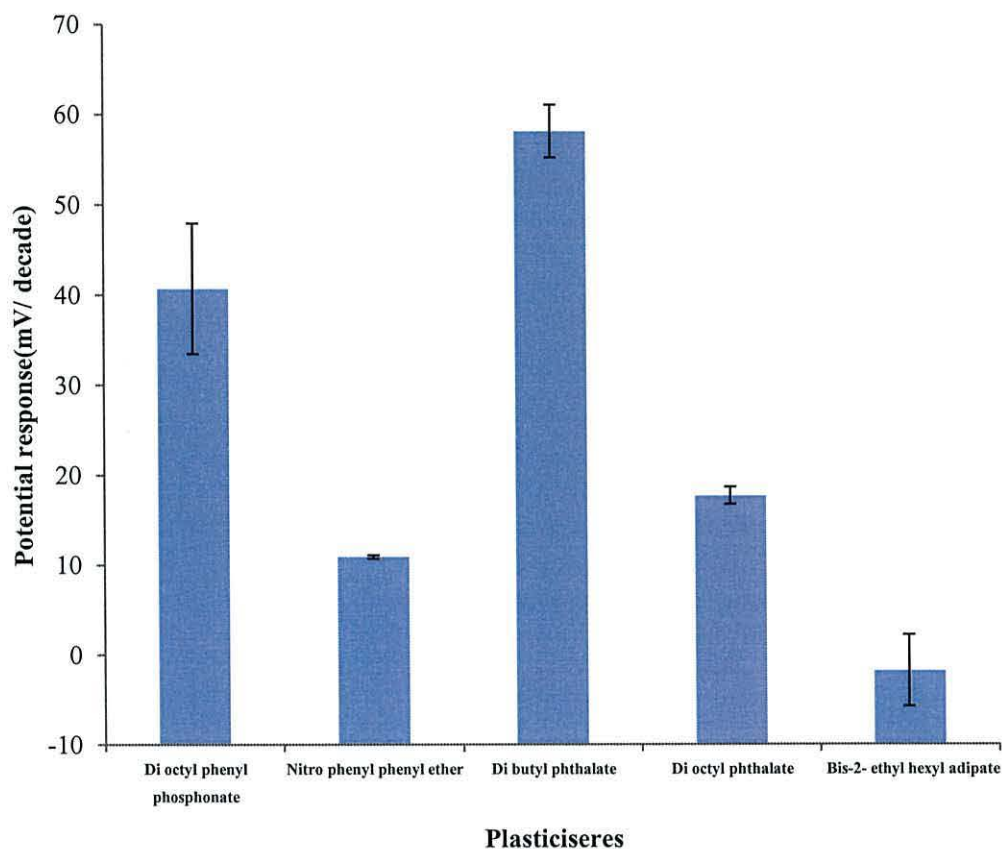


**Figure 4. 17:** The potential response of the potassium ISE of the different plasticisers DBP, DOPP, DOP, NPPE, and BEHA, with dibenzo-18-crown-6 as an ionophore vs. an Ag/AgCl reference electrode, for increasing the polarity of these plasticisers using TLC (petrol: ethyl acetate) 10:1 ( $n = 3$  and error bars [where visible] indicate the standard deviation)

From the graph above, it is clear that the potential response of the PVC membrane effected not just with polarity of the plasticisers used, but as well with chemical structure in the membrane preparation of the ISEs includes compatibility with the polymer used which can be seen from the error bars; it is clear from the highest error bars for the DOPP plasticiser which has an aromatic structure combined with phosphonate group, this is thought to be due to the associated increase in response time for these kind of the structures.



## 4.2 Influence of membrane composition

The sensitivity, selectivity, working range and stability of an ISE depend on many factors, such as the nature of the ionophore, the addition of ion-exchangers, and the nature of various plasticisers. Therefore, membranes with different compositions were prepared and their potentiometric response characteristics were evaluated. The effect of plasticisers on  $K^+$ -selective electrodes based on different solvent mediators is shown in Table 4. 2. It is clear that DBP solvent mediator is a more effective plasticiser than others in preparing the  $K^+$ -ISEs, which can be explained by the fact that DBP-plasticised PVC membranes have much higher dielectric constants than BEHA, DOPP and DOP based membranes. In addition, DBP-plasticised membranes dissolve the ion association complexes and adjust both permittivity and ion-exchanger site mobility to give highest possible selectivity and sensitivity.

*Table 4. 2: Influence of the nature of plasticiser on the characteristics of  $K^+$ -ISEs*

| The plasticiser | Linear range, M                              | Detection limit, M   | Slope, mV/dec. |
|-----------------|--|----------------------|----------------|
| <b>DBP</b>      | $5.0 \times 10^{-5}$ to $1.0 \times 10^{-1}$ | $3.2 \times 10^{-6}$ | 58.1           |
| <b>NPPE</b>     | $5.0 \times 10^{-4}$ to $1.0 \times 10^{-1}$ | $1.2 \times 10^{-4}$ | 5.4            |
| <b>DOPP</b>     | $1.0 \times 10^{-3}$ to $1.0 \times 10^{-1}$ | $4.5 \times 10^{-4}$ | 40.6           |
| <b>DOP</b>      | $5.5 \times 10^{-1}$ to $3.0 \times 10^{-1}$ | $3.1 \times 10^{-3}$ | 17.6           |
| <b>BEHA</b>     | $1.5 \times 10^{-2}$ to $1.3 \times 10^{-1}$ | $4.3 \times 10^{-3}$ | -1.7           |

The performances of sets of membrane-based cation-selective polymeric membrane electrodes with different plasticisers were investigated, since the selectivity of ISEs is greatly influenced by the membrane solvent and also controlled by plasticisers. For the comparison study into the potential response of potassium ISEs containing different plasticisers, dibutyl phthalate, dioctyl phenyl phosphonate, di octyl phthalate, 2- Nitro phenyl phenyl ether, and bis-2-ethyl hexyl adipate were used as plasticisers, with dibenzo-18-crown-6 as an ionophore vs. an Ag/AgCl reference electrode. Increasing concentrations of potassium phosphate ion at pH 9 were used, giving the results shown in (Figure 4. 18).

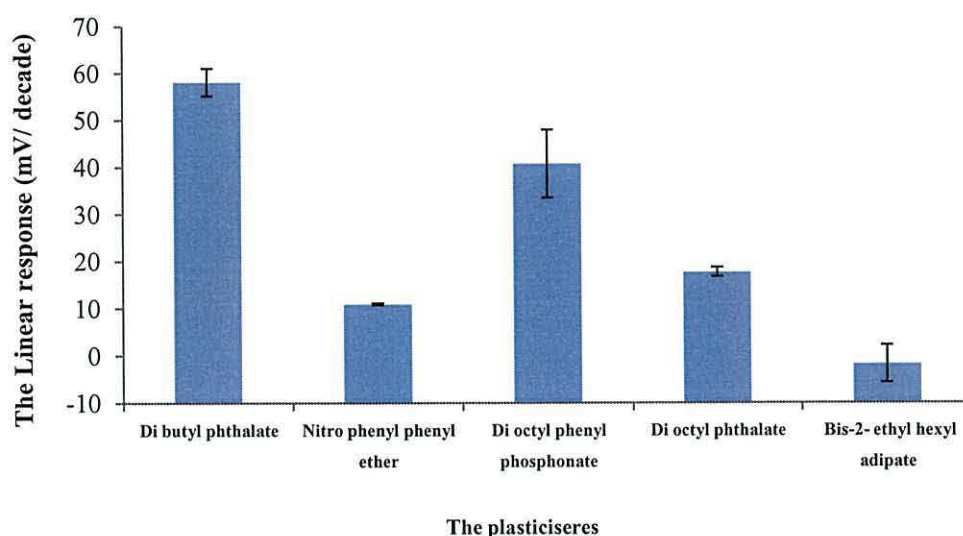


**Figure 4. 18:** The potential response of the potassium ISE of the different plasticisers, with dibenzo-18-crown-6 as an ionophore vs. an Ag/AgCl reference electrode, for increasing concentrations of potassium phosphate ion at pH 9 ( $n = 3$  and error bars [where visible] indicate the standard deviation)

In terms of the correlation coefficient for linearity; the response (Figure 4. 19) shows that DBP gives the best correlation coefficient for potential Nernstian response of the potassium membrane sensor, whilst a non-Nernstian response is seen for bis-2-ethyl hexyl adipate, which also have the highest error bars at one unit of standard deviation.

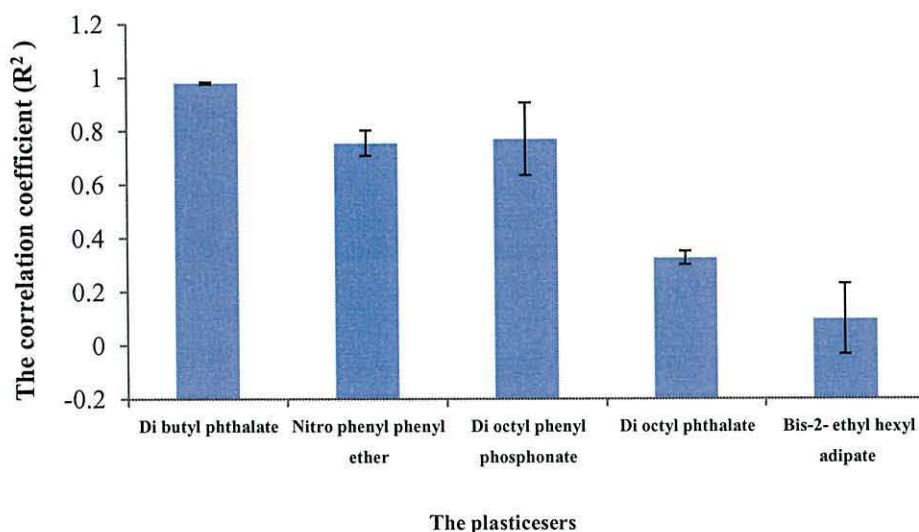


**Figure 4. 19:** The correlation coefficient of the potential response of the potassium ISEs of the different plasticisers, with dibenzo-18-crown-6 as an ionophore vs. an Ag/AgCl reference electrode, for increasing concentrations of potassium phosphate ion at pH 9 ( $n = 3$  and error bars [where visible] indicate the standard deviation)

The combination of these two parameters together indicates the performance of the solvent mediator, and shows that DBP gave linear results, with the other plasticisers following in the order: DBP > DOPP > DOP > NPPE > BEHA as in (Figure 4. 20).

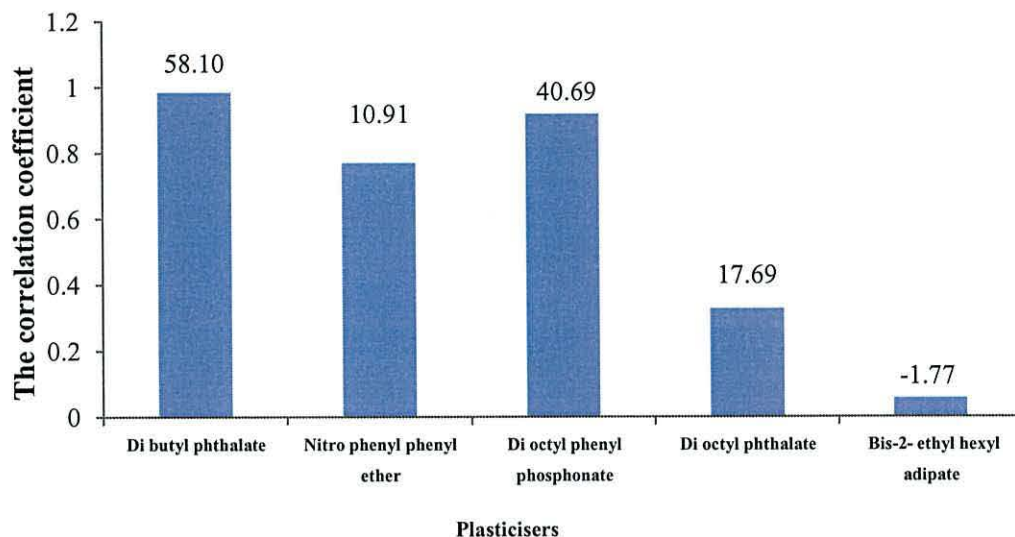


*Figure 4. 20: Comparison study for the potential response slope and the correlation coefficient of the potassium ISEs with different plasticisers and dibenzo-18-crown-6 as an ionophore vs. an Ag/AgCl reference electrode for increasing concentrations of potassium phosphate ion at pH 9 ( $n = 3$  and error bars [where visible] indicate the standard deviation)*

### 4.3 Conclusions

Ion-selective chemical sensors of a liquid membrane type were constructed using DBP, DOP, NPPE, DOPP and BEHA as plasticisers. Some of these sensors showed Nernstian slopes with linear response values in the range  $10^{-5}$  to  $10^{-1}$  mol/l. The best detection limit obtained was for the sensors constructed with DBP as a plasticiser.

It was concluded that electrodes with membranes containing PVC and the above solvent plasticisers exhibit cationic function in solutions of potassium phosphate solution, and in this situation the linearity range and the slope of electrode functions depend on the nature of the plasticiser. Membranes based on DBP lose elasticity after operating for six weeks because of the significant solubility of DBP in water. It was also shown that the introduction of an ionophore significantly improves electrochemical and operating characteristics of electrodes. The nature and type of long chain incorporated into the membrane only insignificantly affected the linearity range of electrode functions. The experimental data on varying the plasticisers in



membranes demonstrated that membranes based on DBP with PVC plasticiser exhibit optimal characteristics.

#### 4.4 References

- [1] P. K. Mohapatra, P. N. Pathak, A. Kelkarz, and V. K. Manchanda, **Novel polymer inclusion membrane containing a macrocyclic ionophore for selective removal of strontium from nuclear waste solution**, *New. J. Chem*, 2004, **28**, 1004-1009.
- [2] N. Ljungberg and B. Wesslen, **The effects of plasticizers on the dynamic mechanical and thermal properties of poly(lactic acid)**, *J. Appl. Polym. Sci.*, 2002, **86**, 1227-1234.
- [3] J. A. Ortuño, C. Serna, A. Molina, and E. Torralba, **Ion transfer square wave voltammetry of ionic liquid cations with a solvent polymeric membrane ion sensor**, *Electroanalysis*, 2009, **21 (21)**, 2297-2302.
- [4] H. Z. Langroodi and S. Meghdadi, **Application of N-quinoline-2-carboxamido-8-aminoquinoline in fabrication of a Ho(III)-PVC membrane sensor**, *J. Chem.*, 2011, **8(S1)**, 237-244.
- [5] A. Rzewuska, M. Wojciechowski, E. Bulska, E. Hall, K. Maksymiuk, and A. Michalska, **Composite polyacrylate–poly(3,4- ethylenedioxythiophene) membranes for improved all-solid-state ion-selective sensors**, *Anal. Chem.*, 2008, **80**, 321-327.
- [6] J. Bobacka, **Conducting polymer-based solid-state ion-selective electrodes**, *Trends Anal. Chem.*, 2006, **18 (1)**, 7-18.
- [7] T. Lindfors and A. Ivaska, **Stability of the inner polyaniline solid contact layer in all-solid-state  $K^+$ -selective electrodes based on plasticized poly(vinyl chloride)**, *Anal. Chem.*, 2004, **76 (15)**, 4387-4394.
- [8] L. Tom, S. Fredrik, H. Lajos, and G. Róbert, **FTIR-ATR study of water uptake and diffusion through ion-selective membranes based on plasticized poly(vinyl chloride)**, *Electroanalysis*, 2009, **21 (17-18)**, 1914-1922.

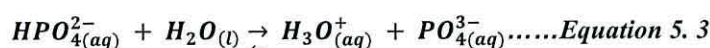
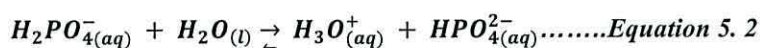
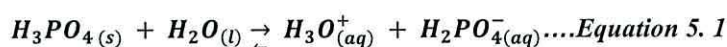
- [9] P. Agnihotri, E. Suresh, B. Ganguly, P. Paul, and P. K. Ghosh, **Study of the competitive binding of mixed alkali and alkaline earth metal ions with dibenzo-30-crown-10**, *Polyhedron*, 2005, **24**, 1023-1032.
- [10] H. Sook Seo, M. Mainul Karim, and S. Hak Lee, **Selective fluorimetric recognition of cesium ion by 15-crown-5-anthracene**, *J. Fluoresc.*, 2008, **18**, 853-857.
- [11] J. Chin, J. Oh, S. Yong Jon, S. Hyun Park, C. Walsdorff, B. Stranix, A. Ghossoub, S. Jong Lee, H. Jei Chung, S. Moon Park, and K. Kim, **Tuning and dissecting electronic and steric effects in ammonium receptors: Nonactin vs Artificial receptors**, *J. Am. Chem. Soc.*, 2002, **124**, 5374-5379.
- [12] M. Novell, M. Parrilla, G. A. Crespo, F. Xavier Rius, and F. J. Andrade, **Paper-based ion- selective potentiometric sensors**, *Anal. Chem.*, 2012, **84**, 4695-4702.
- [13] H. S. Kim, H. J. Park, H. J. Oh, Y. K. Koh, J. H. Choi, D. H. Lee, G. Sig Cha, and H. Nam, **Thiazole-containing benzo-crown ethers: A new class of ammonium-selective ionophores**, *Anal. Chem.*, 2000, **72**, 4683-4688.
- [14] J. Gao, S. Rochat, X. Qian, and K. Severin, **A simple assay for the fluorometric detection of lithium ions in aqueous solution**, *Chem. Eur. J.*, 2010, **16**, 5013-5017.
- [15] A. Loupy, B. Tchoubar, and D. Astruc, **Salt effects resulting from exchange between two ion pairs and their crucial role in reaction**, *Chem. Rev.*, 1992, **92** (6), 1141-1165.
- [16] D. Astruc, **Organometallic electron-reservoir complexes. Concepts and applications**, *Bull. Chem. Soc. Jpn.*, 2007, **80** (9), 1658-1671.
- [17] L. D. Nghiema, P. Mornanea, I. D. Potter, J. M. Perera, R. W. Cattrall, and S. D. Kolev, **Extraction and transport of metal ions and small organic compounds using polymer inclusion membranes (PIMs)**, *J. Membr. Sens.*, 2006, **281**, 7-41.

## **Chapter 5 - Application and assessment of the designed electrode**



## 5.1 Introduction

The phosphorus nutrient is often described or declared as phosphate ( $P_2O_5$ ) rather than phosphorus (P). Orthophosphoric acid is a very polar molecule and highly soluble in water. Triprotic means that an orthophosphoric acid molecule can dissociate up to three times for three equilibrium constants, giving up an  $H^+$  each time, as shown in these dissociation reactions:-



The equilibrium constants for The three equations above are  $K_{a1} = 7.25 \times 10^{-3}$ ,  $K_{a2} = 6.31 \times 10^{-8}$ , and  $K_{a3} = 4.80 \times 10^{-13}$  respectively. Plant-available phosphorus in soil, forming monobasic ( $H_2 PO_4^-$ ) or dibasic ( $HPO_4^{2-}$ ) phosphate, is one of the major essential nutrients for crop growth. However, excessive use this nutrient as fertilizers has been cited as a source of contamination of surface and groundwater ends with eutrophication is when the environment becomes enriched with nutrients. This can be a problem in marine habitats such as lakes as it can cause algal blooms and increase the concentration of these elements in rivers which ends in potable water.<sup>1</sup>

In the last few years the need for the determination of potassium phosphate has considerably increased because of growing environmental problems such as causes atmospheric and water pollution due to its application in various industrial products. In the environment it is generally present as inorganic  $K^+$  which can be easily detected and determined by ISEs are known to offer an excellent low-cost tool for the selective, sensitive and rapid determination of a vast variety of analytes in different fields of application. On the other hand it needs new ISEs for detecting potassium phosphate in aqueous solutions

Therefore; the need for fast, on-site monitoring methods allowing the analysis of a large number of samples has led to the investigation of ion-selective electrode (ISE)

technology for potassium phosphate measurement. This technology offers several advantages over current analytical spectroscopy methods, e.g., simple methodology, direct measurement of analytes, sensitivity over a wide concentration range, low cost, and portability.<sup>2</sup> However, for several reasons, the design of a sensing material (i.e., ionophore) for selective recognition of phosphate is especially challenging.<sup>3,4</sup>

The measurements are performed in a large variety of fields; including physiology,<sup>5</sup> process control,<sup>6</sup> environmental analysis,<sup>7</sup> pollution monitoring, food processing,<sup>8</sup> and water quality.<sup>9</sup> In this type of measurements the internal contact electrodes refer to a type of ISEs in which the internal reference electrode is in direct contact with the electro active membrane and contains internal solution. The concentration of the chloride ions in the internal reference electrode should keep constant concentration which result in the potential stability of internal Ag/AgCl electrode.

These electrodes will have certain advantages over conventional ones, such as the small size, lower cost of production, and ability to operate in high pressure environments where conventional ISEs might be damaged. They are composed entirely of ions and possess unique properties, including low volatility, tuneable viscosity, high conductivity, large electrochemical window and low toxicity. These properties make of the use of water two-phase system appears to be very promising for electroanalytical chemistry.<sup>10</sup> There is increasing interest in the development of ion-selective sensors for detecting electrolytes such as  $K^+$ .<sup>11</sup> To date, several potassium sensors based on plasticized membranes, containing different ionophores have been developed.<sup>12</sup> Most of them however are based on valinomycin,<sup>13,14</sup> or crown ethers<sup>15,16</sup> and report the results of a single crown ether rather than a direct comparison. The mechanism of the potential formation of ISEs with a liquid or (polymeric) membrane depends strongly on extraction and ion-exchange processes between the aqueous and organic phases.<sup>17</sup>

The aim of this chapter was to apply the best designed ion-selective electrode sensor sensitive to potassium phosphate ions (ISE-s) based on a PVC membrane phase containing an ionic liquid in real water samples collected from various sources. These samples were analysed using AAS, quantitative cation and simple anion



qualitative tests to discover the interference matrices. Finally, the polymer sensors were coated in gold and imaged using SEM and EDX which they have been already proved to be a valuable tool for obtaining surface chemical information with high spatial resolution and were developed to image local concentration profiles of  $\text{NH}_4^+$ ,  $\text{K}^+$ , and  $\text{Zn}^{+2}$  ions.<sup>18,19</sup>

## 5.2 Analyses of water samples

Water samples were taken from various sources. These samples ranged from rivers running through farmland, to wells, tap water and potable water, finally waste water. Water samples were collected initially from River Collen which runs through agricultural land in Gwynedd in Wales— with fertilizers being a contributing factor to increased potassium phosphate concentrations in water. Samples were later collected from well from an old natural well in the located in the land of old farm in Rhualt; and also from the potable water at Brecon Carrey and Abbey Well respectively, finally water samples from waste water.

### Qualitative analyses of water samples

The applied sensor belongs to the dibenzo-18-crown-6 has been utilised for the water samples due to the ISEs based on dibenzo-18-crown-6 exhibited a Nernstian response for potassium phosphate over a wide concentration range of  $5 \times 10^{-5} \text{ mol L}^{-1}$  to  $1 \times 10^{-1} \text{ mol L}^{-1}$ .

The ensemble sensor was used to determine  $\text{K}^+$  ions in a range of real samples the results of which showed a strong correlation with the data obtain from the same samples *via* atomic absorption spectroscopy. The use of dibenzo-18-crown-6 showed the potential towards a method for the quantitative determination of potassium phosphate in water samples. A series of qualitative tests for anions were carried out as described in the experimental chapter, to try to determine the possible interference(s) Table 5. 1. By this time, the water samples from the other areas had been collected and so these were also tested at the same time.



Table 5. 1: Observations from qualitative anion analysis.

| Water sample source | Halids                           | Sulphates                         | Sulphites | Nitrate            | Carbonates | Bicarbonates |
|---------------------|----------------------------------|-----------------------------------|-----------|--------------------|------------|--------------|
| Collen river        | White ppt. $\text{NH}_3$ soluble | -                                 | -         | -                  | -          | -            |
| Rhuallt well        | White ppt. $\text{NH}_3$ soluble | White ppt. $\text{HCl}$ insoluble | -         | A faint brown ring | -          | -            |
| Tap water           | White ppt.                       | -                                 | -         | -                  | -          | -            |
| DW1                 | White ppt.                       | -                                 | -         | -                  | -          | -            |
| DW2                 | White ppt.                       | -                                 | -         | -                  | -          | -            |
| Waste water         | White ppt. $\text{NH}_3$ soluble | White ppt. $\text{HCl}$ insoluble | -         | A clear brown ring | -          | -            |

The above table shows that most samples showed a positive result in the halides test present was the chloride ion ( $\text{Cl}^-$ ) as the white precipitate formed was silver chloride. All showed a white precipitate which was completely soluble upon addition of excess  $\text{NH}_3$  solution. Had it been a semi-soluble cream precipitate, the halide would have been bromide ( $\text{Br}^-$ ); an insoluble yellow precipitate would have shown us iodide ( $\text{I}^-$ ).

It has been concluded that sulphites were not detected in any samples either. The test of the sulphates and sulphites would have led to sulphur dioxide gas production. This gas would have turned blue litmus paper red, and potassium dichromate paper green. The third test in this section was also for sulphites and a positive result would have shown the potassium permanganate solution decolourise due to the reduction of manganese. However, the test for sulphates, showed a positive result for the samples taken from Rhuallt well. An insoluble white precipitate was formed due to the formation of barium sulphate ( $\text{BaSO}_4$ ).

The test of the carbonates or bicarbonates was detected during the analysis. Positive results in the first test would have shown fizzing due to the release of  $\text{CO}_2$  gas, which upon addition to limewater would have turned milky. This could have been from either carbonates or bicarbonates. The test carbonates would have distinguished as a white precipitate, which is soluble in  $\text{NH}_3$  solution due to the formation of magnesium carbonate; whereas bicarbonates do not react with magnesium sulphate. The nitrates test was positive only for water samples taken from the Rhuallt well. A

brown ring was visible due to the formation of  $[\text{Fe}(\text{NO})]\text{SO}_4$  at the junction of the layers.

### Elemental analyses

All of the water samples were analysed using pre-prepared calibration standards to determine the presence of Ca, Cd, Ag, Fe, As, Co, Cu, Pb and Zn. All samples showed very small traces of cobalt present, although with concentrations that low this could just be noise and so without further analysis these results could be supposed unreliable. The results for iron were quite low concentrations too as in Table 5. 2.

*Table 5. 2: Results from AAS elemental analysis. Concentrations are in mg/l.*

| Sample source             | [Ca]  | [Cd] | [Ag] | [Fe]  | [As] | [Co]  | [Cu] | [Pb] | [Zn] |
|---------------------------|-------|------|------|-------|------|-------|------|------|------|
| <b>Collen river</b>       | 0.598 | -    | -    | 0.0   | -    | 0.0   | -    | -    | 0.0  |
| <b>Rhuallt well</b>       | 6.324 | -    | -    | 0.0   | -    | 0.02  | -    | -    | 0.0  |
| <b>Tap water (Bangor)</b> | 1.555 | -    | -    | 0.019 | -    | 0.005 | -    | -    | 0.0  |
| <b>DW1(Brecon Carrey)</b> | 0.555 | -    | -    | 0.01  | -    | 0.001 | -    | -    | 0.0  |
| <b>DW2 ( Abbey Well)</b>  | 0.453 | -    | -    | 0.01  | -    | 0.002 | -    | -    | 0.0  |
| <b>Waste water</b>        | 8.955 | -    | -    | 0.09  | -    | 0.05  | -    | -    | 0.0  |

The quantification of the potassium ion in a range of real samples was determined. The unknown concentrations of the samples were confirmed *via* atomic absorption spectroscopy (AAS) (Figure 5. 1).

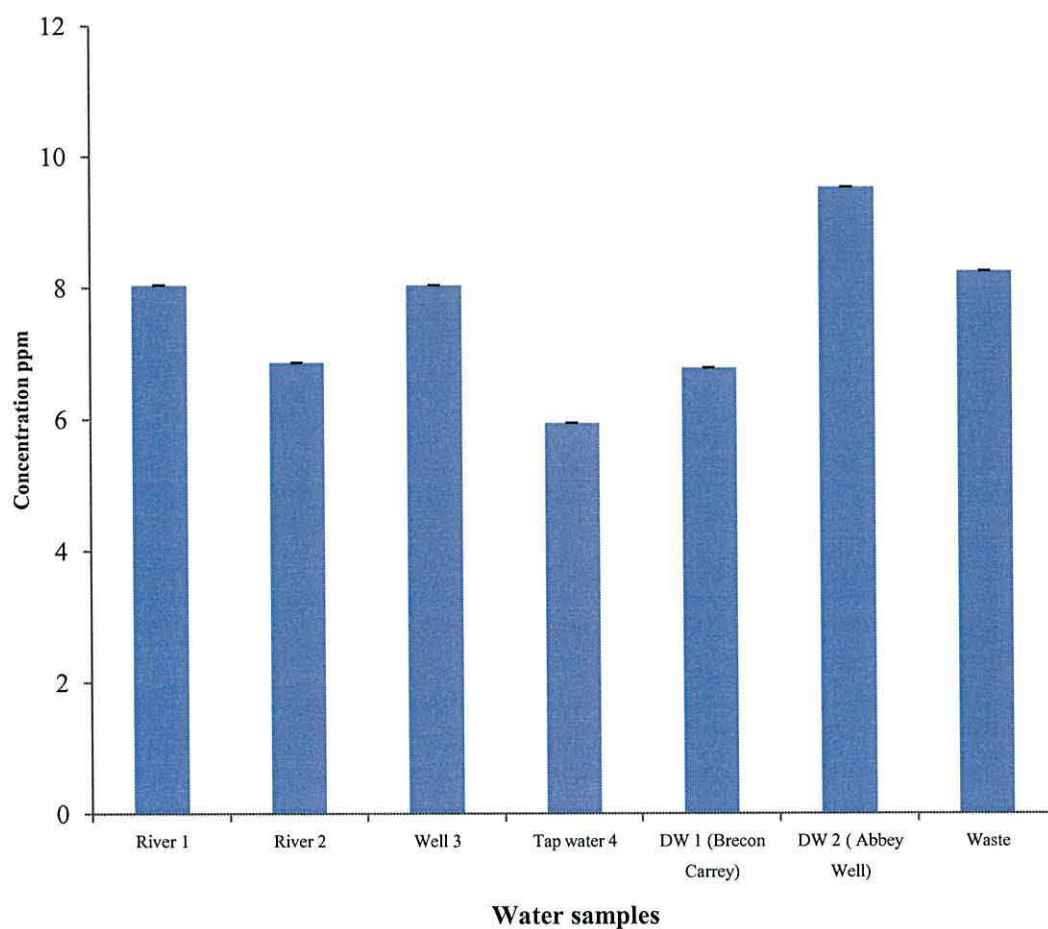


**Figure 5. 1:** Water samples measurements in AAS method ( $n = 3$  and error bars (where visible) indicate the standard deviation)

Potential measurements were carried out with the ISE (Figure 5.2) of dibenzo-18-crown-6 ionophore membrane of DBP as a plasticizer in a PVC matrix.



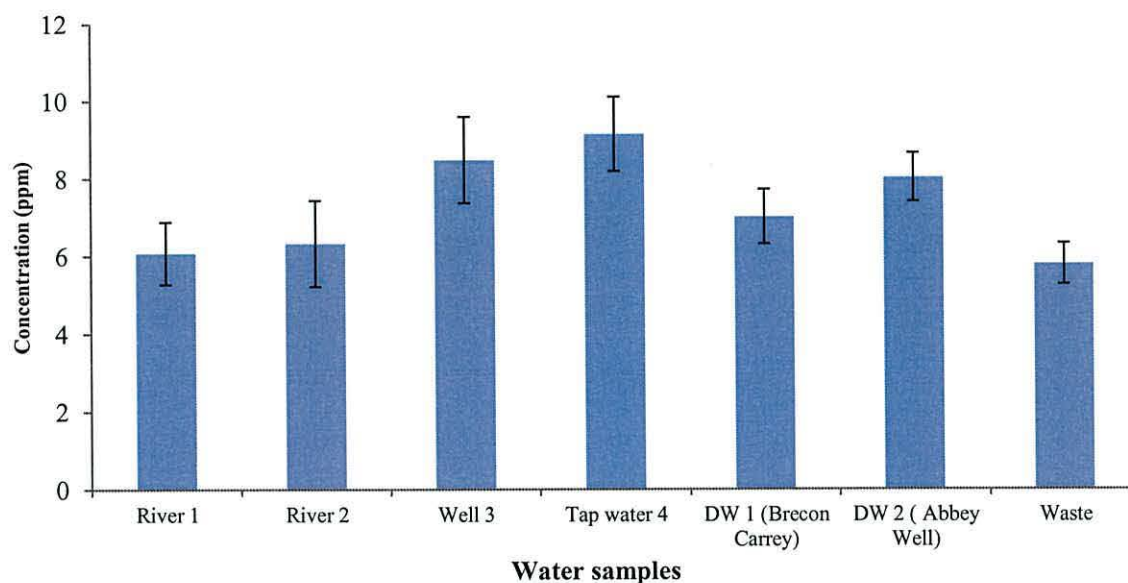


**Figure 5.2:** Water samples measurements for di benzo-18-crown-6 ionophore in ISE method ( $n = 3$  and error bars (where visible) indicate the standard deviation)

The correlation between the potential measurements were carried out with the ISE having a membrane of the dibenzo-18-crown-6 ionophore with comparison of quantification of the potassium ion in a range of real samples was determined and confirmed *via* atomic absorption spectroscopy (AAS) as in (Figure 5.3).

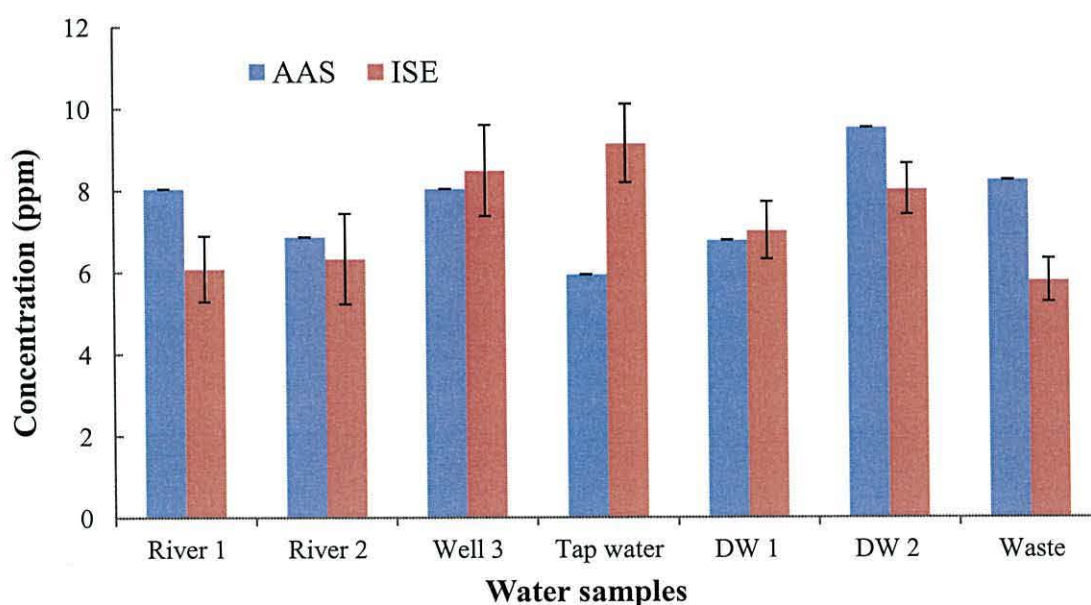


**Figure 5.3:** Water samples measurements for dibenzo-18-crown-6 ionophore in ISE method with comparison with AAS method. ( $n = 3$  and error bars (where visible) indicate the standard deviation)

Linear regression analysis of potassium concentrations measured by the electrode based on dibenzo-18-crown-6 ionophore against values obtained by AAS showed a good correlation albeit with increased error bars.

### **Scanning electrochemical microscopy and EDX analyses**

Energy-dispersive X-ray spectroscopy (EDX) is usually combined into the SEM instrument and is used to gather data about the elemental composition of the samples' surface. X-rays, which are characteristic for different elements are detected and a composition spectrum is produced. The morphologies of the sensor after using it by is imaging of the sensor in scanning electron microscopy which directly imaged.<sup>20,21</sup>

The results are only semi-quantitative since both the sample composition and sample preparation are known to affect the intensity of X-ray emission. Readings were recorded into the membrane by examination of a freshly cut membrane face.

Micrographs were prepared for the membranes evaluated are shown in Micrographs could be taken using a beam current of 10 kV which reduced the level of sample charging. To perform satisfactory EDX analysis a beam current of 14 kV was selected.

The effects of surface fouling and swelling has been noticed for the membrane in a sensor of dibenzo-18-crown-6 ionophore before saturating it in the potassium dihydrogen phosphate solution (dry sensor) as in (Figure 5.4).



*Figure 5.4: A scanning electron microscopic photograph of the PVC potentiometric membrane with dibenzo-18-crown-6 ionophore for a newly made unconditioned (dry) membrane*

The surface of the dibenzo-18-crown-6 was quite smooth in comparison to the others. Energy-dispersive X-ray analysis was carried out on the sensors' surfaces after the SEM images were taken, to get a view of the elemental composition of the surfaces. The dibenzo-18-crown-6 sensor surface (Figure 5.5).

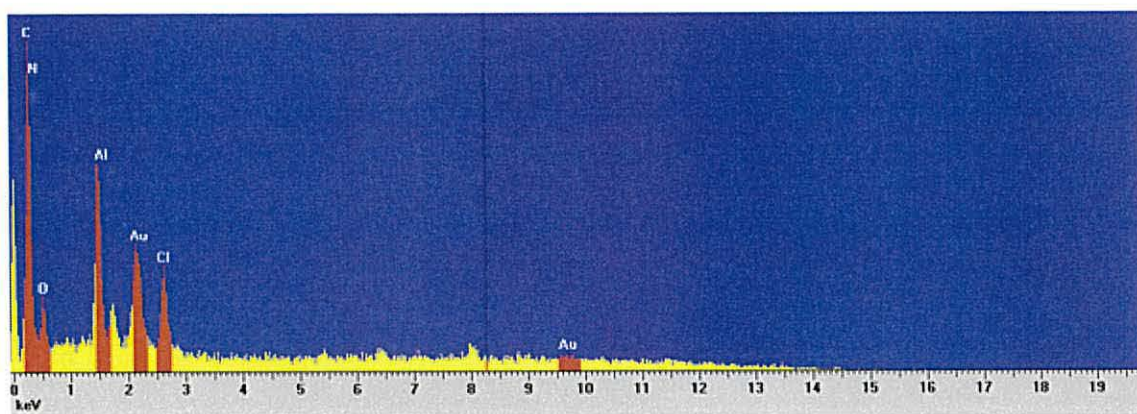


*Figure 5.5: EDX spectrum of di-benzo-18-crown-6 sensor surface*

Compositional examination of the surface particles for all the membrane produced similar results. The particles were composed of C, O, Na, Cl and K. These particles



were confirmed as components for the polymerised sensor. It was proposed that the impurities from the polymer had nucleated on the membrane surface. The Energy-dispersive X-ray analysis of the di benzo-18-crown-6 surface is shown in (Figure 5.6).

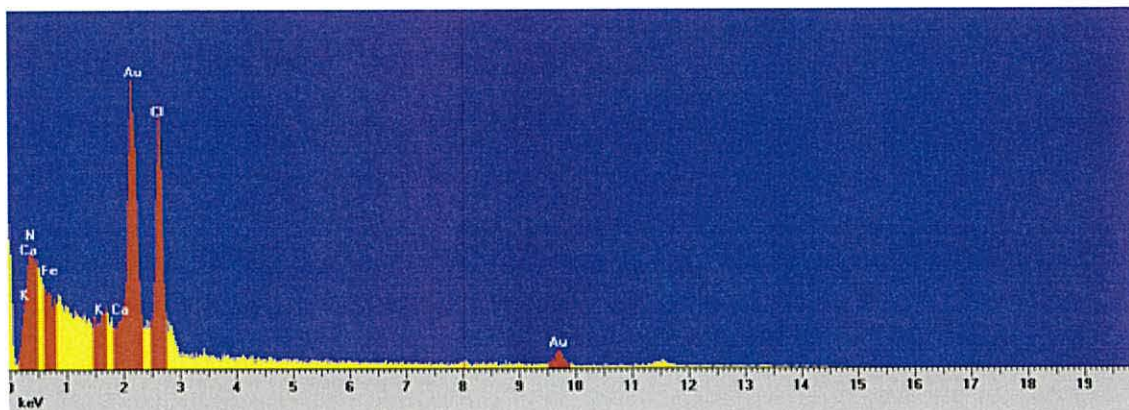


*Figure 5.6: EDX spectrum of di-benzo-18-crown-6 sensor surface after sampling*

The impurities components on the membrane surface were not expected to play any role in the development of the membrane potential. EDX analysis of the membrane surface for both dibenzo-18-crown-6 and 1-aza-18-crown-6 confirmed the presence of potassium from the added saturated solutions.

The surface of the 1-aza-18-crown-6 carried out on the sensors' surfaces after the SEM images were taken, to get a view of the elemental composition of the 1-aza-18-crown-6 surfaces (Figure 5.7).



*Figure 5.7: A scanning electron microscopic photograph of the PVC potentiometric membrane with 1-aza-18-crown-6 ionophore for the PVC membrane with 1-aza- 18 crown-6 ionophore after sampling*

The ion exchange process of potassium during the conditioning process could not be monitored because of the re absorption of the nitrogen X-ray emission. The absence of potassium from the membrane surface after conditioning was considered most significant since this reaffirmed the wave selectivity of the membrane as in (Figure 5.8) of 1-aza-18-crown-6 sensor after using it.

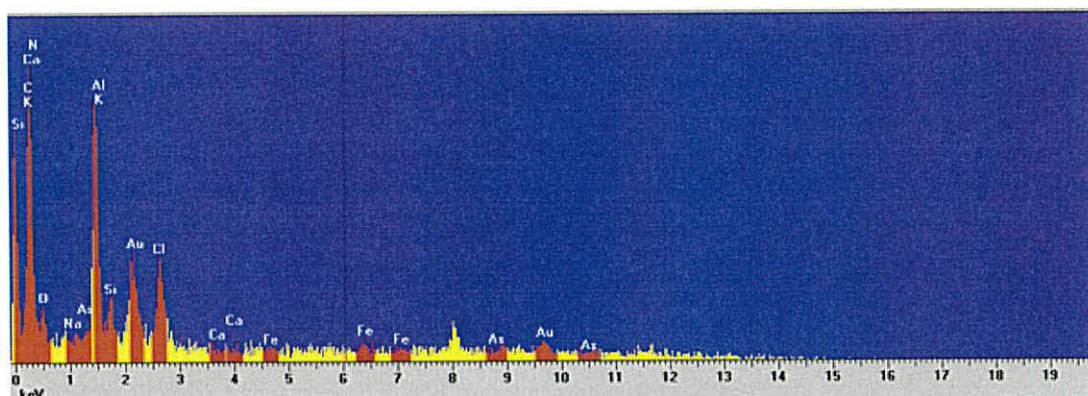


*Figure 5.8: EDX spectrum of 1-aza-18-crown-6 sensor surface after sampling*

The 1-aza-18-crown-6 sensor is different. The spectrum is not as smooth towards the higher end and there are a few elements present that are not in the other spectra. The aluminium peak is there due to the stub the sensor is mounted onto. The C, O and Cl are from the PVC, ionophore and plasticizer. The interesting part is the higher end of the spectrum; which shows Fe, Co and Cu to be present on the sensor surface. On the other hand, the effects of surface fouling and swelling has been noticed for the membrane in a sensor of dibenzo-18-crown-6 ionophore after saturating it in the potassium dihydrogen phosphate solution as in (Figure 5.9).

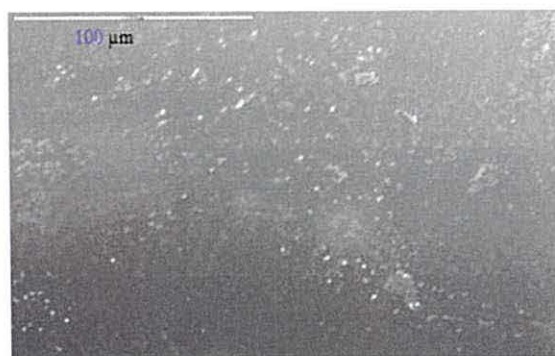


*Figure 5.9: A scanning electron microscopic photograph of the PVC potentiometric membrane with di benzo-18-crown-6 ionophore for a PVC potentiometric membrane after saturating.*



The surface of the benzo-15-crown-5 ionophore (Figure 5.10) and dicyclohexyle-18-crown-6 ionophore (Figure 5.11) carried out on the sensors' surfaces after the SEM images were taken, to get a view of the elemental composition of these surfaces.

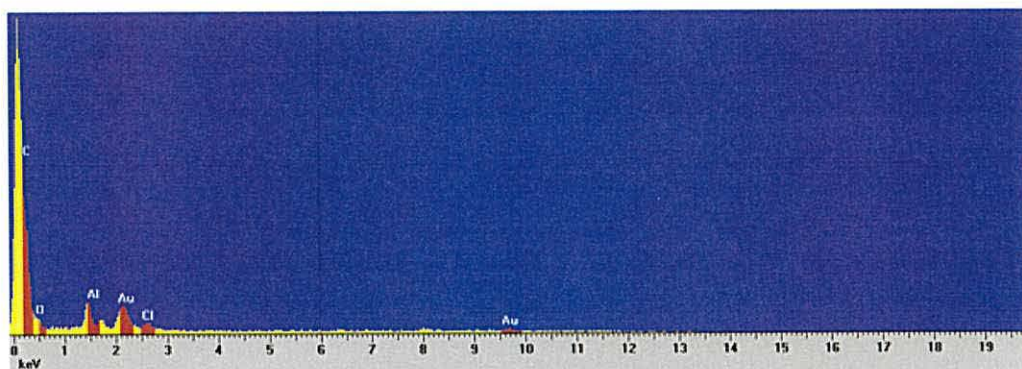


*Figure 5.10: EDX spectrum of benzo-15-crown-5 ionophore sensor surface.*

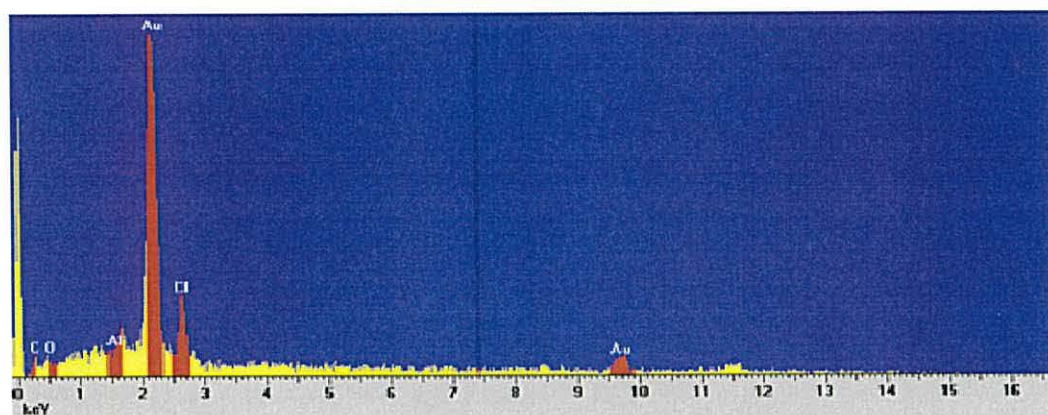


*Figure 5.11: EDX spectrum of di-cyclo hexyl 18-crown-6 ionophore sensor surface*

From all the qualitative and quantitative tests done on the collected water samples, and from the images of the sensor surfaces it can be assumed that the presence of Fe, Co, Cu and Ca could pose interferences for the sensor, along with Cl anions.



## 5.2 Lifetime of the electrode

For analytical applications, the dynamic response time is an important factor for any ISE.<sup>22</sup> and it can be defined as the time in which a stable potential is achieved.<sup>23</sup> In high concentration of potassium phosphate, the response time was longer ( $\approx 60$  s) than at lower concentrations ( $\approx 35$  s). This is because the potassium ions are known to transfer, with a reversible nature, from the aqueous solution under test to the membrane phase and again to the internal solution and hence at higher concentrations the diffusion of the species across the membrane is hindered; as a consequence the electrode needs a longer duration to achieve equilibrium.<sup>24, 25</sup> Additional important characteristic of any ISE membrane is its stability over time.<sup>26</sup> The main reason for the limited lifetimes for carrier-based sensors results from the loss of plasticizer and or ionophores from the polymeric film, due to leaching into the sample solution.<sup>27</sup> Thus, the lifetime of a sensor based on ionophores in solvent polymeric membranes depends on the distribution coefficient of the ionophores and plasticizers between the aqueous and membrane phases.<sup>28</sup>

The stability of the membrane was examined and the membrane was found to be stable over a period of 40 days without showing any significant divergence within the concentration range. The electrodes were stored in air and were re-equilibrated by dipping in a potassium phosphate solution  $1 \times 10^{-2}$  mol L<sup>-1</sup> before use for at least 24 h. After using the electrode for 40 days a slight deviation was observed in response time and slope, which could be corrected by re-equilibrating the membrane with potassium phosphate  $1 \times 10^{-2}$  mol L<sup>-1</sup> solution for 2–3 days. For this reason after use the membranes were stored in the said solution to enhance their lifetime.

### 5.3 The effect of pH

A range of pH values (6 -12) were utilised to examine the effect of the pH on the selective behaviour of potassium based on dibenzo-18-crown-6 ionophore membrane sensor as in (Figure 5.12).

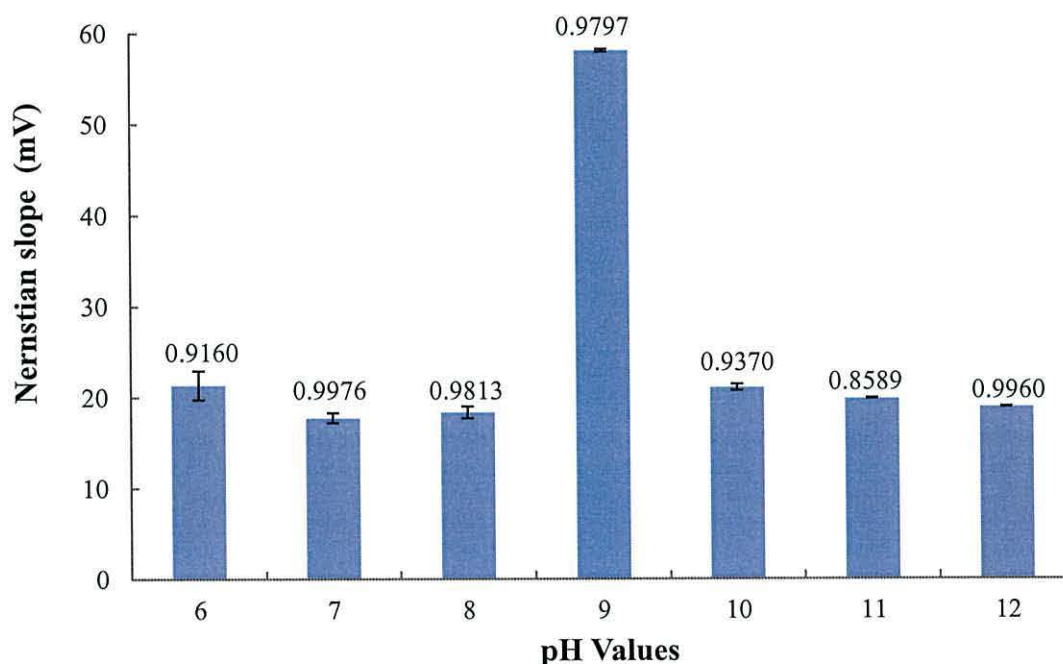


**Figure 5.12:** Nernstian response for di benzo-18-crown-6 ionophore over a range of pH values with their associated correlation coefficients. ( $n = 3$  and error bars (where visible) indicate the standard deviation)

As expected (Figure 5.12) clearly illustrates that the pH has an effect on the response.<sup>29</sup> However, the ion-selective electrode is intended for use in the detection of ions in water samples which typically show pH value variations 7-8. It can be concluded that the most suitable pH for potassium phosphate solutions is at pH 9 because of the significant effect on the electrode Nernstian response. Therefore, it is important to know/adjust the pH value of the samples before conducting ISE measurements.

The electrode potential for solutions with a pH values lower than pH 9 may well be responding to hydrogen ions along with potassium. The deviation from the Nernst equation at pH values high than 9 is thought to be exhibiting Donnan failure,<sup>30,31</sup> due

to the increasing concentration of anions in the solution. At these pH values the potassium ionophore complex in the membrane behaves as an anion-exchanger rather than as cation exchanger, and as such is going to yield a response to the phosphate or hydroxyl anion.

The selectivity coefficients<sup>32, 33</sup> of the electrode ( $k_{i,j}$ ) were determined by a SSM using the respective potassium salts. The concentrations were adjusted to 10 mM. The values were calculated using

$$\text{Log } K_{i,j}^{\text{Pot}} = (E_j - E_i)/S + \log c_i - \log c_j^{1/z_j} \dots \dots \text{Equation 5. 4}$$

Where  $E_i$  and  $E_j$  represent the potential readings measured for  $K^+$  and the interfering ion, respectively,  $S$  is the theoretical slope of the electrode for  $K^+$  (59.2 mV at 25°C),  $c_i$  and  $c_j$  are the concentrations of  $K^+$  and the interfering ion, respectively, and  $z_j$  is the charge of the interfering ion.

The values of the selectivity coefficients were measured against alkali metal ions for dibenzo-18-crown-6 ionophore using a separate potential method according to the table Table 5. 3.

**Table 5. 3: The selectivity coefficient of interfering ions on electrode based on dibenzo-18-crown-6 ionophore**

| Interfering ions | Log $k_{i,j}$ |
|------------------|---------------|
| $K^+$            | -0.342        |
| $Rb^+$           | -0.442        |
| $Na^+$           | -0.418        |
| $Cs^+$           | -0.416        |
| $Li^+$           | -0.508        |
| $NH_4^+$         | -0.315        |

#### 5.4 Effects of the counter ion

The most important characteristic of any ion-selective sensor lies in its ability to distinguish a primary ion. Within this work the selectivity was desired for not only the primary ion but the primary ion with a particular counter ion, namely potassium phosphate. To this end a series of common potassium ions were selected and



evaluated for their response to dibenzo-18-crown-6 ionophore at pH 9, as can be seen from (Figure 5.13) on the following page.

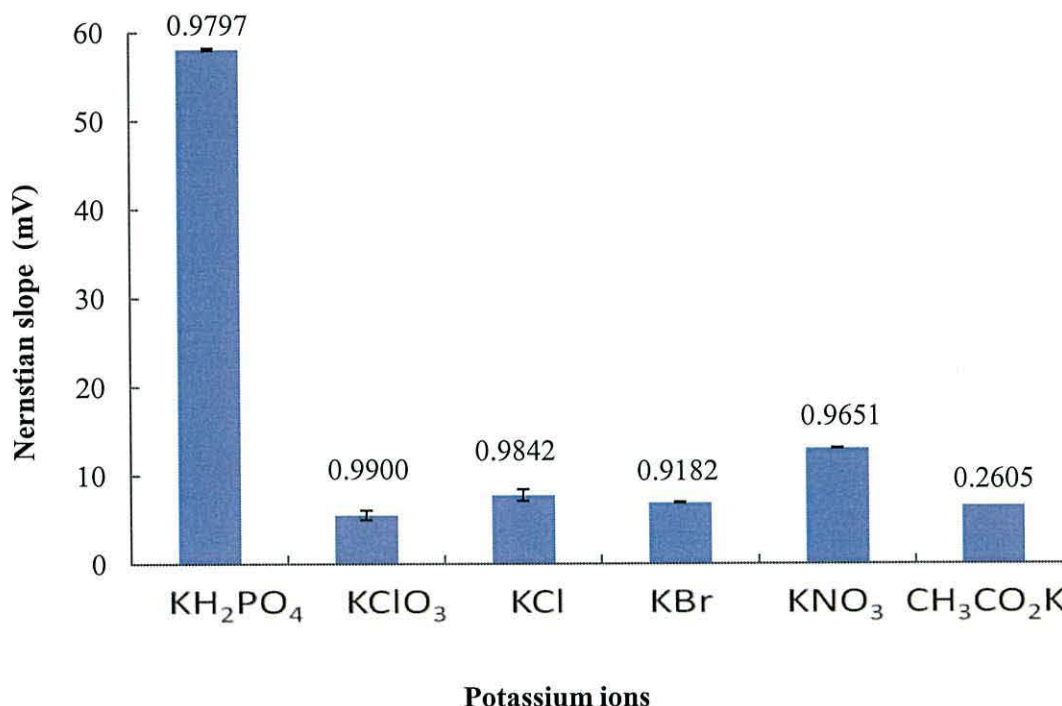


*Figure 5.13: Nernstian response for di benzo-18-crown-6 ionophore against a range of potassium ions with their associated correlation coefficients. ( $n = 3$  and error bars (where visible) indicate the standard deviation)*

Figure 5.13 illustrates that the ISE utilizing dibenzo-18-crown-6 ionophore is clearly selective towards potassium with phosphate as a counter anion. The electrode response toward the counter anion occurs in the following order  $\text{PO}_4^{3-} > \text{NO}_3^- > \text{ClO}_4^- > \text{Cl}^- > \text{Br}^- > \text{CH}_3\text{COO}^-$ . This anti-Hofmeister pattern clearly reveals the mechanism and recognition of  $\text{PO}_4^{3-}$  as a counter anion for the dibenzo-18-crown-6 ionophore,<sup>34</sup> and we believe this is the first work about to combine these two elements together to determine.

Due to the very high hydration energy of phosphate, ion-selective membranes have a very poor selectivity for phosphate alone.<sup>35</sup> According to the characterisation by the Hofmeister series ( $\text{ClO}_4^- > \text{SCN}^- > \text{I}^- > \text{NO}_3^- > \text{Br}^- > \text{Cl}^- > \text{HCO}_3^- > \text{SO}_4^{2-} > \text{HPO}_4^{2-}$ ), phosphate, being at the end of the series, shows the lowest selectivity

response toward the anions because the free energy of the phosphate species is very small and the large size of orthophosphate ions prohibits the use of size-exclusion principles for increased selectivity.<sup>36</sup>

## 5.5 Conclusions

The characteristics of an ISE utilizing a range of crown ethers as ionophores within a PVC membrane have been reported. The electrodes were constructed for the determination of potassium phosphate, with dibenzo-18-crown-6 ionophore proving to be the most effective ionophore with a shelf life of 40 days. It responded in a near Nernstian fashion, and showed a low detection limit of  $3.2 \times 10^{-6} \text{ mol L}^{-1}$ , and a fast response time over a concentration range of  $5 \times 10^{-5} \text{ mol L}^{-1}$  to  $1 \times 10^{-1} \text{ mol L}^{-1}$ .

The resulting electrode signifies a significant advancement in the construction of a potentiometric device for the determination of potassium phosphate concentrations in solution as can be seen from the comparison of the ISE results to that of AAS.

To assess the practical applicability of the sensor in real samples, an attempt was made to obtain recoveries of potassium in tap water and river water samples. Furthermore, the electrode was used for determination of ions in waste water samples. The analysis was performed by ISE technique and the results are comparable with those obtained by the AAS analysis. Thus the electrode provides a good alternative for the determination real samples.

## 5.6 References

- [1] K. W. Staver and R. B. Brinsfield, **Patterns of soil nitrate availability in corn production systems: Implications for reducing groundwater contamination**, *J. Soil. Water. Cons.*, 1990, **45(2)**, 318-323.
- [2] C. M. Carey' and W. B. Rlggan, **Cyclic polyamine ionophore for use in a dibasic phosphate-selective electrode**, *Anal. Chem.*, 1994, **66**, 3587-3591.
- [3] A. Craggs, B. Doyle, S. K. A. G. Hassan, G. J. Moody, and J. D. R. Thomas, **PVC ion-selective electrodes based on calcium bis-[dialkyl- and di-(4-alkylphenyl) phosphates] and mixed solvent mediators**, *Talanta*, 1980, **27**, 277-280.
- [4] R. De Marco and C. Phan, **Determination of phosphate in hydroponic nutrient solutions using flow injection potentiometry and a cobalt-wire phosphate ion-selective electrode**, *Talanta*, 2003, **60**, 1215-1221.
- [5] I. A. Newman, **Ion transport in roots: measurment of fluxes using ion-selective microelectrodes to characterize transporter function**, *Plant Cell Environ.*, 2001, **24**, 1-14.
- [6] J. Izquierdo, L. Nagy, Á. Varga, I. Bitter, G. Nagy, and R. M. Souto, **Scanning electrochemical microscopy for the investigation of corrosion processes: Measurement of  $Zn^{2+}$  spatial distribution with ion selective microelectrodes**, *Electrochim. Acta*, 2012, **59**, 398-403.
- [7] A. Abbaspour, E. Mirahmadi, A. Khalafi-nejad and S. Babamohammadi, **A highly selective and sensitive disposable carbon composite PVC-based membrane for determination of lead ion in environmental samples**, *J. Hazard. Mater.*, 2010, **174**, 656-661.
- [8] L. D. Mello and L. T. Kubota, **Review of the use of biosensors as analytical tools in the food and drink industries**, *Food Chem.*, 2002, **77**, 237-256.
- [9] A. Ceresa, E. Bakker, B. Hattendorf, D. Günther, and E. Pretsch, **Potentiometric polymeric membrane electrodes for measurement of environmental samples at trace levels: New requirements for selectivities and measuring protocols, and comparison with ICPMS**, *Anal. Chem.*, 2001, **73(2)**, 343-351.



- [10] D. Wei and A. Ivaska, **Applications of ionic liquids in electrochemical sensors**, *Anal. Chim. Acta*, 2008, **607**, 126-135.
- [11] J. Ping, Y. Wang, Y. Ying, and J. Wu, **Application of electrochemically reduced graphene oxide on screen-printed ion-selective electrode**, *Anal. Chem*, 2012, **84**, 3473-3479.
- [12] J. Q. Ang, B. T. Nguyen, C. S. Toh, **A dual  $K^+$ - $Na^+$  selective Prussian blue nanotubes sensor**, *Sens. and Actuators B*, 2011, **157**, 417-423.
- [13] N. Zine, J. Bausells, F. Vocanson, R. Lamartine, Z. Asfari, F. Teixidor, E. Crespo, I. A. M. de Oliveira, J. Samitier, and A. Errachid, **Potassium-ion selective solid contact microelectrode based on a novel 1,3-(di-4-oxabutanol)-calix[4]arene-crown-5 neutral carrier**, *Electrochim. Acta*, 2006, **51**, 5075-5079.
- [14] P. C. Hauser, D. W. L. Chiang and G. A. Wright, **A potassium-ion selective electrode with valinomycin based poly(vinyl chloride) membrane and a poly(vinyl ferrocene) solid contact**, *Anal. Chim. Acta*, 1995, **302**, 241-248.
- [15] S. Kim, H. Kim, K. H. Noh, S. H. Lee, S. K. Kim and J. S. Kim, **Potassium ion-selective membrane electrodes based on 1,3-alternate calix[4]crown-5-azacrown-5**, *Talanta*, 2003, **61**, 709-716.
- [16] P. Thuéry, B. Masci, M. Takimoto and T. Yamato, **Supramolecular assemblages from uranyl complexes of calixarenes and potassium complexes of 18-crown-6 or dibenzo-18-crown-6**, *Inorg. Chem. Comm.*, 2007, **10**, 795-799.
- [17] W. E. Morf, M. Badertscher, T. Zwickl, N. F. de Rooij, and E. Pretsch, **Effects of ion transport on the potential response of ionophore-based membrane electrodes: A theoretical approach**, *J. Phys. Chem. B*, 1999, **103**, 11346-11356.
- [18] A. J. Bard, M. V. Mirkin, P. R. Unwin, and D.O. Wipf, **Scanning electrochemical microscopy. 12. Theory and experiment of the feedback mode with finite heterogeneous electron-transfer kinetics and arbitrary substrate size**, *J. Phys. Chem*, 1992, **96**, 1861-1868.
- [19] C. Wei, A. J. Bard, G. Nagy, and K. Toth, **Scanning electrochemical microscopy. 28. Ion-selective neutral carrier based microelectrode potentiometry**, *Anal. Chem.*, 1995, **67**, 1346-1356.

- [20] E. Bakker, D. Diamond, A. Lewenstam, and E. Pretsch, **Ion sensors: current limits and new trends**, *Anal. Chim. Acta*, 1999, **393**, 11-18.
- [21] O. Arous, M. Amara, M. Trari, A. Bouguelia, and H. Kerdjoudj, **Cadmium (II) and lead (II) transport in a polymer inclusion membrane using tributyl phosphate as mobile carrier and CuFeO<sub>2</sub> as a polarized photo electrode**, *J. Hazard. Mater.*, 2010, **180**, 493-498.
- [22] M. N. Kopylovich, K. T. Mahmudov and A. J. L. Pombeiro, **Poly(vinyl) chloride membrane copper-selective electrode based on 1-phenyl-2-(2-hydroxyphenylhydrazo)butane-1,3-dione**, *J. Hazard. Mater.*, 2011, **186**, 1154-1162.
- [23] J. Koryta, **Ion-selective electrodes**, *Ann. Rev. Mater. Sci.*, 1986, **16**, 13-27.
- [24] R.M. Izatt, K. Pawlak, J.S. Bradshaw, and R.L. Bruening, **Thermodynamic and kinetic data for macrocycle interaction with cations and anions**, *Chem. Rev.*, 1991, 1721-1785.
- [25] V. K. Gupta, S. Agarwal, A. Jakob, and H. Lang, **A zinc-selective electrode based on N,N'-bis(acetylaceton)ethylenediimine**, *Sens. Actuators B: Chem.*, 2006, **114**, 812-818.
- [26] M. Jayakannan, O. Babourina, and Z. Rengel, **Improved measurements of Na<sup>+</sup> fluxes in plants using calixarene-based microelectrodes**, *J. Plant Physiol.*, 2011, **168**, 1045-1051.
- [27] V. S. Bhat, V. S. Ijeri, and A. K. Srivastava, **Coated wire lead(II) selective potentiometric sensor based on 4-tert-butylcalix[6]arene**, *Sens. Actuators B: Chem.*, 2004, **99**, 98-105.
- [28] U. Oesch and W. Simon, **Lifetime of neutral carrier based ion-selective liquid-membrane electrodes**, *Anal. Chem.*, 1980, **52**, 692-700.
- [29] C. Wardak, **A highly selective lead-sensitive electrode with solid contact based on ionic liquid**, *J. Hazard. Mater.*, 2011, **186**, 1131-1135.
- [30] M. Hedström and O. Karnland, **Donnan equilibrium in Na-montmorillonite from a molecular dynamics perspective**, *Geochim. Cosmochim. Acta.*, 2012, **77**, 266-274.
- [31] R. P. Buck, V. V. Cosofret and E. Lindner, **Anion effects on Donnan failure of aminated-poly(vinyl chloride)-based and neutral-carrier-based pH sensors**, *Anal. Chim. Acta*, 1993, **282**, 273-281.

- [32] T. Katsu, K. Ido, K. takaishi, and H. Yokosu, **Thallium(I)-selective membrane electrodes based on calix[6]arene or calix[5]arene derivatives**, *Sens. Actuators*, 2002, **87**, 331-335.
- [33] E. Bakker and E. Pretsch, **Potentiometric sensors for trace-level analysis**, *Trends. Analyt. Chem.*, 2005, **24(3)**, 199-207.
- [34] K. Wojciechowski, M. Kucharek, W. Wróblewski, and P. Warszyński, **On the origin of the Hofmeister effect in anion-selective potentiometric electrodes with tetraalkylammonium salts**, *J. Electroanal. Chem.*, 2010, **638**, 204-211.
- [35] M. Fibbioli, M. Berger, F. P. Schmidtchen, and E. Pretsch, **Polymeric membrane electrodes for monohydrogen phosphate and sulfate**, *Anal. Chem.* 2000, **72**, 156-160.
- [36] J. K. Tsagatakis and N. A. Chaniotakis, **190. Multiorganyltin compounds. designing a novel phosphate-selective carrier**, *Helv. Chim. Acta*, 1994, **77**.



## **Chapter 6 – Conclusions and Future work**

### 6.1 Concluding remarks

Phosphorus and potassium are essential nutrients to the life of animals and plants. They both are widely distributed in the earth's surface, seawater, rocks and soil. Higher inputs of potassium together with phosphate from human sources may stimulate plant growth in rivers and causes eutrophication which means of decomposition strips oxygen from the river water. The quantity of drinking-water has been affected strongly by the increasing pollution, and seasonal differences. The rising potassium and phosphate content of the reservoir water led the drinking-water collection company to request the monitoring system to conduct an extensive inquiry into the causes of this pollution.

Eutrophication and reduced water quality is affected by phosphate levels in water which regulated by the EU through the Urban Waste Water Treatment Directive, (annual mean total phosphorus concentrations of 1–2 mg/l) and the Water Framework Directive that will enforce “good ecological and chemical status” by 2015. Legislation is therefore driving the need for increased monitoring of soluble phosphate in water, escalating the desire for a direct, label free approach that could provide remote, continuous monitoring in real-time.<sup>1</sup>

Conventional measuring methods are costly and time consuming, because they require complex processes for pre-treatment and expensive instruments for samples to be quantitatively analyzed. The high cost and long delays of such methods have limited their use in variable-rate fertility management systems. There is thus a clear need for a fast, portable and cost effective sensor for such detection, especially for use *in situ*.

Here a series of macrocyclic compounds with different substituents have been reported. These have been examined for their potential to detect potassium phosphate in the presence of other potassium counter ions. Furthermore, the goal of this work was to develop ionophores that are capable of detecting potassium phosphate ions in aqueous solution. Two types of potassium phosphate sensors, opened and closed ring macrocyclic structure compounds based PVC membranes were evaluated for sensitivity to different potassium phosphate concentrations. The unstable potential readings were showed for the opened ring macrocyclic structure compounds which prevented to be recorded with a very long time. This first attempt to get

this opened ring structure to be comparable with closed ones was studied and showed the effect of the interactions between the cavity ring of the ionophore and the cation itself.

During the last decade, the capabilities of potentiometric analysis have changed fundamentally in that the lower limit of detection (LOD) of ion-selective electrodes (ISEs) has improved and the discrimination factor of interferences from ions. These spectacular improvements are related to the control of ion fluxes through the ion-selective membrane. Nowadays, ISEs can be used for trace measurements in environmental samples. However, by reducing the volume of the samples, the LOD in terms of the amount of analytes has been reduced to the lowest range. This is promising for bioanalysis using selective ionophores. Other recent progress includes the excellent fundamental understanding of the working mechanism.

According to these terms, the electrodes were constructed for the determination of potassium phosphate, with dibenzo-18-crown-6 (ionophore) showing to be the most effective ionophore with a shelf life of 40 days with negligible drift. It exhibited a Nernstian fashion, and showed a low detection limit of  $3.2 \times 10^{-6} \text{ mol L}^{-1}$  at pH 9. In comparison, electrodes using another tin-compound-based PVC membrane containing tributyltin chloride as an ionophore provided unsatisfactory results, showing much less sensitivity to  $\text{H}_2\text{PO}_4^-$ . The cobalt rod-based electrodes exhibited sensitive responses to  $\text{H}_2\text{PO}_4^-$  over a range from  $10^{-5}$  to  $10^{-1} \text{ mol/L}$  total phosphate concentration with a detection limit of  $10^{-5} \text{ mol/L}$ .<sup>2</sup>

In addition to the fast response time was (30-60 sec.) for that electrode over a concentration range of  $5 \times 10^{-5} \text{ mol L}^{-1}$  to  $1 \times 10^{-1} \text{ mol L}^{-1}$ . However, the membranes were based on the synthesised ionophores of 4-amino benzo-15-crown-5 (3) and 4-nitro benzo-18-crown-6 (5) was not usable for determination of potassium phosphates solutions because of their insensitivity and exhibited a non Nernstian response of 1.2657 mV/decade and 0.8525 mV/decade respectively and the correlation coefficient ( $R^2$ ) was 0.0317 and 0.0115 respectively. Moreover, the results of PVC membrane containing nitro benzo-15-crown-5 (1), diamino benzo-15-crown-5 (4), and 4-amino benzo-18-crown-6 (8) were not satisfactory of correlation coefficient ( $R^2$ ) of 0.1184, 0.5394, and 0.4835 respectively, showing much less sensitivity. Single-crystal X-ray structural analysis of (1) and (2) has been confirmed the expected structural arrangement and confirming the closing ring structures’.



On the other hand; the near Nernstian response was obtained for the ionophores of dinitro benzo-18-crown-6 (**6**) dinitro dibenzo-18-crown-6 (**7**), and diamino dibenzo-18-crown-6 (**10**) with ( $R^2$ ) of 0.8600, 0.7471, and 0.858 respectively. Finally the ionophores of dinitro benzo-15-crown-5 (**2**) and diamino benzo-18-crown-6 (**9**) showed a reasonable correlation coefficient ( $R^2$ ) of 0.7117 and 0.7423 with low Nernstian fashion of 14.282 and 8.3982 mV/decade respectively.

In addition to the ionophores study, another important study has been done to select the best plasticiser. The experimental data on varying the plasticisers incorporating the ionophores into the membrane for optimum sensor design. Those plasticisers are dibutyl phthalate, 2-nitrophenyl phenyl ether, dioctyl phenyl phosphonate, dioctyl phthalate, and bis (2-ethylhexyl) adipate demonstrated that membranes based on DBP with PVC plasticiser exhibit optimal characteristics and the sensitivity of the membrane is determined by the linearity range of the plasticiser. The thermal properties of all blends were studied by TG/DSC. All samples showed crystalline melting peaks.

Using only the data for the DBP plasticiser based on PVC membrane and the effect on membrane selectivity was illustrated. In this work, the selectivity for potassium as a cation in the cavity of the ionophore was tested over the interfering cations. However, the selectivity with logarithmic selectivity coefficients which corresponds to sensitivity to potassium than to the others represents in ( $\log K_{i,j}$ ) of -0.342 compared to previously reported data ( $\log K_{i,j}$ ) of -1.420. On the other hand, the selectivity performance for the other cations was decreased due to kinetic limitations in the transfer these cations.<sup>3</sup>

The potassium pollution revolved out to be completely caused by the waste water discharge with combined with the phosphate discharge is fully due to industrial and agricultural activities which cause the water pollution. Preventing the potassium discharge turned out to be impossible on the short term but initiatives on the European level will eventually cause standards as to the potassium with phosphate content of drinking-water to be adopted.

The resulting electrode signifies a significant advancement in the construction of a potentiometric device for the determination of potassium phosphate concentrations in solution. The synthesis of these ionophore molecules is important for the identification of

their structures ability for binding with potassium phosphate in water samples and studying their chemical properties for applying in other fields.

To assess the practical applicability of the sensor in real samples, an attempt was made to obtain recoveries of potassium phosphate in tap water, potable water, well water, and river water samples. Furthermore, the electrode was used for determination of ions in waste water samples. The analysis was performed by ISE technique. The obtained results are comparable with those obtained by the AAS analysis. Thus the electrode provides a good alternative for the determination real samples.

## 6.2 Future work

Further modification of the synthesised ionophores by Surface Plasmon Resonance (SPR) sensor which has been mainly used for the precise detection of biochemical interactions<sup>4</sup> and would provide a significantly useful method for the development of potassium ion sensing with high sensitivity and selectivity based on the coupling of SPR and Surface Analysis Microscopy (SAM). In addition to this the development of the host guest binding between the crown compounds and potassium phosphate by coating sensing on the gold chip<sup>5</sup> In addition, surface plasmon resonance may also be beneficial in sensing the association and formation of crown compounds to get good selectivity and sensitivity of the crown compounds- SAM to the  $K^+$  ion were obtained by SPR spectroscopy.

The crystal structure of the nitro benzo-15-crown-5 (**1**) and dinitro benzo-15-crown-5 (**2**) needs to be established to confirm the structural arrangement of the potassium phosphate ions, and to establish the host–guest interactions of well-formed crown compounds monolayer associated with formation of the transferring complex; this would prove to be a valuable tool for understanding the interaction mechanism.

The unsuccessfully synthesised ionophores will also be further investigated in order to develop the strong host–guest interaction between  $K^+$  ion and well-formed crown compounds monolayer. As it was well known that  $K^+$  ion in the crown cavity of di-benzo-18-crown-6, separating the phosphate as a counter-ion, forming balanced compound in Stoichiometry.



In addition to the critical role of the nature of ionophore in preparing membrane selective electrodes, other important features of the PVC membrane such as the nature of plasticiser,<sup>6</sup> which will be studying more to improve the sensitivity and selectivity of ISEs sensors.

Furthermore; The application of a new Optical scanners to capture images, digitize and quantify light intensity data directly into a computer based on linear imager charge couple device (CCD) technology<sup>7</sup> to the synthesised sensors before and after applying the sensors in real samples.

The designed electrode sensor also needs to be developed and used in scanning electrochemical microscopy (SECM) to measure profiles of ion concentrations in three-dimensional space.<sup>8</sup>

Another important application of the crown ethers compounds and because the energy is the most important issue<sup>9</sup> Therefore; The development of the crown ionophores and their application are as a new insight into dye-sensitized solar cells (DSCs) by giving a little higher short-circuit photocurrent density and little lower fill factor for the dye-sensitized solar cells with 18-crown-ether ionophore.<sup>10</sup>

In addition to the above, the use of enzymatic reactions for modifying a new ionophore for potassium combined with phosphate may prove to reduce the possibility of false response, and enable the sensor to detect the two nutrients in less time and in good selectivity.



### 6.3 References

- [1] C. Warwick, A. Guerreiro, and A. Soares, **Sensing and analysis of soluble phosphates in environmental samples: A review**, *Biosens. Bioelectron.*, 2013, **41**, 1-11.
- [2] H. J. Kim, J. W. Hummel, K. A. Sudduth, and S. J. Birrell, **Evaluation of phosphate ion-selective membranes and cobalt-based electrodes for soil nutrient sensing**, *Am. Soc. Agr. Biol. Eng.*, 2007, **50 (2)**, 415-425.
- [3] H. J. Kim, J. W. Hummel, and S. J. Birrell, **Evaluation of nitrate and potassium ion-selective membranes for soil macronutrient sensing**, *Am. Soc. Agr. Biol. Eng.*, 2006, **49 (3)**, 597-606.
- [4] R.J. Whelan, T. Wohland, L. Neumann, B. Huang, B.K. Kobilka, and R.N. Zare, **Analysis of biomolecular interactions using a miniaturized surface plasmon resonance sensor**, *Anal. Chem.*, 2002, **74**, 4570-4576.
- [5] H. Chen, Y. Gal, S. Kim, H. Choi, M. Oh, J. Lee, and K. Koh, **Potassium ion sensing using a self-assembled calix[4]crown monolayer by surface plasmon resonance**, *Sens. Actuators, B, Chem.*, 2008, **133**, 577-581.
- [6] S. Kim, H. Kim, K. Ho Noh, S. Ho Lee, S. Kuk Kim, and J. Seung Kim, **Potassium ion-selective membrane electrodes based on 1,3-alternate calix[4]crown-5- azacrown-5**, *Talanta*, 2003, **61**, 709-716.
- [7] L. F. C. A. Lapresta-Fernández, **Scanometric potassium determination with ionophore-based disposable sensors**, *Sens. Actuators, B, Chem.*, 2008, **134**, 694-701.
- [8] P. Buhlmann and L. D. Chen, **Ion-selective electrodes with ionophore-doped sensing membranes**, 2012, **1**, 2539-2579.
- [9] J. N. Freitas, A. F. Nogueira, and M. D. Paoli, **New insights into dye-sensitized solar cells with polymer electrolytes**, *J. Mater. Chem.*, 2009, **19**, 5279-5294.
- [10] C. Shi, S. Dai, K. Wang, X. Pan, L. Zeng, L. Hu, F. Kong, and L. Guo, **Influence of various cations on redox behavior of  $I^-$  and  $I_3^-$  and comparison between KI complex with 18-crown-6 and 1,2-dimethyl-3-propylimidazolium iodide in dye-sensitized solar cells**, *Electrochim. Acta*, 2005, **50**, 2597-2602.